AN INTEGRAL-OPERATOR APPROACH TO THE ELECTROMAGNETICS OF INTEGRATED OPTICS

By

Mark Stephen Viola

A DISSERTATION

Submitted to
Michigan State University
in partial fulfillment of the requirements
for the degree of

DOCTOR OF PHILOSOPHY

Department of Electrical Engineering and Systems Science

1988

ABSTRACT

AN INTEGRAL-OPERATOR APPROACH TO THE ELECTROMAGNETICS FOR INTEGRATED OPTICS

By

Mark Stephen Viola

There is an increasing interest in the study of optical and electronic circuits immersed in a layered dielectric surround. Conventional differential-operator formulations for the fields within these circuit devices are ineffective due to the inseparability of the applicable boundary conditions for structures having practical shapes. An integral-operator formulation, based on the identification of equivalent polarization currents, circumvents this difficulty.

An electric field integral equation (EFIE) is developed for the integrated system consisting of electrically heterogeneous dielectric regions embedded within a tri-layered substrate/film/cover background environment. Uniqueness of the solution to this EFIE is established. Special consideration is given to axially uniform integrated dielectric wave guiding systems.

It is observed that the longitudinal invariance of the integrated waveguiding system renders the integral-operator of the EFIE convolutional in the axial variable. Use of the Faltung theorem is prompted and a Fourier transform-domain EFIE is obtained. Analysis of solutions to this transform-domain EFIE in the complex-plane of the transform variable facilitates the identification of a propagation-mode spectrum. Surface wave modes, comprising a discrete spectrum, are associated with

pole singularities. Regimes of purely-guided and leaky surface-wave are determined. A continuous spectrum of radiation-modes arises from solutions to the transform-domain EFIE along an appropriately chosen branch cut contour.

An asymptotic form of the transform-domain EFIE is presented and is applied to the study of dielectric waveguides capable of supporting a surface-wave mode at limitingly low frequency. Examples are given to support the validity of this asymptotic EFIE.

An iterative scheme is devised to generate solutions to the forced transform-domain EFIE. Applications of this method to the graded-index asymmetric slab and graded circular dielectric waveguide indicate that one iteration can provide a reasonably good approximation for high-frequency spectral components of the continuous spectrum when the refractive contrast is small.

TO MY WIFE, LAURA

Ny

Je

re

ACKNOWLEDGEMENTS

The author would like to express sincere thanks to Dennis P. Nyquist for his inspiration and guidance. Special thanks are given to Jes Asmussen, K.M. Chen, and Byron Drachman for their support in this research.

LIS

1.

2.

3.

TABLE OF CONTENTS

Fi

1.

2.

3.

4.

5.

6.

7.

8.

9.

10.

11.

LIST OF FIGURES

12.

13.

14.

15.

16.

17.

18.

19.

20.

21.

22.

23.

24.

25.

26.

27.

28.

29.

30.

31.

32.

33.

34.

35.

36.

IN

im

op

ba

al

vi

so

fo

fi

pe

pr

ti

pr

f(

(

o:

y

d

t

[

CHAPTER ONE

INTRODUCTION

There is an increasing interest in the study of optical circuits immersed in an integrated dielectric surround. Typically, an integrated optical circuit (Figure 1) consists of a layered substrate/film/cover background in which circuit devices (represented by regions of electrical heterogeneity) are immersed. This dissertation is intended to provide a method of analysis appropriate for electromagnetic phenomena associated with this structure. In particular, this method is specialized for, and applied to the study of integrated dielectric waveguides.

Formulating a general analytic description of the electromagnetic fields within integrated dielectric waveguides is complicated by the peculiar geometry of the background/waveguide structure. In fact, it is precisely the inseparability of boundary conditions which render conventional differential-operator formulations ineffective for devices having practical shapes. Approximate solutions have been obtained from a differential-equation approach for the step-index rectangular strip guide (see for example Marcatili [1]) but this method is inaccurate near cutoff. The elaborate mode-matching approach of Peng and Oliner [2,3] yields an exact description for this class of structures, but it used a discretized radiation spectrum.

Recently, integral-operator formulations have been used. Notably, the boundary-element method has been used by a number of investigators [4,5,6]. This method is a generalization of the surface formulation

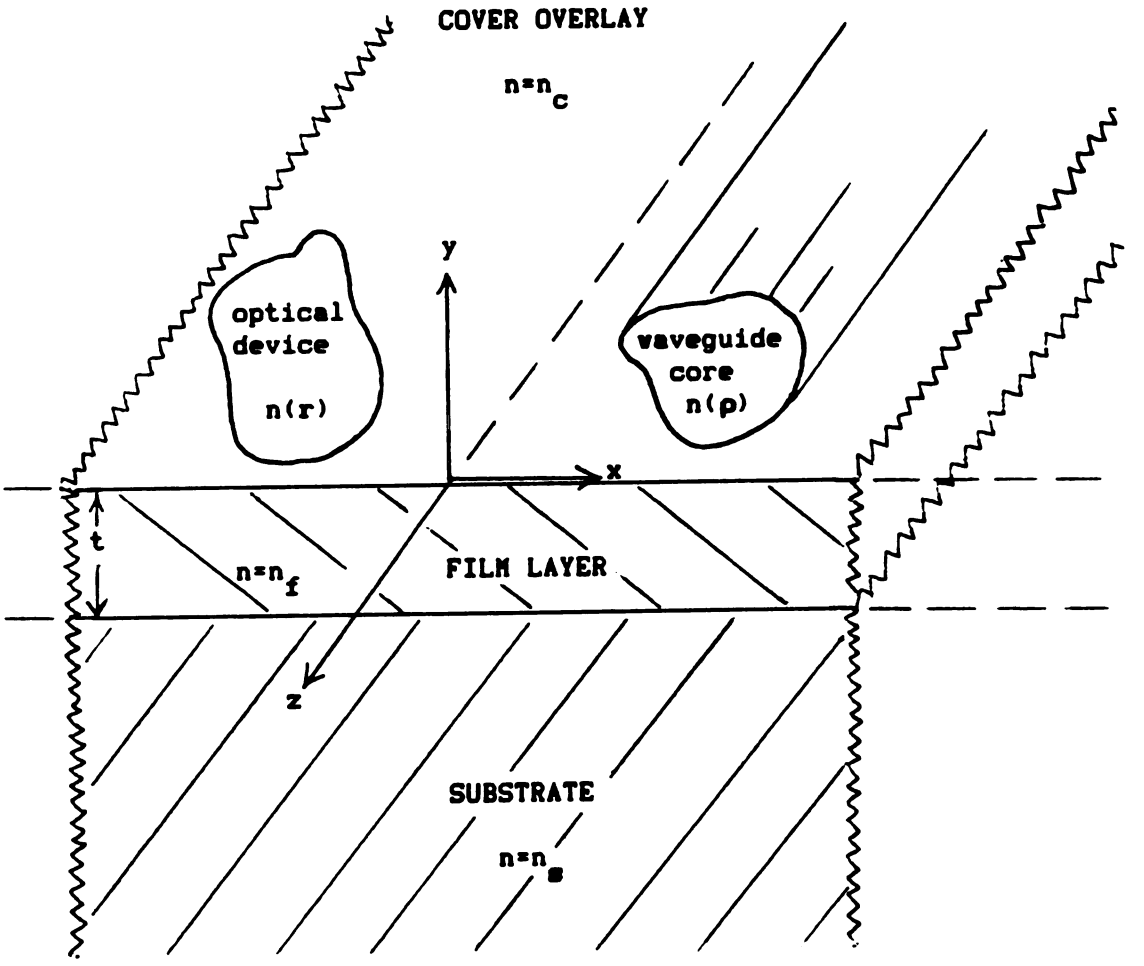

Figure 1. A typical optical circuit.

used by Chang and Harrington [7] and is based on field equivalence principles at surfaces. Although conceptually exact, this method does not account for inhomogeneously-graded structures and fails to address the continuous spectrum.

This dissertation uses an integral-operator approach, based on the identification of equivalent polarization currents, which circumvents the inadequacies of the aforementioned methods. This formulation was developed by Johnson and Nyquist [8] and advanced by Bagby [9] and provides a conceptually exact description of the electric field within an electrically heterogeneous region of arbitrary shape embedded in an integrated surround. All waveguiding phenomena are unified by this description, thus furnishing a powerful model.

The text is divided into seven chapters. In Chapter two, a Green's function for the tri-layered background is developed. Subtleties in the appropriate electric dyadic Green's function for this structure are thoroughly discussed. This dyad is used in Chapter three to construct the integral equation which describes the electric field. A transform-domain version of this integral equation, suitable for the study of longitudinally-uniform waveguides, is developed and forms the basis for all subsequent analyses. In Chapter four, the propagation-mode spectrum of these guides is identified. A discrete spectrum is found to be associated with surface waves, while superposition of the continuous spectrum yields the radiation field. A specialized integral equation, appropriate for the study of waveguides operating at asymptotically low frequency, is developed in Chapter five. Application of this equation to the asymmetric slab [10] and the circular fiber [11] provide asymptotic expressions which are shown to concur with [10] and [11].

An

tr

ci

sl

so

pr

Fi

fa

in

en

as

Und

sim

An iterative scheme is devised in Chapter six to approximate those spectral components of the continuous spectrum having high spatial frequencies. First iterative approximations to the graded-index asymmetric slab and the circular fiber were made. Comparisons to exact well known solutions are given. Finally, conclusions and recommendations are provided in Chapter seven.

Some of the notation which is used liberally should be clarified. First, vector quantities appear bold faced. Similarly, dyads are bold faced and are overstruck with a double bar. Unless stated otherwise, integrals with no specific limits are to imply an integration over the entire domain. Finally, throughout this dissertation the following assumptions are effected:

(1) All media are linear and isotropic;

(2) All of space is magnetically homogeneous such that the magnetic-induction field **B** is related to the magnetic field **H** by the constitutive equation $\mathbf{B} = \mu\mathbf{H}$.

(3) Electrically heterogeneous regions are characterized by permittivity $\varepsilon(r)$ and conductivity $\sigma(r)$ such that the electric displacement **D** and conduction current density $\mathbf{J}^c$ are related to the electric field by the constitutive relations $\mathbf{D} = \varepsilon\mathbf{E}$. and $\mathbf{J}^c = \sigma\mathbf{E}$ respectively.

(4) The time dependence is harmonic ($e^{j\omega t}$) and is suppressed.

Under these assumptions, Maxwell's equations in M-K-S units are greatly simplified and may be written as:

$$\nabla \cdot \epsilon^* \mathbf{E} = \rho \qquad \text{...Gauss' law} \tag{1a}$$

$$\nabla \times \mathbf{E} = -j\omega\mu\mathbf{H} \qquad \text{...Faraday's law} \tag{1b}$$

$$\nabla \times \mathbf{H} = \mathbf{J} + j\omega\epsilon^* \mathbf{E} \qquad \text{...Amperes' law} \tag{1c}$$

$$\nabla \cdot \mathbf{H} = 0 \qquad \text{...Absence of magnetic monopoles} \tag{1d}$$

where $\epsilon^* = \epsilon + \sigma/j\omega$ is the complex permittivity. The complex permittivity may be written as $\epsilon^*(r) = \epsilon_0 n^2(r)$ where n is the complex refractive index and ϵ_0 is the vacuum permittivity.

CHAPTER TWO

ELECTROMAGNETICS OF LAYERED DIELECTRICS

2.1 INTRODUCTION

In this chapter, the electromagnetics of layered dielectric structures is investigated. Description of the fields in a layered environment may be furnished by integrating the inner product of an appropriate Green's dyad with the electric source density maintaining the fields. Knowledge of this dyad is of particular importance since it is used throughout this dissertation as the kernel in the integral equation for the electric field in integrated optical waveguides.

Analysis of electromagnetic fields in a layered environment was first made by Sommerfeld [12] in 1909. Fields produced by electric dipoles oriented normal or tangential to an air-earth interface were considered. Integral-transform techniques were used to obtain integral representations for these fields. These integral expressions were of generic form and have since been categorized as Sommerfeld integrals. Sommerfeld integrals appear in the formulation of fields in layered media for more complicated situations.

Attention is focused on the tri-layered structure depicted in Figure 2. A film layer of thickness t and refractive index n_f is deposited over a substrate region ($y < -t$) which is characterized by index of refraction n_s. The region ($y > 0$) is the cover with refractive index n_c. All dielectrics are assumed to possess limitingly small dissipation with $Re\{n_f\} > Re\{n_s\} > Re\{n_c\}$, where $Re\{\ \}$ designates the real part of the

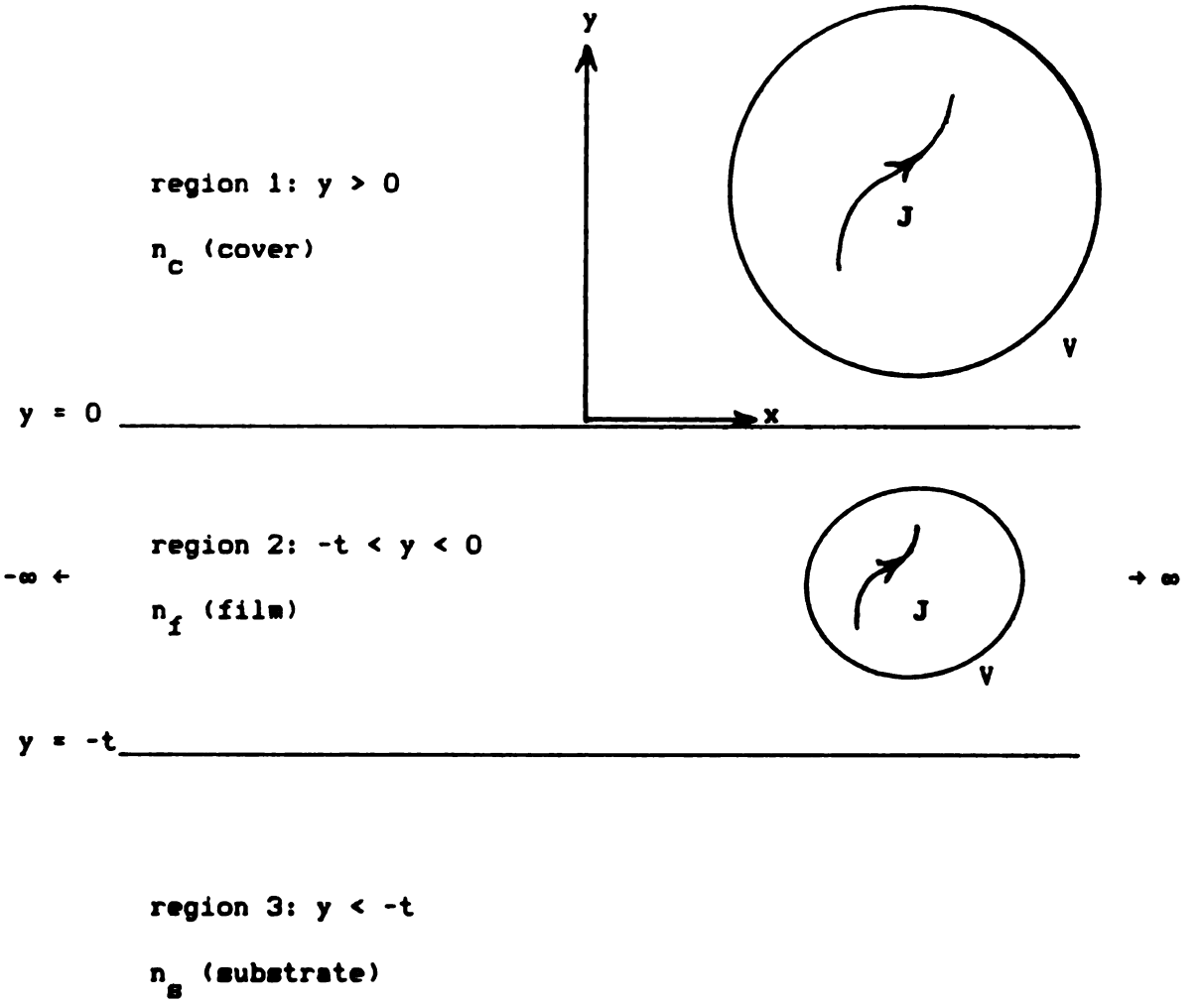

Figure 2. Tri-layered structure used as the background environment for integrated optical and electronic circuits.

quan

tain

havi

atic

of

uitr

die

grou

int

lay

pro

den

ren

are

dep

ele

int

J,

int

the

"pr

Pol

quantity within the braces. Immersed electric current density J maintains electromagnetic fields in all three regions.

Although the ensuing analysis may be generalized for a structure having any number of dielectric layers with embedded currents, the situation in Figure 2 provides a useful model for the background environment of practical electronic, millimeter-wave and optical integrated circuits. Several examples of these structures are shown in Figure 3. A dielectric substrate is used for integrated optics, while a conducting ground plane replaces the substrate for millimeter-wave and electronic integrated circuits.

In the next section, the electric Hertzian potential Π for the trilayered structure is expressed as a superposition integral of the inner product of the appropriate Green's dyad $\bar{\bar{G}}$ with the impressed current density J. Green's dyads are quantified for situations in which currents are embedded exclusively in either the cover or the film region.

In section 3, two equivalent representations of the electric field are given. A spectral representation is used to identify a natural depolarizing dyad $\bar{\bar{L}}$ which is relevant to the Green's dyad $\bar{\bar{G}}^e$ for the electric field. Finally, the electric field is expressed as a volume integration of the inner product of $\bar{\bar{G}}^e$ with the electric current source J, modified by a correction term in which $\bar{\bar{L}}$ appears. The volume of integration extends over the support of the current density but excludes the singularity point of $\bar{\bar{G}}^e$. The excluding region is identified as the "principal volume" which corresponds to the preferred choice of the depolarizing dyad.

n_c(c

n_f(f

////
conc

n_c(c

n_f(f

n_a(a

Figu

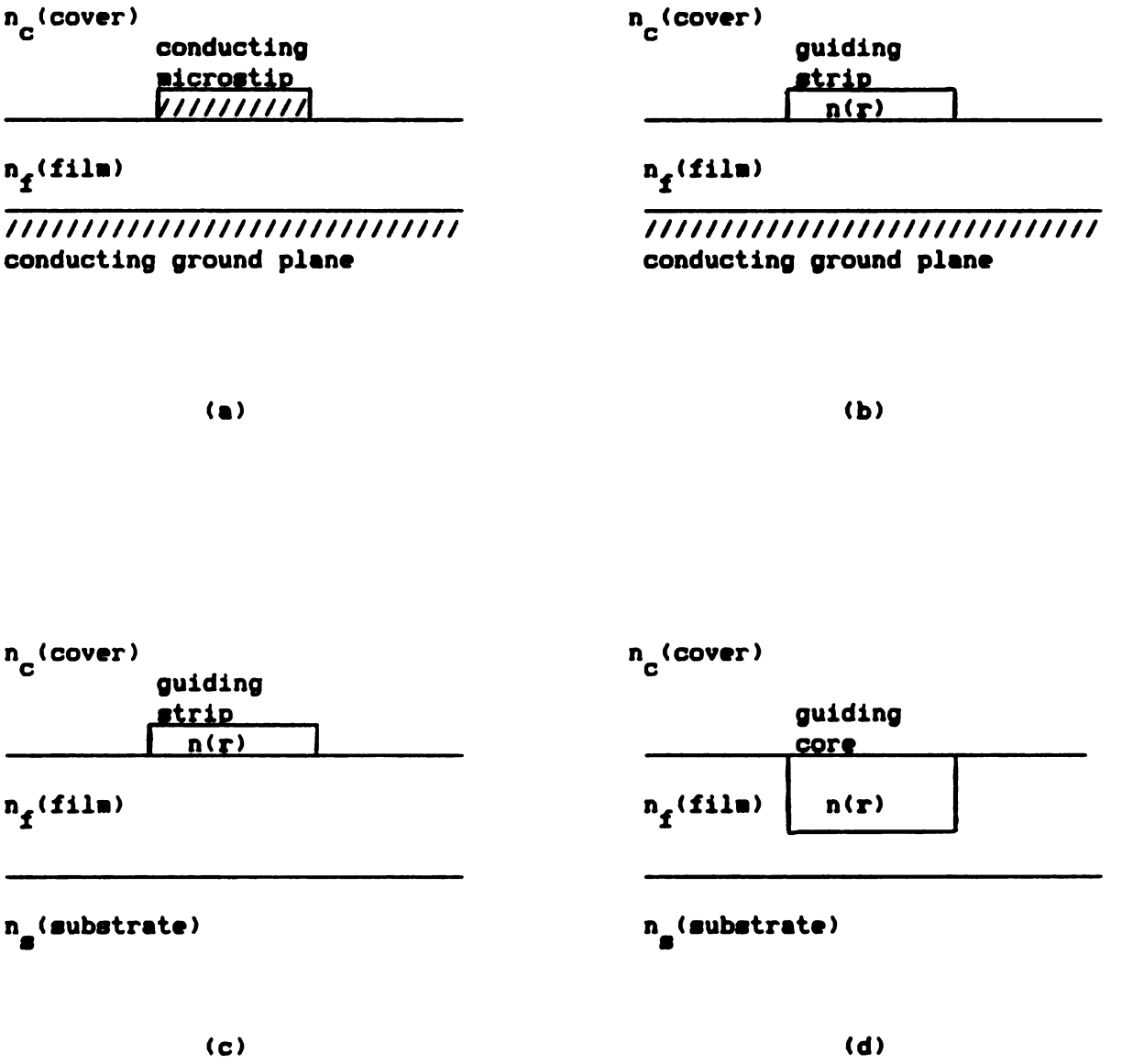

Figure 3. Examples of practical optical, millimeter-wave, and electronic integrated circuits. (a) Micro-strip waveguide. (b) Millimeter-wave dielectric strip waveguide. (c) Optical dielectric strip waveguide. (d) Optical dielectric channel waveguide.

2.2 HERTZIAN POTENTIAL GREEN'S DYAD

For the reader who is unfamiliar with the definition of the Hertzian potential, a review is provided in Appendix A. The relationship of the potential to the electric field, along with the Helmholtz equation which the potential satisfies, are given.

A general development of the Hertzian potential Green's dyad $\bar{\bar{G}}$ for layered dielectrics has been discussed by Bagby and Nyquist [13]. Based on the classical development of Sommerfeld [14], the Hertzian potential dyadic Green's function was shown to have scalar components represented by two-dimensional spectral integrals. In the subsequent development, the analysis in [13] is altered slightly so that identification of a natural depolarizing dyad $\bar{\bar{L}}$, corresponding to the Green's dyad $\bar{\bar{G}}^{e}$ for the electric field, may be made.

Consider the situations shown in Figures 4(a) and 4(b). Electric current density J, immersed in the ith region (i=c(f), for cover(film)) of Figure 4a(b), produces Hertzian potentials in each region of the trilayered structure. The Hertzian potential subject to the Lorentz gauge satisfies the Helmholtz equation

$$(\nabla^2 + k_\ell^2)\Pi_\ell = -J/j\omega\epsilon_i \qquad (1)$$

in each region (ℓ=s,f,c for substrate, film, cover). Note that in (1), $J = 0$ for $\ell \neq i$. Formal operation on (1) with the two-dimensional Fourier transform

$$F\{\cdot\} = \iint \{\cdot\}\, e^{-j\lambda\cdot r}\, dxdz$$

where $\lambda = \hat{x}\xi + \hat{z}\zeta$, reduces equation (1) to the ordinary differential equation

$$(\partial^2/\partial y^2 - p_\ell^2)\pi_\ell(\lambda;y) = -j(\lambda;y)/j\omega\epsilon_i \qquad (2)$$

y = 0

-∞ ←

y = -

y =

-∞

y

Fi

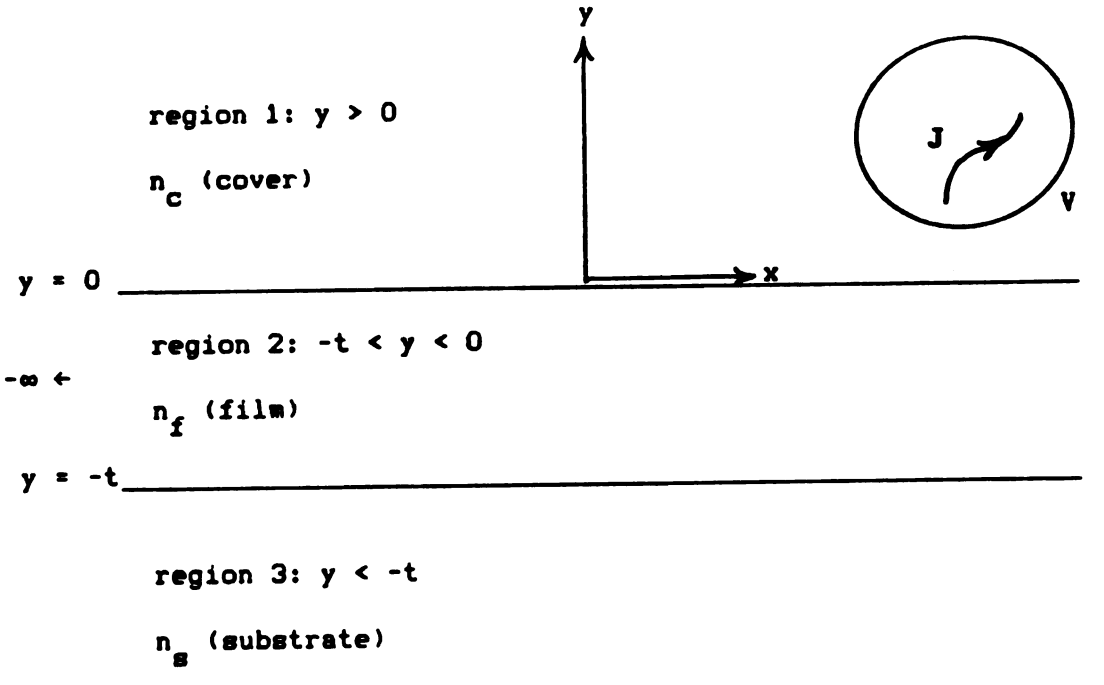

(a)

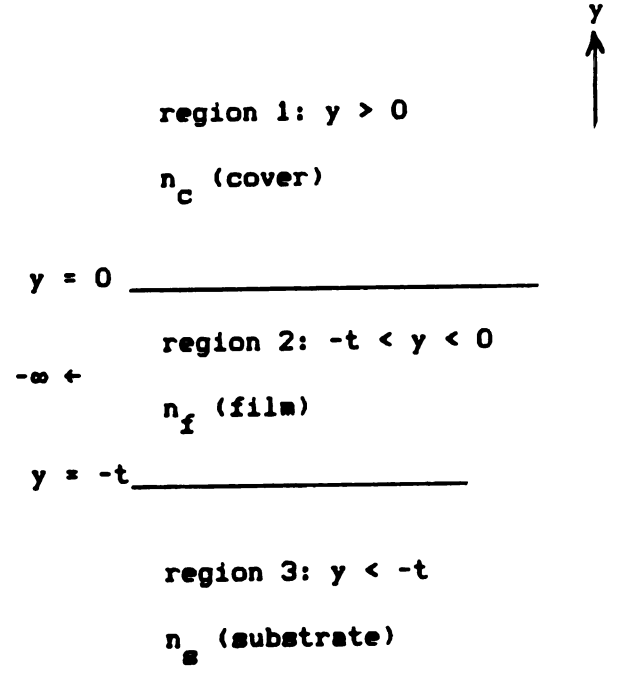

(3)

Figure 4. Tri-layer cover:

essed as a spectral inte-

ibed through the reflected dyad

itten as

y =

-∞ <

y =

y

-∞

y

Fig

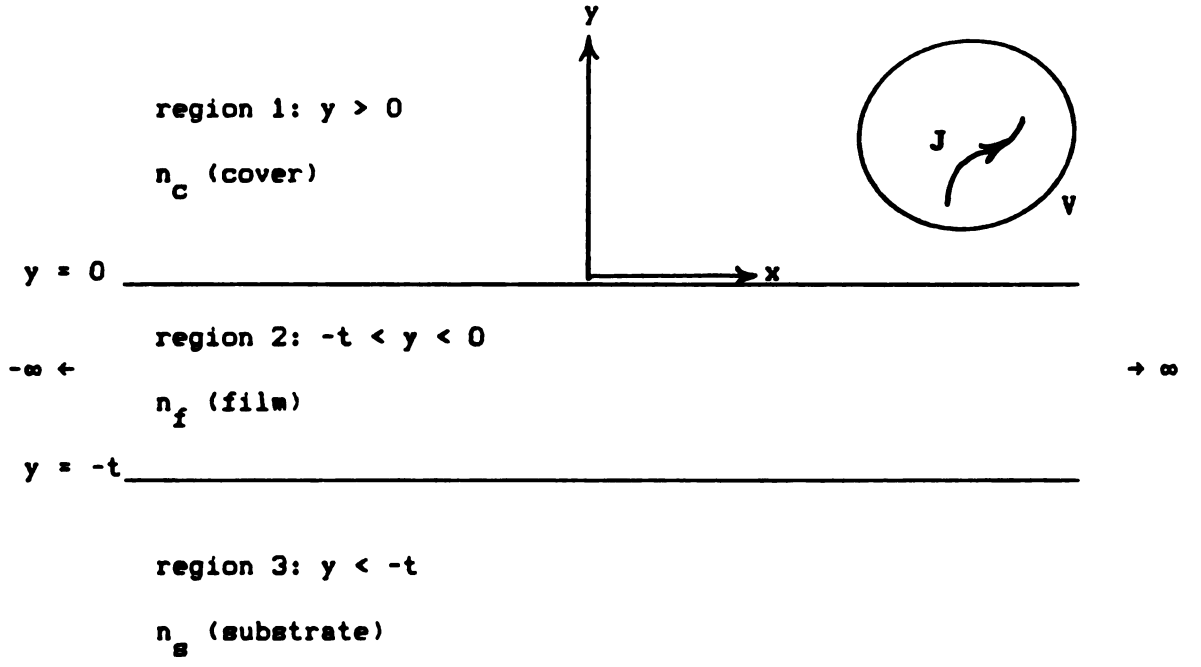

(a)

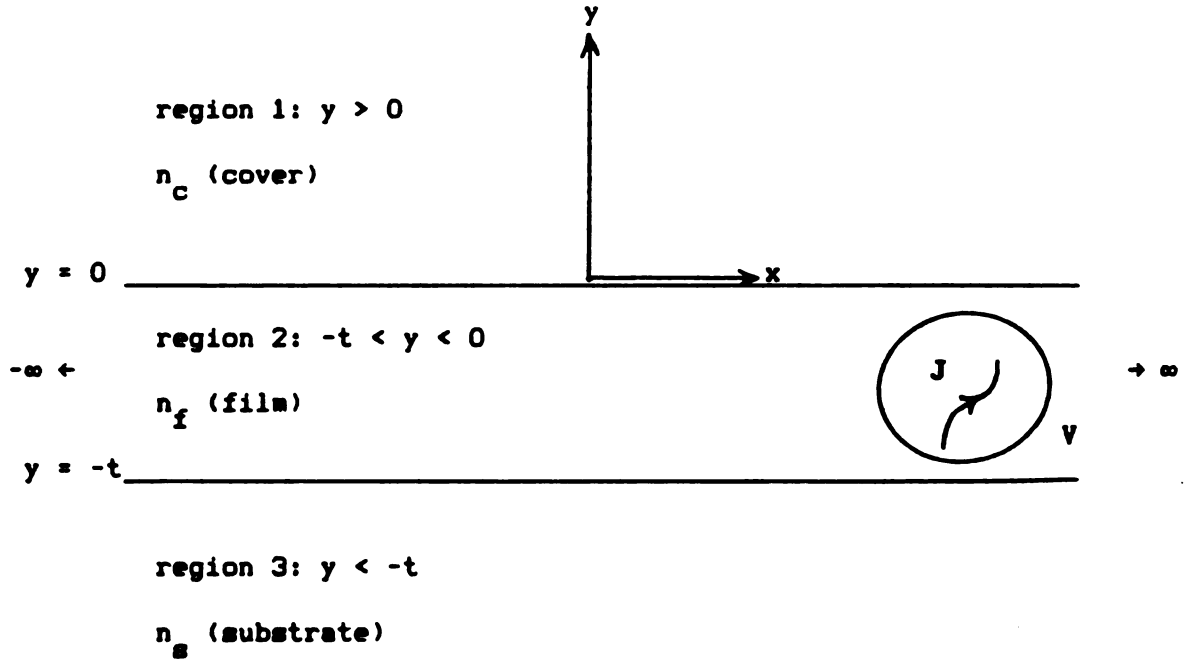

(b)

Figure 4. Tri-layered structure with (a) sources exclusively in the cover: (b) sources exclusively in the film.

where $\pi_\ell = F(\Pi_\ell)$, $j = F(J)$, and $p_\ell^2 = \xi^2 + \zeta^2 - k_\ell^2$. Solution of (2) is elementary, and may be written as a sum of particular and complementary solutions. Physically, the particular solution represents the primary wave which radiates in the hypothetical unbounded region of space, while the complementary solution represents the reflected wave maintained by the surface polarization current at the interfaces of dielectric discontinuity. This decomposition for the transform-domain potentials is

$$\pi_\ell(\lambda;y) = \delta_{i\ell}\left\{\int_V g^p(\lambda;y,r')\,\frac{J(r')}{j\omega\epsilon_i}\,dV'\right\} + W_\ell^+(\lambda)\,e^{p_\ell y} + W_\ell^-(\lambda)\,e^{-p_\ell y}$$

where $g^p(\lambda;y,r') = e^{-j\lambda\cdot r'}\,e^{-p_i|y-y'|}/2p_i$ and $\delta_{i\ell}$ is a Kronecker delta. The coefficients $W_\ell^\pm$ are determined by satisfying the appropriate boundary conditions [13] across the dielectric interfaces and as $y\to\pm\infty$. These boundary conditions and their implementation are given in Appendix B for currents immersed exclusively in the film. The result for currents in the cover is discussed in Section 2.2.2. Solution to the problem with sources in the substrate may be obtained from the solution to the problem with sources in the cover by interchanging n_s with n_c and making the coordinate transformation $y = -t - y$.

Inversion of the transform-domain potentials may be performed and yields the solution to (1) with the potential in the ith region given by

$$\Pi_i(r) = \frac{1}{(2\pi)^2}\iint e^{j\lambda\cdot r}\left\{\int_V g^p(\lambda;y,r')\,\frac{J(r')}{j\omega\epsilon_i}\,dV'\right\}d\xi d\zeta \qquad (3)$$

$$+ \int_V \bar{\bar{G}}^r(r|r')\cdot\frac{J(r')}{j\omega\epsilon_i}\,dV'.$$

The principal portion of potential Π^p is expressed as a spectral integral and the reflected part Π^r is described through the reflected dyad $\bar{\bar{G}}^r$. The reflected dyad may be written as

wher

diel

nent

curr

of $\bar{\bar{G}}$

late

2.2.

more

[15,

a pr

The

inte

this

p. 4

theo

inte

wher

$$\bar{\bar{G}}^r(r|r') = \hat{x}G_t^r\hat{x} + \hat{y}\left(\frac{\partial G_c^r}{\partial x}\hat{x} + G_n^r\hat{y} + \frac{\partial G_c^r}{\partial z}\hat{z}\right) + \hat{z}G_t^r\hat{z}$$

where G_t^r (G_n^r) yields components of potential tangential (normal) to the dielectric interface maintained by tangential (normal) current components. G_c^r accounts for the coupling between tangential components of current with the normal component of potential. The scalar components of $\bar{\bar{G}}^r$ have spectral integral representations which are elaborated in later sections.

2.2.1 PRIMARY GREEN'S DYAD

The principal part of the Hertzian potential in (3) may assume a more familiar form by use of Fubini's theorem for improper integrals [15, p.473]. Although the integrand of the spectral integral in (3) is a proper volume integral, the principal part of (3) may be written

$$\Pi^p(r) = \frac{1}{(2\pi)^2}\iint e^{j\lambda\cdot r}\lim_{v\to 0}\left\{\int_{V-v} g^p(\lambda;y,r')\frac{J(r')}{j\omega\epsilon_i}dV'\right\}d\xi d\zeta \quad (4a)$$

$$= \frac{1}{(2\pi)^2}\lim_{v\to 0}\iint e^{j\lambda\cdot r}\left\{\int_{V-v} g^p(\lambda;y,r')\frac{J(r')}{j\omega\epsilon_i}dV'\right\}d\xi d\zeta. \quad (4b)$$

The volume v is any volume which excludes the singular point r'=r. The interchange of the limit with the spectral integral is justified since this integral converges uniformly [15, p.473]. Use of Abel's test [15, p.472] for uniform convergence of improper integrals along with Fubini's theorem for improper integrals allows the spatial integration to be interchanged with the spectral integration. Therefore, (4b) becomes

$$\Pi^p(r) = \lim_{v\to 0}\int_{V-v}\bar{\bar{G}}^p(r|r')\cdot\frac{J(r')}{j\omega\epsilon_i}dV'$$

where the principal dyad $\bar{\bar{G}}^p$ is given by $\bar{\bar{G}}^p = \bar{\bar{I}}G^p$. $\bar{\bar{I}}$ is a unit dyad and

the pri

An alte

transfo

loving

where

G^p

where J

going f

J_0 foun

may be

ticular

= t_m.

The for

tegrate

the principal Green's function G^p is given by

$$G^p(r|r') = \frac{1}{(2\pi)^2} \iint \frac{e^{-p_i|y-y'|}}{2p_i} e^{j\lambda\cdot(r-r')}\, d\xi d\zeta. \qquad (5)$$

An alternative integral representation of G^p can be obtained from (5) by transforming the double integral to polar coordinates. Making the following substitutions

$$\xi = \lambda \cos\theta$$

$$\zeta = \lambda \sin\theta$$

$$p_i = (\lambda^2 - k_i^2)^{1/2}$$

$$d\xi d\zeta = \lambda\, d\theta d\lambda$$

$$x - x' = |\tau-\tau'| \cos\varphi$$

$$z - z' = |\tau-\tau'| \sin\varphi$$

where $|\tau-\tau'| = [(x-x')^2 + (z-z')^2]^{1/2}$, equation (5) becomes

$$G^p(r|r') = \frac{1}{(2\pi)^2} \int_0^\infty \frac{e^{-p_i|y-y'|}}{2p_i} \left\{ \int_0^{2\pi} e^{j\lambda|\tau-\tau'|\cos(\theta-\varphi)}\, d\theta \right\} \lambda d\lambda \qquad (6a)$$

$$= \frac{1}{2\pi} \int_0^\infty \frac{e^{-p_i|y-y'|}}{2p_i} J_0(\lambda[(x-x')^2+(z-z')^2]^{1/2})\, \lambda d\lambda. \qquad (6b)$$

where J_0 is the zeroeth order Bessel function of the first kind. In going from (6a) to (6b), use was made of an integral representation of J_0 found in [16, p.360]. Evaluation of the integrals in (5) and (6b) may be performed, but need not be when it is realized that Π^p is a particular solution to (1) with conditions on its asymptotic behavior at $y = \pm\infty$. Whence, the familiar free space Green's function obtains as

$$G^p(r|r') = \frac{e^{-jk_i|r-r'|}}{4\pi|r-r'|}. \qquad (7)$$

The form of (7) is not a convenient representation of $\bar{\bar{G}}^p$ for use in integrated optics. For practical applications, the spectral

repre

tenti

where

2.2.2

situ

the

the

disc

sugg

phas

wher

coup

ulat

due

line

representations (5) or (6b) are recommended. Finally, the Hertzian potential in (3) may assume the standard form

$$\Pi_i(r) = \lim_{v \to 0} \int_{V-v} \bar{\bar{G}}(r|r') \cdot \frac{J(r')}{j\omega\epsilon_i} \, dV'$$

where $\bar{\bar{G}}$ is given by $\bar{\bar{G}} = \bar{\bar{G}}^p + \bar{\bar{G}}^r$.

2.2.2 REFLECTED GREEN'S DYAD FOR SOURCES IN THE COVER

In this section, the reflected Green's dyad $\bar{\bar{G}}^r$ is detailed for the situation shown in Figure 5. Source and field points are situated in the cover region. The reflected wave, which is illustrated, represents the grand sum of all waves reflected from the interfaces of dielectric discontinuity which travel in the positive y direction. Intuitive appeal suggests that the y dependent part of the reflected wave should have a phase of $y + y'$. In fact, the scalar components of $\bar{\bar{G}}^r$ are given as

$$\begin{Bmatrix} G_t^r(r|r') \\ G_n^r(r|r') \\ G_c^r(r|r') \end{Bmatrix} = \iint \begin{Bmatrix} R_t(\lambda) \\ R_n(\lambda) \\ C(\lambda) \end{Bmatrix} \frac{e^{-p_c(y+y')}}{2(2\pi)^2 p_c} e^{j\lambda\cdot(r-r')} \, d^2\lambda$$

where $d^2\lambda = d\xi d\zeta$. The reflection coefficients R_t and R_n as well as the coupling coefficient C have been derived in [9, pp. 163-172] and are tabulated below.

Computation of the reflection and coupling coefficients is tedious due to their complicated dependence on environmental parameters. Outlined below is a simple procedure for obtaining these coefficients.

1. Calculate tangential reflection and transmission coefficients associated with the cover-film interface as

y = 0

-∞ ←

y =

Figu

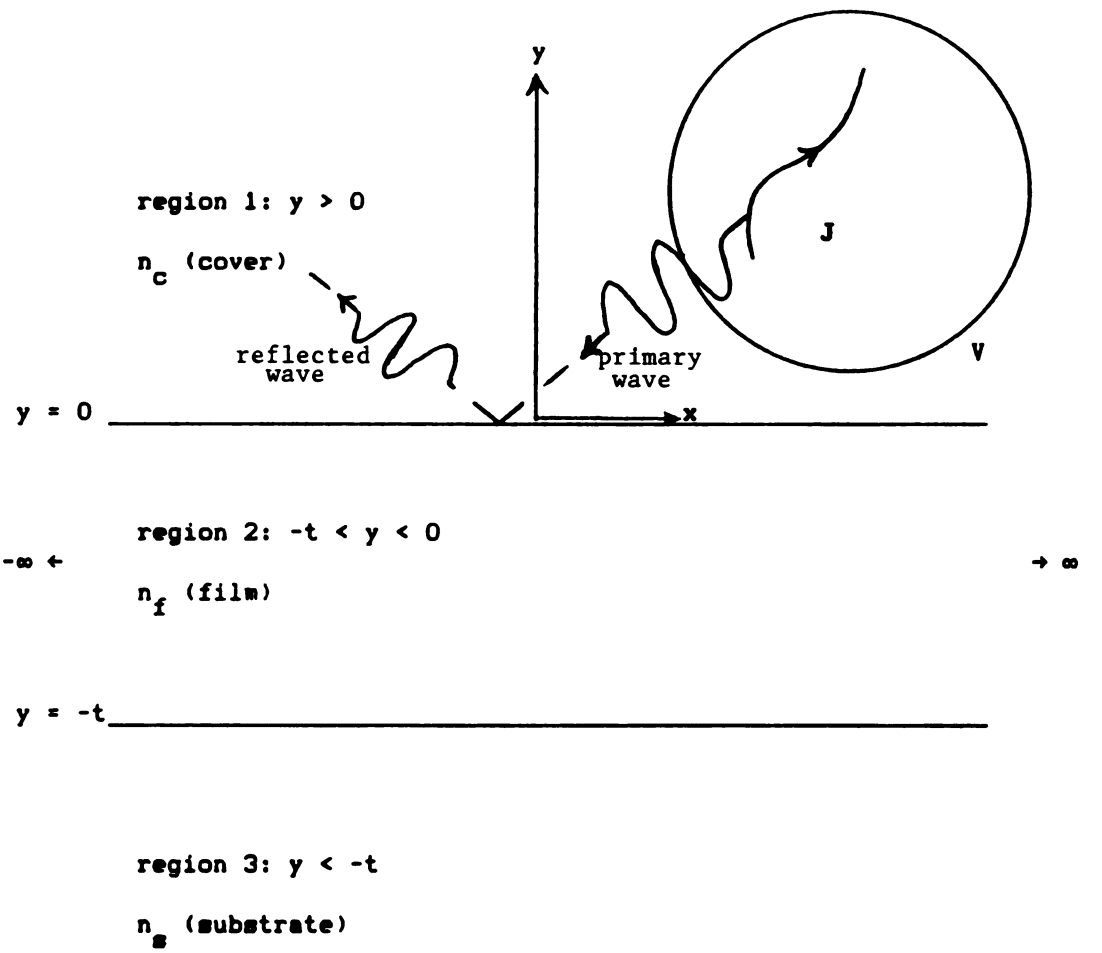

Figure 5. Tri-layered structure with currents immersed exclusively in the cover region.

$$R^t_{fc} = (p_c - p_f)/(p_c + p_f) \qquad R^t_{cf} = (p_f - p_c)/(p_c + p_f)$$
$$T^t_{fc} = 2N^2_{fc}p_f/(p_c + p_f) \qquad T^t_{cf} = 2N^{-2}_{fc}p_c/(p_c + p_f)$$

where $N_{fc} = (n_f/n_c)$.

2. Calculate tangential reflection and transmission coefficients associated with the film-substrate interface as

$$R^t_{sf} = (p_f - p_s)/(p_f + p_s) \qquad T^t_{fs} = 2N^{-2}_{sf}p_f/(p_f + p_s)$$

where $N_{sf} = (n_s/n_f)$.

3. Calculate the normal reflection and transmission coefficients associated with the cover-film interface as

$$R^n_{fc} = (N^2_{fc}p_c - p_f)/(N^2_{fc}p_c + p_f) \qquad T^n_{cf} = 2p_c/(N^2_{fc}p_c + p_f)$$
$$T^n_{fc} = 2N^2_{fc}p_f/(N^2_{fc}p_c + p_f).$$

4. Calculate the normal reflection and transmission coefficients associated with the film-substrate interface as

$$R^n_{sf} = (N^2_{sf}p_f - p_s)/(N^2_{sf}p_f + p_s) \qquad T^n_{fs} = 2p_f/(N^2_{sf}p_f + p_s).$$

5. Calculate intermediate expressions

$$D^t = 1 - R^t_{cf}R^t_{sf}e^{-2p_f t}$$
$$D^n = 1 + R^n_{fc}R^n_{sf}e^{-2p_f t}.$$

6. Calculate the intermediate coupling coefficients as

$$C_1 = N^2_{fc}(N^2_{fc} - 1)T^t_{cf}(1 + R^t_{sf}e^{-2p_f t})/D^t(N^2_{fc}p_c + p_f)$$
$$C_2 = N^2_{sf}(N^2_{sf} - 1)T^t_{cf}T^t_{fs}/D^t(N^2_{sf}p_f + p_s).$$

7. Finally, the reflection and coupling coefficients are evaluated as

2.2.

J, i

regi

dete

poin

miss

adja

towa

tion

in

obs

is

pat

Ψ_2(

Sca

$$R_t = R_{fc}^t + T_{cf}^t T_{fc}^t R_{sf}^t e^{-2p_f t}/D^t = (R_{fc}^t + R_{sf}^t e^{-2p_f t})/D^t$$

$$R_n = R_{fc}^n + T_{cf}^n T_{fc}^n R_{sf}^n e^{-2p_f t}/D^n = (R_{fc}^n + R_{sf}^n e^{-2p_f t})/D^n$$

$$C = C_1 + T_{fc}^n (R_{sf}^n N_{fc}^{-2} C_1 + C_2) e^{-2p_f t}/D^n$$
$$= \left[C_1(1 + R_{sf}^n e^{-2p_f t}) + C_2 T_{fc}^n e^{-2p_f t}\right]/D^n$$

2.2.3 REFLECTED GREEN'S DYAD FOR SOURCES IN THE FILM

Consider the situation shown in Figure 6. Electric current density J, immersed in the film region, maintains electromagnetic fields in each region. Again, the y dependence of the reflected wave may be correctly determined by use of a physical picture. As seen in Figure 6, a source point at y' produces a primary disturbance in the film region. Transmission and reflection of the primary wave occur at the interfaces of adjacent regions. A wave which is reflected from one interface travels toward the other interface where it experiences transmission and reflection. Figure 7 shows that there are four fundamentally different ways in which a wave from a source at y' may arrive, via reflection, at the observation point at y. The y dependence of the reflected Green's dyad is comprised of four terms with phases associated with these distinct paths. Using Figure 7, the phase path lengths are $\varphi_1(y,y',t) = -y-y'$, $\varphi_2(y,y',t) = y+y'+2t$, $\varphi_3(y,y',t) = y-y'+2t$, and $\varphi_4(y,y',t) = -y+y'+2t$. Scalar components of $\bar{\bar{G}}^r$ may be written as

$$\begin{Bmatrix} G_t^r(r|r') \\ G_n^r(r|r') \\ G_c^r(r|r') \end{Bmatrix} = \iint \sum_{i=1}^{4} \begin{Bmatrix} R_i^t(\lambda) \\ R_i^n(\lambda) \\ C_i(\lambda) \end{Bmatrix} \frac{e^{-p_f(\varphi_i(y,y',t))}}{2(2\pi)^2 p_f} e^{j\lambda\cdot(r-r')} d^2\lambda$$

re

n_c

y = 0

re

$-\infty \leftarrow$

n_f

y = -

re

n_s

Figure

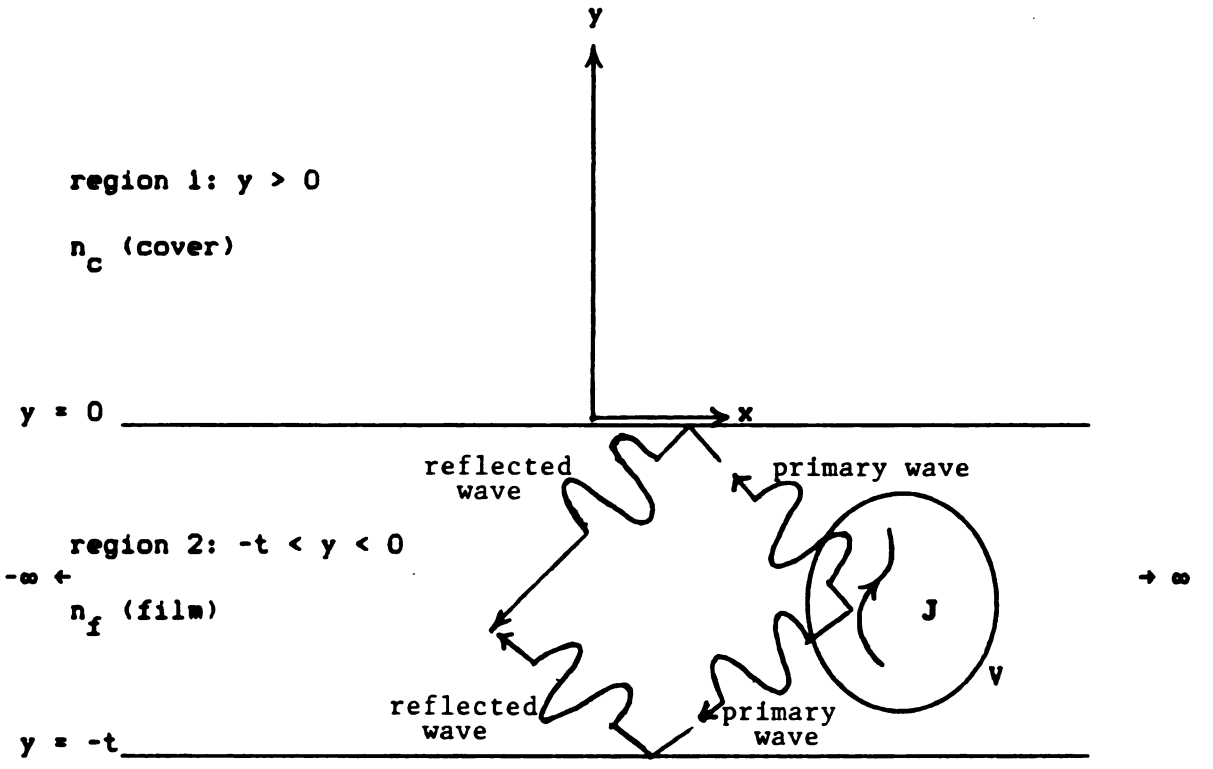

Figure 6. Tri-layered structure with currents immersed exclusively in the film region.

y = 0

-∞ ←

y = -t

y = 0

-∞ ←

y = -

y = 0

-∞ ←

y = .

y = (

-∞ ←

y =

Figur

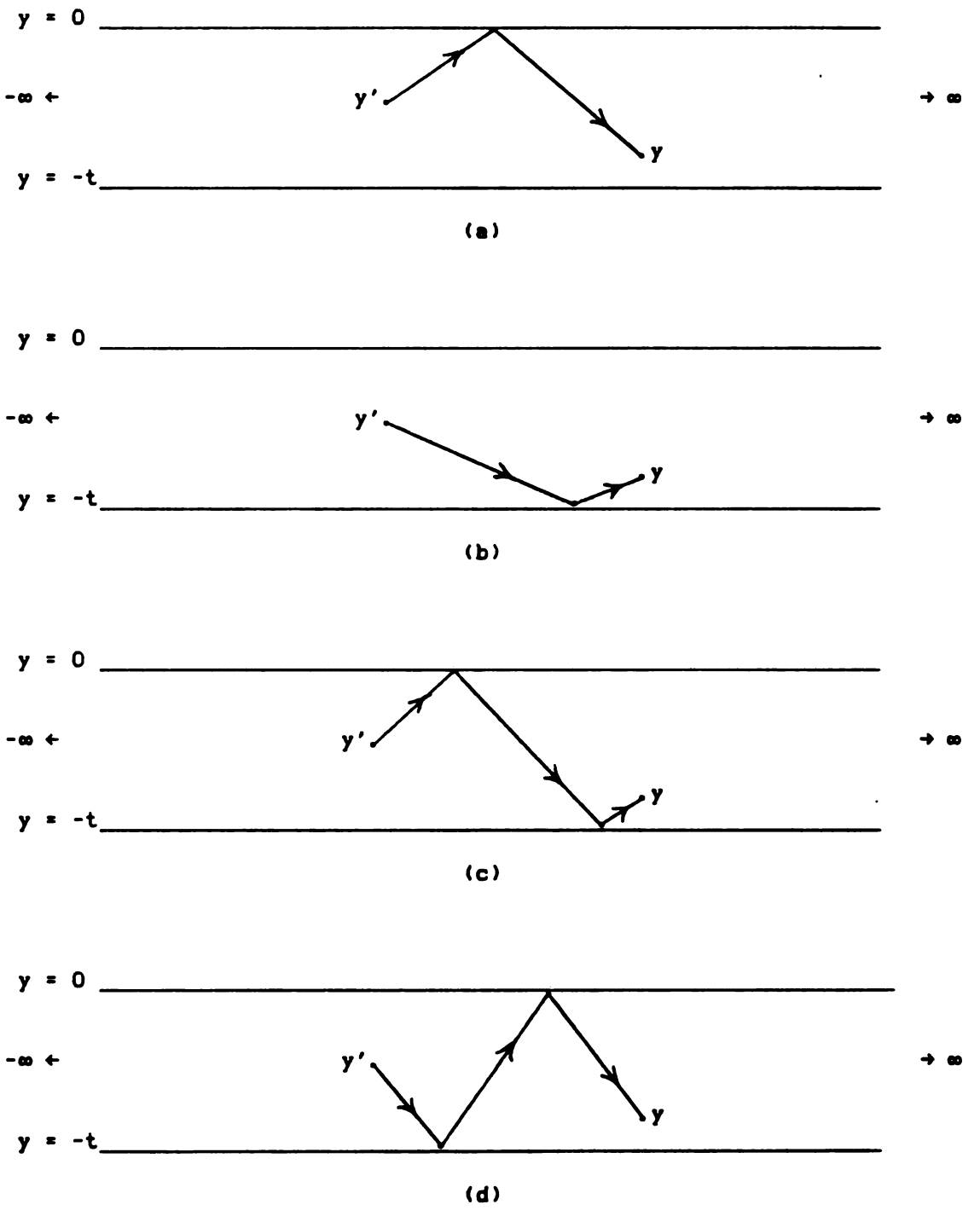

Figure 7. Four paths with different y-dependent phases. (a) -y-y'. (b) y+y'+2t. (c) y-y'+2t. (d) -y+y'+2t

whe

2.3

ere

pot

evi

ti

2.

re

a

p

d

t

g

where R_i^t, R_i^n, and C_i are derived and detailed in Appendix B.

2.3 ELECTRIC DYADIC GREEN'S FUNCTION

In this section, calculation of the electric field in the tri-layered environment is made. The electric field is related to the Hertzian potential as given in equation (A.5) by $\mathbf{E} = (k^2 + \nabla\nabla\cdot)\boldsymbol{\Pi}$. Obviously, evaluation of derivatives of $\boldsymbol{\Pi}$ are required to calculate $\mathbf{E}$. The evaluation of these derivatives demands the use of strict mathematical rigor.

2.3.1 DERIVATIVES OF THE HERTZIAN POTENTIAL

Each of the reflection and coupling coefficients appearing in the reflected dyad is a bounded function of λ as $|\lambda| \to \infty$. Pole singularities are present in the complex λ-plane and are associated with surface-wave phenomena. Under the assumption that all media have limitingly small dissipation, these surface wave poles are located off the real axis in the complex λ-plane. Due to the decaying exponential term in the integrand of the spectral integrals of the scalar components of $\bar{\bar{G}}^r$, these integrals converge uniformly and absolutely for all r in the domain over which they are integrated. Hence, derivatives of the reflected part Π^r of the Hertzian potential are obtained by formally differentiating under the volume integral. In fact, the second order derivatives of Π^r are given by

$$\frac{\partial^2 \Pi^r(\mathbf{r})}{\partial x_\alpha \partial x_\beta} = \int_V \frac{\partial^2 \bar{\bar{G}}^r(\mathbf{r}|\mathbf{r}')}{\partial x_\alpha \partial x_\beta} \cdot \frac{\mathbf{J}(\mathbf{r}')}{j\omega\epsilon_i}\, dV'.$$

Special attention is required in determining derivatives of the principal part of $\boldsymbol{\Pi}$.

The principal part Π^p of the Hertzian potential is represented by

the

C th

pact

by f

Spli

diff

$\nabla\nabla$

Tang

brac

deri

pria

the

$= \int$

$= \int$

whic

the

the spectral integral on the right side of (3). It is shown in Appendix C that under the assumption that J and $\nabla\cdot J$ are continuous and of compact support in V, derivatives up to second order of Π^p may be obtained by formally differentiating under the spectral integral. Therefore,

$$\nabla\nabla\cdot\Pi^p(r) = \frac{1}{(2\pi)^2}\iint \nabla\nabla\cdot\left\{ e^{j\lambda\cdot r}\left[\int_V g^p(\lambda;y,r')\,\frac{J(r')}{j\omega\epsilon_i}\,dV'\right]\right\} d^2\lambda.$$

Splitting the spatial integral into regions in which g^p is continuously differentiable yields

$$\nabla\nabla\cdot\Pi^p(r) = \frac{1}{(2\pi)^2}\left(\iint \nabla\nabla\cdot\left\{ e^{j\lambda\cdot r}\left[\int_{y'<y} g^p(\lambda;y,r')\,\frac{J(r')}{j\omega\epsilon_i}\,dV'\right]\right\} d^2\lambda \right.$$

$$\left. + \iint \nabla\nabla\cdot\left\{ e^{j\lambda\cdot r}\left[\int_{y'>y} g^p(\lambda;y,r')\,\frac{J(r')}{j\omega\epsilon_i}\,dV'\right]\right\} d^2\lambda \right).$$

Tangential derivatives (i.e. derivatives with respect to x and z) of the bracketed terms above operate only on $e^{j\lambda\cdot r}$. However, performing the derivatives with respect to y demands additional considerations. Appropriate use of Leibnitz's rule [15, pp.321-325] for differentiation under the integral sign reveals that

$$\frac{\partial}{\partial y}\left\{ \int_{y'<y} g^p(\lambda;y,r')\,\frac{J(r')}{j\omega\epsilon_i}\,dV' + \int_{y'>y} g^p(\lambda;y,r')\,\frac{J(r')}{j\omega\epsilon_i}\,dV'\right\}$$

$$= \int_{y'<y} \frac{\partial}{\partial y} g^p(\lambda;y,r')\,\frac{J(r')}{j\omega\epsilon_i}\,dV' + \int_{y'>y} \frac{\partial}{\partial y} g^p(\lambda;y,r')\,\frac{J(r')}{j\omega\epsilon_i}\,dV'$$

$$+ \iint e^{-j\lambda\cdot r'}\left\{\left[\frac{e^{-p_i(y-y')}}{2p_i} - \frac{e^{-p_i(y'-y)}}{2p_i}\right]\frac{J(r')}{j\omega\epsilon_i}\right\}\Big|_{y'=y} dx'dz'$$

$$= \int_{y'<y} \frac{\partial}{\partial y} g^p(\lambda;y,r')\,\frac{J(r')}{j\omega\epsilon_i}\,dV' + \int_{y'>y} \frac{\partial}{\partial y} g^p(\lambda;y,r')\,\frac{J(r')}{j\omega\epsilon_i}\,dV'$$

which is the result obtained by formally passing the derivative under the integral sign. However, performing a subsequent differentiation

with respect to y shows

$$\frac{\partial^2}{\partial y^2}\left\{\int_{y'<y} g^p(\lambda;y,r')\,\frac{J(r')}{j\omega\epsilon_i}\,dV' + \int_{y'>y} g^p(\lambda;y,r')\,\frac{J(r')}{j\omega\epsilon_i}\,dV'\right\}$$

$$= \int_{y'<y} \frac{\partial^2}{\partial y^2} g^p(\lambda;y,r')\,\frac{J(r')}{j\omega\epsilon_i}\,dV' + \int_{y'>y} \frac{\partial^2}{\partial y^2} g^p(\lambda;y,r')\,\frac{J(r')}{j\omega\epsilon_i}\,dV'$$

$$+ \iint e^{-j\lambda\cdot r'}\left\{\left[\frac{\partial}{\partial y}\frac{e^{-p_i(y-y')}}{2p_i} - \frac{\partial}{\partial y}\frac{e^{-p_i(y'-y)}}{2p_i}\right]\frac{J(r')}{j\omega\epsilon_i}\right\}\Big|_{y'=y} dx'dz'$$

$$= \int_{y'<y} \frac{\partial^2}{\partial y^2} g^p(\lambda;y,r')\,\frac{J(r')}{j\omega\epsilon_i}\,dV' + \int_{y'>y} \frac{\partial^2}{\partial y^2} g^p(\lambda;y,r')\,\frac{J(r')}{j\omega\epsilon_i}\,dV'$$

$$- \iint \frac{J(x',y,z')}{j\omega\epsilon_i}\,e^{-j\lambda\cdot r'}\,dx'dz'.$$

which is altered from the formal result by the presence of a correction term. Finally, evaluation of $\nabla\nabla\cdot\Pi^p$ yields

$$\nabla\nabla\cdot\Pi^p(r) = \iint\left[\int_V \bar{\bar{g}}(\lambda;r,r')\cdot\frac{J(r')}{j\omega\epsilon_i}\,dV'\right]d^2\lambda$$

$$- \frac{1}{(2\pi)^2}\iint\left[\iint \frac{\hat{y}\,J_y(x',y,z')}{j\omega\epsilon_i}\,e^{-j\lambda\cdot r'}dx'dz'\right]e^{j\lambda\cdot r}\,d^2\lambda$$

$$= \iint\left[\int_V \bar{\bar{g}}(\lambda;r,r')\cdot\frac{J(r')}{j\omega\epsilon_i}\,dV'\right]d^2\lambda - \bar{\bar{L}}\cdot J(r)/j\omega\epsilon_i \qquad (8)$$

where $\bar{\bar{L}} = \hat{y}\hat{y}$ and the dyad $\bar{\bar{g}}$ is given by the expression

$$\bar{\bar{g}}(\lambda;r,r') = \begin{cases} \nabla\nabla\,[e^{j\lambda\cdot(r-r')}\,e^{-p_i(y-y')}/8\pi^2 p_i], & y'<y \\ \nabla\nabla\,[e^{j\lambda\cdot(r-r')}\,e^{-p_i(y'-y)}/8\pi^2 p_i], & y'>y. \end{cases}$$

The term $\bar{\bar{L}}\cdot J$ was extracted from exploitation of the Fourier inversion theorem [17, p.315], and is found to correspond exactly with that exposed in [18] for a "pillbox" principal volume. The form of $\bar{\bar{g}}$ suggests

that the "slice" exclusion in Figure 8 might be a more natural principal volume pertaining to $\bar{\bar{L}}$. This assertion is verified below.

2.3.2 DEVELOPMENT OF THE PRINCIPAL DYAD

Using (8), the principal part of the electric field may be written as

$$\mathbf{E}^{p}(\mathbf{r}) = -j\omega\mu_0 \iint \left\{ \int_V \bar{\bar{g}}^{e}(\lambda;\mathbf{r},\mathbf{r}')\cdot\mathbf{J}(\mathbf{r}')\, dV' \right\} d^2\lambda - \bar{\bar{L}}\cdot\mathbf{J}(\mathbf{r})/j\omega\epsilon_i \qquad (9)$$

where the dyad $\bar{\bar{g}}^{e} = \bar{\bar{g}}/k_i^2 + (1/4\pi^2)\bar{\bar{I}}g^{p}e^{j\lambda\cdot\mathbf{r}}$.

Equation (9) is a useful expression for the principal part of the electric field due to the simple nature of the integrand appearing in the volume integral. However, (9) is not written in the standard form as a volume integration of the inner product of a Green's dyad with the electric current density. Since the depolarizing dyad $\bar{\bar{L}}$ has manifested itself naturally, a corresponding principal volume is sought.

In appendix C, it is shown that the spectral integral in (9) converges uniformly. Hence, proceeding analogously as in the development of the principal part of the Hertzian potential Green's dyad, (9) may be written

$$\mathbf{E}^{p}(\mathbf{r}) = -j\omega\mu_0 \iint \left\{ \lim_{v\to 0} \int_{V-v} \bar{\bar{g}}^{e}(\lambda;\mathbf{r},\mathbf{r}')\cdot\mathbf{J}(\mathbf{r}')\, dV' \right\} d^2\lambda - \bar{\bar{L}}\cdot\mathbf{J}(\mathbf{r})/j\omega\epsilon_i$$

$$= -j\omega\mu_0 \lim_{v\to 0} \iint \left\{ \int_{V-v} \bar{\bar{g}}^{e}(\lambda;\mathbf{r},\mathbf{r}')\cdot\mathbf{J}(\mathbf{r}')\, dV' \right\} d^2\lambda - \bar{\bar{L}}\cdot\mathbf{J}(\mathbf{r})/j\omega\epsilon_i$$

where v is any region excluding r. In order to exchange the order of integrations, uniform convergence of the spectral integral of $\bar{\bar{g}}^{e}$ is desired. Observing that the spectral integration of $\bar{\bar{g}}^{e}$ does not even converge unless $y' \neq y$, interchanging the order of integrations may be illegitimate. Hence, the choice of v is limited to volumes which exclude y. The form of $\bar{\bar{g}}^{e}$ suggests that the slice region is the

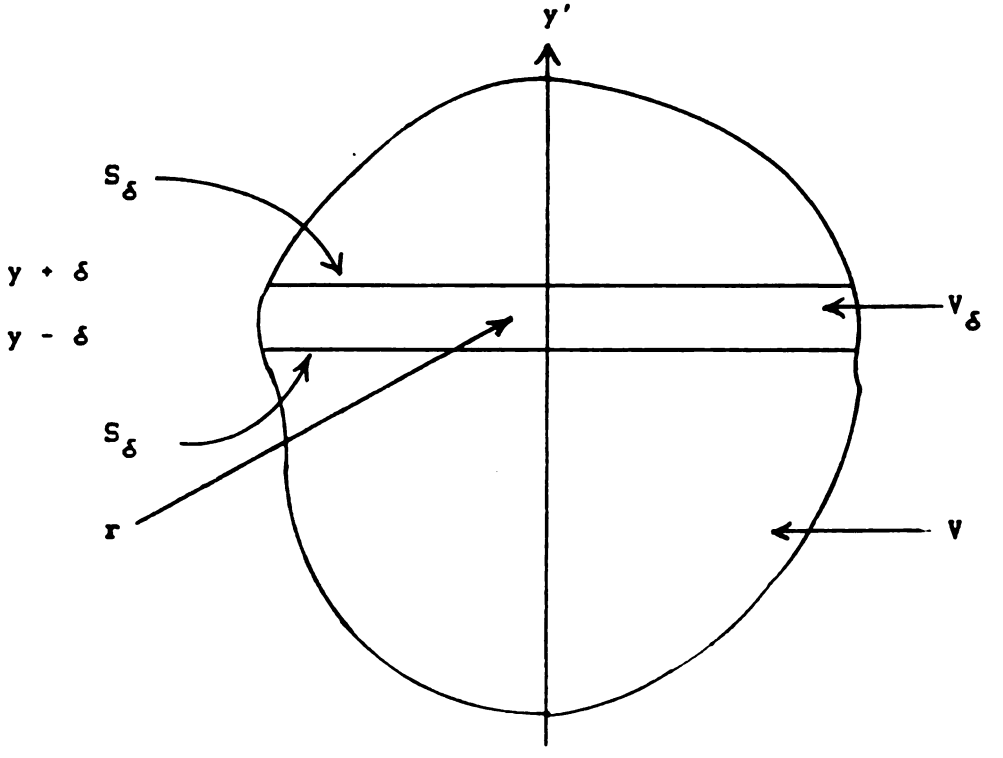

Figure 8. A "slice" principal volume excluding the singularity point r of the electric dyadic Green's function; closed surface S_δ is the boundary of the slice volume.

approp

slice,

gral t

princi

where

and $\bar{\bar{G}}$

$\bar{\bar{G}}$

Note

spect

to a

devel

2.3.3

funct

for a

dyadi

where

to co

(10).

appropriate choice for the principal volume. Choosing v to be the slice, Fubini's theorem for improper integrals allows the spatial integral to be interchanged with the spectral integral. Therefore, the principal part of the electric field may be written

$$\mathbf{E}^{p}(\mathbf{r}) = -j\omega\mu_0 \lim_{\delta\to 0} \int_{V-V_\delta} \bar{\bar{G}}^{e}(\mathbf{r}|\mathbf{r}')\cdot\mathbf{J}(\mathbf{r}')\, dV' - \bar{\bar{L}}\cdot\mathbf{J}(\mathbf{r})/j\omega\epsilon_i \qquad (10)$$

where V_δ is the slice in Figure 8 excluding the singularity of $\bar{\bar{G}}^{e}$ at r, and $\bar{\bar{G}}^{e}$ is given by

$$\bar{\bar{G}}^{e}(\mathbf{r}|\mathbf{r}') = \begin{cases} \iint (\bar{\bar{I}} + \nabla\nabla/k_i^2) \left[e^{j\lambda\cdot(\mathbf{r}-\mathbf{r}')} \dfrac{e^{-p_i(y-y')}}{2(2\pi)^2 p_i} \right] d^2\lambda, & y'<y \\ \iint (\bar{\bar{I}} + \nabla\nabla/k_i^2) \left[e^{j\lambda\cdot(\mathbf{r}-\mathbf{r}')} \dfrac{e^{-p_i(y'-y)}}{2(2\pi)^2 p_i} \right] d^2\lambda, & y'>y. \end{cases} \qquad (11)$$

Note that the differential operator in (11) may be passed outside of the spectral integration. In fact, the slice principal volume is equivalent to a pillbox when the differentiation is performed lastly. A classical development is used below to establish this equivalence.

2.3.3 EQUIVALENCE OF PRINCIPAL VOLUMES

Starting with the common representation for the free space Green's function $\psi(\mathbf{r}|\mathbf{r}') = e^{-jk_i|\mathbf{r}-\mathbf{r}'|}/4\pi|\mathbf{r}-\mathbf{r}'|$, it is shown in Appendix D that for a slice principal volume, the correction term $\mathbf{E}^{c}(\mathbf{r})$ for the electric dyadic Green's function for field points in the source region is

$$\mathbf{E}^{c}(\mathbf{r}) = -\frac{1}{j\omega\epsilon_i} \lim_{\delta\to 0} \int_{S_\delta} \nabla'\psi(\mathbf{r}|\mathbf{r}')\hat{\mathbf{n}}'\cdot\mathbf{J}(\mathbf{r}')\, dS' \qquad (12)$$

where S_δ is shown in Figure 8. The correction term above is now shown to correspond to the correction terms appearing in equations (9) and (10). The surface integral term in (12) is split into integration over

S_1 and S_2 (planes at $y\pm\delta$ respectively). This yields for (12)

$$E^c(r) = -\frac{1}{j\omega\epsilon_i}\lim_{\delta\to 0}\left(-\int_{S_1}\nabla'\psi(r|r')\Big|_{y'=y+\delta} J_y(x',y+\delta,z')dx'dz' + \int_{S_2}\nabla'\psi(r|r')\Big|_{y'=y-\delta} J_y(x',y-\delta,z')dx'dz'\right). \tag{13}$$

As $\delta\to 0$, S_1 approaches S_2 and $J_y(x',y\pm\delta,z')$ approaches $J_y(x',y,z')$ due to the smoothness of the boundary of V and the continuity of J at $y'=y$. Thus, (13) simplifies to

$$E^c(r) = \frac{1}{j\omega\epsilon_i}\lim_{\delta\to 0}\int_S \nabla'\psi(r|r')\Big|_{y'=y-\delta}^{y'=y+\delta} J_y(x',y,z')dx'dz' \tag{14}$$

where S extends over the x'-z' plane. Expressing $\nabla'\psi$ in Cartesian form as

$$\nabla'\psi(r|r') = (-jk_i-1/R)\frac{e^{-jk_iR}}{4\pi R^2}[\hat{x}(x'-x)+\hat{y}(y'-y)+\hat{z}(z'-z)]$$

where $R=|r-r'|$, it is found that

$$\nabla'\psi(r|r')\Big|_{y'=y-\delta}^{y'=y+\delta} = (-jk_i-1/R)\frac{e^{-jk_iR_\delta}}{4\pi R_\delta^2}\hat{y}2\delta \tag{15}$$

where $R_\delta = [(x-x')^2+(z-z')^2+\delta^2]^{1/2}$. Substitution of (15) into (14) yields

$$E^c(r) = \frac{1}{j\omega\epsilon_i}\lim_{\delta\to 0}\{\hat{y}\int_S 2\delta(-jk_i-1/R_\delta)\frac{e^{-jk_iR_\delta}}{4\pi R_\delta^2}J_y(x',y,z')dx'dz'\}. \tag{16}$$

The integral in (16) may be decomposed into the sum of integrals over $S - C_\nu$ and C_ν. C_ν is a circle centered at (x,z) with radius ν. As $\delta\to 0$, integration over $S-C_\nu$ vanishes. If ν is chosen sufficiently small, then $J_y(x',y,z') \approx J_y(r)$ and $e^{-jk_cR_\delta} \approx 1$ so that (16) becomes

$$E^c(r) = -\frac{1}{j\omega\epsilon_i}\hat{y}J_y(r)\lim_{\delta\to 0}\{\delta\int_{C_\nu}\frac{jk_i+1/R_\delta}{2\pi R_\delta^2}dx'dz'\} \tag{17a}$$

$$= -\frac{1}{j\omega\epsilon_i}\hat{y}J_y(r)\lim_{\delta\to 0}\left(\delta\int_0^{2\pi}d\phi\int_0^{\nu}\frac{jk_i+1/r_\delta}{2\pi r_\delta^2}\rho d\rho\right) \tag{17b}$$

$$= -\frac{1}{j\omega\epsilon_i}\hat{y}J_y(r)\lim_{\delta\to 0}\left(\delta\int_0^{\nu}\frac{jk_i+1/r_\delta}{r_\delta^2}\rho d\rho\right) \tag{17c}$$

where $r_\delta = (\rho^2+\delta^2)^{1/2}$. In going from (17a) to (17b), integration over C_ν has been transformed to polar coordinates. Performing the angular integration is trivial and yields (17c). Noting that the integrand in (17c) is a perfect differential, the term in braces becomes

$$\delta\int_0^{\nu}\frac{jk_i+1/r_\delta}{r_\delta^2}\rho d\rho = \delta\left(jk_i\ln(\rho^2+\delta^2)^{1/2} - (\rho^2+\delta^2)^{-1/2}\right)\Big|_0^{\nu}$$

$$= \delta\left(jk_i\left[\ln(\nu^2+\delta^2)^{1/2} - \ln\delta\right] + \left[1/\delta - (\nu^2+\delta^2)^{-1/2}\right]\right)$$

$$= 1 \quad (\text{as } \delta\to 0). \tag{18}$$

Finally, substitution of (18) into (17c) yields

$$E^C(r) = -\frac{1}{j\omega\epsilon_i}\hat{y}\,J_y(r)$$

which is precisely the same correction term appearing in (10). Therefore, the correction term for the slice exclusion is identical to that for a pillbox. Hence, this establishes the equivalence of these principal volumes.

2.4 SUMMARY

In a tri-layered dielectric configuration, the Hertzian potential Π in a current carrying region decomposes into principal and reflected parts. The principal wave is that wave which propagates directly from the source to the point of observation. Surface polarization currents, which are induced at the boundary of adjacent regions by the primary

wave, account for the reflected part of the disturbance.

Integral representations for Π may be expressed in either spectral form as

$$\Pi_i(r) = \frac{1}{(2\pi)^2} \iint e^{j\lambda\cdot r} \left\{ \int_V g^p(\lambda; y, r') \frac{J(r')}{j\omega\epsilon_i} dV' \right\} d\xi d\zeta \qquad (19)$$

$$+ \int_V \bar{\bar{G}}^r(r|r') \cdot \frac{J(r')}{j\omega\epsilon_i} dV',$$

or in a more standard form as

$$\Pi_i(r) = \lim_{v \to 0} \int_{V-v} \bar{\bar{G}}(r|r') \cdot \frac{J(r')}{j\omega\epsilon_i} dV' \qquad (20)$$

where $\bar{\bar{G}} = \bar{\bar{G}}^p + \bar{\bar{G}}^r$ and v is any volume which excludes the singularity point $r'=r$ of $\bar{\bar{G}}^p$. Scalar components of $\bar{\bar{G}}$ are represented as two dimensional spectral integrals. The spectral form (19) is useful in practical applications, while the standard form in (20) may be more suitable for theoretical purposes.

The electric field corresponding to the Hertzian potential is given by $E = (k^2 + \nabla\nabla\cdot)\Pi$. It is found that use of the spectral representation for the principal part of Π yields a natural depolarizing dyad $\bar{\bar{L}} = \hat{y}\hat{y}$ in the formulation of E. Integral representations E are expressible in either spectral form as

$$E(r) = -j\omega\mu_0 \iint \left\{ \int_V \bar{\bar{g}}^e(\lambda; r, r') \cdot J(r')\, dV' \right\} d^2\lambda - \bar{\bar{L}} \cdot J(r)/j\omega\epsilon_i \qquad (21)$$

$$+ (k_i^2 + \nabla\nabla\cdot) \int_V \bar{\bar{G}}^r(r|r') \cdot \frac{J(r')}{j\omega\epsilon_i} dV'$$

or in the standard form

$$E(r) = (k_i^2 + \nabla\nabla\cdot) \lim_{v \to 0} \int_{V-v} \bar{\bar{G}}(r|r') \cdot \frac{J(r')}{j\omega\epsilon_i} dV' \qquad (22a)$$

$$= -j\omega\mu_0 \lim_{\delta\to 0} \int_{V-V_\delta} \bar{\bar{G}}^{e}(r|r')\cdot J(r')\, dV' - \bar{\bar{L}}\cdot J(r)/j\omega\epsilon_i \qquad (22b)$$

$$+ \int_V (k_i^2 + \nabla\nabla\cdot)\, \bar{\bar{G}}^{r}(r|r')\cdot \frac{J(r')}{j\omega\epsilon_i}\, dV'$$

where $\bar{\bar{G}}^{e}$ is given in (11) and V_δ is a the slice exclusion in Figure 8. As with the Hertzian potential, the spectral form (21) of E is useful for numerical analysis, while equations (22a) and (22b) are appropriate for theoretical use.

CHAPTER THREE

AN INTEGRAL-OPERATOR APPROACH TO INTEGRATED OPTICS

3.1 INTRODUCTION

Many problems in mathematical physics, which are described by a differential equation subject to particular boundary conditions, may be expressed alternatively by an integral equation. In an integral equation, an unknown function appears as part of an integrand.

There are several advantages to using an integral equation over its differential counterpart. First, when placed in the context of linear operator theory, integral operators often have desirable properties (e.g. boundedness) which are absent in the differential problem. Consequently, poverful analytic theorems may be used to generate, and study properties of, solutions to the problem. Second, an integral equation relates an unknown function to its values throughout an entire region, including its boundary. Therefore, boundary conditions are incorporated naturally in an integral equation. In fact, when boundary conditions are inseparable, a differential formulation is highly impractical. With these considerations in mind, study of optical circuits immersed in an integrated surround may proceed.

Figure 9 illustrates the configuration which is to be investigated. A dielectric obstacle, characterized by refractive index n(r), is embedded in a volume V within the cover of the tri-layered structure of Chapter two. Electric current J, immersed in the source volume V_s, is the source of electromagnetic fields. Unfortunately, none of the eleven

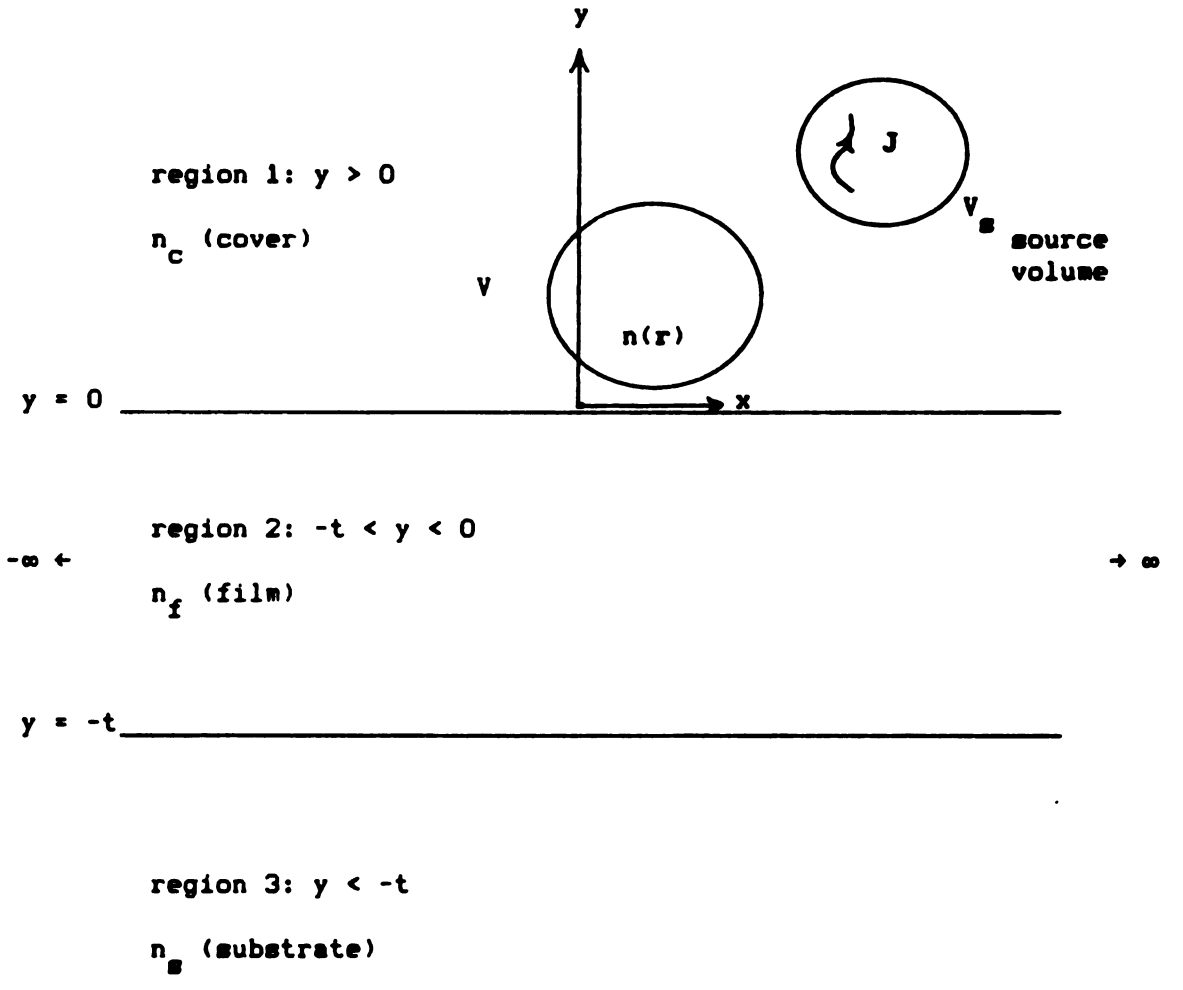

Figure 9. A general optical device immersed within a tri-layered dielectric surround.

orthogonal coordinate systems, for which the Helmholtz equation is separable, match the boundaries associated with this optical system. Hence, development of a Hertzian potential Green's dyad for this system is at best, intractable. An integral-operator formulation, based on identification of equivalent volume polarization currents, circumvents this difficulty.

In the next section, this equivalent polarization source is identified. The electric field integral equation (EFIE) for the field within the obstacle is constructed. Solution to the EFIE is shown directly to satisfy Maxwell's equations along with the appropriate boundary conditions.

In section 3, the EFIE is specialized for axially invariant waveguides in the integrated surround. A transform-domain integral equation is introduced which is used extensively throughout this dissertation. Transverse field components are shown to satisfy an integral equation which is independent of the longitudinal components.

3.2 ELECTRIC FIELD INTEGRAL EQUATION

Consider the physical system depicted in Figure 10(a). The trilayered structure of Chapter two is perturbed by introducing an optical device, of refractive index n(r), into a volume V of the cover. System excitation is provided by an impressed current source J, within a volume V_s, which maintains an impressed field $\mathbf{E}^i$. Scattering of the impressed field occurs due to the contrast $\delta n^2(r) = n^2(r) - n_c^2$ of refractive indices between the optical device and the uniform cover. The scattered field $\mathbf{E}^s$ superposes with the impressed field so that at any point the total field $\mathbf{E}$ is given by $\mathbf{E} = \mathbf{E}^i + \mathbf{E}^s$.

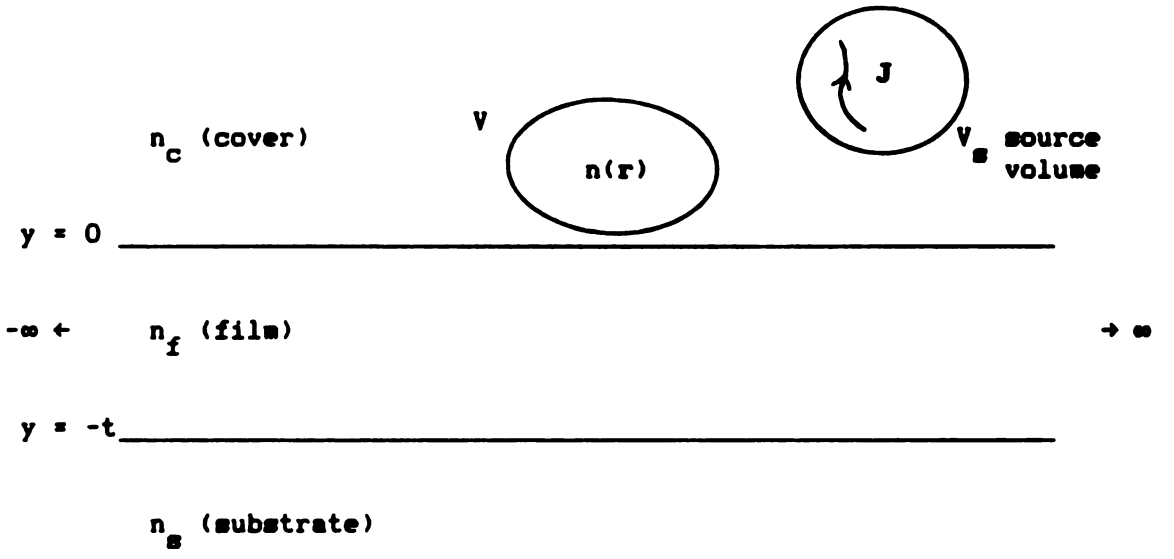

(a)

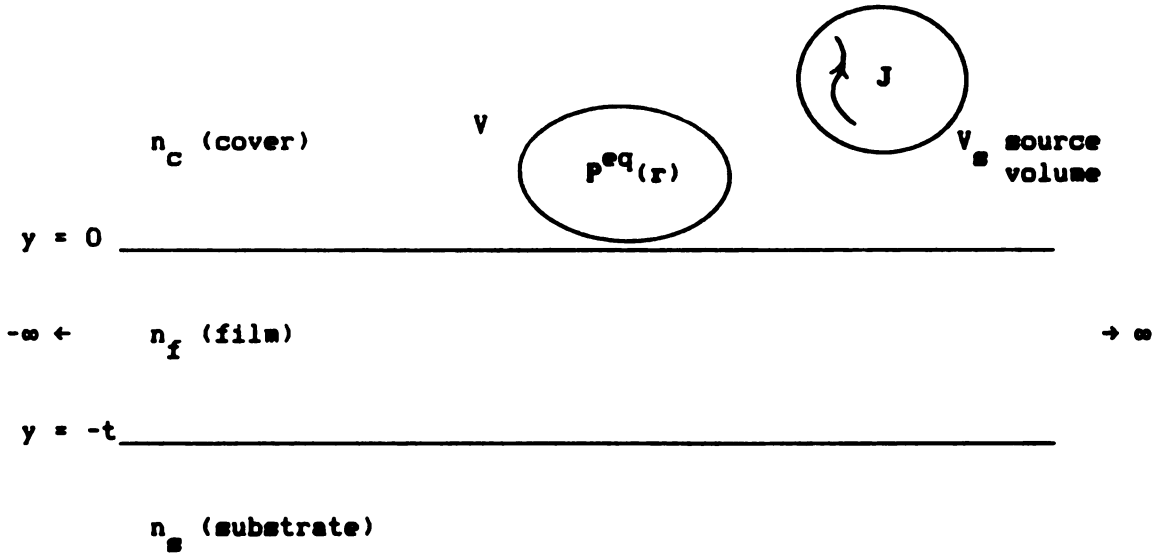

(b)

Figure 10. (a) The physical system of an optical device within an integrated surround. (b) An equivalent system in which P^{eq} accounts for all effects of the inhomogeneous dielectric obstacle .

The electric field of the optical circuit in Figure 10(a) remains unaffected by replacing the dielectric obstacle with an equivalent polarization source P^{eq} as shown in Figure 10(b). This equivalent polarization radiates in the uniform cover surround and is the source for the scattered field E^s. Ampère's law is used below to identify P^{eq}.

3.2.1 EQUIVALENT SOURCE IDENTIFICATION

For the physical system in Figure 10(a), Ampère's law within V is given by

$$\nabla \times H(r) = j\omega\epsilon_0 n^2(r) E(r) \tag{1}$$

while for the equivalent system in Figure 10(b), Ampère's law is

$$\nabla \times H(r) = j\omega P^{eq}(r) + j\omega\epsilon_0 n_c^2 E(r) \tag{2}$$

where $j\omega P^{eq} = J^{eq}$. Subtracting (1) from (2), and solving for P^{eq} yields

$$P^{eq}(r) = \epsilon_0 \delta n^2(r) E(r) \tag{3}$$

where P^{eq} is the excess induced polarization which augments the polarization existing in the cover background. With the Green's function of the integrated surround known, construction of the EFIE for the field within the optical device may now be accomplished.

3.2.2 CONSTRUCTION OF THE INTEGRAL EQUATION

Impressed field E^i is the field maintained by J in the unperturbed integrated surround. Therefore, use of equation (2.22a) yields

$$E^i(r) = (k_c^2 + \nabla\nabla\cdot) \int_V \bar{\bar{G}}_s(r|r') \cdot \frac{J(r')}{j\omega\epsilon_c} \, dV' \tag{4}$$

where the limit on the improper integral has been omitted since the

excluding region is shape independent.

Similarly, scattered field $\mathbf{E}^s$, maintained by $\mathbf{P}^{eq}$, may be expressed as

$$\mathbf{E}^s(\mathbf{r}) = (k_c^2 + \nabla\nabla\cdot) \int_V \bar{\mathbf{G}}(\mathbf{r}|\mathbf{r}') \cdot \frac{\mathbf{P}^{eq}(\mathbf{r}')}{\varepsilon_c} \, dV' \tag{5a}$$

$$= (k_c^2 + \nabla\nabla\cdot) \int_V \frac{\delta n^2(\mathbf{r}')}{n_c^2} \bar{\mathbf{G}}(\mathbf{r}|\mathbf{r}') \cdot \mathbf{E}(\mathbf{r}') \, dV' \tag{5b}$$

where use of (3) has been made in going from (5a) to (5b) .

Using linear superposition, the total field may be written as

$$\mathbf{E}(\mathbf{r}) = (k_c^2 + \nabla\nabla\cdot) \int_V \frac{\delta n^2(\mathbf{r}')}{n_c^2} \bar{\mathbf{G}}(\mathbf{r}|\mathbf{r}') \cdot \mathbf{E}(\mathbf{r}') \, dV' + \mathbf{E}^i(\mathbf{r}) \tag{6}$$

so that transposition of the scattered field to the left side of (6) yields

$$\mathbf{E}(\mathbf{r}) - (k_c^2 + \nabla\nabla\cdot) \int_V \frac{\delta n^2(\mathbf{r}')}{n_c^2} \bar{\mathbf{G}}(\mathbf{r}|\mathbf{r}') \cdot \mathbf{E}(\mathbf{r}') \, dV' = \mathbf{E}^i(\mathbf{r}). \tag{7}$$

It should be remarked that (7) is a valid expression for all r such that $y > 0$. However, to the extent that knowledge of E within V determines the field everywhere throughout the region $y > 0$, (7) is an integral equation for E with domain $\mathbf{r} \in V$. More precisely, (7) is an integro-differential equation for the unknown electric field within the optical device. Although use of (1.17b) allows (7) to be converted into a pure integral equation, the degree in singularity of the resulting kernel is much greater than that of $\bar{\mathbf{G}}$. Hence, use of (7) is preferred for most analytical purposes.

3.2.3 UNIQUENESS OF SOLUTION

It is well known that the solution to (7) is unique if it satisfies Maxwell's equations along with the appropriate boundary conditions. By

construction, solution of (7) satisfies Maxvell's equations. Therefore, to prove uniqueness of solution, it is sufficient to show that the field has the proper behavior at the boundary of the optical device.

Figure 11 assists in the discussion of the applicable boundary conditions. Observation point r lies on the boundary S of the optical device. Without loss of generality, r^- (r^+) is interior (exterior) to V and displaced a distance δ from r along a linear path defined by the surface normal $\hat{n}$. Field behavior across S may be determined by evaluating the field at r^+ and r^- and forming the difference ΔE given by

$$\Delta E = \lim_{\delta \to 0} \left(E(r^+) - E(r^-) \right)$$

$$= \lim_{\delta \to 0} \left\{ \left[E^i(r^+) - E^i(r^-) \right] + \left[E^s(r^+) - E^s(r^-) \right] \right\}. \qquad (8)$$

Consider now, each bracketed term in (8) separately. First, it is shown that the impressed field is continuous at r. Under the assumption that V and V_s are disjoint, the volume integration in (4) never passes through the singularity point r of $\bar{\bar{G}}$. Hence, $\bar{\bar{G}}$ and its partial derivatives are continuous for all $r' \in V$ and $r \notin V$, whereby a standard theorem of advanced calculus [15, p.322] guarantees continuity of E^i at r. Thus, the first bracketed term in (8) vanishes as $\delta \to 0$.

Next, examine the scattered field E^s as given by (5a). Since the reflected dyad $\bar{\bar{G}}^r$ and its partial derivatives are continuous throughout the cover, that portion of the scattered field originating from properties of the layered surround is also continuous. However, analysis of the principal part of the scattered field reveals a discontinuity in the component of field which is normal to the boundary of the optical device. This claim is asserted below.

Using (5a), the principal part of the scattered field may be

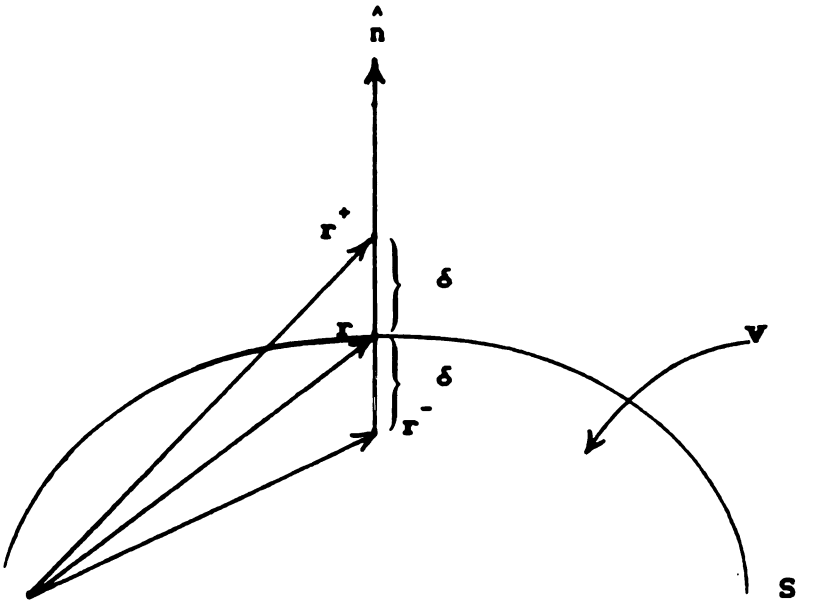

Figure 11. Geometry for field behavior at the boundary surface S of an optical device immersed in a uniform surround.

written as

$$\underline{E}_p^s(r) = (k_c^2 + \nabla\nabla\cdot) \int_V \underline{\bar{G}}^p(r|r') \cdot \frac{J^{eq}(r')}{j\omega\epsilon_c} \, dV' \tag{9}$$

$$= I_1(r) + I_2(r)$$

where the integrals I_1 and I_2 are given by

$$I_1(r) = k_c^2 \int_V \underline{\bar{G}}^p(r|r') \cdot \frac{J^{eq}(r')}{j\omega\epsilon_c} \, dV' \tag{10a}$$

$$I_2(r) = \nabla\nabla\cdot \int_V \underline{\bar{G}}^p(r|r') \cdot \frac{J^{eq}(r')}{j\omega\epsilon_c} \, dV' \tag{10b}$$

Under the assumption that J^{eq} and $\nabla\cdot J^{eq}$ are continuous and of compact support in V, use of (D.4) allows (10b) to be written

$$I_2(r) = \frac{1}{j\omega\epsilon_c} \left(- \int_V \nabla' G^p(r|r') \, \nabla'\cdot J^{eq}(r') \, dV' + \int_S \hat{n}'\cdot J^{eq}(r') \, \nabla' G^p(r|r') \, dS' \right). \tag{11}$$

In general, J^{eq} will not be zero at the boundary surface S. Therefore, unlike in (D.6), the surface integration in (11) must be retained.

Continuity of I_1 in (10a) as well as the volume integral in (11) may be established by arguments used by Kellogg [19, pp.150-151] in showing continuity of static potentials and thus will not be given here. It is in fact precisely the surface integral of (11) which leads to discontinuity in the component of electric field which is normal to S. Thus, the difference ΔE becomes

$$\Delta E = \frac{1}{j\omega\epsilon_c} \lim_{\delta\to 0} \int_S \left[\nabla' G^p(r^+|r') - \nabla' G^p(r^-|r') \right] \hat{n}'\cdot J^{eq}(r') \, dS'$$

$$= \frac{1}{j\omega\epsilon_c} \lim_{\delta\to 0} \int_S \nabla' G^p(r|r') \Big|_{r=r^-}^{r=r^+} \hat{n}'\cdot J^{eq}(r') \, dS'.$$

Decomposing this surface integral into the sum of integrals over $S\text{-}S_v$

and S_ν yields

$$\Delta\mathbf{E} = \frac{1}{j\omega\epsilon_c} \lim_{\delta\to 0} \left\{ \int_{S-S_\nu} \nabla' G^p(\mathbf{r}|\mathbf{r}') \Big|_{r=r^-}^{r=r^+} \hat{n}' \cdot \mathbf{J}^{eq}(\mathbf{r}')\, dS' \right. \\ \left. + \int_{S_\nu} \nabla' G^p(\mathbf{r}|\mathbf{r}') \Big|_{r=r^-}^{r=r^+} \hat{n}' \cdot \mathbf{J}^{eq}(\mathbf{r}') dS' \right\} \tag{12}$$

where S_ν is a subset of S such that $\mathbf{r} \in S_\nu$ and ν is the maximum chord of S_ν.

The first integral in (12) vanishes as $\delta\to 0$ since $\nabla' G^p$ is a bounded and continuous function for $\mathbf{r}' \in S - S_\nu$ as $\delta\to 0$. Evaluation of the integration over S_ν may be simplified by an appropriate choice of S_ν. Let C_ν be a circle of radius ν and center $\mathbf{r}$ lying in the tangent plane to S at $\mathbf{r}$. Choose S_ν to be the projection along $\hat{n}$ of C_ν onto S. For ν sufficiently small, $\hat{n}' \cdot \mathbf{J}^{eq}(\mathbf{r}') \approx \hat{n} \cdot \mathbf{J}^{eq}(\mathbf{r}^-)$ and the surface integral over S_ν may be approximated by integration over C_ν. Therefore (12) reduces to

$$\Delta\mathbf{E} = \frac{1}{j\omega\epsilon_c} \hat{n} \cdot \mathbf{J}^{eq}(\mathbf{r}^-) \lim_{\delta\to 0} \int_{C_\nu} \nabla' G^p(\mathbf{r}|\mathbf{r}') \Big|_{r=r^-}^{r=r^+} dS'.$$

Aligning the unit normal $\hat{n}$ along the y-axis by an appropriate coordinate rotation, it is found that

$$\nabla' G^p(\mathbf{r}|\mathbf{r}') \Big|_{r=r^-}^{r=r^+} = (-jk_c - 1/R) \frac{e^{-jk_c R_\delta}}{4\pi R_\delta^2} (-\hat{n} 2\delta).$$

If ν is chosen so small that $e^{-jk_c R_\delta} \approx 1$, then $\Delta\mathbf{E}$ becomes

$$\Delta\mathbf{E} = \frac{1}{j\omega\epsilon_c} \hat{n}\hat{n} \cdot \mathbf{J}^{eq}(\mathbf{r}^-) \lim_{\delta\to 0} (\delta \int_{C_\nu} \frac{jk_c + 1/R_\delta}{2\pi R_\delta^2} dx'dz') \tag{13}$$

which is essentially the same quantity (with $\hat{n}=\hat{y}$), modulo sign, as that in (2.17a) for the correction term $\bar{\mathbf{E}}^c$ to the electric Green's dyad for a slice principal volume. Using this result, (13) becomes

$$\Delta \mathbf{E} = \frac{1}{j\omega\epsilon_c} \hat{\mathbf{n}}\hat{\mathbf{n}} \cdot \mathbf{J}^{eq}(\mathbf{r}^-)$$

whereupon substitution of $j\omega\epsilon_0 \, \delta n^2 \mathbf{E}$ for $\mathbf{J}^{eq}$ reveals

$$\mathbf{E}(\mathbf{r}^+) - \mathbf{E}(\mathbf{r}^-) = \hat{\mathbf{n}} \left(\frac{\delta n^2(\mathbf{r}^-)}{n_c^2} \right) \left(\hat{\mathbf{n}} \cdot \mathbf{E}(\mathbf{r}^-) \right)$$

from which the relations

$$\mathbf{E}_{tan}(\mathbf{r}^+) = \mathbf{E}_{tan}(\mathbf{r}^-)$$

$$n_c^2 \mathbf{E}_{norm}(\mathbf{r}^+) = n^2(\mathbf{r}^-) \mathbf{E}_{norm}(\mathbf{r}^-)$$

where $\mathbf{E}_{tan} = \hat{\mathbf{n}} \times \mathbf{E}$ and $\mathbf{E}_{norm} = \hat{\mathbf{n}} \cdot \mathbf{E}$, are found to agree with the well known boundary conditions for the electric field at the interface of dielectric discontinuity. This establishes uniqueness to the solution of (7).

3.3 AXIALLY-UNIFORM WAVEGUIDES

Unless the geometry and electrical characteristics of the optical device discussed above are specified, there is not much that can be said about solution to (7). However, there are several interesting simplifications which can be made when this device is a longitudinally-uniform waveguide. Figure 12 depicts a typical integrated optical waveguide having infinite extent along the z-axis and a general cross sectional shape CS in the transverse (x,y) plane. This guide is assumed to be optically dense with refractive index $n(\rho) > n_f$, where $\rho = \hat{\mathbf{x}}x + \hat{\mathbf{y}}y$ designates the transverse position vector. As a consequence of the axial independence of the index of refraction, the integral operator in (5b) is rendered convolutional in z with

$$\bar{\bar{\mathbf{G}}} \cdot \mathbf{E} = \int \bar{\bar{\mathbf{G}}}(\rho|\rho';z-z') \cdot \mathbf{E}(\rho',z') \, dz'$$

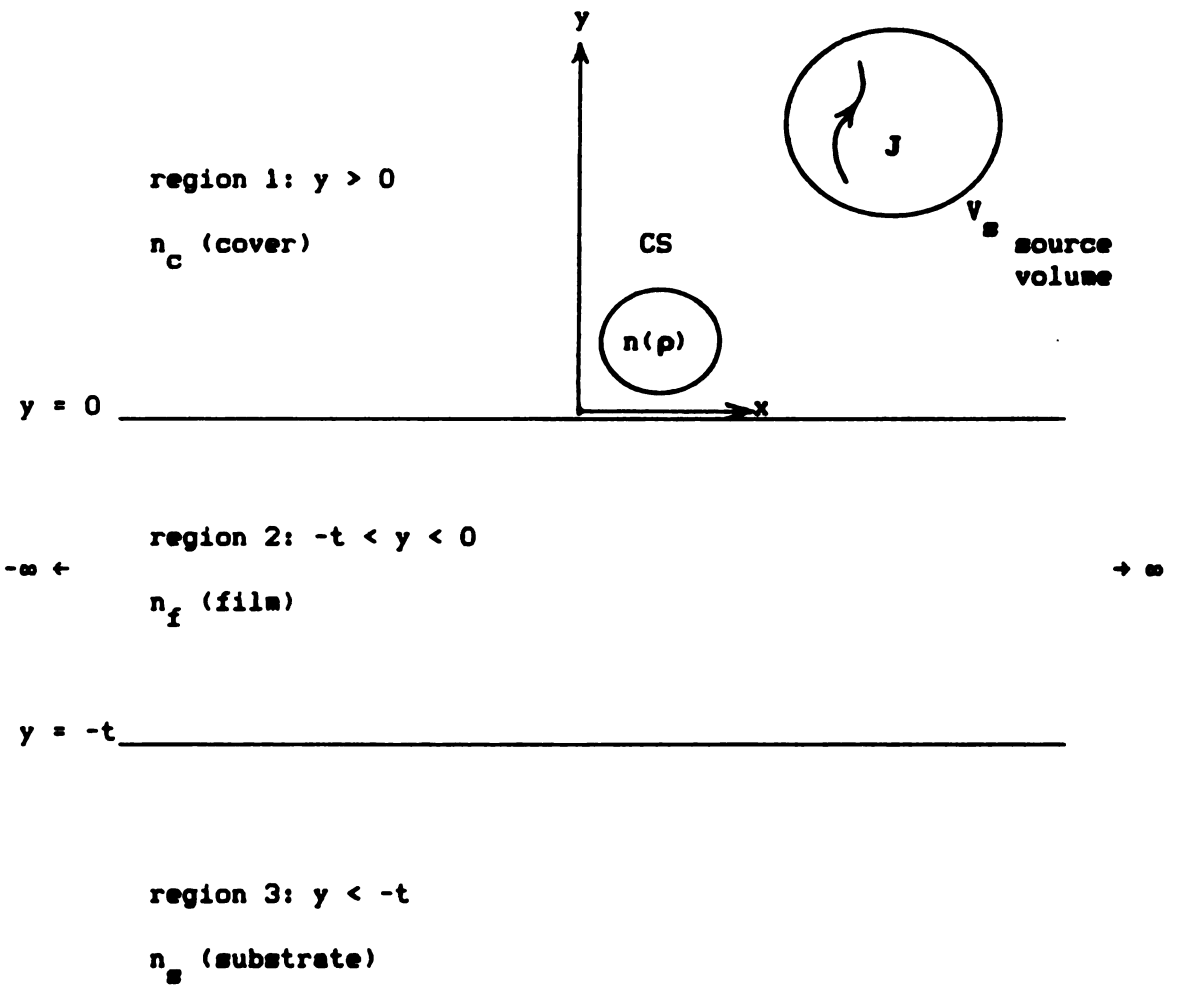

Figure 12. A longitudinally invariant waveguide deposited within the cover of an integrated background environment.

thereby prompting use of the Faltung theorem [16, p.1020]. Formal operation on (7) with the one dimensional Fourier transform

$$F_z(\cdot) = \int (\cdot)\, e^{-j\zeta z}\, dz$$

leads to the transform-domain EFIE

$$e(\rho,\zeta) - (k_c^2 + \tilde{\nabla}\tilde{\nabla}\cdot) \int_{CS} \frac{\delta n^2(\rho')}{n_c^2}\, \bar{\bar{g}}_\zeta(\rho|\rho')\cdot e(\rho',\zeta)\, dS' = e^i(\rho,\zeta) \quad (14)$$

where $e = F_z(E)$, $e^i = F_z(E^i)$, $\tilde{\nabla} = \nabla_t + \hat{z}j\zeta$, and $\nabla_t = \hat{x}\frac{\partial}{\partial x} + \hat{z}\frac{\partial}{\partial z}$. The transform-domain Green's dyad $\bar{\bar{g}}_\zeta$ decomposes as before into principal and reflected parts with

$$\bar{\bar{g}}_\zeta(\rho|\rho') = \bar{\bar{g}}_\zeta^p(\rho|\rho') + \bar{\bar{g}}_\zeta^r(\rho|\rho').$$

The principal dyad $\bar{\bar{g}}_\zeta^p$ is given by

$$\bar{\bar{g}}_\zeta^p = \bar{\bar{I}} g_\zeta^p$$

where the principal transform-domain Green's function g_ζ^p is given by

$$g_\zeta^p(\rho|\rho') = \int \frac{e^{-p_c|y-y'|}}{4\pi p_c}\, e^{j\xi(x-x')}\, d\xi. \quad (15)$$

An alternative integral representation of g_ζ^p can be obtained from (15) by considering a mapping of the real ξ-line into a contour C_η in a complex η-plane by letting $\xi = \gamma_c \sinh\eta$ (where $\gamma_c = (\zeta^2 - k_c^2)^{1/2}$). Figure 13 shows the contour C_η which is determined by requiring $\mathrm{Im}(\gamma_c \sinh\eta) = 0$, $\mathrm{Re}(\gamma_c) > 0$, and $\mathrm{Im}(\gamma_c) > 0$. Invoking these restrictions, it is found that $\theta^+ = \tan^{-1}(\mathrm{Im}(\gamma_c)/\mathrm{Re}(\gamma_c)) < \pi/2$. After transforming the spatial variables to polar coordinates, extensive complex-plane analysis shows that (15) can be transformed into

$$g_\zeta^p(\rho|\rho') = \frac{1}{4\pi} \int_{-\infty}^{\infty - j\pi} e^{-j\gamma_c|\rho-\rho'|\sinh\eta}\, d\eta \quad (16a)$$

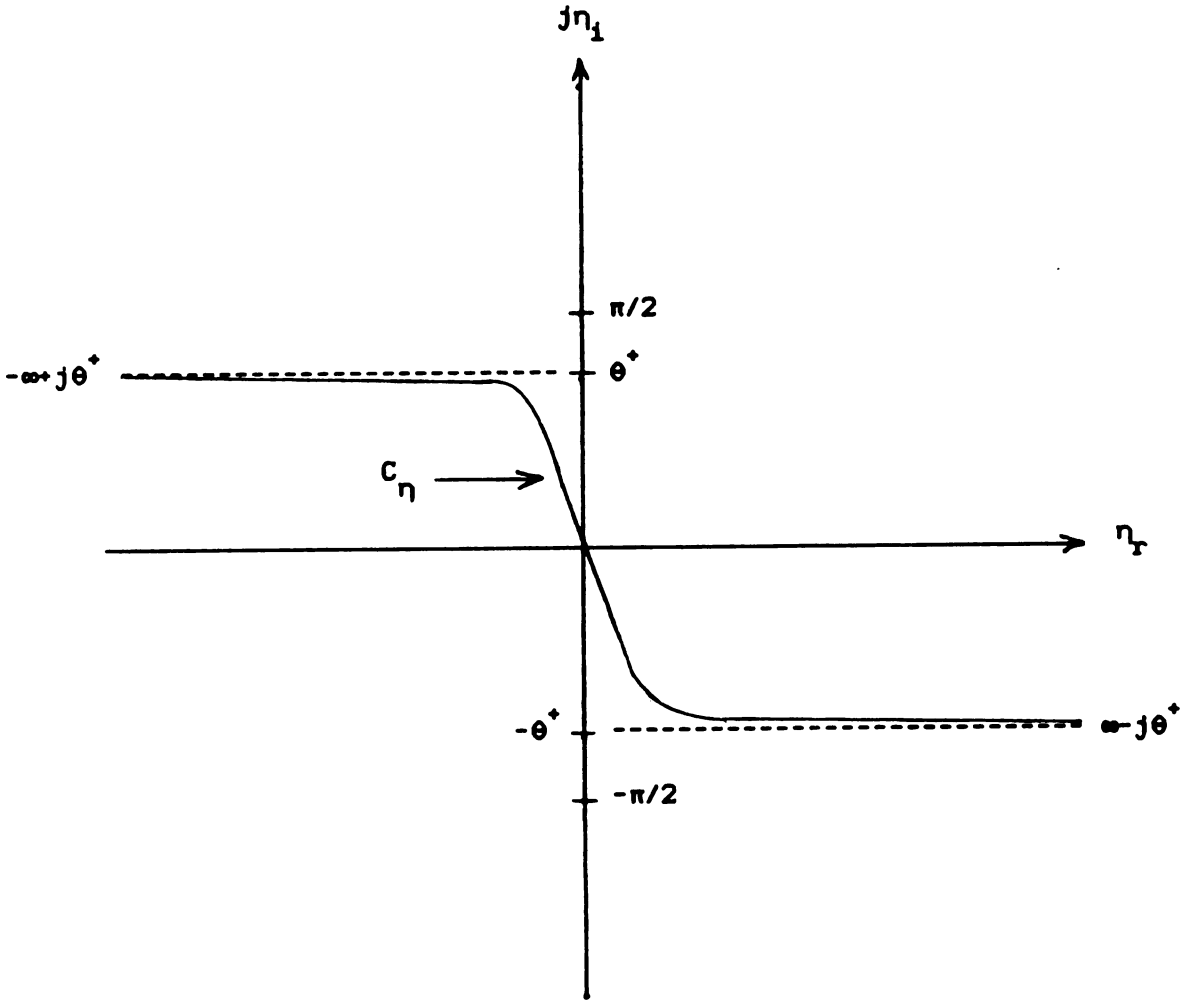

Figure 13. Complex η-plane with contour C_η.

$$= \frac{1}{4\pi}(-j\pi)\, H_0^{(2)}(-j\gamma_c|\rho-\rho'|) \quad \ldots |\arg(-j\gamma_c|\rho-\rho'|)| < \pi/2 \qquad (16b)$$

$$= \frac{1}{2\pi} K_0(\gamma_c|\rho-\rho'|) \qquad \ldots\ 0 < \arg(\gamma_c) < \pi/2 \qquad (16c)$$

where $H_0^{(2)}$ is the Hankel function of order zero and K_0 is a modified Bessel function of order zero. In going from (16a) to (16b), use was made of an integral representation of $H_0^{(2)}$ found in [16, p.360] while the relationship between K_0 and $H_0^{(2)}$ [16, p.375] was used to obtain (16c). It can be shown that (16c) is valid for $-\pi/2 < \arg(\gamma_c) < \pi/2$.

The reflected dyad $\bar{\bar{g}}_\zeta^r$ has the form

$$\bar{\bar{g}}_\zeta^r = \hat{x} g_{\zeta t}^r \hat{x} + \hat{y}\left(\frac{\partial g_{\zeta c}^r}{\partial x}\hat{x} + g_{\zeta n}^r \hat{y} + j\zeta g_{\zeta c}^r \hat{z}\right) + \hat{z} g_{\zeta t}^r \hat{z}.$$

where the scalar components of $\bar{\bar{g}}_\zeta$ are represented as spectral integrations with

$$\begin{Bmatrix} g_{\zeta t}^r(\rho|\rho') \\ g_{\zeta n}^r(\rho|\rho') \\ g_{\zeta c}^r(\rho|\rho') \end{Bmatrix} = \int \begin{Bmatrix} R_t(\lambda) \\ R_n(\lambda) \\ C(\lambda) \end{Bmatrix} \frac{e^{-p_c(y+y')}}{4\pi p_c} e^{j\xi(x-x')}\, d\xi$$

where as before $p_c^2 = \xi^2 + \zeta^2 - k_c^2$ and the reflection coefficients R_t and R_n as well as the coupling coefficient C are given by the expressions tabulated in the preceding chapter.

There are several advantages to using the transform domain EFIE in (14) over the EFIE in (7). First, numerical approximation to the solution of (7) for each ζ is more readily accomplished since both spatial and spectral integrations have been reduced in dimension. Second, differentiation with respect to z transforms to multiplication by the transform variable ζ. Third, as shown in the next section, field

components which are transverse to z satisfy an integral equation which is independent of the longitudinal component. Fourth, and perhaps most important, identification of a propagation-mode spectrum may be effected by a study of solutions to (14) in the complex ζ-plane. Chapter 4 is devoted to a detailed discussion of this topic.

3.3.1 EFIE FOR THE TRANSVERSE FIELD

It is possible to formulate a transform domain EFIE which uncouples the longitudinal component from the transverse components. Development of this transverse EFIE relies upon use of the Fourier transform of Gauss' law (1.1a)

$$\tilde{\nabla}\cdot(n^2\mathbf{e}) = 0. \tag{17}$$

Writing $\mathbf{e} = \mathbf{e}_t + \hat{z}e_z$, (17) may be written as

$$\nabla_t\cdot(n^2\mathbf{e}_t) + j\zeta n^2 e_z = 0. \tag{18}$$

Solving (18) for $j\zeta e_z$ yields

$$j\zeta e_z = -\frac{1}{n^2}\nabla_t\cdot(n^2\mathbf{e}_t) \tag{19a}$$

$$= -\nabla_t\cdot\mathbf{e}_t - \left[\frac{\nabla_t n^2}{n^2}\right]\cdot\mathbf{e}_t \tag{19b}$$

where use of the vector identity $\nabla_t\cdot(\phi\mathbf{A}) = \phi\nabla_t\cdot\mathbf{A} + \nabla_t\phi\cdot\mathbf{A}$ has been made.

Operating on (14) with $\hat{z}\hat{z}\cdot$ yields

$$\hat{z}e_z(\rho,\zeta) = k_c^2\int_{CS}\frac{\delta n^2(\rho')}{n_c^2}\{\hat{z}\cdot\bar{\bar{g}}_\zeta(\rho|\rho')\cdot\mathbf{e}(\rho',\zeta)\}\hat{z}\,dS'$$

$$+ j\zeta\hat{z}\tilde{\nabla}\cdot\int_{CS}\frac{\delta n^2(\rho')}{n_c^2}g_\zeta(\rho|\rho')\cdot\mathbf{e}(\rho',\zeta)\,dS' + \hat{z}e_z^i(\rho,\zeta). \tag{20}$$

Subtracting (20) from (14) yields

$$e_t(\rho,z) = k_c^2 \int_{CS} \frac{\delta n^2(\rho')}{n_c^2} \{\bar{\bar{g}}_z(\rho|\rho')\cdot e(\rho',z) - \hat{z}[\hat{z}\cdot\bar{\bar{g}}_z(\rho|\rho')\cdot e(\rho',z)]\}\, dS'$$

$$+ \nabla_t\tilde{\nabla}\cdot \int_{CS} \frac{\delta n^2(\rho')}{n_c^2} \bar{\bar{g}}_z(\rho|\rho')\cdot e(\rho',z)\, dS' + e_t^i(\rho,z)$$

$$= k_c^2 \int_{CS} \frac{\delta n^2(\rho')}{n_c^2} \{\bar{\bar{g}}_z(\rho|\rho')\cdot e(\rho',z) - \hat{z}[\hat{z}\cdot\bar{\bar{g}}_z(\rho|\rho')\cdot e(\rho',z)]\}\, dS'$$

$$+ \nabla_t \int_{CS} \frac{\delta n^2(\rho')}{n_c^2} \tilde{\nabla}\cdot\{\bar{\bar{g}}_z(\rho|\rho')\cdot e(\rho',z)\}\, dS' + e_t^i(\rho,z). \tag{21}$$

The inner products appearing in (21) may be expanded as

$$\bar{\bar{g}}_z\cdot e = \bar{\bar{g}}_z\cdot e_t + \bar{\bar{g}}_z\cdot\hat{z}e_z$$
$$= \bar{\bar{g}}_z\cdot e_t + [\hat{z}g_z^p + \hat{z}g_{zt}^r + \hat{y}jzg_{zc}^r]e_z \tag{22a}$$

$$\hat{z}[\hat{z}\cdot\bar{\bar{g}}_z\cdot e] = \hat{z}(\,\hat{z}\cdot\bar{\bar{g}}_z\cdot e_t + \hat{z}\cdot\bar{\bar{g}}_z\cdot\hat{z}e_z\,)$$
$$= \hat{z}(\,g_z^p e_z + g_{zt}^r e_z\,) \tag{22b}$$

$$\tilde{\nabla}\cdot(\bar{\bar{g}}_z\cdot e) = \nabla_t\cdot[\bar{\bar{g}}_z\cdot e] + jz\hat{z}\cdot\bar{\bar{g}}_z\cdot e$$
$$= \nabla_t\cdot[\bar{\bar{g}}_z\cdot e_t + \bar{\bar{g}}_z\cdot\hat{z}e_z] + jz(\,\hat{z}\cdot\bar{\bar{g}}_z\cdot e_t + \hat{z}\cdot\bar{\bar{g}}_z\cdot\hat{z}e_z\,)$$
$$= \nabla_t\cdot[\bar{\bar{g}}_z\cdot e_t] + \left(g_z^p + g_{zt}^r + \frac{\partial g_{zc}^r}{\partial y}\right) jze_z$$
$$= [\nabla_t\cdot\bar{\bar{g}}_z]\cdot e_t + \left(g_z^p + g_{zt}^r + \frac{\partial g_{zc}^r}{\partial y}\right) jze_z \tag{22c}$$

so that substitution of equations (22) into (21) leads to

$$e_t(\rho,z) = k_c^2 \int_{CS} \frac{\delta n^2(\rho')}{n_c^2} \{\bar{\bar{g}}_z(\rho|\rho')\cdot e_t(\rho',z) + \hat{y}g_{zc}^r(\rho|\rho')jze_z(\rho',z)\}\, dS'$$

$$+ e_t^i(\rho,z) \tag{23}$$

$$+ \nabla_t \int_{CS} \frac{\delta n^2(\rho')}{n_c^2} \{[\nabla_t\cdot\bar{\bar{g}}_z(\rho|\rho')]\cdot e_t(\rho',z) + g_1(\rho|\rho')jze_z(\rho',z)\}\, dS'$$

where the function g_1 is given by

$$g_1(\rho|\rho') = g_z^p + g_{zt}^r + \frac{\partial g_{zc}^r}{\partial y} .$$

Using (19b), $j\zeta e_z$ may be eliminated from (23) resulting in

$$\begin{aligned} e_t(\rho,z) &= e_t^i(\rho,z) + k_c^2 \int_{CS} \frac{\delta n^2(\rho')}{n_c^2} \bar{\bar{g}}_z(\rho|\rho')\cdot e_t(\rho',z)\, dS' \\ &+ \nabla_t \int_{CS} \frac{\delta n^2(\rho')}{n_c^2} [\nabla_t \cdot \bar{\bar{g}}_z(\rho|\rho')]\cdot e_t(\rho',z)\, dS' \\ &- \hat{y} k_c^2 \int_{CS} \frac{\delta n^2(\rho')}{n_c^2} g_{zc}^r(\rho|\rho') \left\{ \nabla_t' \cdot e_t(\rho',z) + \frac{\nabla_t' n^2(\rho')}{n^2(\rho')} \cdot e_t(\rho',z) \right\} dS' \\ &- \nabla_t \int_{CS} \frac{\delta n^2(\rho')}{n_c^2} g_1(\rho|\rho') \left\{ \nabla_t' \cdot e_t(\rho',z) + \frac{\nabla_t' n^2(\rho')}{n^2(\rho')} \cdot e_t(\rho',z) \right\} dS'. \end{aligned} \tag{24}$$

It is desirable to eliminate the terms in (24) which contain $\nabla_t \cdot e_t$ by integrating by parts. This is accomplished by using the two-dimensional divergence theorem

$$\int_{CS} \nabla_t \cdot A(\rho)\, dS = \int_\Gamma \hat{n} \cdot A(\rho)\, dl$$

where CS has boundary contour Γ and $\hat{n}$ is the outward unit normal vector. Let g represent either g_{zc}^r or g_1 in (24). Using the vector identity $\nabla_t \cdot (\varphi A) = \varphi\, \nabla \cdot A + \nabla\varphi \cdot A$, it is discovered that

$$\begin{aligned} &\frac{\delta n^2(\rho')}{n_c^2} g(\rho|\rho') \left\{ \nabla_t' \cdot e_t(\rho',z) + \frac{\nabla_t' n^2(\rho')}{n^2(\rho')} \cdot e_t(\rho',z) \right\} \\ &\quad = \nabla_t' \cdot \left\{ \frac{\delta n^2(\rho')}{n_c^2} g(\rho|\rho') e_t(\rho',z) \right\} - \frac{\delta n^2(\rho')}{n_c^2} e_t(\rho',z) \cdot \nabla_t' g(\rho|\rho') \\ &\qquad - g(\rho|\rho') e_t(\rho',z) \cdot \frac{\nabla_t' n^2(\rho')}{n^2(\rho')} . \end{aligned} \tag{25}$$

Application of (25) along with the two dimensional divergence theorem

allows (24) to be written

$$\mathbf{e}_t(\rho,z) = \mathbf{e}_t^i(\rho,z) + k_c^2 \int_{CS} \frac{\delta n^2(\rho')}{n_c^2} \overline{\overline{g}}_z(\rho|\rho')\cdot\mathbf{e}_t(\rho',z)\,dS' \qquad (26)$$

$$+ \nabla_t \int_{CS} \frac{\delta n^2(\rho')}{n_c^2} [\nabla_t \cdot \overline{\overline{g}}_z(\rho|\rho')]\cdot\mathbf{e}_t(\rho',z)\,dS'$$

$$+ \hat{y}k_c^2 \left\{ \int_{CS} \frac{\delta n^2(\rho')}{n_c^2} \nabla_t' g_{zc}^r(\rho|\rho')\cdot\mathbf{e}_t(\rho',z)\,dS' \right.$$

$$+ \int_{CS} \frac{\nabla_t' n^2(\rho')}{n^2(\rho')} \cdot \mathbf{e}_t(\rho',z)\, g_{zc}^r(\rho|\rho')\,dS'$$

$$\left. - \int_\Gamma \frac{\delta n^2(\rho')}{n_c^2} g_{zc}^r(\rho|\rho')\, \mathbf{e}_t(\rho',z)\cdot\hat{n}'\,dl' \right\}$$

$$+ \nabla_t \left\{ \int_{CS} \frac{\delta n^2(\rho')}{n_c^2} \nabla_t' g_1(\rho|\rho')\cdot\mathbf{e}_t(\rho',z)\,dS' \right.$$

$$+ \int_{CS} \frac{\nabla_t' n^2(\rho')}{n^2(\rho')} \cdot \mathbf{e}_t(\rho',z)\, g_1(\rho|\rho')\,dS'$$

$$\left. - \int_\Gamma \frac{\delta n^2(\rho')}{n_c^2} g_1(\rho|\rho')\, \mathbf{e}_t(\rho',z)\cdot\hat{n}'\,dl' \right\}.$$

Finally, after combining terms and performing a considerable amount of algebraic manipulation, (26) simplifies to

$$\mathbf{e}_t(\rho,z) = \mathbf{e}_t^i(\rho,z) + k_0^2 \int_{CS} \delta n^2(\rho')\, \overline{\overline{g}}_{t1}(\rho|\rho')\cdot\mathbf{e}_t(\rho',z)\,dS' \qquad (27)$$

$$+ \int_{CS} \frac{\nabla_t' n^2(\rho')}{n^2(\rho')} \cdot \mathbf{e}_t(\rho',z)\, g_{t2}(\rho|\rho')\,dS'$$

$$- \int_\Gamma \frac{\delta n^2(\rho')}{n_c^2} g_{t2}(\rho|\rho')\, \mathbf{e}_t(\rho',z)\cdot\hat{n}'\,dl'$$

$$+ \int_{CS} \frac{\delta n^2(\rho')}{n_c^2} \overline{\overline{g}}_{t3}(\rho|\rho')\cdot\mathbf{e}_t(\rho',z)\,dS'$$

where the quantities $\bar{\bar{g}}_{t1}$, g_{t2}, and $\bar{\bar{g}}_{t3}$ are given by

$$\bar{\bar{g}}_{t1} = \bar{\bar{I}} g^p_\zeta + \hat{x} g^r_{\zeta t} \hat{x} + \hat{y} \left(g^r_{\zeta n} + \frac{\partial g^r_{\zeta c}}{\partial y} \right) \hat{y}$$

$$g_{t2} = \hat{y} k_c^2 g^r_{\zeta c} + \nabla_t \left(g^p_\zeta + g^r_{\zeta t} + \frac{\partial g^r_{\zeta c}}{\partial y} \right)$$

$$\bar{\bar{g}}_{t3} = \nabla_t \left\{ \hat{y} \frac{\partial}{\partial y} \left[g^r_{\zeta n} + g^r_{\zeta t} + \frac{\partial g^r_{\zeta c}}{\partial y} \right] \right\}.$$

It should be noted that while $\bar{\bar{g}}_{t1}$ and $\bar{\bar{g}}_{t3}$ are dyadic functions, g_{t2} is simply a vector quantity.

3.4 SUMMARY

Due to the inseparability of boundary conditions for the general integrated optical circuit, development of a Hertzian potential Green's dyad for this system is intractable. An integral equation, based on identifying an equivalent source system, circumvents this difficulty. An electric field integral equation (EFIE) for a generally heterogeneous dielectric, immersed within the cover of the tri-layered background, may be written as

$$\mathbf{E}(\mathbf{r}) = (k_c^2 + \nabla\nabla\cdot) \int_V \frac{\delta n^2(\mathbf{r}')}{n_c^2} \bar{\bar{G}}(\mathbf{r}|\mathbf{r}') \cdot \mathbf{E}(\mathbf{r}') \, dV' + \mathbf{E}^i(\mathbf{r}) \qquad (28)$$

where $\bar{\bar{G}}$ is the Hertzian potential Green's dyad for the layered surround and $\mathbf{E}^i$ is the impressed field which radiates in the absence of the dielectric obstacle. Solution to (28) is unique since it solution satisfies Maxwell's equations along with the appropriate boundary conditions across the surface of the optical device.

For an axially uniform guiding structure deposited within the cover, the integrand of (28) becomes convolutional in z as $\bar{\bar{G}} \cdot \mathbf{E}$. A Fourier

transform in z is prompted and leads to the transform domain EFIE

$$e(\rho, z) - (k_c^2 + \tilde{\nabla}\tilde{\nabla}\cdot) \int_{CS} \frac{\delta n^2(\rho')}{n_c^2} \bar{\bar{g}}_z(\rho|\rho') \cdot e(\rho', z)\, dS' = e^i(\rho, z) \quad (29)$$

where $e = F\{E\}$, $\bar{\bar{g}} = F\{\bar{\bar{G}}\}e^{-jzz'}$, and $\tilde{\nabla} = \nabla_t + \hat{z}jz$ is the transform of the del-operator.

Finally, in the transform domain, the transverse field components are uncoupled from the longitudinal component. The transform domain EFIE for the transverse components is written as

$$\begin{aligned} e_t(\rho, z) = e_t^i(\rho, z) &+ k_0^2 \int_{CS} \delta n^2(\rho')\, \bar{\bar{g}}_{t1}(\rho|\rho') \cdot e_t(\rho', z)\, dS' \\ &+ \int_{CS} \frac{\nabla_t' n^2(\rho')}{n^2(\rho')} \cdot e_t(\rho', z)\, g_{t2}(\rho|\rho')\, dS' \\ &- \int_\Gamma \frac{\delta n^2(\rho')}{n_c^2} g_{t2}(\rho|\rho')\, e_t(\rho', z) \cdot \hat{n}'\, dl' \\ &+ \int_{CS} \frac{\delta n^2(\rho')}{n_c^2} \bar{\bar{g}}_{t3}(\rho|\rho') \cdot e_t(\rho', z)\, dS' \end{aligned} \quad (30)$$

where the dyads $\bar{\bar{g}}_{t1}$ and $\bar{\bar{g}}_{t3}$, as well as the vector g_{t2} are given by

$$\bar{\bar{g}}_{t1} = \bar{\bar{I}} g_z^p + \hat{x} g_{zt}^r \hat{x} + \hat{y} \left(g_{zn}^r + \frac{\partial g_{zc}^r}{\partial y} \right) \hat{y}$$

$$g_{t2} = \hat{y} k_c^2 g_{zc}^r + \nabla_t \left(g_z^p + g_{zt}^r + \frac{\partial g_{zc}^r}{\partial y} \right)$$

$$\bar{\bar{g}}_{t3} = \nabla_t \left\{ \hat{y} \frac{\partial}{\partial y} \left[g_{zn}^r + g_{zt}^r + \frac{\partial g_{zc}^r}{\partial y} \right] \right\}.$$

CHAPTER FOUR

THE PROPAGATION-MODE SPECTRUM

4.1 INTRODUCTION

As was stated in Chapter three, the transform-domain EFIE (3.29) may be used to identify the propagation-mode spectrum of longitudinally invariant integrated dielectric waveguides. Analysis of solutions to (3.29) in the complex ζ-plane facilitates this identification. Use of Cauchy's theorem for contour integrals [17, pp.218-220] allows the initial real-line inversion-integral of the transform-domain electric field to be deformed. An appropriate choice of contour deformation reveals that the field decomposes into two types of modes.

Before identification of the propagation-modal types may be made, location of ζ-plane singularities of the transform-domain field must be determined. Due to the complicated nature of the integro-differential operator appearing in (3.29), firm mathematical statements regarding the locality of these singularities do not exist. Nevertheless, heuristic arguments which have intuitive appeal may be made to determine the placement of these singularities. These arguments are supported by situations for which solutions (or numerical approximation to solutions) are known (e.g. [20, pp.485-508]).

Existing singularities in the ζ-plane are either isolated (e.g. poles) or branch points with associated branch cuts. It is shown that at simple poles, modal fields satisfy the homogeneous transform-domain EFIE. These modes comprise a discrete spectrum which is associated with

surface waves supported by the waveguide. A continuous spectrum arises from solutions to the forced EFIE (3.29) along an appropriately chosen branch cut. It is argued that superposition of this continuous spectrum leads to the radiation field of the waveguide.

4.2 COMPLEX ζ-PLANE ANALYSIS

Inversion of the unknown transform-domain electric field in (3.29) can be obtained as the Cauchy principal value [17, p.317]

$$E(r) = \lim_{R\to\infty} \frac{1}{2\pi} \int_{-R}^{R} e(\rho, \zeta)\, e^{j\zeta z}\, d\zeta. \tag{1}$$

Deformation of this real-line integration requires knowledge of the singularities of e in the complex ζ-plane. Since e is described in (3.29) through the Green's dyad $\bar{\bar{g}}_\zeta$, it makes sense to discuss ζ-plane singularities associated with $\bar{\bar{g}}_\zeta$. It is argued that any ζ-plane branch point of $\bar{\bar{g}}_\zeta$ is also a branch point of e. After locating these branch points, a discussion of the appropriate branch cuts is given. Finally, Cauchy's theorem for contour integrals is used to determine the appropriate contour used in identifying the propagation spectrum.

4.2.1 GREEN'S DYAD ζ-PLANE SINGULARITIES

As seen in the previous chapter, scalar components $g_{\zeta\alpha\beta}$ of $\bar{\bar{g}}_\zeta$ are represented by spectral integrals having the generic form

$$g_{\zeta\alpha\beta}(\rho|\rho') = \int W_{\alpha\beta}(\lambda)\, \frac{e^{-p_c|y\pm y'|}}{4\pi p_c}\, e^{j\xi(x-x')}\, d\xi. \tag{2}$$

The integrand of (2) has a complicated functional dependence on the wavenumbers $p_i = (\xi^2 + \zeta^2 - k_i^2)^{1/2}$. The signs of these square roots are chosen to satisfy the physical constraints which require waves to decay

and propagate outwardly. These conditions are satisfied when $Re(p_i) > 0$ and $Im(p_i) > 0$.

Note that integration in (2) passes through $\zeta = 0$, whence $p_i = \gamma_i$ where $\gamma_i = (\zeta^2 - k_i^2)^{1/2}$. In order to ensure that p_i remain single-valued, it is necessary that γ_i is single-valued with $Re(\gamma_i) > 0$ and $Im(\gamma_i) > 0$. Therefore, $\bar{\bar{g}}_\zeta$ has branch points at $\pm k_i$ in the complex ζ-plane. Branch points at $\pm k_f$ are removable singularities, hence not implicated, since all integrands for the components of $\bar{\bar{g}}_\zeta$ are even functions of p_f.

4.2.2 ELECTRIC FIELD ζ-PLANE SINGULARITIES

An indirect method of proof may now be used to show that e shares the branch points of $\bar{\bar{g}}_\zeta$. Assume that e is an even function of γ_c (γ_s) so that the singularities at $\zeta = \pm k_c$ ($\zeta = \pm k_s$) are removable. Then the inner product of $\bar{\bar{g}}_\zeta$ with e, which appears in the integral operator for the scattered field of (3.29), yields a function which has branch points at $\pm k_c$ ($\pm k_s$). Since both the scattered and impressed fields have these singularities, so does their sum. The sum of the scattered and impressed fields is the total field e which was assumed to have removable singularities at $\zeta = \pm k_c$ ($\zeta = \pm k_s$). This is the desired contradiction which establishes that e must have branch points at $\pm k_c$ ($\pm k_s$).

In addition to the branch point singularities, e may have a finite number of isolated singularities. The existence of a pole singularity depends on the cutoff characteristics associated with the waveguide. Chapter five is devoted to a detailed discussion of this topic. For the present, it is assumed that a finite number 2N of simple poles exist at $\zeta = \pm\zeta_n$ ($n=1,\ldots,N$). The possibility that e has poles of higher order is discussed.

Figure 14 shows the location of the singularities of e in the complex ζ-plane. Real and imaginary parts of ζ are designated ζ_r and ζ_i respectively. Under the assumption that the optical system has limitingly small loss, all singularities reside in quadrants two and four and are infinitesimally displaced off the real ζ-axis. Simple poles are confined to the region such that $|k|_{max} > |(\zeta_n)|_{max} > |k_s|$ where $|k|_{max}$ is the maximum value of $k = n(\rho)k_0$. Branch cut lines originate from each branch point and extend to the point at infinity. At this stage, these cuts may be chosen arbitrarily so long as they do not intersect the initial inversion integral. Subsequent analysis involving contour deformation demands a particular choice for the branch cuts.

4.2.3 CONTOUR DEFORMATION

Calculus of residues provides a poverful analytic technique for evaluating certain types of definite integrals. Specifically, the residue theorem [17, p.275] may be used to deform the initial real-line inversion integral in (1). The details of this deformation are given below.

Consider the closed contour C in the complex ζ-plane as shown in Figure 15. The line segment $-R < \zeta_r < R$ is closed in the upperhalf (loverhalf) plane with a contour consisting of the upperhalf (loverhalf) C_R of the circle $|\zeta| = R$ which detours around the branch cuts C_b. Since $e(\rho, \zeta)\ \exp(j\zeta z)$ is analytic inside and on C except at the points ζ_n $(\pm\zeta_n)$, the residue theorem guarantees

$$\int_C e(\rho, \zeta)\ e^{j\zeta z}\ d\zeta = 2\pi j \sum_n \mathrm{Res}_n[e(\rho, \zeta)e^{j\zeta z}]$$

where C is taken in the positive sense and $\mathrm{Res}_n[\ ]$ denotes the residue

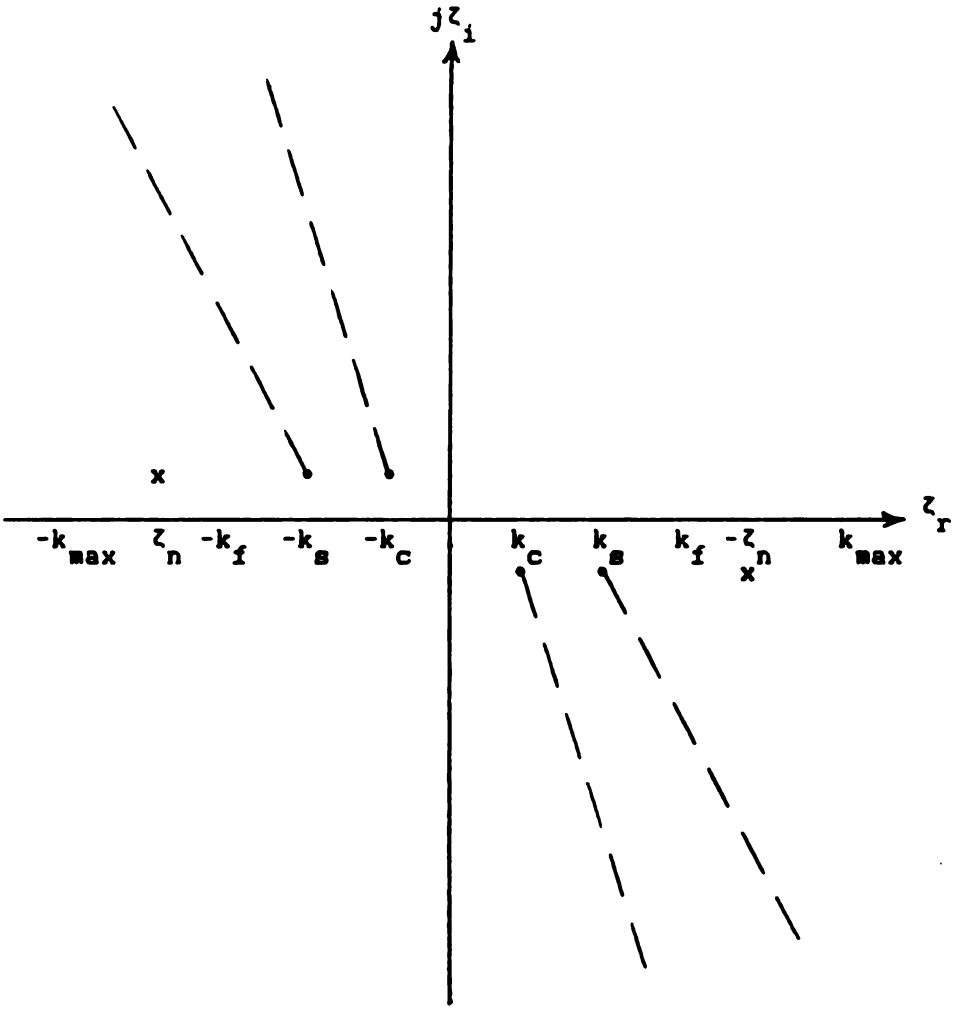

Figure 14. Complex ζ-plane singularities of the transform-domain electric field.

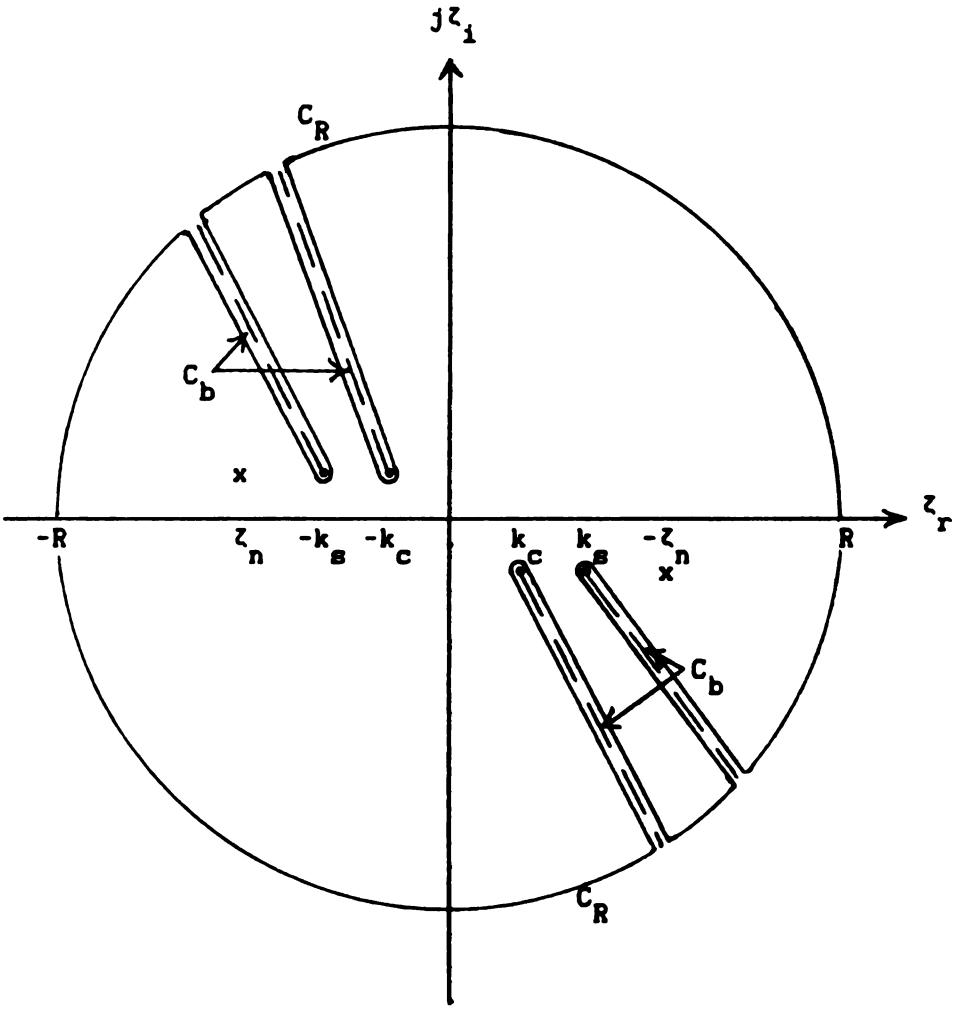

Figure 15. Closed contour C in and on which the transform-domain electric field is analytic except at $\zeta = \zeta_n$.

of the bracketed quantity at ζ_n ($\pm\zeta_n$) within the closed contour C. It is now seen that

$$\int_{-R}^{R} e(\rho,\zeta)\, e^{j\zeta z}\, d\zeta = 2\pi j \sum \mathrm{Res}_n\{e(\rho,\zeta)e^{j\zeta z}\} - \int_{C_b+C_R} e(\rho,\zeta)\, e^{j\zeta z}\, d\zeta. \quad (3)$$

If the contours C_b of the branch cuts are chosen so that the integration over C_R vanishes as $R\to\infty$, then the space-domain electric field as given by (1) may be expressed as

$$E(r) = \frac{1}{2\pi}\{2\pi j \sum \mathrm{Res}_n\{e(\rho,\zeta)e^{j\zeta z}\} - \int_{C_b} e(\rho,\zeta)\, e^{j\zeta z}\, d\zeta\}. \quad (4)$$

It is now apparent that the electric field decomposes into the sum of two fundamentally different spectral superpositions. This decomposition is recognized as a sum of a discrete spectrum and an integration of a continuous spectrum. The considerations necessary to determine the appropriate branch cuts C_b, for which (4) is valid, are subsequently shown.

First, it must be decided in which half-plane the contour C is to be closed. Without loss of generality, this may be accomplished by assuming that the space-domain impressed source is a surface current located at z' such that $J(\rho',z) = J(r')\,\delta(z-z')\,dz'$ where $\delta(z-z')$ is a Dirac delta. Then the impressed field e^i is of the form

$$e^i(\rho,\zeta) = e^{-j\zeta z'} \int_{CS_\infty} (k_c^2 + \tilde{\tilde{\nabla}}\nabla\cdot)\, \tilde{\tilde{g}}_\zeta(\rho|\rho')\cdot \frac{J(r')}{j\omega\varepsilon_c}\, dS'\, dz'$$

where CS_∞ is the infinite transverse cross section. Obviously, e^i is proportional to $e^{-j\zeta z'}$. Exploiting the linearity of (3.29), the total field e must also be proportional to $e^{-j\zeta z'}$. Hence, the exponential factor $e^{j\zeta(z-z')}$ appears as part of the integrand in (3). In the upper-half (loverhalf) plane, this exponential factor is decaying for $z-z' > 0$

$(z-z^{*} < 0)$ while it increases exponentially for $z-z^{*} < 0$ $(z-z^{*} > 0)$. Hence, C must be closed in the upperhalf (loverhalf) plane when $z > z^{*}$ $(z < z^{*})$ so that on C_R, $e^{-j\zeta(z-z^{*})}$ vanishes as $R\to\infty$.

Second, the branches for each γ_i must be chosen so that the integrand of (2) represents a decaying and outward-propagating wave. This requires that $\mathrm{Re}\{\gamma_i\} > 0$ and $\mathrm{Im}\{\gamma_i\} > 0$ along the initial real-line inversion contour. Figure 16 is helpful in determining these branches. Writing $\gamma_i = (\zeta - k_i)^{1/2}\,(\zeta + k_i)^{1/2}$, it is seen that the arguments of each factor satisfy the inequalities

$$0 < \arg(\zeta - k^{i})^{1/2} < \pi/2$$

$$-\pi/2 < \arg(\zeta + k_i)^{1/2} < 0$$

since $0 < \theta_i^{+} < \pi$ and $-\pi < \theta_i^{-} < 0$. A careful examination shows that the sum of these arguments satisfies $0 < \theta_i^{+} + \theta_i^{-} < \pi$. Hence, the argument of γ_i lies in the interval $0 < \arg(\gamma_i) < \pi/2$. Thus, on the proper branch, the positive root of γ_i must be chosen.

Finally, consider the behavior of e along C_R. Inasmuch as e is described in (3.29) through the Green's dyad $\bar{\bar{g}}_{\zeta}$, it is intuitively expected that as $|\zeta|\to\infty$, e should exhibit asymptotic properties similar to those of $\bar{\bar{g}}_{\zeta}$. It can be seen that for $\zeta \in C_R$, $\bar{\bar{g}}$ increases without limit (approaches zero) as $R\to\infty$ for $\mathrm{Re}\{\gamma_i\} < 0$ $(\mathrm{Re}\{\gamma_i\} > 0)$. Hence,

$$\lim_{R\to\infty} \max\, |e(\rho,\zeta)\, e^{j\zeta z^{*}}| = 0. \tag{5}$$

In order to ensure that C_R remains on the proper branch for which $\mathrm{Re}\{\gamma_i\} > 0$, the branch cut emanating from k_i must be the boundary which separates the proper and improper branches. Thus, C_b must be the contour defined by $\mathrm{Re}\{\gamma_i\} = 0$. Observe that when $\mathrm{Re}\{\gamma_i\} = 0$, γ_i^2 satisfies

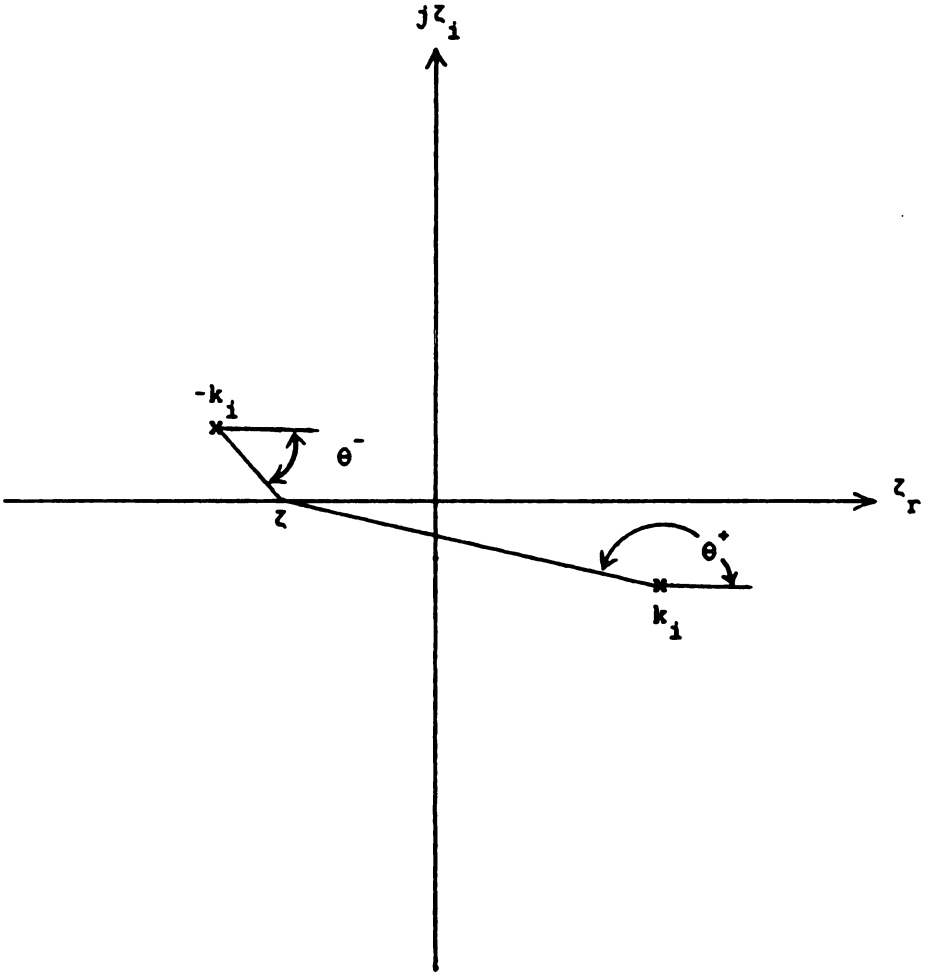

Figure 16. Determination of the proper branch for each γ_i.

both (i) $\mathrm{Im}(\gamma_i^2) = 0$ and (ii) $\mathrm{Re}(\gamma_i^2) < 0$. Writing $k_i = k_i' - jk_i''$, γ_i^2 may be written as

$$\gamma_i^2 = [(\zeta_r^2 - \zeta_i^2) - (k_i'^2 - k_i''^2)] + j2[\zeta_r\zeta_i + k_i'k_i'']$$

from which it can be seen that condition (i) is satisfied if and only if

$$\zeta_r\zeta_i = -k_i'k_i''. \tag{6}$$

Along the hyperbolas defined by (6), $\mathrm{Re}(\gamma_i^2) = \zeta_r^{-2}(\zeta_r^2 - k_i'^2)(\zeta_r^2 + k_i''^2)$. In order to satisfy condition (ii), ζ_r must satisfy the inequality

$$-k_i' < \zeta_r < k_i'. \tag{7}$$

Conditions (6) and (7) describe the portions of the hyperbolas shown in Figure 17. A decrease in the losses associated with the cover and substrate implies a decrease in k_s'' and k_c''. In the limit of zero loss, the hyperbolic branch cuts emanating from k_s and k_c coalesce resulting in the contour depicted in Figure 18. In either the case of moderate loss or limitingly low loss, these branch cuts guarantee that for all $\zeta \in C_R$, $\mathrm{Re}(\gamma_i) > 0$. Use of Jordan's Lemma [17, pp.303-305] along with (5) assure that

$$\lim_{R\to\infty} \int_{C_R} e(\rho,\zeta)\, e^{j\zeta z}\, d\zeta = 0$$

assuring the validity of (4). With the appropriate contour deformation determined, analysis of the discrete and continuous spectrums proceeds.

4.3 THE DISCRETE SPECTRUM

A discrete-mode propagation spectrum has been shown to arise from evaluation of the residues of e at poles in the complex ζ-plane. In practice, it is an extremely difficult task to determine these residues

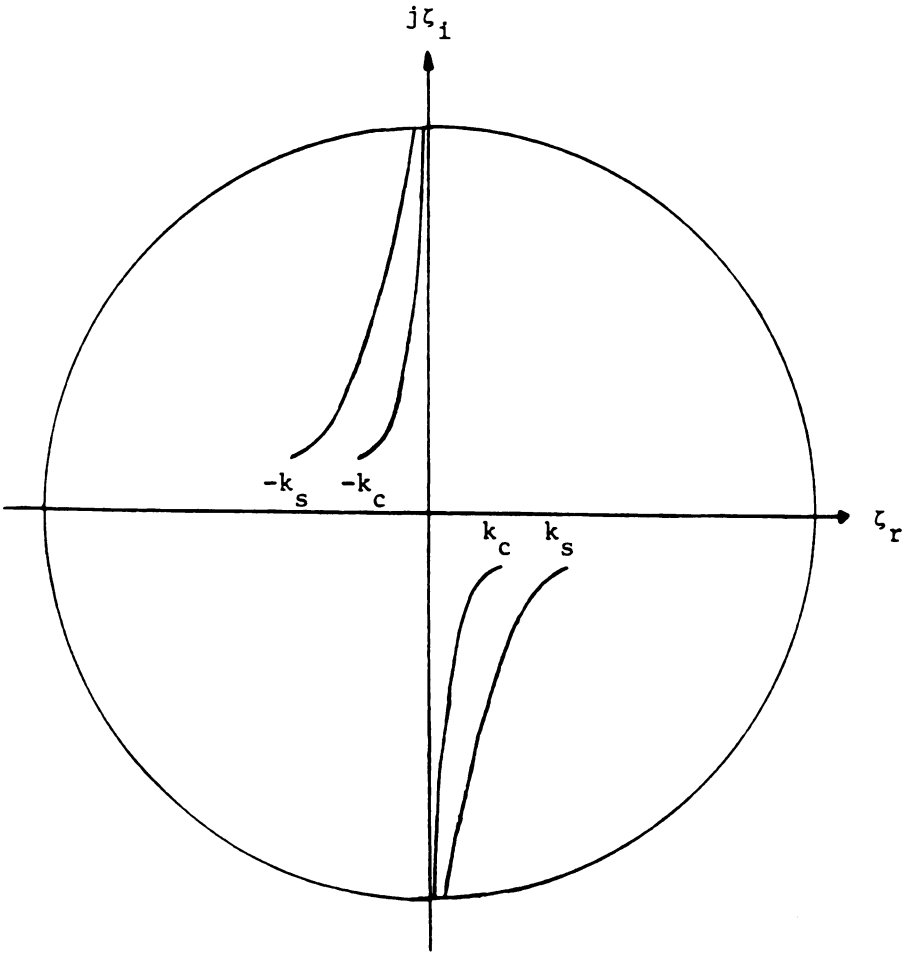

Figure 17. Hyperbolic branch cuts.

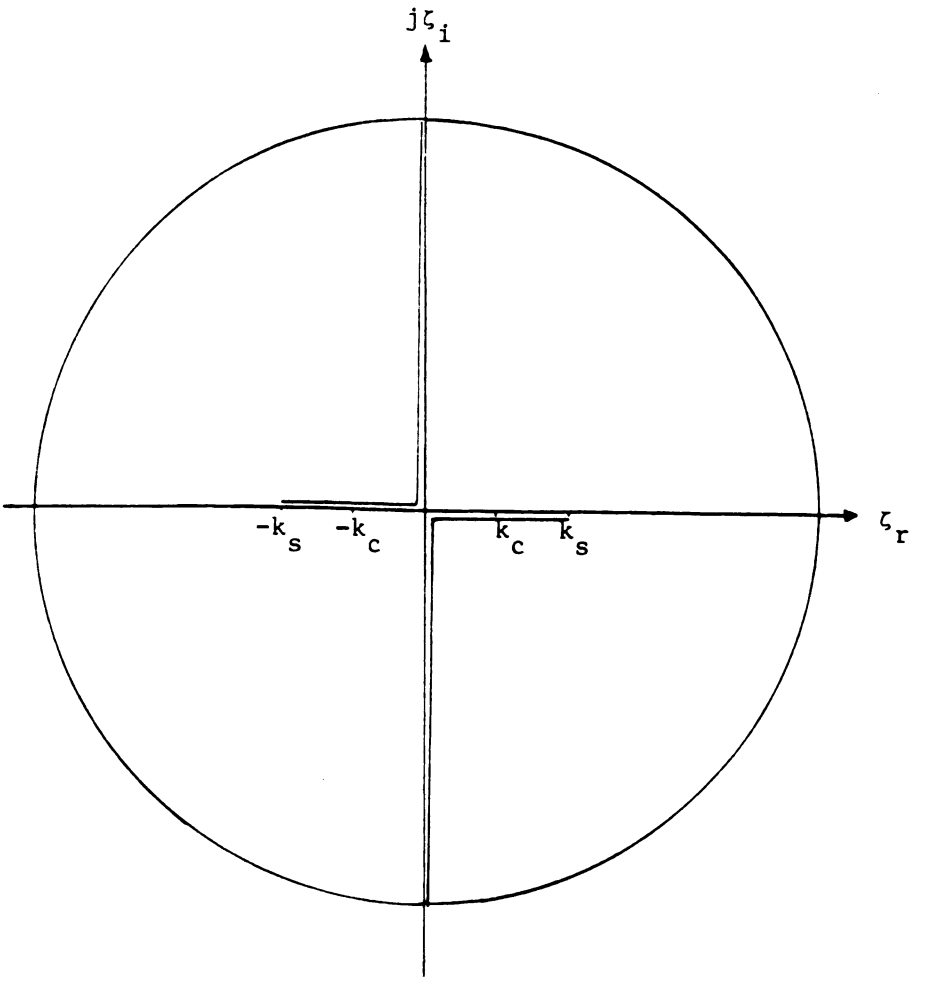

Figure 18. Coalesced branch cuts.

due to the unknown order of the pole singularity. In this section, a recursive procedure for obtaining the residue through knowledge of the order of the pole is presented along with a method to determine the pole order. Finally, a discussion of the regimes of surface-wave leakage and purely-guided waves is given.

4.3.1 DETERMINING THE RESIDUE

Under the assumption that e has no essential singularities, the principal part of its Laurent series terminates in some neighborhood of ζ_n. Assuming that e has a pole of order M at ζ_n, its Laurent series may be written

$$e(\rho,\zeta) = \frac{e_{-M}(\rho)}{(\zeta-\zeta_n)^M} + \ldots + \frac{e_{-1}(\rho)}{(\zeta-\zeta_n)^1} + \sum_{m=0}^{\infty} e_m(\rho)\,(\zeta-\zeta_n)^m \tag{8}$$

for $0 < |\zeta - \zeta_n| < \bar{\zeta}$ for some $\bar{\zeta}$. Substituting (8) into (3.29) yields

$$\sum_{m=-M}^{\infty} e_m(\rho)\,(\zeta-\zeta_n)^m = \mathcal{L}_{op}\left\{\sum_{m=-M}^{\infty} e_m(\rho)\,(\zeta-\zeta_n)^m\right\} + e^i(\rho,\zeta) \tag{9}$$

where the linear operator $\mathcal{L}_{op}$ is defined by

$$\mathcal{L}_{op}(\cdot) = (k_c^2 + \tilde{\tilde{\nabla}}\tilde{\tilde{\nabla}}\cdot)\int_{CS} \frac{\delta n^2(\rho')}{n_c^2}\,\tilde{\tilde{g}}_\zeta(\rho|\rho')\cdot(\cdot)\,dS'. \tag{10}$$

By choosing $\bar{\zeta}$ sufficiently small, the impressed field e^i and the operator $\mathcal{L}_{op}$ are analytic functions of ζ for all $|\zeta - \zeta_n| < \bar{\zeta}$ and may be expressed by the Taylor series at ζ_n

$$e^i(\rho,\zeta) = \sum_{m=0}^{\infty} e_m^i(\rho)\,(\zeta-\zeta_n)^m \tag{11a}$$

$$\mathcal{L}_{op}(\cdot) = \sum_{m=0}^{\infty} \mathcal{L}_{op_m}(\cdot)\,(\zeta-\zeta_n)^m \tag{11b}$$

where the coefficients in the series are given by

$$e_m^i(\rho) = \frac{1}{m!} \frac{\partial^m e^i(\rho, \zeta_n)}{\partial \zeta_n^m}$$

$$\ell_{op_m}(\cdot) = \frac{1}{m!} \frac{\partial^m \ell_{op}(\cdot)}{\partial \zeta^m} \Bigg|_{\zeta=\zeta_n}.$$

Substitution of expressions (11a) and (11b) into (9) reveals

$$\sum_{m=-M}^{\infty} e_m(\rho)\ (\zeta - \zeta_n)^m = \sum_{i=0}^{\infty} \ell_{op_i} \left\{ \sum_{m=-M}^{\infty} e_m(\rho)\ (\zeta - \zeta_n)^m \right\} (\zeta - \zeta_n)^i + \sum_{m=0}^{\infty} e_m^i(\rho)\ (\zeta - \zeta_n)^m$$

$$= \sum_{m=-M}^{\infty} \sum_{i=0}^{\infty} \ell_{op_i}\{e_m(\rho)\}\ (\zeta - \zeta_n)^{i+m} + \sum_{m=0}^{\infty} e_m^i(\rho)\ (\zeta - \zeta_n)^m \tag{12}$$

By making the change of indices $q=i+m$ and appropriately changing the order of summations, the double series may be converted into a single series so that (12) becomes

$$\sum_{m=-M}^{\infty} e_m(\rho)\ (\zeta - \zeta_n)^m = \sum_{m=-M}^{\infty} \left[\sum_{i=0}^{M+m} \ell_{op_i}\{e_{m-i}(\rho)\} \right] (\zeta - \zeta_n)^m + \sum_{m=0}^{\infty} e_m^i(\rho)\ (\zeta - \zeta_n)^m. \tag{13}$$

Uniqueness of series representation allows coefficients to be equated term by term from which the following relations are obtained:

$$e_m(\rho) = \sum_{i=0}^{M+m} \ell_{op_i}\{e_{m-i}(\rho)\} \qquad \ldots\ -M \le m < 0$$

$$e_m(\rho) = \sum_{i=0}^{M+m} \ell_{op_i}\{e_{m-i}(\rho)\} + e_m^i(\rho) \quad \ldots\ \ 0 \le m. \tag{14}$$

As can be seen from (14), $e_{-M}(\rho)$ satisfies the homogeneous form of the transform-domain EFIE (3.29)

$$e_{-M}(\rho) - (k_c^2 + \tilde{\nabla}_n \tilde{\nabla}_n \cdot) \int_{CS} \frac{\delta n^2(\rho')}{n_c^2} \bar{g}_{\zeta_n}(\rho|\rho') \cdot e_{-M}(\rho)\, dS' = 0 \tag{15}$$

where $\tilde{\nabla}_n$ and $\tilde{\bar{g}}_{\zeta_n}$ are respectively the del-operator and the transform-domain Hertzian potential Green's dyad evaluated at $\zeta=\zeta_n$. After solving (15) for e_{-M}, (14) may be used to obtain the forced EFIE

$$e_{1-M}(\rho) - \mathcal{L}_{op_0}\{e_{1-M}(\rho)\} = \mathcal{L}_{op_1}\{e_{-M}(\rho)\}.$$

A recursive relation results and the residue e_{-1} satisfies the EFIE

$$e_{-1}(\rho) - \mathcal{L}_{op_0}\{e_{-1}(\rho)\} = \sum_{i=1}^{M-1} \mathcal{L}_{op_i}\{e_{-1-i}(\rho)\}.$$

In the special case where $M = 1$, the residue satisfies the homogeneous transform-domain EFIE

$$e_{-1}(\rho) - (k_c^2 + \tilde{\nabla}_n\tilde{\nabla}_n\cdot) \int_{CS} \frac{\delta n^2(\rho')}{n_c^2} \tilde{\bar{g}}_{\zeta_n}(\rho|\rho')\cdot e_{-1}(\rho)\, dS' = 0. \quad (16)$$

In order for this recursive procedure to be useful, knowledge of the order of the pole is required. A method for establishing the order of a pole singularity is now given.

4.3.2 DETERMINATION OF POLE ORDER

As was shown in the previous section, solution to the homogeneous transform-domain EFIE (15) yields a function proportional to the leading term in the Laurent expansion of the solution to the forced EFIE. Operating on each side of (3.29) with the inner product operator defined by

$$\langle e_{-M}| = \int_{CS} dS\ \frac{\delta n^2(\rho)}{n_c^2} e_{-M}(\rho)\ \cdot$$

leads to the equation

$$\langle e_{-M}|e\rangle = \langle e_{-M}|\mathcal{L}_{op}(e)\rangle + \langle e_{-M}|e^i\rangle. \quad (17)$$

As asserted by Bagby, Nyquist and Drachman [21], the reciprocity relation for the electric Green's dyad as stated by Collin [20] is valid for the transform-domain Green's dyad. Therefore, (17) can be written

$$\langle e_{-M} | e \rangle = \langle e | \mathcal{L}_{op}(e_{-M}) \rangle + \langle e_{-M} | e^{i} \rangle \tag{18}$$

whereby substitution of the Taylor series (11b) for the operator $\mathcal{L}_{op}$ into (18) results in

$$\langle e_{-M} | e \rangle = \sum_{m=0}^{\infty} \langle e | \mathcal{L}_{op_m}(e_{-M}) \rangle (\zeta - \zeta_n)^m + \langle e_{-M} | e^{i} \rangle. \tag{19}$$

Notice that the first term in the series of (19) contains the inner product $\langle e | \mathcal{L}_{op_m}(e_{-M}) \rangle$. Use of (15) along with the commutative property of the inner product allows (19) to be written

$$\sum_{m=1}^{\infty} \langle e | \mathcal{L}_{op_m}(e_{-M}) \rangle (\zeta - \zeta_n)^m = - \langle e_{-M} | e^{i} \rangle \tag{20}$$

Substituting the Laurent series (8) for e into (20) and manipulating the resulting double series reveals

$$\sum_{m=1-M}^{\infty} \left[\sum_{i=1}^{M+m} \langle e_{m-i} | \mathcal{L}_{op_i}(e_{-M}) \rangle \right] (\zeta - \zeta_n)^m = - \langle e_{-M} | e^{i} \rangle. \tag{21}$$

Since the right side of (21) is not singular at $\zeta = \zeta_n$, uniqueness of series representation implies that either M = 1 or

$$\sum_{i=1}^{M+m} \langle e_{m-i} | \mathcal{L}_{op_i}(e_{-M}) \rangle = 0 \quad \text{... for } m = 1-M,\ 2-M, \ldots,\ -1. \tag{22}$$

Pole order M may be deduced from (22) by determining the number of values m for which $1-M \leq m \leq -1$. However, in all of the waveguiding structures which have thus far been investigated, all poles have been simple [22]. In this case, M=1 and the amplitude coefficient a_n of the modal function e_{-1} can be extracted from (20). Let $e(\rho) = a_n e_{-1}(\rho)$ in (20).

Equating the leading terms of each series in (20) and solving for a_n yields

$$a_n = - \langle e_{-1} | e_0^i \rangle / \langle e_{-1} | \mathcal{L}_{op_1} (e_{-1}) \rangle .$$

By exploiting the reciprocal property of the electric Green's dyad and using (15) with M=1, a_n assumes the familiar form

$$a_n = - \frac{1}{j\omega\epsilon_c} \int_V J(r) \cdot e_{-1}(\rho)\, e^{-j\zeta_n z}\, dV \; / \; \langle e_{-1} | \mathcal{L}_{op_1} (e_{-1}) \rangle$$

which agrees, modulo the form of the normalization, to that given by Collin [20, pp. 483-485].

4.3.3 SURFACE-WAVE LEAKAGE

The physical phenomenon of surface-wave leakage from open-boundary integrated dielectric waveguides was identified Peng and Oliner [2,3] through use of an elaborate mode-matching method. A leaky wave is a surface wave which propagates in a direction deviating from the wave-guiding axis. As stated in [2,3], leakage may actually be a desirable effect in certain applications of novel devices such as a leaky-wave directional coupler. However, the waveguide is usually used as a component in an optical or millimeter-wave integrated circuit, and this leakage can cause unwanted coupling between circuit devices. It is therefore essential to know which modes, if any, of a particular guiding structure are leaky. An examination of the homogeneous transform-domain EFIE is used to predict whether a mode is leaky or purely guided.

Suppose that e has a simple pole at $\zeta = \zeta_n$. Then the residue e_{-1} satisfies the homogeneous transform-domain EFIE (16). Scalar components $(g^r_{\zeta_n})_{\alpha\beta}$ of the reflected Green's dyad appearing in (16) are of the form

$$(g^{r}_{\zeta_n})_{\alpha\beta}(\rho|\rho') = \int W_{\alpha\beta}(\lambda)\, \frac{e^{-p_c(\lambda)(y+y')}}{4\pi p_c(\lambda)}\, e^{j\xi(x-x')}\, d\xi \qquad (23)$$

where $W_{\alpha\beta}$ is representative of R_t, R_n and C. An alternative form for (23) may obtained by deforming the initial real-line integral in the complex ξ-plane. The ξ-plane singularities of the integrand of (23) consist of branch points at $\pm(\zeta_n - k_c^2)^{1/2}$ and $\pm(\zeta_n - k_s^2)^{1/2}$ along with associated branch cuts and a finite number of poles at $\xi_p = \pm(\lambda_p^2 - \zeta_n^2)^{1/2}$ where λ_p corresponds to the poles of $W_{\alpha\beta}$. If the branch cuts are taken along the familiar infinitesimal-loss hyperbolic contours shown in Figure 19, then the analysis of section 4.2.3 applies to the deformation of the initial real-line integral in (23) and the scalar components of $g^{r}_{\zeta_n}$ may be written

$$(g^{r}_{\zeta_n})_{\alpha\beta}(\rho|\rho') = \sum_p \mathrm{Res}[W_{\alpha\beta}(\lambda)]\, \frac{e^{-p_c(\lambda_p)(y+y')}}{4\pi p_c(\lambda_p)}\, e^{j\xi_p|x-x'|}$$

$$- \int_{C_b} W_{\alpha\beta}(\lambda)\, \frac{e^{-p_c(\lambda)(y+y')}}{4\pi p_c(\lambda)}\, e^{j\xi|x-x'|}\, d\xi \qquad (24)$$

where evidently $(g^{r}_{\zeta_n})_{\alpha\beta}$ decomposes into the sum of a discrete spectrum and integration of a continuous spectrum.

Observing that λ_p is confined in the interval $k_s < \lambda_p < k_f$ whereas ζ_n lies within the interval $k_s < \zeta_n < k_{max}$, it is clear that either $\zeta_n > \lambda_p$ or $\zeta_n < \lambda_p$ are possible. If $\zeta_n > \lambda_p$, then $\xi_p = (\lambda_p^2 - \zeta_n^2)^{1/2}$ must be purely imaginary and the x-dependent function appearing in the residue series of (24) is exponentially decaying. In this case, the time-averaged transverse power flow is zero and the surface wave is purely bound. On the other hand, if $\zeta_n < \lambda_p$, then ξ_p is purely real and power is transported transversely. This leaky wave propagates in the direction

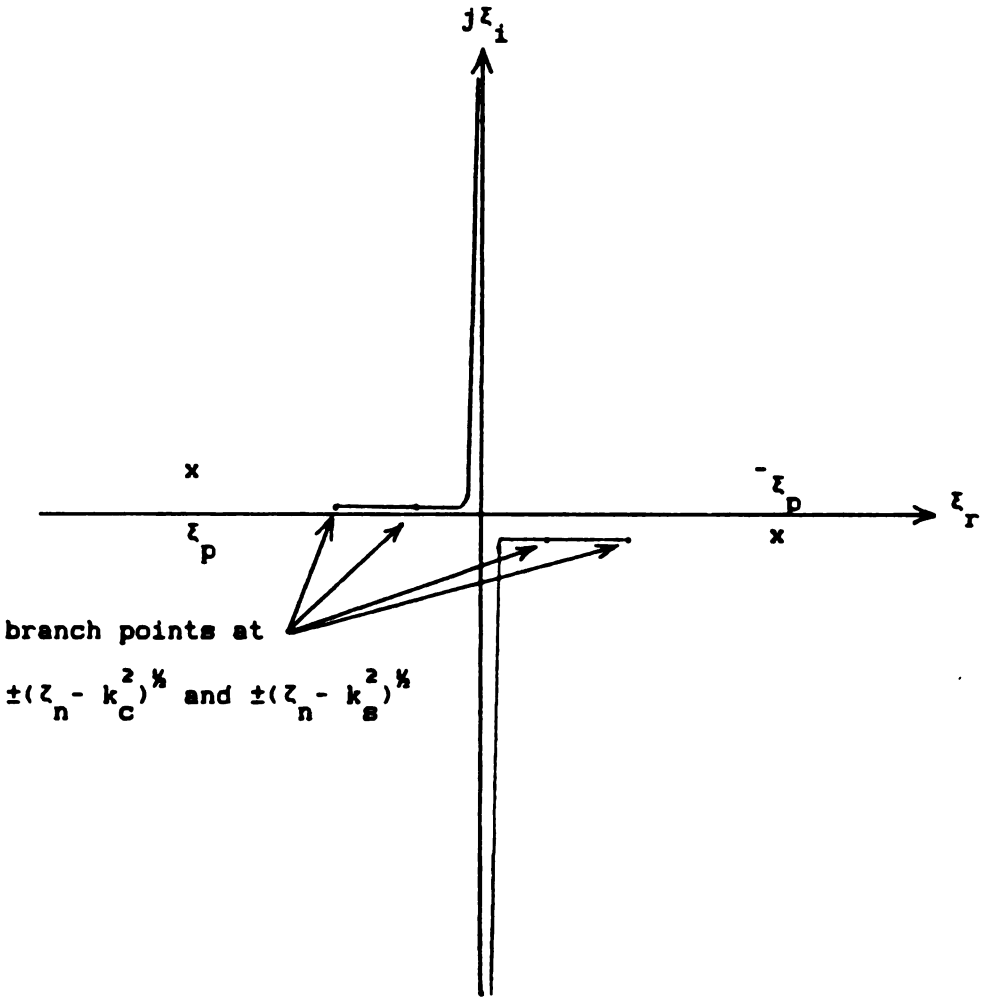

Figure 19. Hyperbolic branch cuts in the complex ξ-plane in the limit of low loss.

which makes an angle $\theta = \tan^{-1}[\mathrm{Re}(\xi_p)/\mathrm{Re}(\zeta_n)]$ with the waveguiding axis. This agrees with the result given in [2,3].

4.4 THE CONTINUOUS SPECTRUM

A continuous-mode propagation spectrum has been shown to arise from solutions to the forced transform-domain EFIE (3.29) at each point along the hyperbolic branch cut C_b shown in Figure 18. An examination of the spatially dependent functions which appear in the integrand of $\bar{\bar{g}}_\zeta$ reveals that $\bar{\bar{g}}_\zeta$ is a spectral superposition of oscillatory y-dependent waves. Hence, the continuous spectrum is appropriately called the radiation spectrum.

Each spectral component of the radiation spectrum may be regarded as a superposition of solutions to the transform-domain EFIE with elementary (point source) excitation. Consider the form of the impressed field e^i as given by

$$e^i(\rho,\zeta) = \int_{CS_\infty} (k_c^2 + \tilde{\tilde{\nabla}}\tilde{\tilde{\nabla}}\cdot)\, \bar{\bar{g}}_\zeta(\rho|\rho^s)\cdot \frac{j(\rho^s,\zeta)}{j\omega\epsilon_c}\, dS^s$$

$$= \int_{CS_\infty} \left(\int \bar{\bar{I}}_g(\rho|\rho^s;\xi,\zeta)\cdot \frac{j(\rho^s,\zeta)}{j\omega\epsilon_c}\, d\xi \right) dS^s$$

where $\bar{\bar{I}}_g(\rho|\rho^s;\xi,\zeta)$ is the integrand of the spectral representation of $(k_c^2 + \tilde{\tilde{\nabla}}\tilde{\tilde{\nabla}}\cdot)\, \bar{\bar{g}}_\zeta(\rho|\rho^s)$. A unit point source of current located at $\rho^s = \rho'$ and polarized along $\hat{\alpha}$ ($\hat{\alpha} = \hat{x}$, $\hat{y}$, or $\hat{z}$) produces a component of impressed field given by $[\bar{\bar{I}}_g(\rho|\rho^s;\xi,\zeta)\cdot\hat{\alpha}]/j\omega\epsilon_c$. This elementary impressed field maintains the elementary radiation spectral component $R_\alpha(\rho|\rho^s;\xi,\zeta)$ which satisfies the transform-domain EFIE

$$R_\alpha(\rho|\rho';\xi,\zeta) = (k_c^2 + \tilde{\tilde{\nabla}}\tilde{\tilde{\nabla}}\cdot) \int_{CS_\infty} \frac{\delta n^2(\rho')}{n_c^2} \bar{\bar{g}}_\zeta(\rho|\rho') \cdot R_\alpha(\rho'|\rho';\xi,\zeta)\, dS'$$

$$+ [\bar{\bar{I}}_g(\rho|\rho';\xi,\zeta) \cdot \hat{\alpha}]/j\omega\epsilon_c .$$

Defining a radiation spectral dyad $\bar{\bar{R}}$ by

$$\bar{\bar{R}}(\rho|\rho';\xi,\zeta) = \sum_\alpha R_\alpha(\rho|\rho';\xi,\zeta)\, \hat{\alpha}$$

the total radiation field E^R is given by

$$E^R(r) = -\frac{1}{2\pi} \int_{C_b} d\zeta\, e^{j\zeta z} \int d\xi \int_{CS_\infty} \bar{\bar{R}}(\rho|\rho';\xi,\zeta) \cdot \frac{j(\rho',\zeta)}{j\omega\epsilon_c}\, dS'$$

which verifies the conjecture [23] that the total radiation field may be obtained by a two dimensional spectral integration.

4.5 SUMMARY

Identification of the propagation-mode spectrum of axially uniform integrated dielectric waveguides may be made by analyzing solutions to (3.29) in the complex ζ-plane. By appropriately deforming the initial real-line inversion integral of the transform-domain electric field, the space-domain field E may be expressed as

$$E(r) = \frac{1}{2\pi} \left(2\pi j \sum \mathrm{Res}_n [e(\rho,\zeta) e^{j\zeta z}) - \int_{C_b} e(\rho,\zeta)\, e^{j\zeta z}\, d\zeta\right) \qquad (25)$$

where C_b is the hyperbolic branch cut shown in Figure 17. It can be seen from (25) that E decomposes into a superposition of two types of modes. A discrete-mode spectrum arises from evaluation of the residues of e at poles in the complex ζ-plane while spectral components of the continuous spectrum are solutions to (3.29) along the branch cut C_b.

The residue e_{-1} of e at a pole ζ_n is obtained by a recursive procedure. Under the assumption that e has no essential singularities, the

principal part of its Laurent series terminates. The leading term in the Laurent series e_{-M} ($M \geq 1$) is shown to satisfy the homogeneous EFIE

$$e_{-M}(\rho) - (k_c^2 + \tilde{\nabla}_n \tilde{\nabla}_n \cdot) \int_{CS} \frac{\delta n^2(\rho')}{n_c^2} \bar{g}_{\zeta_n}(\rho|\rho') \cdot e_{-M}(\rho)\, dS' = 0.$$

If $M > 1$, then higher order terms are solutions to the forced EFIE

$$e_m(\rho) = \sum_{i=0}^{M+m} \ell_{op_i}(e_{m-i}(\rho)) \quad \ldots\ 1-M \leq m \leq -1 \tag{26}$$

with ℓ_{op} given by (10). In order for (26) to be useful, it is necessary to determine M. This is accomplished by deducing the number of values m such that

$$\sum_{i=1}^{M+m} \langle e_{m-i} | \ell_{op_i}(e_{-M}) \rangle = 0 \quad \ldots \text{ for } m = 1-M,\ 2-M, \ldots,\ -1$$

is satisfied.

Surface-wave leakage is the phenomenon in which a surface wave propagates in a direction which deviates from the axis of the guiding structure. Through an analysis of the homogeneous transform-domain EFIE, regimes of leaky and purely-bounded waves are identified. If λ_p is a pole of the integrated background, then a purely-guided wave has a pole $\zeta_n < \lambda_p$. If $\zeta_n > \lambda_p$, then the surface wave is leaky and propagates in the direction which makes an angle $\theta = \tan^{-1}[\mathrm{Re}(\zeta_p)/\mathrm{Re}(\zeta_n)]$ with the waveguiding axis.

CHAPTER FIVE

AN ASYMPTOTIC EFIE

5.1 INTRODUCTION

In this chapter, an asymptotic form of the transform-domain EFIE (henceforth designated an AEFIE) is developed which is appropriate to the study of dielectric waveguides capable of supporting a surface-wave mode with no low-frequency cutoff. It is a conjecture that such a surface wave can exist on any axially-invariant dielectric waveguide immersed in a uniform surround. Although it is beyond the scope of this discussion to prove this claim, examples are given which provide evidence to support it.

By the simple example of the graded-index asymmetric slab waveguide, it is shown that unless the guiding surround is uniform, the existence of a surface-wave at limitingly low frequency cannot be guaranteed. Allowing the surround to become uniform, the asymptotic form of the fields and propagation numbers for the TE and TM modes are computed directly from the integral equation formulation. Specializing the situation to the step-index symmetric slab waveguide, these limiting forms are shown to agree with the small argument approximation of the well known results as given by Marcuse [10, pp.13,16].

Next, the step-index circular fiber is examined. Again, both the asymptotic field and propagation number are extracted from the AEFIE. These results are shown to concur with a small argument approximation to the well known results as given by Johnson [24].

Aside from the academic purpose of proving the aforementioned hypothesis, the (AEFIE) provides a favorable alternative to numerically implementing the non-asymptotic EFIE in the investigation of surface waves propagating in the regime where the phase constant approaches the wavenumber of the surround. While no numerical results are given here, this is suggested as possible research for the future.

5.2 THE GRADED-INDEX ASYMMETRIC SLAB WAVEGUIDE

The geometry of the graded-index asymmetric slab is shown in Figure 20. A guiding region of thickness t and refractive index n(y) is deposited over a substrate region ($y < 0$) which is characterized by index of refraction n_s. The cover region ($y > t$) has refractive index n_c. Obviously, the background of this guide is a specialization of the tri-layered surround with $n_f = n_s$. It is assumed that the excitation of this system is uniform along x, thereby rendering the total electric field e independent of x.

The x-invariance of e allows a specialized form of the transform-domain EFIE (3.30) for the transverse field to be formulated from which a pair of uncoupled integral equations for e_x and e_y are readily developed. This latter derivation is lengthy but the resulting equations simplify the subsequent analysis. The EFIE for the x-component of field is used to show that dielectric waveguides immersed in a non-uniform surround can be incapable of supporting a surface wave which has no low-frequency cutoff. For the special case in which the background is uniform, the uncoupled integral equations are used to obtain asymptotic ($\gamma_c \to 0$) forms of the propagation wavenumbers for two independent modal types which agree with well known results for step-index guides.

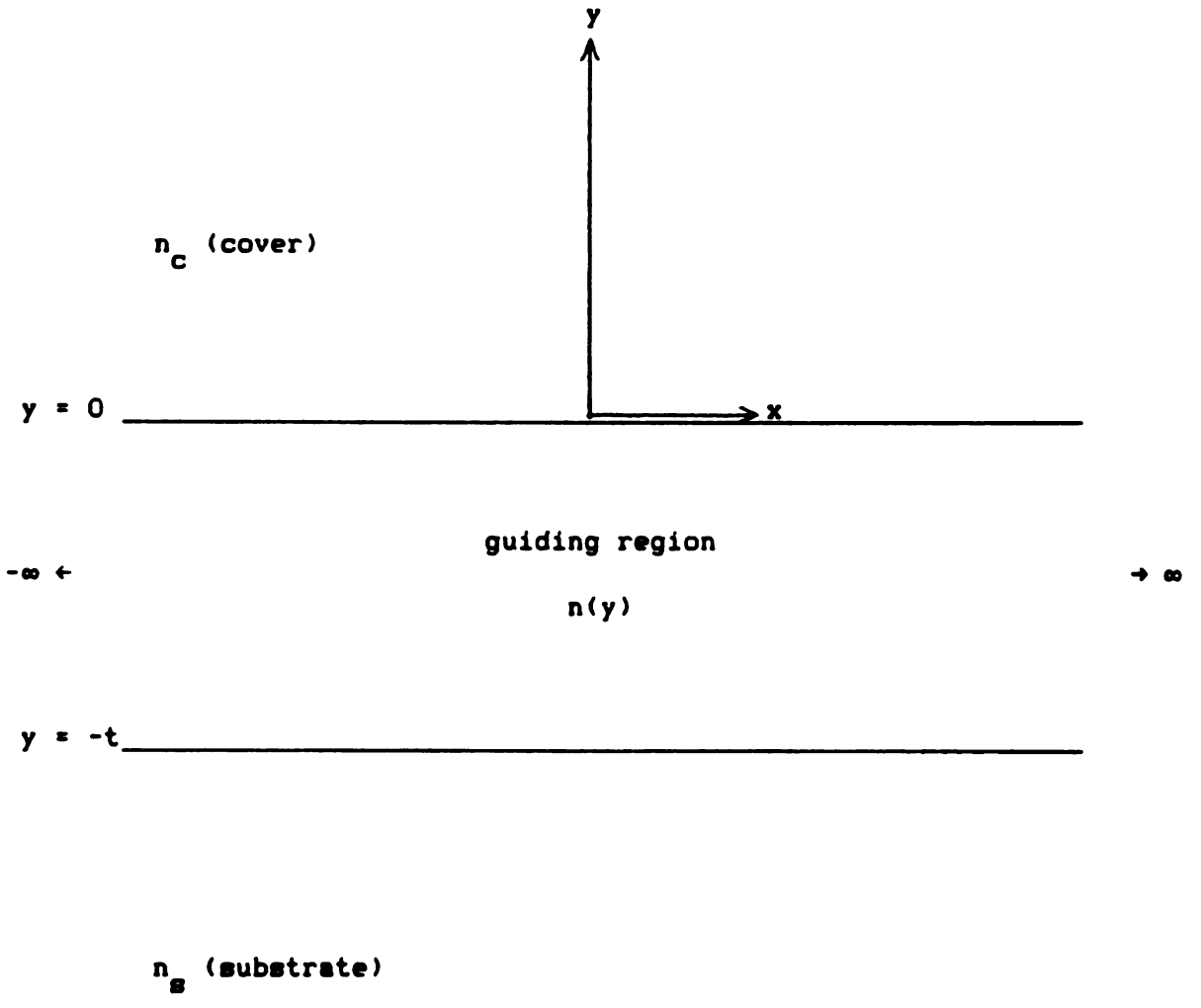

Figure 20. The graded-index asymmetric slab waveguide.

5.2.1 EFIE FOR THE ASYMMETRIC SLAB

Since both the refractive index n and the field are not functions of x, the vector g_{t2} and the dyads $\bar{\bar{g}}_{t1}$ and $\bar{\bar{g}}_{t3}$ are the only functions appearing in equation (3.30) which depend on x'. Notice that these quantities are composed of functions $g_t(\rho|\rho')$ which have the generic form

$$g_t(\rho|\rho') = \int W_t(\lambda) \frac{e^{-p_c|y\pm y'|}}{4\pi p_c} e^{j\xi(x-x')}\, d\xi.$$

Therefore, carrying out the x'-integration in (3.30) involves integrals of the type

$$\int g_t(\rho|\rho')\, dx' = \int \left\{ \int W_t(\lambda) \frac{e^{-p_c|y\pm y'|}}{4\pi p_c} e^{j\xi(x-x')}\, d\xi \right\} dx'. \qquad (1)$$

Exploiting the Fourier inversion theorem [17, p.317], (1) simplifies to

$$\int g_t(\rho|\rho')\, dx' = W_t(\xi=0) \frac{e^{-\gamma_c|y\pm y'|}}{2\gamma_c} \qquad (2)$$

where it is seen that each of these integrals is independent of x. Use of equation (2) reduces (3.30) to the specialized EFIE

$$\begin{aligned} e_t(y,z) = e_t^i(y,z) &+ k_0^2 \int_0^t \delta n^2(y')\, \bar{\bar{h}}_{t1}(y|y') \cdot e_t(y',z)\, dy' \qquad (3) \\ &+ \int_0^t \frac{2n'(y')}{n(y')} h_{t2}(y|y')\, e_y(y',z)\, dy' \\ &- \left\{ \frac{\delta n^2(y')}{n_c^2} h_{t2}(y|y')\, e_y(y',z) \right\} \Big|_{y'=0}^{y'=t} \\ &+ \int_0^t \frac{\delta n^2(y')}{n_c^2} \bar{\bar{h}}_{t3}(y|y') \cdot e_t(y',z)\, dy' \end{aligned}$$

where the dyads $\bar{\bar{h}}_{t1}$ and $\bar{\bar{h}}_{t3}$ as well as the vector h_{t2} are given by the expressions

$$\bar{h}_{t1} = \bar{\imath} h^p_\zeta + \hat{x} h^r_{\zeta t} \hat{x} + \hat{y} \left(h^r_{\zeta n} + \frac{\partial h^r_{\zeta c}}{\partial y} \right) \hat{y} \tag{4a}$$

$$h_{t2} = \hat{y} \left\{ k_c^2 h^r_{\zeta c} + \frac{\partial}{\partial y} \left[h^p_\zeta + h^r_{\zeta t} + \frac{\partial h^r_{\zeta c}}{\partial y} \right] \right\} \tag{4b}$$

$$\bar{h}_{t3} = \hat{y} \left\{ \frac{\partial^2}{\partial y^2} \left[h^r_{\zeta n} + h^r_{\zeta t} + \frac{\partial h^r_{\zeta c}}{\partial y} \right] \right\} \hat{y}. \tag{4c}$$

Scalar functions h^p_ζ, $h^r_{\zeta t}$, $h^r_{\zeta n}$, and $h^r_{\zeta c}$ may be written as

$$h^p_\zeta(y|y') = \frac{e^{-\gamma_c|y-y'|}}{2\gamma_c}$$

$$\begin{Bmatrix} h^r_{\zeta t}(y|y') \\ h^r_{\zeta n}(y|y') \\ h^r_{\zeta c}(y|y') \end{Bmatrix} = \begin{Bmatrix} r_t \\ r_n \\ c \end{Bmatrix} \frac{e^{-\gamma_c(y+y')}}{2\gamma_c}$$

where the reflection coefficients r_t and r_n as well as the coupling coefficient c can be calculated by letting $n_f = n_s$ and $\xi=0$ in the expressions for R_t, R_n, and C tabulated in Chapter two. Effecting these specializtions, it is found that

$$r_t = \frac{\gamma_c - \gamma_s}{\gamma_c + \gamma_s}$$

$$r_n = \frac{N^2\gamma_c - \gamma_s}{N^2\gamma_c + \gamma_s}$$

$$c = \frac{2(N^2-1)\gamma_c}{(N^2\gamma_c+\gamma_s)(\gamma_c+\gamma_s)}$$

where $N = (n_s/n_c)$ and as before $\gamma_i = (\zeta^2 - k_i^2)^{1/2}$ with i=s,c.

As stated in Marcuse [10, pp.7-8], the invariance along x allows modes of the asymmetric slab to be classified as TE (transverse-electric with $e_z=0$) or TM (transverse-magnetic with $h_z=0$). Examination of Maxwell's equations reveals that the TE modes have $e = \hat{x} e_x$, while the TM

modes have $e = \hat{y}e_y + \hat{z}e_z$. Through a careful inspection of EFIE (3) and equations (4a)-(4c), this uncoupling of the transverse field components becomes apparent and is manifested by a further decomposition of this EFIE into two independent equations for the x and y-components of field. TE modes are described entirely by an EFIE for the x-component of field, while the TM modes can be characterized through an EFIE for the y-component. By writing the x-component of equation (3), the EFIE for the TE modes is found to be given by

$$e_x(y,z) = k_0^2 \int_0^t \delta n^2(y')\, h_{xx}(y|y')\, e_x(y',z)\, dy' + e_x^i(y,z) \tag{5}$$

where the function h_{xx} is defined as

$$h_{xx}(y|y') = h_z^p + h_{zt}^r$$

$$= \frac{e^{-\gamma_c|y-y'|} + r_t e^{-\gamma_c(y+y')}}{2\gamma_c}. \tag{6}$$

Similarly, the TM modes arise from the y-component of equation (3) and are described by the EFIE

$$e_y(y,z) = k_c^2 \int_0^t \frac{\delta n^2(y')}{n_c^2}\, h_{1yy}(y|y')\, e_y(y',z)\, dy' + e_x^i(y,z) \tag{7}$$

$$+ \int_0^t \frac{2n'(y')}{n(y')}\, h_{t2}(y|y')\, e_y(y',z)dy'$$

$$- \left\{ \frac{\delta n^2(y')}{n_c^2}\, h_{t2}(y|y')\, e_y(y',z) \right\}\Bigg|_{y'=0}^{y'=t}$$

where h_{t2} and the function h_{1yy} are defined as

$$h_{1yy}(y|y') = k_c^2\, h_z^p + \frac{\partial^2 h_{zt}^r}{\partial y^2} + \left(k_c^2 + \frac{\partial^2}{\partial y^2}\right)\left[h_{zn}^r + \frac{\partial h_{zc}^r}{\partial y}\right] \tag{8a}$$

$$h_{t2}(y|y') = k_c^2\, h_{zc}^r + \frac{\partial}{\partial y}\left\{h_z^p + h_{zt}^r + \frac{\partial h_{zc}^r}{\partial y}\right\}. \tag{8b}$$

Elementary forms for (8a) and (8b) can be established through insightful administrations of the following relationships:

$$\frac{\partial}{\partial y}\begin{Bmatrix} h^r_{\zeta t} \\ h^r_{\zeta n} \\ h^r_{\zeta c} \end{Bmatrix} = -\gamma_c \begin{Bmatrix} h^r_{\zeta t} \\ h^r_{\zeta n} \\ h^r_{\zeta c} \end{Bmatrix} \tag{9a}$$

$$\gamma_c^2 + k_c^2 = \zeta^2 \tag{9b}$$

$$\zeta^2 c - \gamma_c r_t = \gamma_c r_n. \tag{9c}$$

Performing the required algebra is straightforward and thus the details have been omitted. Using equations (9a)-(9c) allow (8a) and (8b) to be reduced to

$$h_{1yy}(y|y') = k_c^2 \left(h^p_\zeta + h^r_{\zeta n}\right)$$

$$= k_c^2 \frac{e^{-\gamma_c|y-y'|} + r_n e^{-\gamma_c(y+y')}}{2\gamma_c}$$

$$h_{t2}(y|y') = \frac{\partial}{\partial y}\left(h^p_\zeta - h^r_{\zeta n}\right)$$

$$= \frac{\partial}{\partial y} \frac{e^{-\gamma_c|y-y'|} - r_n e^{-\gamma_c(y+y')}}{2\gamma_c}.$$

Finally, a simplified form for EFIE (7) is obtained and can be expressed as

$$e_y(y,\zeta) = e^i_y(y',\zeta) + k_0^2 \int_0^t \delta n^2(y')\, h_{yy}(y|y')\, e_y(y',\zeta)\, dy' \tag{10}$$

$$+ \int_0^t \frac{2n'(y')}{n(y')} \frac{\partial \tilde{h}_{yy}(y|y')}{\partial y} e_y(y',\zeta)\, dy'$$

$$- \left\{ \frac{\delta n^2(y')}{n_c^2} \frac{\partial \tilde{h}_{yy}(y|y')}{\partial y} e_y(y',\zeta) \right\} \Bigg|_{y'=0}^{y'=t}$$

where h_{yy} and $\tilde{h}_{yy}$ are given by

$$h_{yy}(y|y') = \frac{e^{-\gamma_c|y-y'|} + r_n\, e^{-\gamma_c(y+y')}}{2\gamma_c}$$

$$\tilde{h}_{yy}(y|y') = \frac{e^{-\gamma_c|y-y'|} - r_n\, e^{-\gamma_c(y+y')}}{2\gamma_c} .$$

With the development of the uncoupled pair of integral equations (5) and (10) completed, investigation of dielectric waveguides which support surface waves at limitingly low frequency.

5.2.2 TE MODE AEFIE FOR THE ASYMMETRIC SLAB

It is now shown by means of an indirect proof that there is no TE surface-wave mode of the graded-index asymmetric slab which exists for arbitrarily small frequency. As an obvious consequence of this observation, a surface wave with no low-frequency cutoff cannot be assured to exist on every dielectric waveguide which is placed in a non-uniform surround.

Recall from Chapter four that solutions to the homogeneous version of (5) are modal fields for surface waves. Hence, TE surface-wave modes of the asymmetric slab satisfy

$$e_x(y) = k_0^2 \int_0^t \delta n^2(y')\, h_{xx}(y|y')\, e_x(y')\, dy' \qquad (11)$$

for discrete eigenvalues $\zeta_n \in (k_s, k_{max})$ where $k_{max} = \max_y\{n(y)k_0\}$.

Now, it is assumed that equation (11) has a non-trivial solution for limitingly low frequency. As k_0 approaches zero, ζ_n must also tend to zero since it lies in the interval (k_s, k_{max}). Therefore, for asymptotically small k_0, $\gamma_i = (\zeta_n^2 - k_i^2)^{1/2} \sim 0$. Now, the limiting form for

small γ_i of the Green's function h_{xx} is found by approximating the exponentials in (6) by the leading term in their Maclaurin series. As $\gamma_i \to 0$, h_{xx} is asymptotic as

$$h_{xx} \sim \frac{1 + r_t}{2\gamma_c}$$

$$= 1/(\gamma_c + \gamma_s).$$

Therefore, the asymptotic form of (5) is given by the AEFIE

$$e_x(y) \sim \frac{k_0^2}{\gamma_c + \gamma_s} \int_0^t \delta n^2(y')\, e_x(y')\, dy'. \tag{12}$$

Noting that the right side of (12) is independent of y, it is necessary that e_x is a spatial constant. Solution to (12) is assumed to be non-trivial so that each each side of this equation may be divided by e_x. Effecting this division reveals

$$1 \sim \frac{k_0^2}{\gamma_c + \gamma_s} \langle \delta n^2 \rangle t \tag{13}$$

where $\langle \delta n^2 \rangle$ designates the average of δn^2 and is expressed as

$$\langle \delta n^2 \rangle = \frac{1}{t} \int \delta n^2(y)\, dy.$$

For $n_c \neq n_s$, the right side of (13) may be multiplied and divided by the quantity $\gamma_c - \gamma_s$ so that

$$1 \sim k_0^2 \langle \delta n^2 \rangle t \, \frac{\gamma_c - \gamma_s}{\gamma_c^2 - \gamma_s^2}$$

$$= \frac{\langle \delta n^2 \rangle t}{n_s^2 - n_c^2} (\gamma_c - \gamma_s). \tag{14}$$

It is apparent that (14) is inconsistent with the hypothesis that $\gamma_i \to 0$ unless $n_s = n_c$ thereby establishing the desired contradiction. That is

to say that unless the guiding surround is uniform, there is no TE surface waves which exist at limitingly low frequency.

A direct result of this development is that determination of the asymptotic propagation wavenumber for the dominant TE mode of the graded-index symmetric slab is facilitated. Letting $n_c = n_s$ in (13) the asymptotic form of γ_c is found to be

$$\gamma_c \sim k_0^2 <\delta n^2> t/2. \tag{15}$$

It should be emphasized that in order for (15) to be valid, it is not necessary to assume that $k_0 \to 0$. Letting $n_c = n_s$ in (11), the only assumption which needs to be effected is that the exponential may be approximated by the leading term in its Maclaurin series. This demands that $\gamma_c t$ is asymptotically small from which (15) implies that the product $k_0^2 <\delta n^2> t/2$ tends to zero. Therefore, subsequent developments do not impose the restriction that k_0 must be small but rather assume that the product of γ_c with the maximum chord of the guide approaches zero.

The asymptotic expression (15) may be specialized for step-index guides. If the index of refraction n of the guiding region is a constant, then the contrast of refractive indices is designated Δn^2. The asymptotic form of γ_c for the step-index symmetric slab becomes

$$\gamma_c \sim \Delta k^2 t/2 \tag{16}$$

where $\Delta k^2 = \Delta n^2 k_0^2$. This expression is now shown to agree with the small argument approximation of the well known result given in [10, p.13].

It is shown in [10, p.13] that the mode of the step-index symmetric slab which exhibits no low frequency cutoff has as its characteristic equation

$$\kappa \tan(\kappa t/2) = \gamma_c$$

where $\kappa = (n^2 k_0^2 - \zeta_n^2)^{1/2}$. Approximating $\tan(\kappa t/2)$ by the leading term of its Maclaurin series, it is discovered that

$$(\kappa t/2)^2 \sim \gamma_c t/2.$$

Using the fact that $\kappa^2 + \gamma_c^2 = \Delta k^2$, it is easily seen that $\gamma_c \sim \Delta k^2 t/2$ which is precisely the relationship given by (16).

5.2.3 TM MODE AEFIE FOR THE SYMMETRIC SLAB

Deriving the AEFIE for the TM modes of the graded-index symmetric slab is slightly more involved than the corresponding development for the TE modes. Again, surface-wave modal fields are solutions to the homogeneous version of (10). In addition, the symmetry of the background implies $r_n = 0$. Then the small γ_c approximation for h_{yy} becomes

$$h_{yy}(y|y') \sim 1/2\gamma_c$$

while the derivative of $\tilde{h}_{yy}$ has as its limiting form

$$\frac{\partial}{\partial y} \tilde{h}_{yy}(y|y') \sim \begin{cases} -1/2 \ldots \text{for } y > y' \\ 1/2 \ldots \text{for } y < y' \end{cases}$$

Effecting all of these simplifications results in the AEFIE

$$e_y(y) \sim \frac{k_0^2}{2\gamma_c} \int_0^t \delta n^2(y')\, e_y(y')\, dy' \qquad (17)$$

$$- \left\{ \int_0^y \frac{n'(y')}{n(y')} e_y(y')\, dy' - \int_y^t \frac{n'(y')}{n(y')} e_y(y')\, dy' \right\}$$

$$- \frac{1}{2n_c^2} \left\{ \delta n^2(t)\, e_y(t) + \delta n^2(0)\, e_y(0) \right\}.$$

A closed form solution to this AEFIE exists and can be obtained by differentiating (17) with respect to y. This transforms (17) into the first-order ordinary differential equation

$$e_y'(y) \sim - \frac{2n'(y)}{n(y)} e_y(y)$$

which has the well known solution $e_y(y) \propto n^{-2}(y)$. A substitution of this solution into (17) leads to

$$n^{-2}(y) \sim \frac{k_o^2}{2\gamma_c} \int_0^t \frac{\delta n^2(y)}{n^2(y)} dy + \frac{1}{2} \left\{ n^{-2}(y') \Big|_0^y - n^{-2}(y') \Big|_y^t \right\}$$

$$- \frac{1}{2n_c^2} \left\{ \frac{\delta n^2(t)}{n^2(t)} + \frac{\delta n^2(0)}{n^2(0)} \right\}$$

from which the asymptotic form for γ_c emerges as

$$\gamma_c \sim \frac{k_o^2}{2} \int_0^t \delta n^2(y) \, (n_c/n(y))^2 \, dy.$$

If the index of refraction n of the guiding region is a constant, then the limiting form of γ_c simplifies to

$$\gamma_c \sim (n_c/n)^2 \, \Delta k^2 t/2.$$

This expression is now shown to agree with the small argument approximation of the well known result expressed in [10, p.16].

It is shown in [10, p.16] that the characteristic equation for the dominant TM mode is written

$$(n_c/n)^2 \, \kappa \tan(\kappa t/2) = \gamma_c$$

where as before $\kappa = (n^2 k_o^2 - \zeta_n^2)^{1/2}$. A similar development to that for the TE characteristic equation shows that the asymptotic behavior of γ_c can be expressed as $\gamma_c \sim (n_c/n)^2 \, \Delta k^2 t/2$. This agrees with the result

obtained above.

5.3 A GENERAL AEFIE

Attention is now directed towards obtaining an asymptotic form of the transform-domain EFIE (3.30). Since the example of the asymmetric slab demonstrates that an integrated dielectric waveguide can be incapable of supporting a surface wave at arbitrarily low frequency, an AEFIE is developed only for those guides placed in a uniform surround. In the absence of a layered background, EFIE (3.30) becomes

$$\begin{aligned} e_t(\rho,z) = e_t^i(\rho) &+ k_0^2 \int_{CS} \delta n^2(\rho')\, g_z^p(\rho|\rho')\, e_t(\rho')\, dS' \\ &+ \int_{CS} \frac{\nabla_t' n^2(\rho')}{n^2(\rho')} \cdot e_t(\rho')\, \nabla_t g_z^p(\rho|\rho')\, dS' \\ &- \int_\Gamma \frac{\delta n^2(\rho')}{n_c^2} \nabla_t g_z^p(\rho|\rho')\, e_t(\rho',z)\cdot\hat{n}\, dl' \end{aligned} \tag{18}$$

where the principal Green's function and its gradient can be expressed in terms of the K_0 Bessel function as

$$g_z^p(\rho|\rho') = \frac{1}{2\pi} K_0(\gamma_c|\rho-\rho'|)$$

$$\nabla_t g_z^p(\rho|\rho') = \frac{1}{2\pi} K_0'(\gamma_c|\rho-\rho'|)\, \gamma_c \frac{\rho-\rho'}{|\rho-\rho'|}\,. \tag{19}$$

In order to derive the AEFIE which pertains to the homogeneous version of (18), an examination of the behavior of g_z^p and $\nabla_t g_z^p$ as $\gamma_c r_m \to 0$ (r_m is the maximum chord of the waveguide) is appropriate. Approximating K_0 by the limiting form for small argument as found in [16, p.375] shows that the asymptotic expression for the principal Green's function is

$$g_\zeta^p(\rho|\rho') \sim -\frac{1}{2\pi}\log(\gamma_c|\rho-\rho'|). \tag{20a}$$

$$\sim -\frac{1}{2\pi}\log(\gamma_c r_m) \tag{20b}$$

The small argument approximation for the gradient of g_ζ^p can be obtained by using either the small argument approximation of (19) or by directly formulating the gradient of the right side of (20a). Taking the latter approach, it can be seen that the asymptotic form of $\nabla_t g_\zeta^p$ becomes

$$\nabla_t g_\zeta^p(\rho|\rho') \sim -\frac{1}{2\pi}\frac{\rho-\rho'}{|\rho-\rho'|}. \tag{21}$$

Finally, simple substitution of equations (20b) and (21) into (18) results in the general AEFIE

$$e_t(\rho) \sim -\frac{1}{2\pi}\log(\gamma_c r_m)\, k_0^2 \int_{CS} \delta n^2(\rho)\, e_t(\rho)\, dS \tag{22}$$

$$-\frac{1}{2\pi}\int_{CS}\frac{\nabla_t' n^2(\rho')}{n^2(\rho')}\cdot e_t(\rho')\,\frac{\rho-\rho'}{|\rho-\rho'|^2}\,dS'$$

$$+\frac{1}{2\pi}\int_\Gamma \frac{\delta n^2(\rho')}{n_c^2}\,\frac{\rho-\rho'}{|\rho-\rho'|^2}\,e_t(\rho')\cdot\hat{n}'\,dl'.$$

This AEFIE provides a formulation which affords a description of field behavior in the regime where the propagation phase constant is limitingly close to the wavenumber of the background. It was stated in the introduction that no attempt will be made to prove that a solution to (22) exists for all possible guiding structures. A general existence proof seems precarious at this time due to the lack of available theory on coupled systems of integral equations. In all practicality, numerical investigation of (22) for specific waveguides may be pursued and is usually required. An exact analysis of the step-index circular fiber is

possible and is the topic for the next section.

5.4 AEFIE OF THE CIRCULAR FIBER

Figure 21 illustrates the geometry of the step-index circular fiber. A guiding region of radius a and refractive index n is centered at the origin of coordinates. As usual, the cover region is characterized by index of refraction n_c. A natural choice of the polar coordinates (ρ, φ) is invoked so that AEFIE (22) can be appropriately specialized. Outward unit normal is the unit radial vector $\hat{\rho}$ where $\hat{\rho}$ is given in terms of cartesian unit vectors as $\hat{\rho} = \hat{x}\cos\varphi + \hat{y}\sin\varphi$. Application of (22) to the circular fiber is greatly assisted by use of the following expressions:

$$|\rho-\rho'| = \rho^2 + \rho'^2 - 2\rho\rho'\cos(\varphi-\varphi')$$

$$\rho-\rho' = \rho\hat{\rho} - \rho'\hat{\rho}'$$

Use of these expressions results in the specialized AEFIE

$$e_t(\rho) \sim -\frac{1}{2\pi}\log(\gamma_c a)\,\Delta k^2 \int_0^a \int_{-\pi}^{\pi} e_t(\rho)\,\rho\,d\varphi\,d\rho \qquad (23)$$

$$+\frac{1}{2\pi}\frac{\Delta n^2}{n_c^2}\int_{-\pi}^{\pi} \hat{\rho}'\cdot e_t(a,\varphi')\,\frac{\rho - a\hat{\rho}'}{\rho^2 + a^2 - 2a\rho\cos(\varphi-\varphi')}\,a\,d\varphi'$$

Consideration of the axial symmetry of this waveguide suggests that an angularly invariant solution to (23) might exist. In fact, further considerations suggest that this solution is spatially independent. Without loss of generality, the field may be written as $e_t(\rho) = \hat{x}e_x$. Then, the x-component of (23) simplifies to

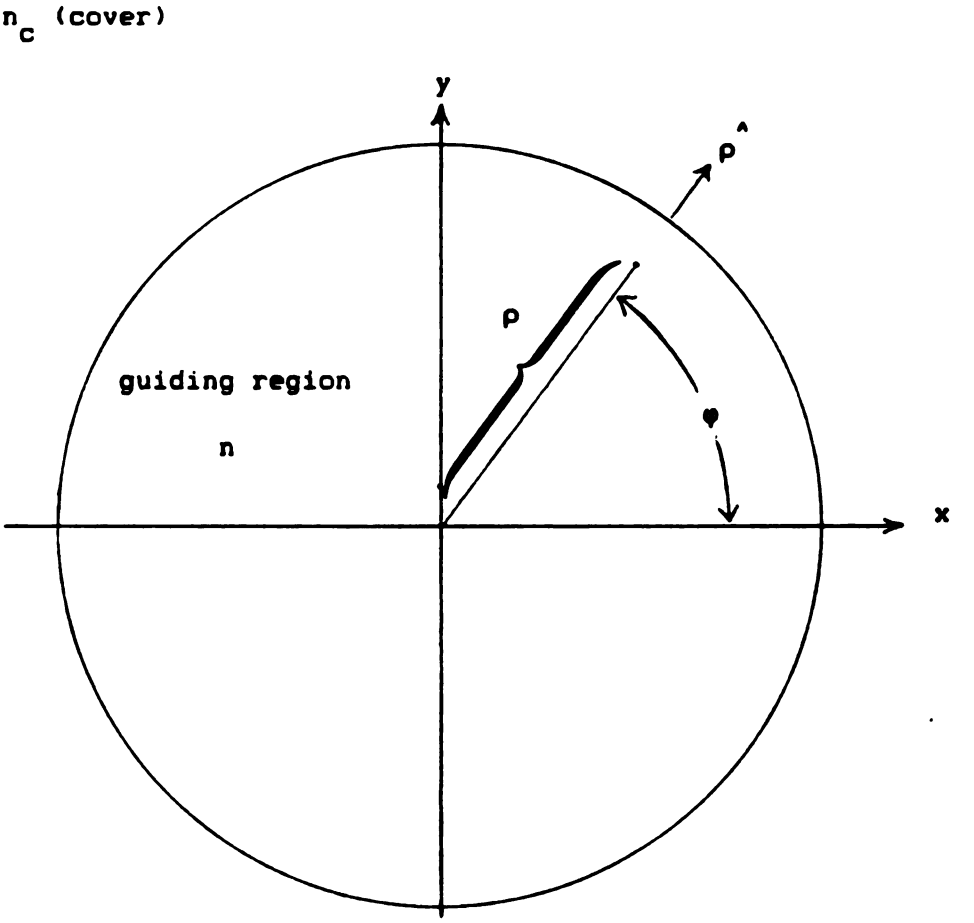

Figure 21. Geometry of the step-index circular fiber.

$$e_x \sim -\log(\gamma_c a)\,\Delta k^2\, e_x \int_0^a \rho\, d\rho \tag{24}$$

$$+\frac{1}{2\pi}\frac{\Delta n^2}{n_c^2} e_x \int_{-\pi}^{\pi} \cos\varphi' \frac{\rho\cos\varphi - a\cos\varphi'}{\rho^2 + a^2 - 2a\rho\cos(\varphi-\varphi')}\, a\, d\varphi'$$

Evaluation of the angular integral above can be performed in closed form. Make the substitution $\varphi-\varphi' = \theta$ and exploiting the periodicity of the integrand results in

$$I(\rho,\varphi) = \int_{-\pi}^{\pi} \cos\varphi' \frac{\rho\cos\varphi - a\cos\varphi'}{\rho^2 + a^2 - 2a\rho\cos(\varphi-\varphi')}\, d\varphi'$$

$$= \int_{-\pi}^{\pi} \cos(\varphi-\theta) \frac{\rho\cos\varphi - a\cos(\varphi-\theta)}{\rho^2 + a^2 - 2a\rho\cos\theta}\, d\theta$$

whereby use of the addition formula for the cosine leads to

$$I(\rho,\varphi) = \rho\cos^2\varphi\, I_c^{(1)} - a\cos^2\varphi\, I_c^{(2)} + \rho\cos\varphi\sin\varphi\, I_s^{(1)} - a\sin^2\varphi\, I_s^{(2)} - 2a\cos\varphi\sin\varphi\, I_{sc} \tag{25}$$

where the quantities $I_c^{(1)}$, $I_c^{(2)}$, $I_s^{(1)}$, $I_s^{(2)}$, and I_{sc} abbreviate the following integrals which have been evaluated in [25, pp. 366-368]:

$$I_c^{(1)} = \int_{-\pi}^{\pi} \frac{\cos\theta\, d\theta}{\rho^2 + a^2 - 2a\rho\cos\theta} = \frac{2\pi(\rho/a)}{a^2 - \rho^2} \tag{26a}$$

$$I_c^{(2)} = \int_{-\pi}^{\pi} \frac{\cos^2\theta\, d\theta}{\rho^2 + a^2 - 2a\rho\cos\theta} = \frac{\pi}{a^2}\frac{a^2+\rho^2}{a^2-\rho^2} \tag{26b}$$

$$I_s^{(1)} = \int_{-\pi}^{\pi} \frac{\sin\theta\, d\theta}{\rho^2 + a^2 - 2a\rho\cos\theta} = 0 \tag{26c}$$

$$I_s^{(2)} = \int_{-\pi}^{\pi} \frac{\sin^2\theta\, d\theta}{\rho^2 + a^2 - 2a\rho\cos\theta} = \frac{\pi}{a^2} \tag{26d}$$

$$I_{sc} = \int_{-\pi}^{\pi} \frac{\sin\theta\cos\theta\, d\theta}{\rho^2 + a^2 - 2a\rho\cos\theta} = 0. \tag{26e}$$

Therefore, the integral $I(\rho,\varphi)$ is indeed independent of φ. Substituting equations (26a)-(26e) into (25) yields

$$I(\rho) = \rho\cos^2\varphi\,\frac{2\pi(\rho/a)}{a^2-\rho^2} - a\cos^2\varphi\,\frac{\pi}{a^2}\,\frac{a^2+\rho^2}{a^2-\rho^2} - a\sin^2\varphi\,\frac{\pi}{a^2}$$

$$= -\frac{\pi}{a}\,.$$

Thus, the angular integral is in fact a spatially independent function which implies that e_x is a constant. Equation (24) finally reduces to the asymptotic form

$$1 \sim -\log(\gamma_c a)\,\Delta k^2 a^2/2 - \Delta n^2/2n_c^2$$

which upon solving for $\log(\gamma_c a)$ yields

$$\log(\gamma_c a) \sim -\left(\frac{n^2+n_c^2}{n_c^2}\right)\frac{1}{\Delta k^2 a^2}\,. \tag{27}$$

This expression is now shown to agree with the small argument approximation of the well known result given in [24, p.175].

It is shown in [10, p.175] that the characteristic equation for the dominant mode of the circular fiber can be written as

$$\frac{n^2+n_c^2}{(\kappa a)^2(\gamma_c a)^2} = -\frac{n^2 J_0(\kappa a)J_2(\kappa a)}{(\kappa a)^2 J_1^2(\kappa a)} + \frac{(n^2+n_c^2)J_1'(\kappa a)K_1'(\gamma_c a)}{(\kappa a)(\gamma_c a)J_1(\kappa a)K_1(\gamma_c a)} + \frac{n_c^2 K_0(\gamma_c a)K_2(\gamma_c a)}{(\gamma_c a)^2 K_1^2(\gamma_c a)} \tag{28}$$

where J_n and K_n $(n = 0,1,2)$ are the first kind Bessel function of order n and the modified Bessel function of order n respectively. As with the characteristic equations for the symmetric slab, $\kappa = (n^2k_0^2 - \zeta_n^2)^{1/2}$. The small argument approximations for the Bessel functions of order n are found in [16, pp.360,375] and can be written as

$$J_n(z) \sim (z/2)^n/n!$$

$$K_n(z) \sim \begin{cases} -\log z & \ldots\ n = 0 \\ 2^{n-1}(n-1)!\, z^{-n} & \ldots\ n \geq 1 \end{cases}$$

Using these expressions in (28) and simplifying quotients leads to the asymptotic characteristic equation

$$\frac{n^2 + n_c^2}{(\kappa a)^2(\gamma_c a)^2} \sim -\frac{n^2}{2(\kappa a)^2} - \frac{n^2 + n_c^2}{(\kappa a)^2(\gamma_c a)^2} - \frac{2n_c^2 \log(\gamma_c a)}{(\gamma_c a)^2} \qquad (29)$$

which can be further simplified as follows:

$$2(n^2 + n_c^2) \sim -2n_c^2(\kappa a)^2 \log(\gamma_c a) - n^2(\gamma_c a)^2/2$$

$$\sim -2n_c^2(\kappa a)^2 \log(\gamma_c a) \qquad (30)$$

since $\gamma_c a$ is tending towards zero. Observing that $\kappa^2 = \Delta k^2 - \gamma_c^2$ allows (30) to be written as

$$2(n^2 + n_c^2) \sim -2n_c^2(\Delta k^2 a^2 - \gamma_c^2 a^2)\log(\gamma_c a)$$

where the product of $\gamma_c^2 a^2$ and $\log(\gamma_c a)$ vanishes with $\gamma_c a$. Hence,

$$2(n^2 + n_c^2) \sim -2n_c^2\, \Delta k^2 a^2 \log(\gamma_c a)$$

whereby simple division yields the asymptotic expression

$$\log(\gamma_c a) \sim -\left(\frac{n^2 + n_c^2}{n_c^2}\right) \frac{1}{\Delta k^2 a^2}$$

which is precisely the the relationship given by (27).

5.5 SUMMARY

It is postulated that all axially-invariant dielectric waveguides immersed in a uniform surround are capable of supporting a surface-wave

mode with no low-frequency cutoff. The example of the asymmetric slab shows that unless the background is uniform, an arbitrary guiding structure cannot be assured to support such a surface wave.

For the x-invariant modes of the graded-index asymmetric slab, EFIE (3.30) can be greatly simplified. This independence along x allows modes to be classified as TE or TM. This uncoupling is manifested by a decomposition of the EFIE into two independent equations for the transverse field components. The TE modes are characterized by an EFIE for the x-component of field:

$$e_x(y,z) = e_x^i(y,z) + k_0^2 \int_0^t \delta n^2(y')\, h_{xx}(y|y')\, e_x(y',z)\, dy' \qquad (31)$$

where the function h_{xx} is defined as

$$h_{xx}(y|y') = \frac{e^{-\gamma_c|y-y'|} + r_t e^{-\gamma_c(y+y')}}{2\gamma_c} . \qquad (32)$$

The asymptotic form of the homogeneous version of (31) has no solution unless the guiding surround is uniform. Allowing the background to be uniform, the asymptotic field is a constant and the limiting form for the wavenumber γ_c is given by

$$\gamma_c \sim k_0^2 \langle \delta n^2 \rangle t/2$$

where $\langle \delta n^2 \rangle$ is the average value of δn^2. In the case of step-index waveguides, this asymptotic expression agrees with the small argument approximation of the well known result given in [10, p.13]

The TM modes are described entirely by an EFIE for the y-component of field:

$$e_y(y,z) = e_y^i(y',z) + k_o^2 \int_0^t \delta n^2(y')\, h_{yy}(y|y')\, e_y(y',z)\, dy' \qquad (33)$$

$$+ \int_0^t \frac{2n'(y')}{n(y')} \frac{\partial \tilde{h}_{yy}(y|y')}{\partial y} e_y(y',z)\, dy'$$

$$- \left\{ \frac{\delta n^2(y')}{n_c^2} \frac{\partial \tilde{h}_{yy}(y|y')}{\partial y} e_y(y',z) \right\} \Bigg|_{y'=0}^{y'=t}$$

where h_{yy} and $\tilde{h}_{yy}$ are given by

$$h_{yy}(y|y') = \frac{e^{-\gamma_c|y-y'|} + r_n e^{-\gamma_c(y+y')}}{2\gamma_c} \qquad (34a)$$

$$\tilde{h}_{yy}(y|y') = \frac{e^{-\gamma_c|y-y'|} - r_n e^{-\gamma_c(y+y')}}{2\gamma_c} . \qquad (34b)$$

For guides in a uniform surround, the asymptotic form of the homogeneous versions of (33) has a solution $e_y \sim 1/n^2$. The limiting form for γ_c is established as

$$\gamma_c \sim \frac{k_o^2}{2} \int_0^t \delta n^2(y)\, (n_c/n(y))^2\, dy.$$

For step-index waveguides, this asymptotic form concurs with the limiting form of the well known results in [10, p.16].

For dielectric waveguides immersed in a uniform surround, EFIE (3.30) becomes

$$e_t(\rho,z) = e_t^i(\rho) + k_o^2 \int_{CS} \delta n^2(\rho')\, g_z^p(\rho|\rho')\, e_t(\rho')\, dS' \qquad (35)$$

$$+ \int_{CS} \frac{\nabla_t' n^2(\rho')}{n^2(\rho')} \cdot e_t(\rho')\, \nabla_t g_z^p(\rho|\rho')\, dS'$$

$$- \int_\Gamma \frac{\delta n^2(\rho')}{n_c^2} \nabla_t g_z^p(\rho|\rho')\, e_t(\rho',z) \cdot \hat{n}\, dl'$$

where the principal Green's function and its gradient can be expressed in terms of the K_0 Bessel function as

$$g_\zeta^p(\rho|\rho') = \frac{1}{2\pi} K_0(\gamma_c|\rho-\rho'|)$$

$$\nabla_t g_\zeta^p(\rho|\rho') = \frac{1}{2\pi} K_0'(\gamma_c|\rho-\rho'|)\ \gamma_c\ \frac{\rho-\rho'}{|\rho-\rho'|}\ .$$

An asymptotic form of this transform-domain EFIE (designated as an AEFIE), which is appropriate for the study of surface waves propagating in the regime where the product of γ_c with the maximum chord of CS is approaching zero, is expressed by

$$\begin{aligned} e_t(\rho) \sim & -\frac{1}{2\pi}\log(\gamma_c r_m)\ k_0^2 \int_{CS} \delta n^2(\rho)\ e_t(\rho)\ dS \\ & -\frac{1}{2\pi}\int_{CS} \frac{\nabla_t' n^2(\rho')}{n^2(\rho')} \cdot e_t(\rho')\ \frac{\rho-\rho'}{|\rho-\rho'|^2}\ dS' \\ & +\frac{1}{2\pi}\int_\Gamma \frac{\delta n^2(\rho')}{n_c^2}\ \frac{\rho-\rho'}{|\rho-\rho'|^2}\ e_t(\rho')\cdot\hat{n}'\ dl'. \end{aligned} \tag{36}$$

Application of (35) to the step-index circular fiber allows the asymptotic field and propagation wavenumber to be determined. It is found that the field asymptotically becomes constant while the limiting form for γ_c is expressed as

$$\log(\gamma_c a) \sim -\left(\frac{n^2 + n_c^2}{n_c^2}\right)\frac{1}{\Delta k^2 a^2}\ .$$

These results to agree with a small argument approximation to the well known results as given in [24].

CHAPTER SIX

APPROXIMATION OF THE CONTINUOUS SPECTRUM

6.1 INTRODUCTION

In Chapter four, complex-plane analysis was used to identify the complete propagation-mode spectrum of longitudinally invariant integrated dielectric waveguides. It was found that spectral components of a continuous spectrum are solutions to the forced transform-domain EFIE (3.29) at each point along the familiar hyperbolic branch cut. Due to the complexity of (3.29), numerical approximations of solutions to this EFIE are required for all but a few guiding structures.

Standard numerical techniques such as the method of moments (MoM) [26] may be used to approximate spectral components along a finite portion of the branch cut. As the spatial frequency increases, the corresponding spectral component of field oscillates more rapidly. This increasingly oscillatory behavior demands that an extensive number of basis functions be used in implementing the MoM. Accompanying matrix sizes become so large that the MoM technique is rendered ineffective due to limitations on computation. Therefore, an alternative method is sought to approximate spectral components of high spatial frequencies.

In the next section, an iterative scheme is devised which may be used to generate solutions to (3.29) for high spatial frequencies. The aforementioned inadequacies of the MoM are not present in the iterative method, since each iterate is a closed-form analytic function of z.

In section 3, the iterative method is applied to the graded-index

asymmetric slab. Error estimates of the nth iterate along with convergence criteria and are established for both the TE and TM modes. These criteria are shown to differ fundamentally from one another due to the absence of charge in the TE case.

Finally, the graded-index circular fiber is examined. Fourier series analysis is performed and angular modes are shown to uncouple by exploiting orthogonality. The first iterate of the angularly-invariant mode is calculated for the step-index fiber which is excited by an axially-polarized point source of current. A comparison of the first iterate to the exact solution is made.

6.2 ITERATIVE METHOD

The method of successive approximations is a standard mathematical technique which has a vide variety of applications. This technique is used to generate a sequence of iterates which converges to the solution of the prescribed problem. Heuristic arguments are given below to motivate the application of the iterative method towards obtaining spectral components of the continuous spectrum.

Consider the transform-domain EFIE (3.29) which is expressed in operator form as

$$e = \mathcal{L}_{op}\{e\} + e^{i} \tag{1}$$

where the operator $\mathcal{L}_{op}$ is given by

$$\mathcal{L}_{op}\{\cdot\} = (k_c^2 + \tilde{\tilde{\nabla}}\tilde{\tilde{\nabla}}\cdot) \int_{CS} \frac{\delta n^2(\rho')}{n_c^2} \tilde{\tilde{g}}_z(\rho|\rho')\cdot\{\cdot\}\, dS'.$$

If δn^2 is in some sense small, then it is plausible to claim that e can be approximated by the impressed field. Hence, the initial approximation is denoted $e^{(0)} = e^{i}$. A better approximation is found by

substituting $e^{(0)}$ for e in the right side of (1). This yields for the first iterate $e^{(1)} = \mathcal{L}_{op}\{e^{(0)}\} + e^{i}$. Continuing in this fashion, a sequence of iterates is generated and is given by

$$\begin{aligned} e^{(0)} &= e^{i} \\ e^{(1)} &= \mathcal{L}_{op}\{e^{(0)}\} + e^{i} \\ &\vdots \\ e^{(n)} &= \mathcal{L}_{op}\{e^{(n-1)}\} + e^{i} \\ &= e^{i} + \sum_{m=1}^{n} (\mathcal{L}_{op})^{m}\{e^{i}\}. \end{aligned} \tag{2}$$

Formally, this sequence converges to solution of (1). Error analysis makes discussion of convergence rigorous.

6.2.1 ERROR ANALYSIS

It is natural to inquire how closely $e^{(n)}$ approximates e. Typically, this accuracy is measured by the absolute error $\varepsilon^{(n)}$ which is defined as

$$\varepsilon^{(n)} \equiv \|e - e^{(n)}\|$$

where $\|\cdot\|$ is a suitable norm chosen to make complete a vector space of complex-valued functions (complete normed vector spaces are called Banach spaces [27]). Forming the difference $e - e^{(n)}$ by subtracting (2) from (1) reveals

$$\varepsilon^{(n)} = \|\mathcal{L}_{op}\{e - e^{(n-1)}\}\|$$

which by inductive reasoning becomes

$$\varepsilon^{(n)} = \|(\mathcal{L}_{op})^{n}\{e - e^{(0)}\}\|$$

$$= \| (\mathcal{L}_{op})^{n} (e - e^{i}) \|$$

$$= \| (\mathcal{L}_{op})^{n+1} (e) \|. \tag{3}$$

If $\lim \epsilon^{(n)} = 0$, then $\lim e^{(n)} = e$ with convergence being in the norm. Sufficient conditions under which the sequence of iterates converges to solution of (1) are made precise below by borrowing a theorem from linear operator theory [27, pp.86-87].

6.2.2 NEUMANN SERIES THEOREM

Suppose that $\mathcal{L}_{op}$ is a bounded linear operator on a Banach space B such that the operator norm, defined by

$$\| \mathcal{L}_{op} \| \equiv \sup_{f \in B} \frac{\| \mathcal{L}_{op} (f) \|}{\| f \|}, \quad (f \neq 0)$$

satisfies the inequality $\| \mathcal{L}_{op} \| < 1$. Then solution to (1) is unique and is given by the Neumann series [27, pp.86-87]

$$e = e^{i} + \sum_{n=1}^{\infty} (\mathcal{L}_{op})^{n} (e^{i}) \tag{4}$$

with convergence of the series being in the norm.

For sufficiently small $|\delta n^{2}|_{max}$, it is expected that $\| \mathcal{L}_{op} \| < 1$. Unfortunately, the notoriously complex nature of the $\mathcal{L}_{op}$ makes formulating a rigorous proof of this statement rather dubious. Therefore, numerical investigation of conditions for which the iterative process successfully approximates the continuous spectrum is usually imperative.

6.2.3 RELATIVE ERROR OF ONE ITERATION

Since each successive iterate obviously becomes more difficult to generate than the preceding one, subsequent analysis involves the

determination of the accuracy of one iteration. A useful gauge of this accuracy is the relative error $\epsilon_{rel}^{(1)}$ which is defined by

$$\epsilon_{rel}^{(1)} = \frac{\|e-e^{(1)}\|}{\|e\|} . \tag{5}$$

An estimate of the relative error can be obtained in terms of the operator norm as follows. First, substituting the right side of (3) (with n = 1) for the numerator of (5) yields

$$\epsilon_{rel}^{(1)} = \frac{\|(\mathcal{L}_{op})^2\{e\}\|}{\|e\|} . \tag{6}$$

Next, multiplying and dividing the right side of (6) by $\|\mathcal{L}_{op}\{e\}\|$ and invoking the definition of the operator norm, it is found that

$$\begin{aligned} \epsilon_{rel}^{(1)} &= \frac{\|\mathcal{L}_{op}\{\mathcal{L}_{op}\{e\}\}\|}{\|\mathcal{L}_{op}\{e\}\|} \frac{\|\mathcal{L}_{op}\{e\}\|}{\|e\|} \\ &\leq \|\mathcal{L}_{op}\| \, \|\mathcal{L}_{op}\| \\ &= \|\mathcal{L}_{op}\|^2 . \end{aligned} \tag{7}$$

Therefore, the relative error of the first iterate is bounded by the square of the operator norm. Inductive reasoning can be used to show that the relative error of the nth iterate is bounded by $\|\mathcal{L}_{op}\|^{n+1}$.

6.2.4 REMARK

As a final note, an observation on the consequence of the definition of the operator norm is given. Whenever an upper bound of the quantity $\|\mathcal{L}_{op}\{e\}\|/\|e\|$ is found, it must be greater than or equal to the operator norm. That is to say, that if a number α is found by some method such that $\|\mathcal{L}_{op}\{e\}\| \leq \alpha \|e\|$, then $\|\mathcal{L}_{op}\| \leq \alpha$.

6.3 ANALYSIS OF THE ASYMMETRIC SLAB

In this section, the iterative scheme is applied to the graded-index asymmetric slab of Chapter five. Estimates of operator norms and relative errors $\epsilon_{rel}^{(n)}$ for both the TE and TM modes are obtained on the space of bounded and continuous complex-valued functions equipped with the sup norm where the sup norm is defined by

$$\|e_\alpha\|_\infty = \sup_y |e_\alpha(y,\zeta)|, \quad (\alpha=x,y).$$

It is well known [27, pp.21-22] that this space is a Banach space, whence the theorem of the previous section applies.

Spectral components of the continuous spectrum for the TE and TM modes are solutions to the forced equations (5.31) and (5.33) respectively, at adjacent points on each side of the branch cut C_b shown in Figure 22. Noting that the Green's functions appearing in (5.31) and (5.33) depend explicitly on $(1/\gamma_c)$, analysis is focused on approximating spectral components of field on the portion of C_b where $|Re(\zeta)| < k_c$. In this regime, both γ_c and γ_s are purely imaginary with

$$\gamma_c = jQ_c$$

$$\gamma_s = jQ_s$$

where $Q_c = (k_c^2 - \zeta^2)^{1/2}$ and $Q_s = (k_s^2 - \zeta^2)^{1/2}$.

6.3.1 TE MODE OPERATOR ANALYSIS

The EFIE which describes the x-invariant TE radiation modes of the asymmetric slab is expressed in operator form as

$$e_x = \mathcal{L}_{op}^{TE}(e_x) + e_x^i$$

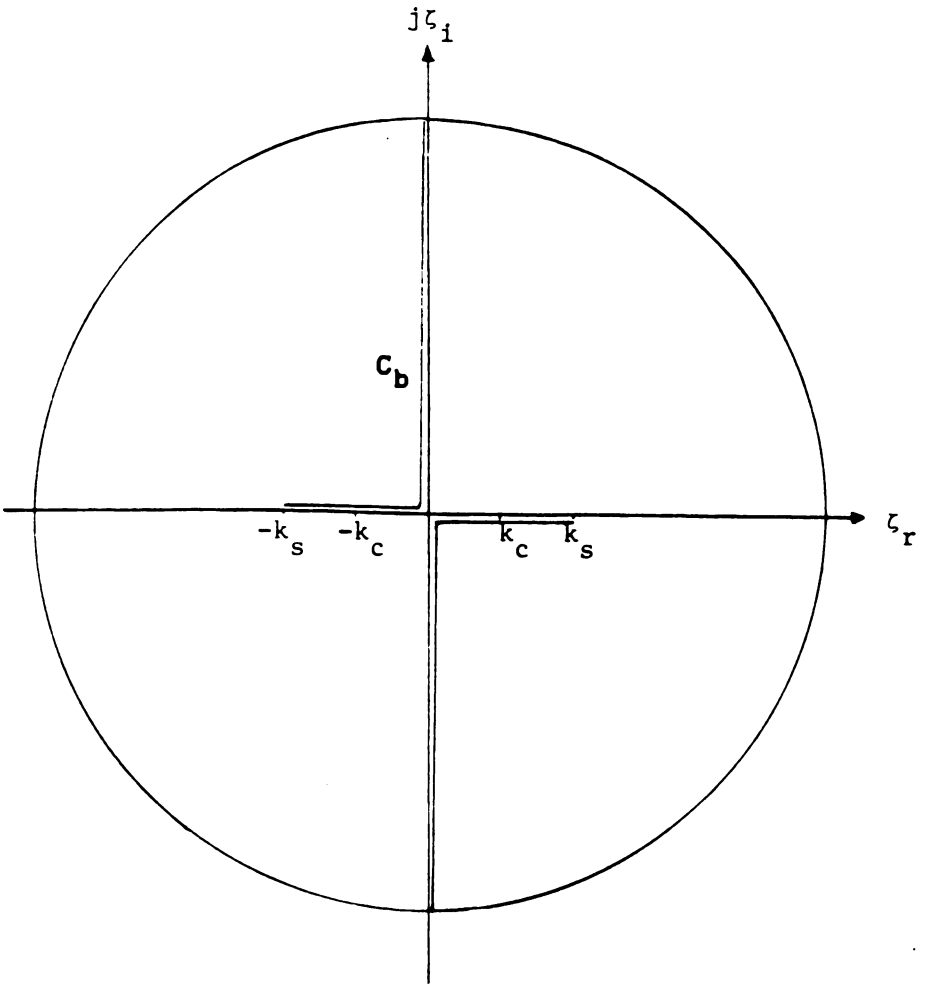

Figure 22. Complex ζ-plane with branch cut C_b.

where the operator $\mathcal{L}_{op}^{TE}$ is defined by

$$\mathcal{L}_{op}^{TE}\{e_x\} = k_0^2 \int_0^t \delta n^2(y') \, h_{xx}(y|y') \, e_x(y', \zeta) \, dy'$$

for $\zeta \in C_b$. Along that portion of C_b where $|\mathrm{Re}\{\zeta\}| < k_c$, the Green's function h_{xx} specializes to

$$h_{xx}(y|y') = \frac{e^{-jQ_c|y-y'|} + r_t e^{-jQ_c(y+y')}}{2jQ_c}$$

and the tangential reflection coefficient r_t becomes the negative and real-valued function of ζ given by

$$r_t = \frac{Q_c - Q_s}{Q_c + Q_s} .$$

An estimate for the operator norm is obtained from the following relations.

$$|\mathcal{L}_{op}^{TE}\{e_x\}| = \left| k_0^2 \int_0^t \delta n^2(y') \, h_{xx}(y|y') \, e_x(y', \zeta) \, dy' \right|$$

$$\leq k_0^2 \int_0^t \left| \delta n^2(y') \, h_{xx}(y|y') \, e_x(y') \right| dy'$$

$$\leq k_0^2 \langle \delta n^2 \rangle t \left[\sup_{y, y'} |h_{xx}| \right] \|e_x\|_\infty .$$

Using the triangle inequality for complex numbers [17, p. 205], the supremum of $|h_{xx}|$ is seen to be bound by $(1 + |r_t|)/2Q_c$. This provides the following estimate for the operator norm.

$$\|\mathcal{L}_{op}^{TE}\| \leq \frac{\langle \delta n^2 \rangle (\bar{k}_0)^2}{2\bar{Q}_c} (1 + |r_t|) \qquad (8)$$

$$= \frac{\langle \delta n^2 \rangle (\bar{k}_0)^2}{2\bar{Q}_c} \frac{2\bar{Q}_s}{\bar{Q}_s + \bar{Q}_c}$$

where $\bar{k}_0 = k_0 t$ and $\bar{Q}_c = Q_c t$ are normalized wavenumbers.

It is apparent from (8) that the operator norm becomes less than unity for either sufficiently small $\langle \delta n^2 \rangle$ or sufficiently large $\bar{Q}_c$. Hence, convergence of the iterative sequence can be guaranteed with the relative error of the nth iterate satisfying the inequality

$$\epsilon_{rel}^{(n)} \leq \left(\frac{\langle \delta n^2 \rangle (\bar{k}_0)^2}{2\bar{Q}_c} \frac{2\bar{Q}_s}{\bar{Q}_s + \bar{Q}_c} \right)^{n+1}. \tag{9}$$

Actual error may be considerably less than the upper bound predicted by (9). An investigation of the accuracy of one iteration for the step-index symmetric slab excited by an infinite line source is given below. Equivalence of the first iterate and a first-order expansion in Δn^2 of the exact solution is directly established. Comparison between actual relative error $\epsilon_{rel}^{(1)}$ and its estimate in (9) is made.

6.3.2 TE MODES OF THE STEP-INDEX SYMMETRIC SLAB

Excitation of the x-invariant TE radiation modes of the symmetric slab is provided by an x-independent current source which is directed along the x-axis. Without loss of generality, the source density J_x is taken to be $J_x(y,z) = I\,\delta(y-y^s)\,\delta(z-z^s)$ with $y^s > t$. The impressed field e_x^i in the guiding region is given by

$$\begin{aligned} e_x^i(y,z) &= \hat{x} \cdot \left\{ (k_c^2 + \tilde{\tilde{\nabla}}\tilde{\tilde{\nabla}} \cdot) \int_{CS_\infty} \tilde{\tilde{g}}_z(\rho|\rho') \cdot \frac{F_z(J)}{j\omega\epsilon_c}\, dS' \right\} \\ &= k_0^2 \int_0^t \frac{e^{-j\bar{Q}_c(y'-y)}}{2j\bar{Q}_c} (I/j\omega\epsilon_0)\, \delta(y'-y^s)\, e^{-j\zeta z^s}\, dy' \\ &= C(\zeta)\, e^{j\bar{Q}_c y} \end{aligned}$$

where $C(\zeta) = -(\omega\mu_0 I/2\bar{Q}_c)\, e^{-j\bar{Q}_c y^s}\, e^{-j\zeta z^s}$ is a spatial constant. The resulting total field e_x can be found in closed form by any of several

methods (e.g. [9, Appendix B]) and can be written as

$$e_x(y,z) = A(z)\, e^{j\beta y} + B(z)\, e^{-j\beta y} \tag{10}$$

where $\beta = (n^2 k_0^2 - \zeta^2)^{1/2}$ and the coefficients $A(z)$ and $B(z)$ are given by

$$A(z) = \frac{\beta_c(\beta + \beta_c)\, e^{j\beta_c t}}{2\beta_c\beta\cos\beta t + j(\beta_c^2 + \beta^2)\sin\beta t}\, C(z) \tag{11a}$$

$$B(z) = \frac{\beta_c(\beta - \beta_c)\, e^{j\beta_c t}}{2\beta_c\beta\cos\beta t + j(\beta_c^2 + \beta^2)\sin\beta t}\, C(z). \tag{11b}$$

A first iterative approximation to (10) is generated by the procedure discussed in the previous section. Specializing $\mathcal{L}_{op}^{TE}$ for the step-index symmetric slab, the first iterate becomes

$$\begin{aligned} e_y^{(1)}(y,z) &= C(z)\left\{ e^{j\beta_c y} + k_0^2 \int_0^t \Delta n^2\, \frac{e^{-j\beta_c|y-y'|}}{2j\beta_c}\, e^{j\beta_c y'}\, dy' \right\} \\ &= C(z)\left\{ \left(1 - \frac{\Delta n^2 k_0^2}{4\beta_c^2}\right) e^{j\beta_c y} - j\left(\frac{\Delta n^2 k_0^2}{2\beta_c}\right)(t-y)\, e^{j\beta_c y} \right. \\ &\qquad \left. + \frac{\Delta n^2 k_0^2}{4\beta_c^2}\, e^{-j\beta_c y} \right\}. \end{aligned} \tag{12}$$

The inequality in (9) implies that the relative error of the first iterate is of the order $(\Delta n^2)^2$. In fact, a first-order expansion of e_x in powers of Δn^2 is identical to the first iterate. A direct proof of this statement is given below.

Approximation of e_x by the first two terms in its Maclaurin series in Δn^2 is greatly assisted by use of the following relations.

$$\beta = \beta_c + (k_0^2/2\beta_c)\, \Delta n^2 + O((\Delta n^2)^2) \tag{13a}$$

$$e^{\pm j\beta t} = [1 \pm j(k_0^2 t/2\beta_c)\, \Delta n^2]\, e^{\pm j\beta_c t} + O((\Delta n^2)^2) \tag{13b}$$

$$\sin\Omega t = \sin\Omega_c t + [(k_0^2 t/2\Omega_c)\,\Delta n^2]\cos\Omega_c t + O((\Delta n^2)^2) \qquad (13c)$$

$$\cos\Omega t = \cos\Omega_c t - [(k_0^2 t/2\Omega_c)\,\Delta n^2]\sin\Omega_c t + O((\Delta n^2)^2) \qquad (13d)$$

where $O(\cdot)$ notates "big O" [15, pp.141-142] of the term in braces. Now, $A(\zeta)$ and $B(\zeta)$ can be approximated to first order in Δn^2 by substituting (13a)-(13d) into (11a)-(11b), retaining terms up to order Δn^2, and manipulating the resulting expressions. Thus,

$$A(\zeta) \approx \frac{2\Omega_c^2\, e^{j\Omega_c t}\,(1 + \Delta n^2 k_0^2/4\Omega_c^2)}{2\Omega_c^2\, e^{j\Omega_c t}\,(1 + (1 + j\Omega_c t)(\Delta n^2 k_0^2/2\Omega_c^2))}\, C(\zeta)$$

$$\approx 1 - (1 + j2\Omega_c t)\,\frac{\Delta n^2 k_0^2}{4\Omega_c^2}$$

$$B(\zeta) \approx \frac{2\Omega_c^2\, e^{j\Omega_c t}\,(\Delta n^2 k_0^2/4\Omega_c^2)}{2\Omega_c^2\, e^{j\Omega_c t}\,(1 + (1 + j\Omega_c t)(\Delta n^2 k_0^2/2\Omega_c^2))}\, C(\zeta)$$

$$\approx \frac{\Delta n^2 k_0^2}{4\Omega_c^2}\, C(\zeta).$$

These expressions along with (13b) with $t = y$ yield the first order approximation of the field

$$e_x(y,\zeta) \approx C(\zeta)\left\{\left(1 - (1 + j2\Omega_c t)\,\frac{\Delta n^2 k_0^2}{4\Omega_c^2}\right)\left(1 + j\,\frac{\Delta n^2 k_0^2}{2\Omega_c}\,y\right)e^{j\Omega_c y} + \frac{\Delta n^2 k_0^2}{4\Omega_c^2}\left(1 - j\,\frac{\Delta n^2 k_0^2}{2\Omega_c}\,y\right)e^{-j\Omega_c y}\right\}$$

$$\approx C(\zeta)\left\{\left(1 - \frac{\Delta n^2 k_0^2}{4\Omega_c^2}\right)e^{j\Omega_c y} - j\,\frac{\Delta n^2 k_0^2}{2\Omega_c}\,(t - y)\,e^{j\Omega_c y} + \frac{\Delta n^2 k_0^2}{4\Omega_c^2}\,e^{-j\Omega_c y}\right\}$$

which is precisely the first iterate.

A plot of the relative error versus $\bar{Q}_c$ is shown in Figure 23. The cover is assumed to be vacuum with $n_c = 1.0$. In order to guarantee monomode surface-wave propagation, $\Delta n^2 \bar{k}_0^2$ must be less than π^2. If $\bar{k}_0$ is chosen such that $k_0 = .57k_{co}$, where k_{co} is the cutoff wavenumber of the first higher order surface-wave mode, then $\Delta n^2 \bar{k}_0^2 = 3.25$. It is clear that actual relative error follows the curve of its estimate closely. Figures 24 through 26 show relative field amplitudes $e_x/C(\zeta)$ and $e_x^{(1)}/C(\zeta)$ versus the normalized y-coordinate. In Figure 24, $Q_c t = 2$ and a relative error of 0.3 results. Observation of Figure 25 indicates clearly that for $Q_c t = 5$, field amplitude is very closely approximated by the first iterate. Finally, Figure 26 has $Q_c t = 10$ and the first iterate is nearly indistinguishable from the exact field. The absence of charge in the TE mode situation affords the luxury of improving accuracy of one iteration to any desired tolerance by merely increasing Q_c. However, in most instances, charge is present and it is the contrast of refractive indices which sets a limit on the relative error. This effect can be seen from examination of the TM modes and is the topic of the next section.

6.3.3 TM OPERATOR ANALYSIS

Analysis of the TM modes proceeds in the same manner as that of the TE modes. A complete description of the TM modes is provided by an EFIE for the y-component of field. In operator form, this EFIE is written as

$$e_y = \mathcal{L}_{op}^{TM}(e_y) + e_y^i$$

where the operator $\mathcal{L}_{op}^{TM}$ is defined by

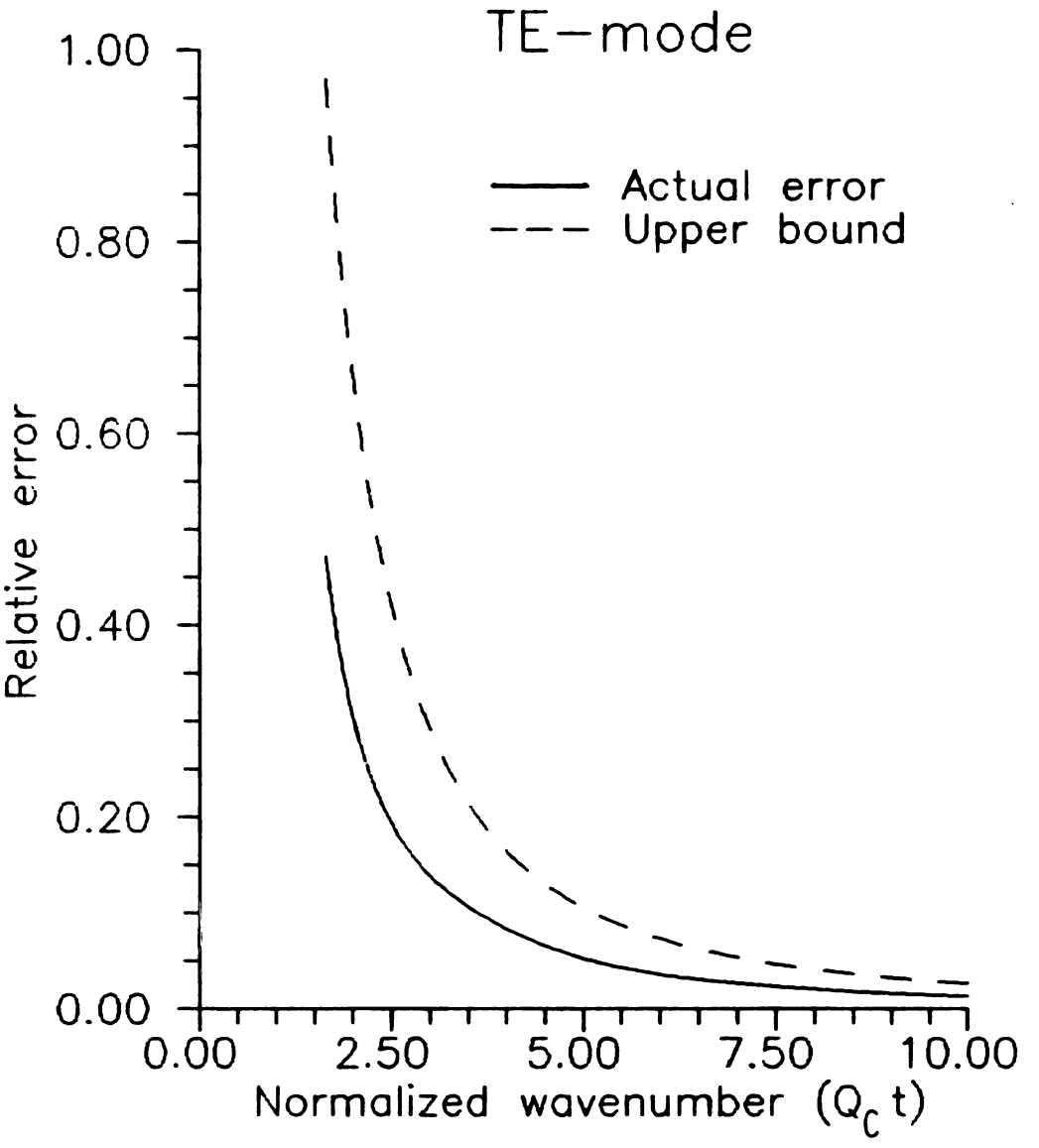

Figure 23. Relative error vs. $\bar{Q}_c$ for TE modes.

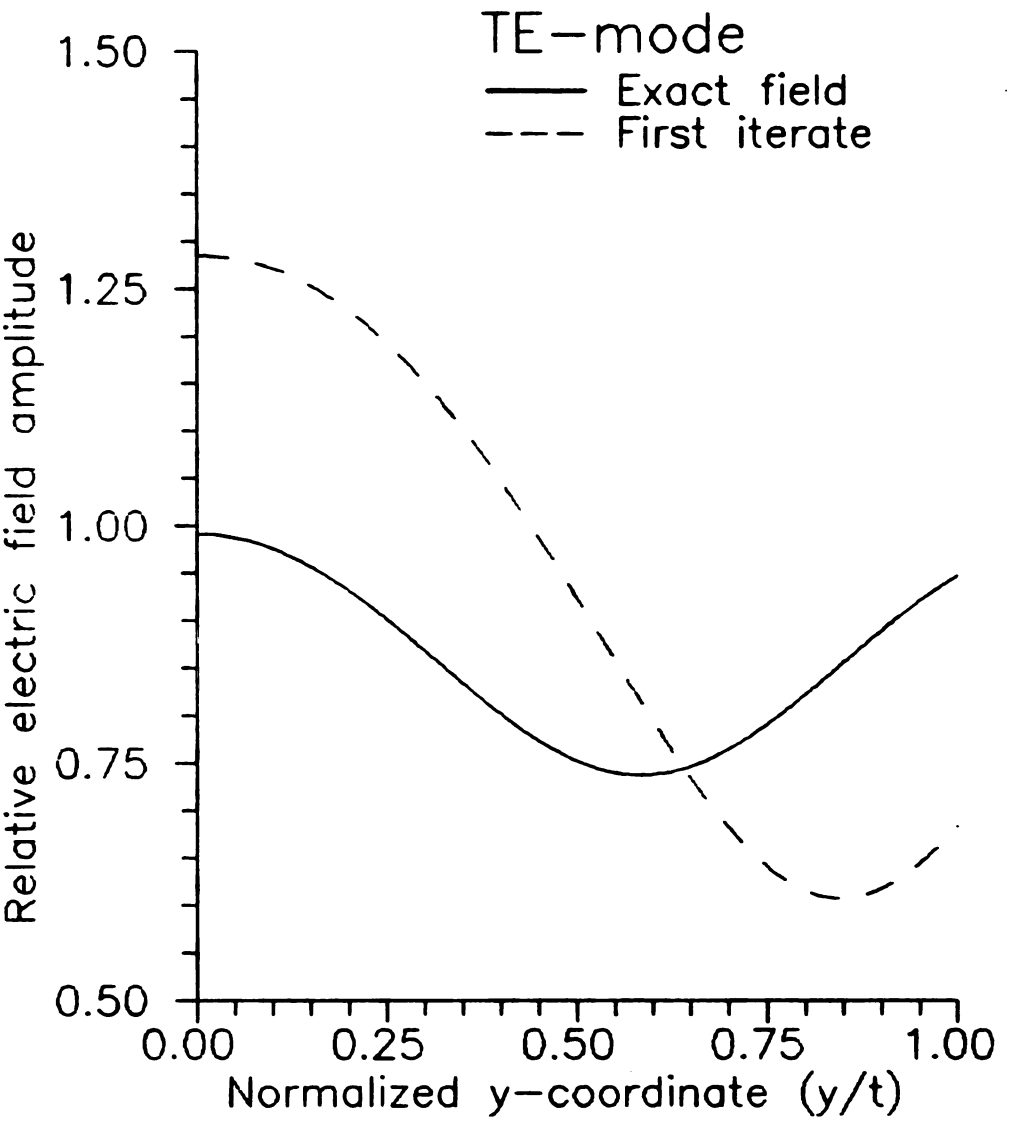

Figure 24. Relative field amplitudes for TE mode ($\bar{\theta}_c$ = 2.0).

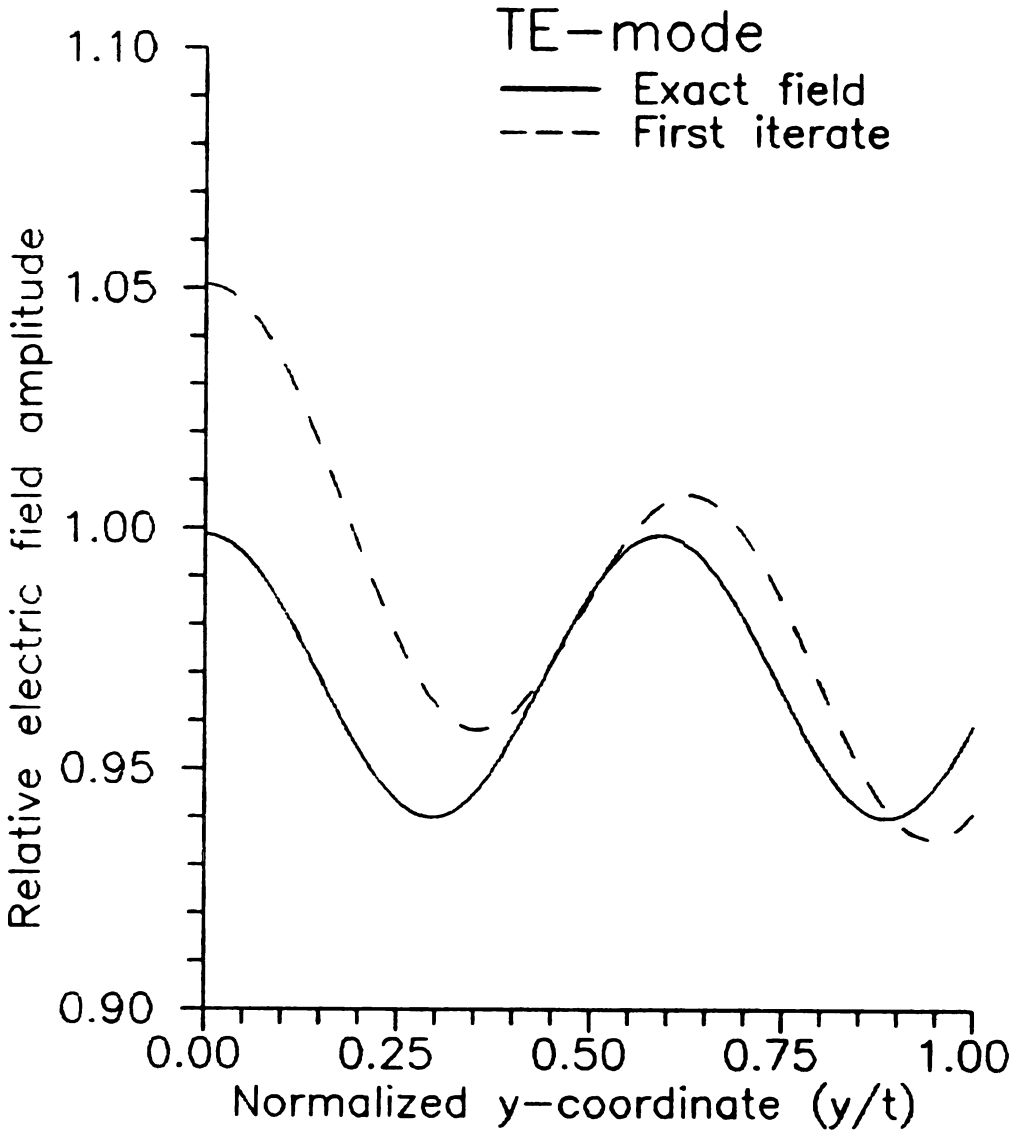

Figure 25. Relative field amplitudes for TE mode ($\bar{Q}_c$ 5.0).

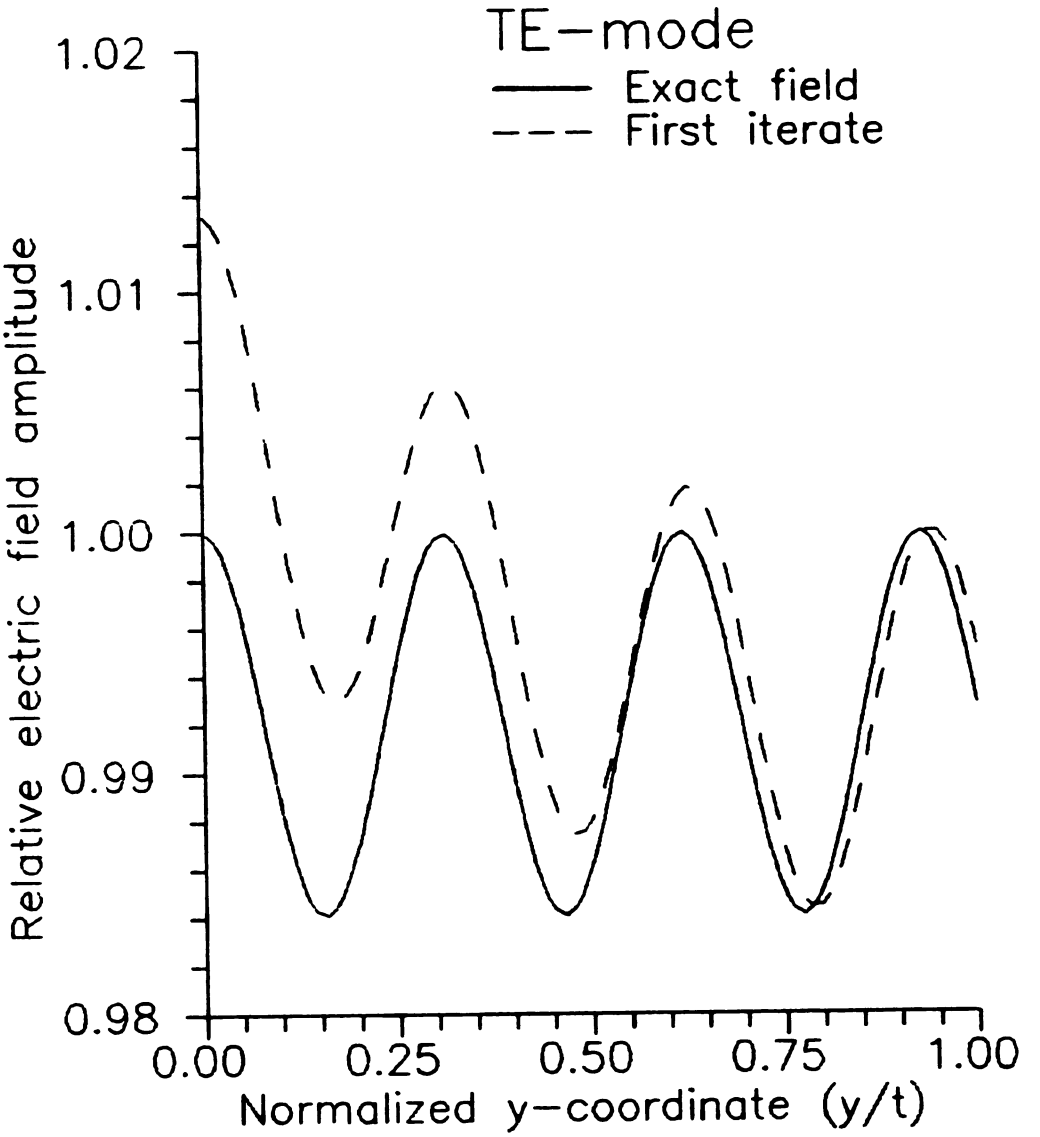

Figure 26. Relative field amplitudes for TE mode ($\tilde{\theta}_c$ = 10.0).

$$\mathcal{L}_{op}^{TM}(e_y) = k_o^2 \int_0^t \delta n^2(y')\, h_{yy}(y|y')\, e_y(y',\zeta)\, dy'$$

$$+ \int_0^t \frac{2n'(y')}{n(y')} \frac{\partial \tilde{h}_{yy}(y|y')}{\partial y} e_y(y',\zeta)\, dy'$$

$$- \left\{ \frac{\delta n^2(y')}{n_c^2} \frac{\partial \tilde{h}_{yy}(y|y')}{\partial y} e_y(y',\zeta) \right\} \Bigg|_{y'=0}^{y'=t}$$

for $\zeta \in C_b$. Again, the iterative scheme is applied to spectral components along that part of C_b where $|\mathrm{Re}\{\zeta\}| < k_c$. Then, the Green's functions h_{yy} and $\tilde{h}_{yy}$ specialize to

$$h_{yy}(y|y') = \frac{e^{-jQ_c|y-y'|} + r_n e^{-jQ_c(y+y')}}{2jQ_c}$$

$$\tilde{h}_{yy}(y|y') = \frac{e^{-jQ_c|y-y'|} - r_n e^{-jQ_c(y+y')}}{2jQ_c}$$

and the normal reflection coefficient r_n becomes a real-valued function of ζ given by

$$r_n = \frac{N^2 Q_c - Q_s}{N^2 Q_c + Q_s}$$

where $N = (n_s/n_c)$.

Obtaining an estimate for the operator norm is achieved from the following relations.

$$|\mathcal{L}_{op}^{TM}(e_y)| = \left| k_o^2 \int_0^t \delta n^2(y')\, h_{yy}(y|y')\, e_y(y',\zeta)\, dy' \right.$$

$$+ \int_0^t \frac{2n'(y')}{n(y')} \frac{\partial \tilde{h}_{yy}(y|y')}{\partial y} e_y(y',\zeta)\, dy'$$

$$\left. - \left\{ \frac{\delta n^2(y')}{n_c^2} \frac{\partial \tilde{h}_{yy}(y|y')}{\partial y} e_y(y',\zeta) \right\} \Bigg|_{y'=0}^{y'=t} \right|$$

$$\leq \left| k_0^2 \int_0^t \delta n^2(y') \, h_{yy}(y|y') \, e_y(y',z) \, dy' \right|$$

$$+ \left| \int_0^t \frac{2n'(y')}{n(y')} \frac{\partial \tilde{h}_{yy}(y|y')}{\partial y} e_y(y',z) \, dy' \right|$$

$$+ \left| \left\{ \frac{\delta n^2(y')}{n_c^2} \frac{\partial \tilde{h}_{yy}(y|y')}{\partial y} e_y(y',z) \right\} \Big|_{y'=0}^{y'=t} \right|$$

$$\leq \left\{ k_0^2 \langle \delta n^2 \rangle t \left[\sup_{y,y'} |h_{yy}| \right] + 2\langle |n'/n| \rangle \left[\sup_{y,y'} |\partial \tilde{h}_{yy}/\partial y| \right] \right.$$

$$\left. + \left[(\delta n^2(t) + \delta n^2(0))/2n_c^2 \right] \left[\sup_{y,y'} |\partial \tilde{h}_{yy}/\partial y| \right] \right\} \|e_y\|_\infty .$$

where very crude estimates have been used. Upper bounds for the suprema of h_{yy} and the derivative of $\tilde{h}_{yy}$ can be obtained by using the triangle inequality. These provide the following estimate for the operator norm.

$$\|\mathcal{L}_{op}^{TM}\| \leq \left\{ \frac{\langle \delta n^2 \rangle (\bar{k}_0)^2}{2\bar{Q}_c} + \langle |n'/n| \rangle + \frac{\delta n^2(t) + \delta n^2(0)}{2n_c^2} \right\} (1 + |r_n|) \quad (14)$$

$$\leq \left\{ \frac{\langle \delta n^2 \rangle (\bar{k}_0)^2}{2\bar{Q}_c} + \langle |n'/n| \rangle + \frac{\delta n^2(t) + \delta n^2(0)}{2n_c^2} \right\} \frac{2N^2 \bar{Q}_s}{N^2 \bar{Q}_c + \bar{Q}_s}$$

which does not vanish as Q_c tends to infinity. Hence, this result is fundamentally different from the TE case. Indeed, if the contrast δn^2 is not sufficiently small, then the iterative solution might fail. Nevertheless, an upper bound for the relative error of the nth iterate can be obtained by using (14). For the special case of the step-index symmetric slab, the relative error of the first iterate satisfies the inequality

$$\varepsilon_{rel}^{(1)} \leq \frac{\Delta n^2}{n_c^2} + \frac{\Delta n^2 (\bar{k}_0)^2}{2\bar{Q}_c} .$$

In the next section, a comparison of the actual error with this upper

bound is made.

6.3.4 TM MODES OF THE STEP-INDEX SYMMETRIC SLAB

Excitation of the x-invariant TM radiation modes of the symmetric slab is provided by an x-independent current source which is polarized along either the y-axis or the z-axis. For simplicity, the source density is taken to be $J(y,z) = \hat{z}\, I\, \delta(y-y^{*})\, \delta(z-z^{*})$ with $y^{*} > t$. Then, the y-component of impressed field is given by

$$e_y^i(y,\zeta) = \hat{y} \cdot \left\{ (k_c^2 + \tilde{\nabla}\tilde{\nabla}\cdot) \int_{CS_\infty} \bar{\bar{g}}_z(\rho|\rho') \cdot \frac{F_z(J)}{j\omega\epsilon_0}\, dS' \right\}$$

$$= k_0^2 \int_0^t \frac{e^{-jQ_c(y'-y)}}{2jQ_c}\, (I/j\omega\epsilon_0)\, \delta(y-y^{*})\, e^{-j\zeta z^{*}}\, dy'$$

$$= D(\zeta)\, e^{jQ_c y}$$

where $D(\zeta) = (\zeta I/2\omega\epsilon_c)\, e^{-jQ_c y^{*}}\, e^{-j\zeta z^{*}}$ is a spatial constant. The resulting total field e_y is given by

$$e_y(y,\zeta) = \tilde{A}(\zeta)\, e^{jQy} + \tilde{B}(\zeta)\, e^{-jQy} \qquad (15)$$

where as before $Q = (n^2 k_0^2 - \zeta^2)^{1/2}$ and the coefficients $\tilde{A}(\zeta)$ and $\tilde{B}(\zeta)$ are

$$\tilde{A}(\zeta) = \frac{Q_c(Q + \tilde{n}^2 Q_c)\, e^{jQ_c t}}{2\tilde{n}^2 Q_c Q \cos Qt + j(\tilde{n}^4 Q_c^2 + Q^2) \sin Qt}\, D(\zeta)$$

$$\tilde{B}(\zeta) = \frac{Q_c(Q - \tilde{n}^2 Q_c)\, e^{jQ_c t}}{2\tilde{n}^2 Q_c Q \cos Qt + j(\tilde{n}^4 Q_c^2 + Q^2) \sin Qt}\, D(\zeta)$$

with $\tilde{n} = (n/n_c)$ a normalized refractive index.

A first iterative approximation to (15) is generated by the procedure discussed in the section 6.2. Specializing $\mathcal{L}_{op}^{TM}$ for the step-index symmetric slab, the first iterate becomes

$$e_y^{(1)}(y,z) = D(z)\left\{ e^{jQ_c y} + k_0^2 \int_0^t \Delta n^2 \frac{e^{-jQ_c|y-y'|}}{2jQ_c} e^{jQ_c y'}\, dy' \right.$$

$$\left. - \frac{\Delta n^2}{2n_c^2}\left(e^{-jQ_c|y-y'|}\, e^{jQ_c y'}\Big|_{y=0}^{y=t} \right) \right\}$$

$$= D(z)\left\{ \left(1 - \frac{\Delta n^2 k_0^2}{4Q_c^2} - \frac{\Delta n^2}{2n_c^2} \right) e^{jQ_c y} - j\frac{\Delta n^2 k_0^2}{2Q_c}(t-y)\, e^{jQ_c y} \right.$$

$$\left. + \left(\frac{\Delta n^2 k_0^2}{4Q_c^2} - \frac{\Delta n^2}{2n_c^2} \right) e^{-jQ_c y} \right\}. \qquad (16)$$

As with the TE modes, the first iterate is equivalent to a first order expansion of e_y in powers of Δn^2. The proof of the statement is virtually identical to that given in section 6.3.2 and is therefore omitted here.

Three plots of relative error versus Q_c/k_c are given in Figures 27 through 29. Again, $n_c = 1.0$ and the operating wavenumbers are chosen so that only the dominant surface-wave mode propagates. It is clear that the actual relative errors are much less than the upper bounds obtained through the rather crude estimates used in section 6.3.3. The explanation of this result can be seen by examining the relative field amplitudes shown in Figures 30 through 35. It can be seen that estimating the field at $y = 0$ and $y = t$ by the maximum value of field can be a gross over estimate. However, the analysis provides a starting point from which more detailed studies can proceed.

6.4 ANALYSIS OF THE CIRCULAR FIBER

In the preceding section, the Banach space of continuous complex-valued functions equipped with sup norm provided a space on which upper bounds for relative errors $\varepsilon_{rel}^{(1)}$ could be obtained analytically. The

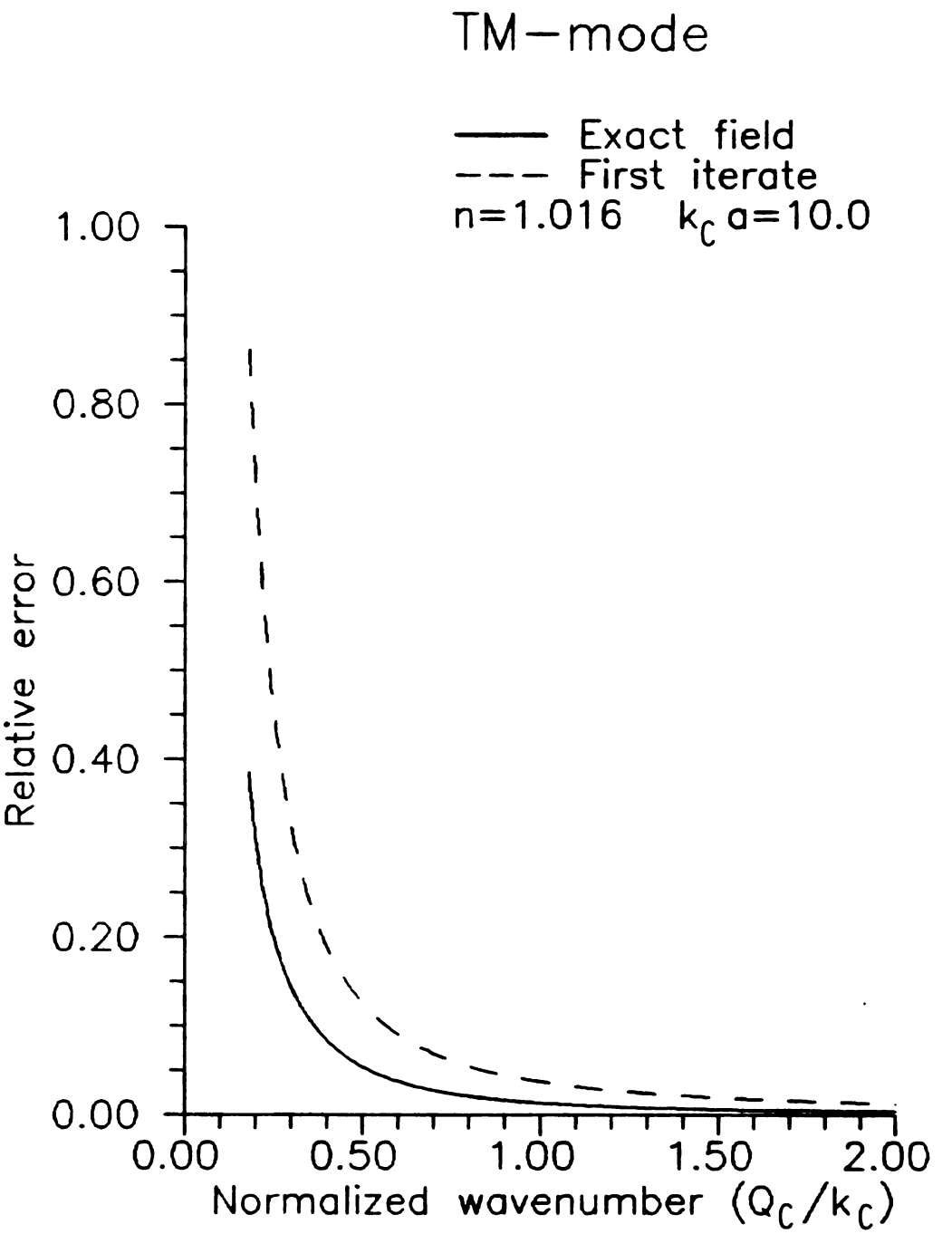

Figure 27. Relative error vs. (Q_c/k_c) for TM mode (Δn^2 = .032).

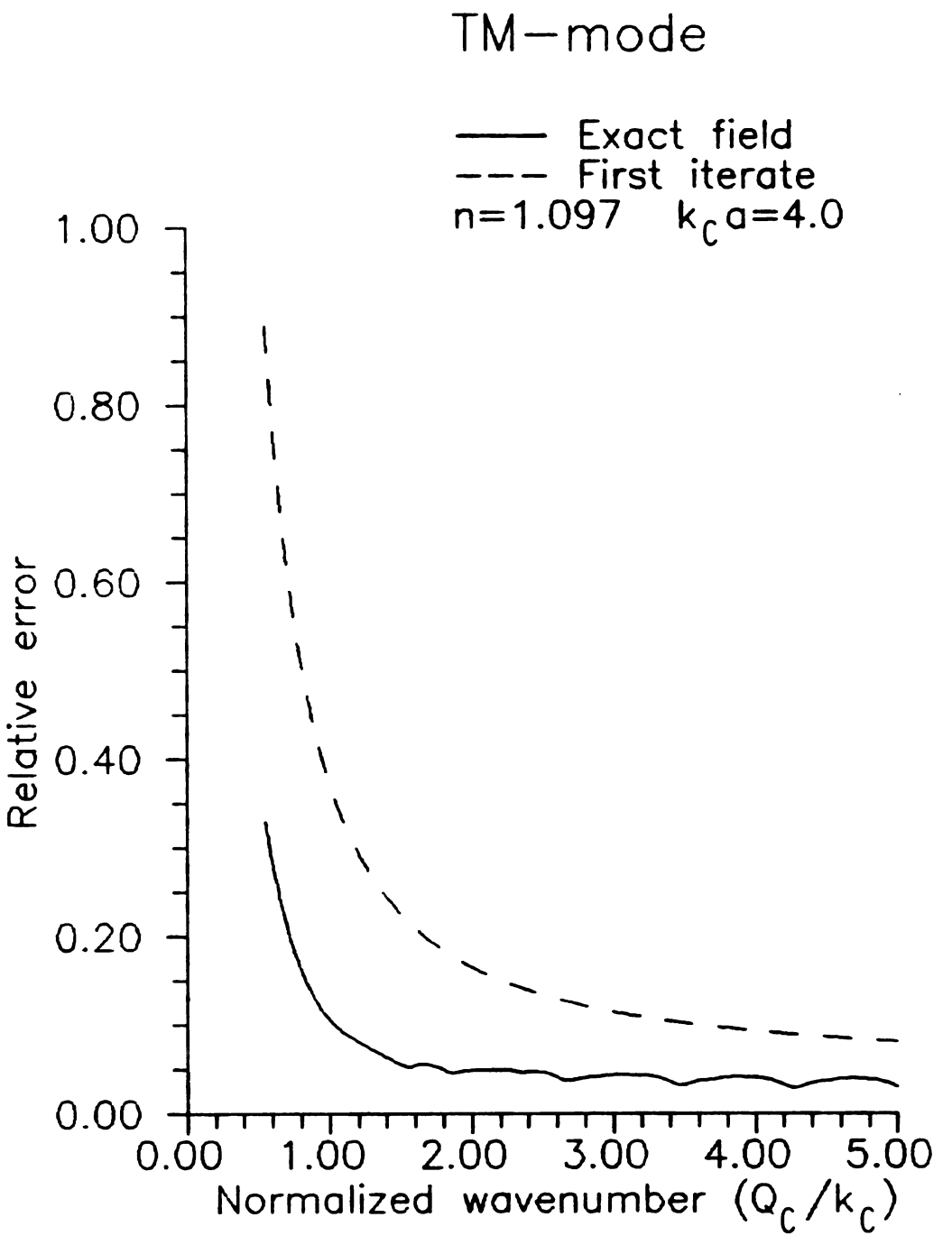

Figure 28. Relative error vs. (Q_c/k_c) for TM mode (Δn^2 = .203).

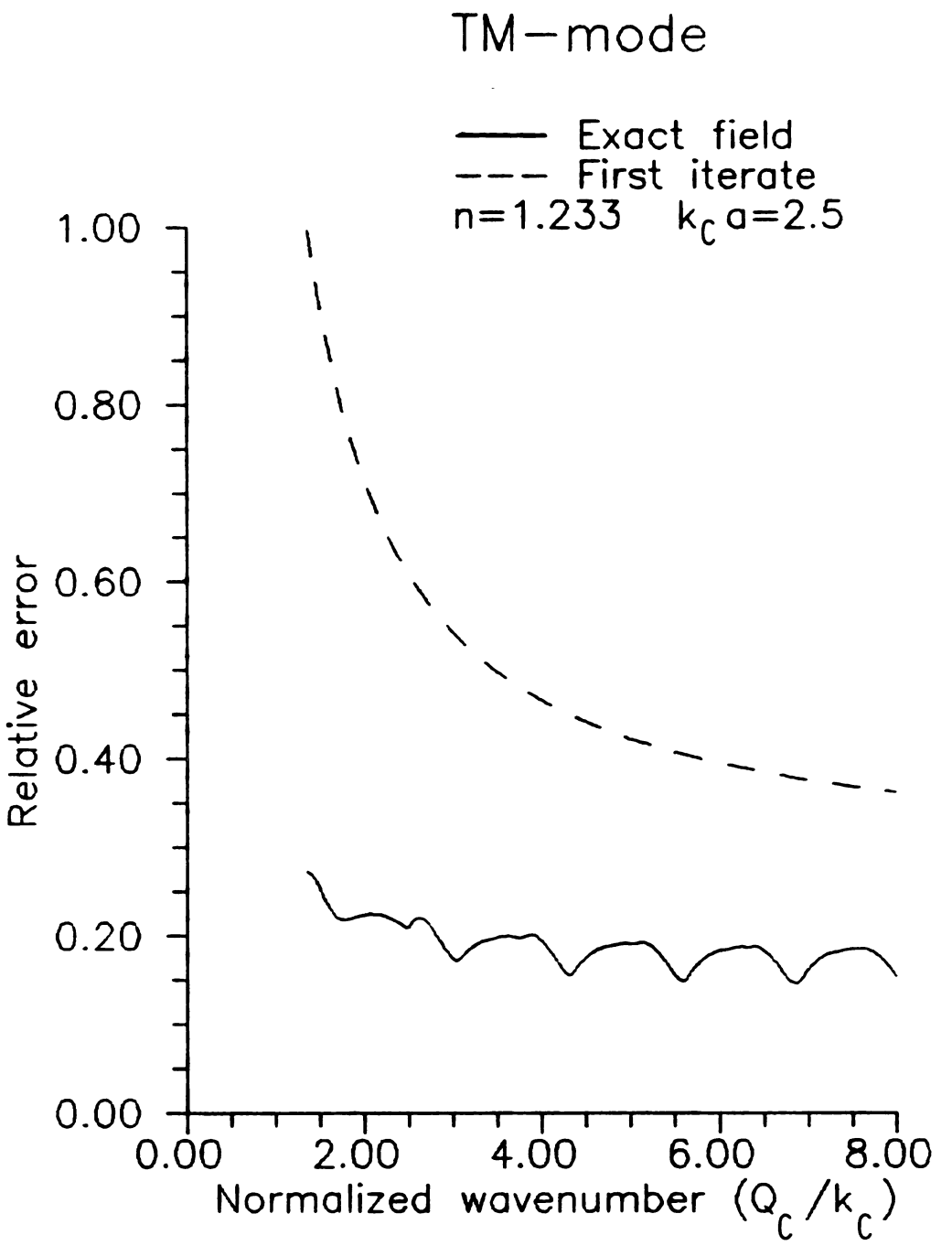

Figure 29. Relative error vs. (Q_c/k_c) for TM mode (Δn^2 = .520).

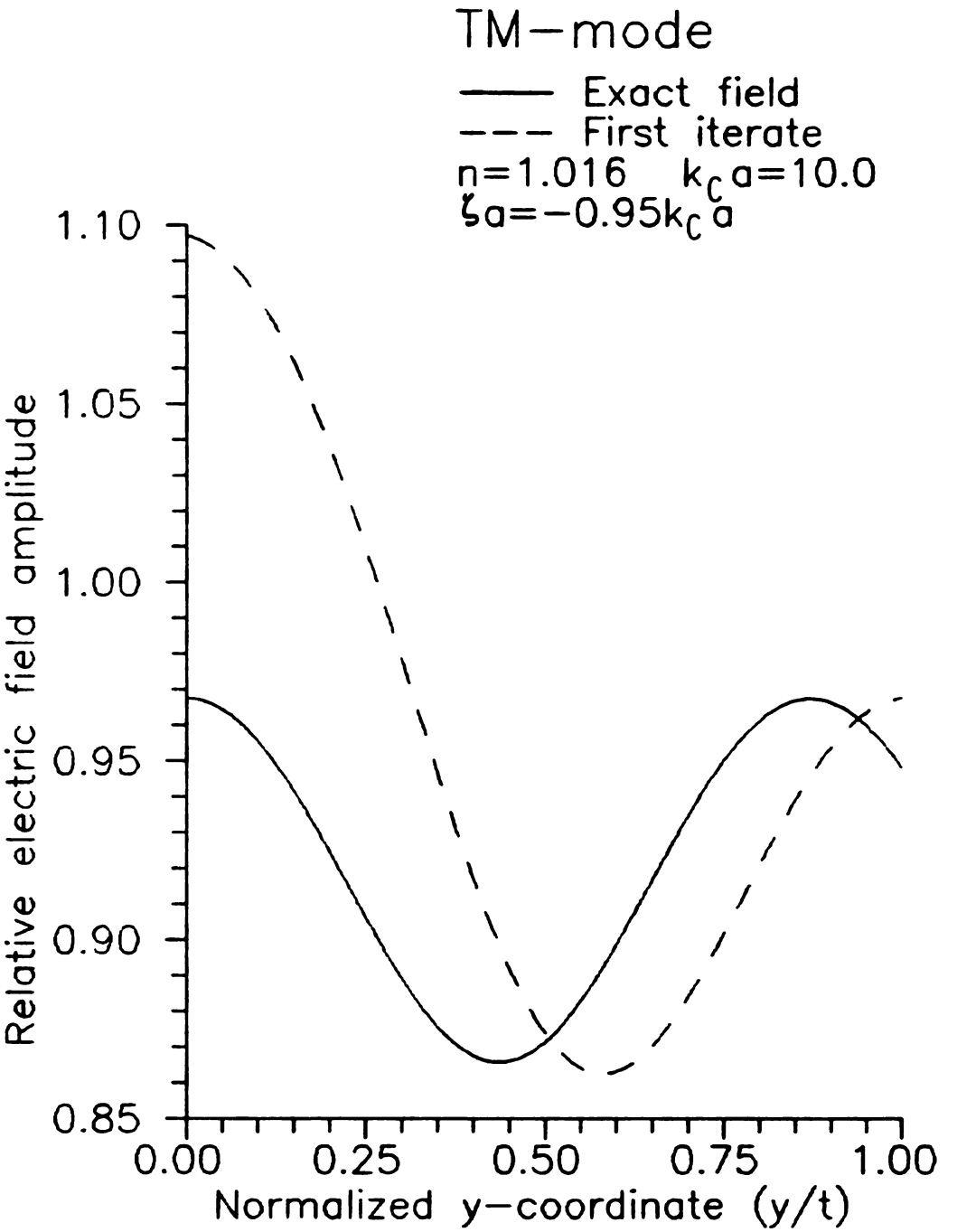

Figure 30. Relative field amplitudes for TM mode (Δn^2 = .032).

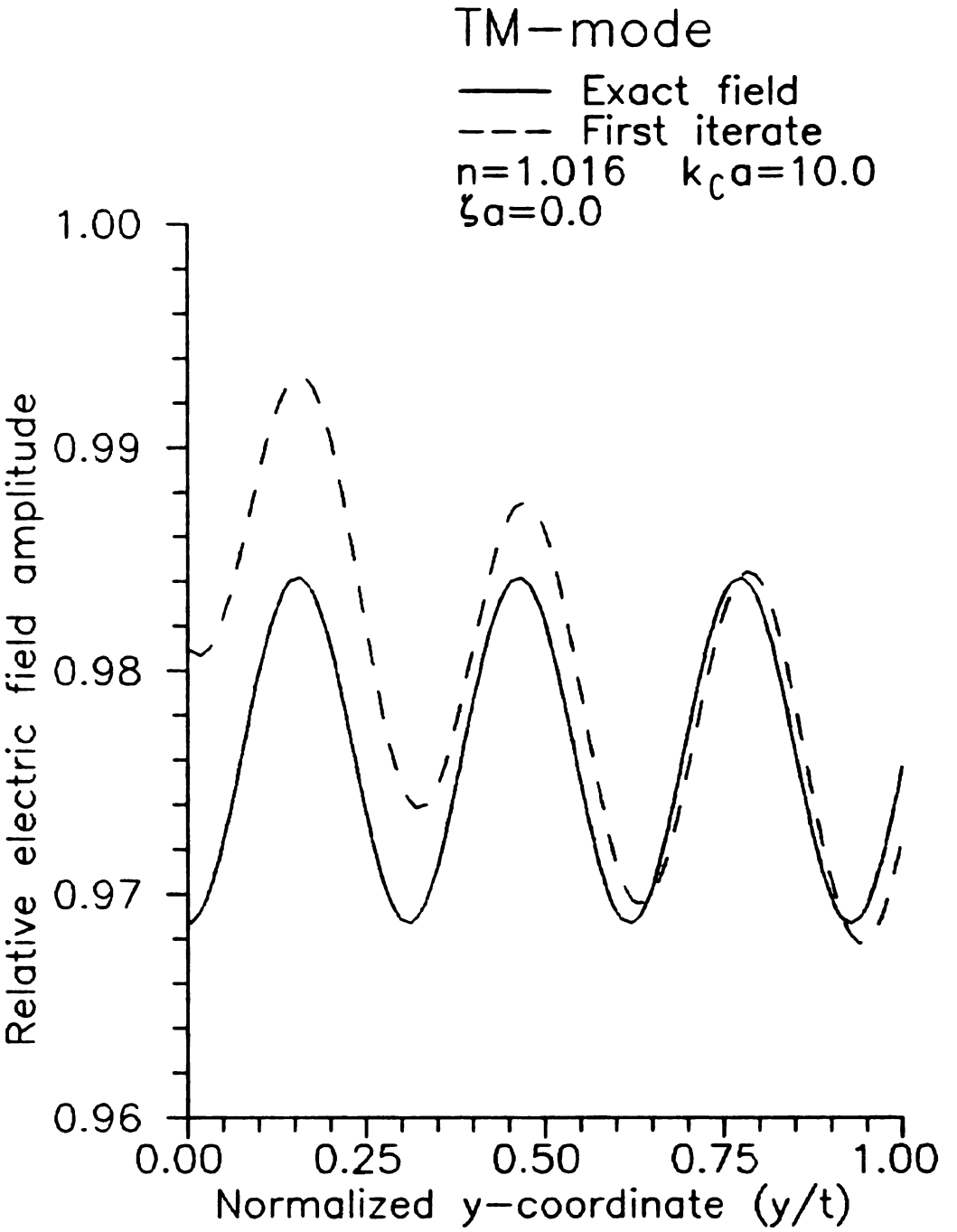

Figure 31. Relative field amplitudes for TM mode (Δn^2 = .032).

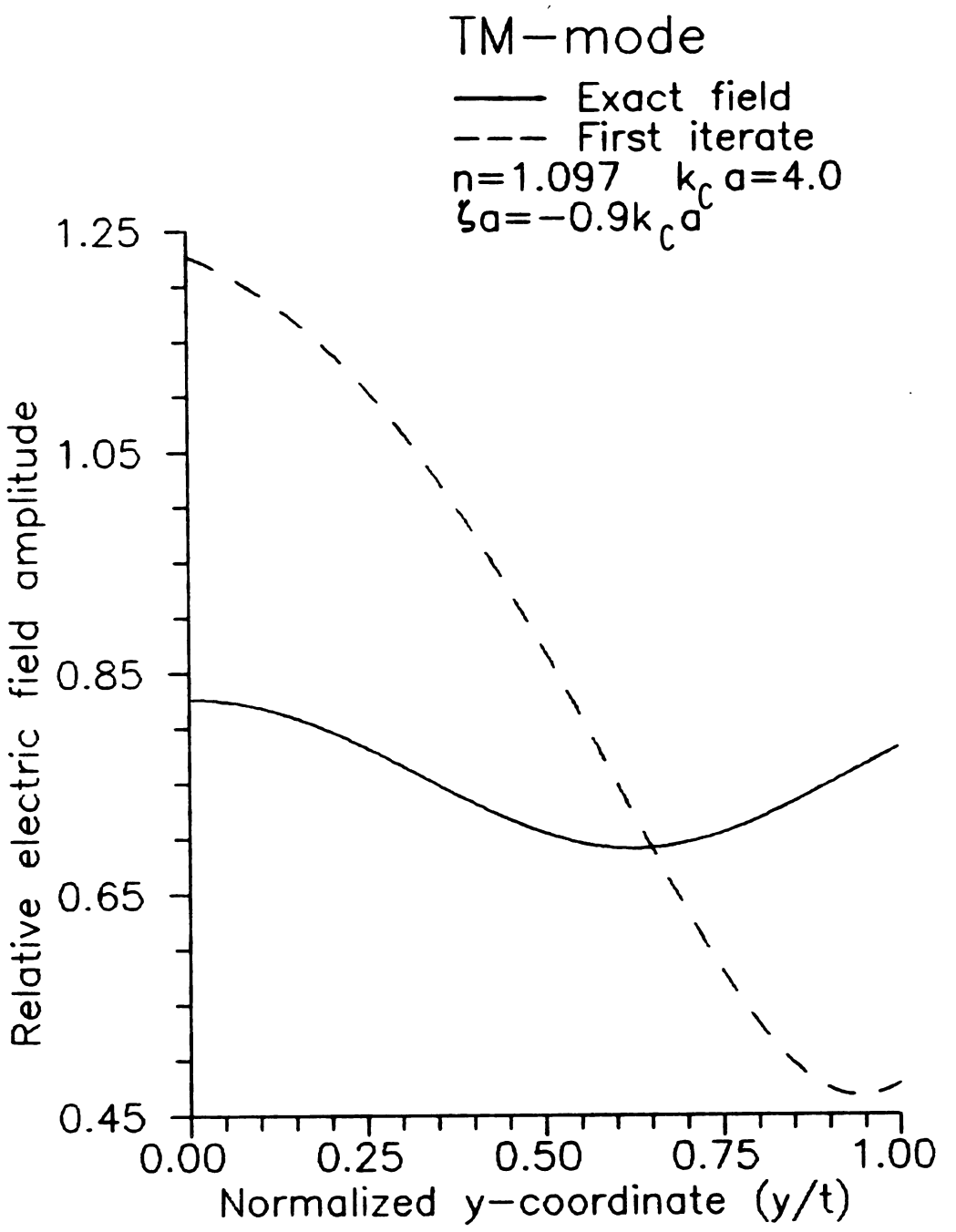

Figure 32. Relative field amplitudes for TM mode (Δn^2 = .203).

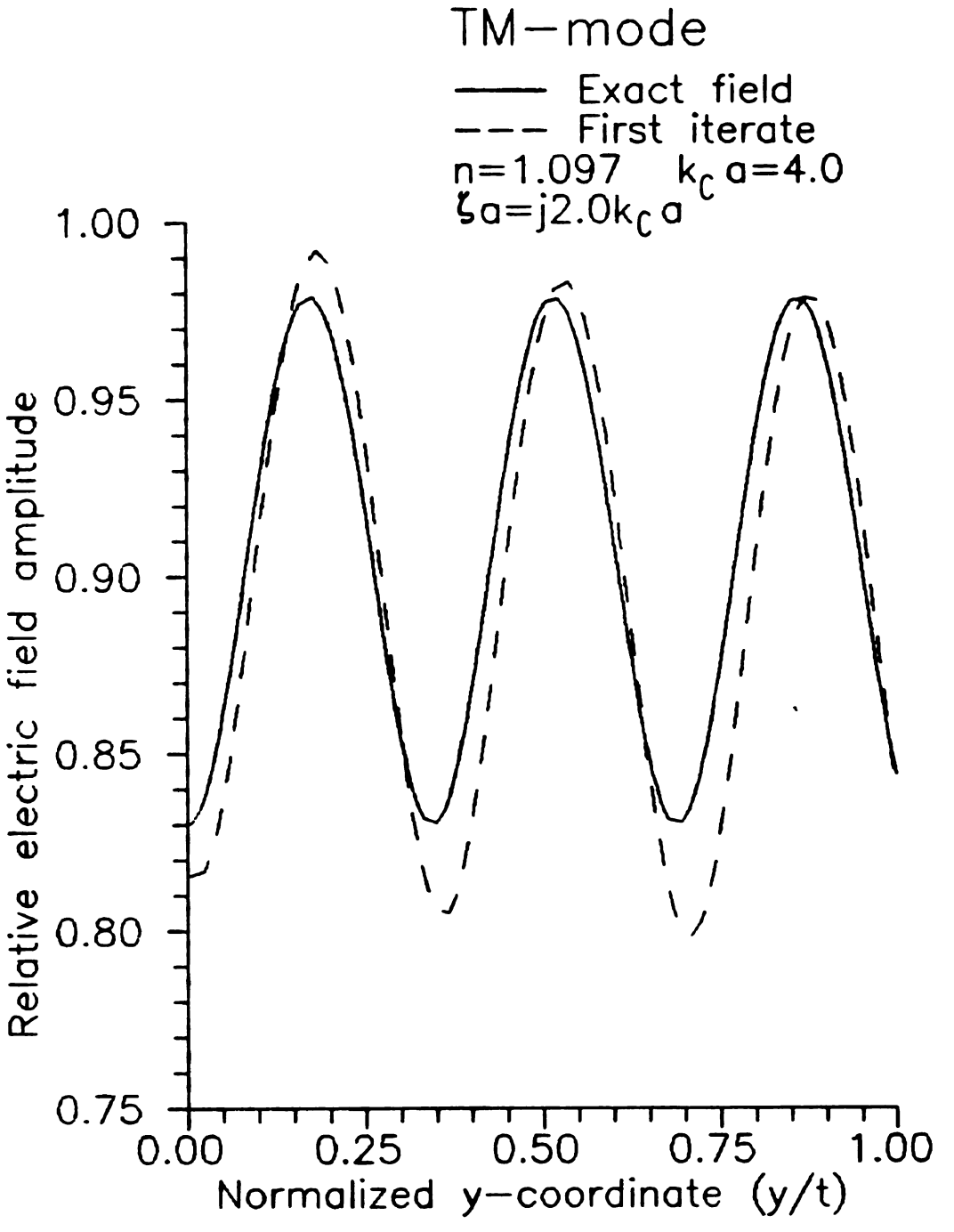

Figure 33. Relative field amplitudes for TM mode (Δn^2 = .203).

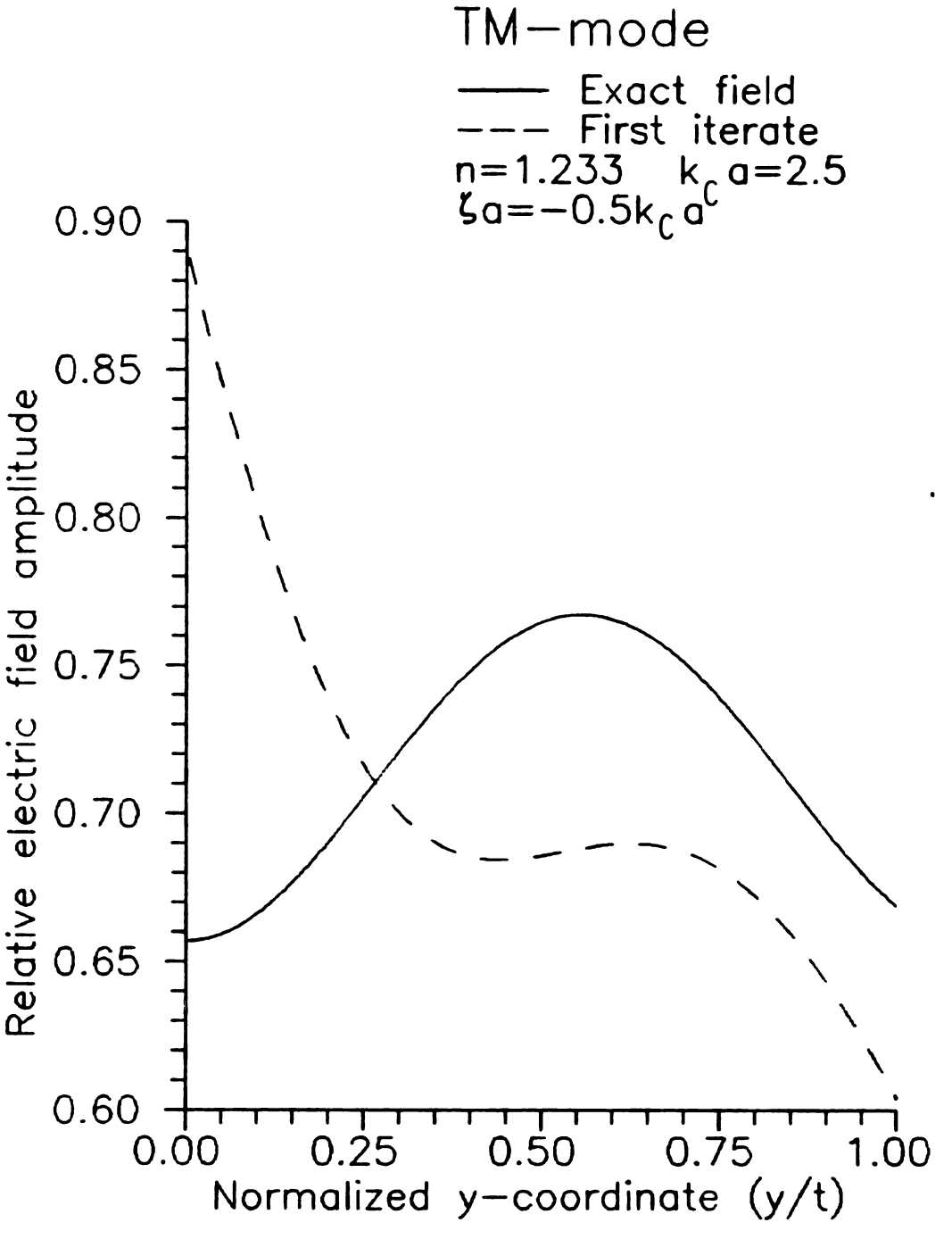

Figure 34. Relative field amplitudes for TM mode (Δn^2 = .520).

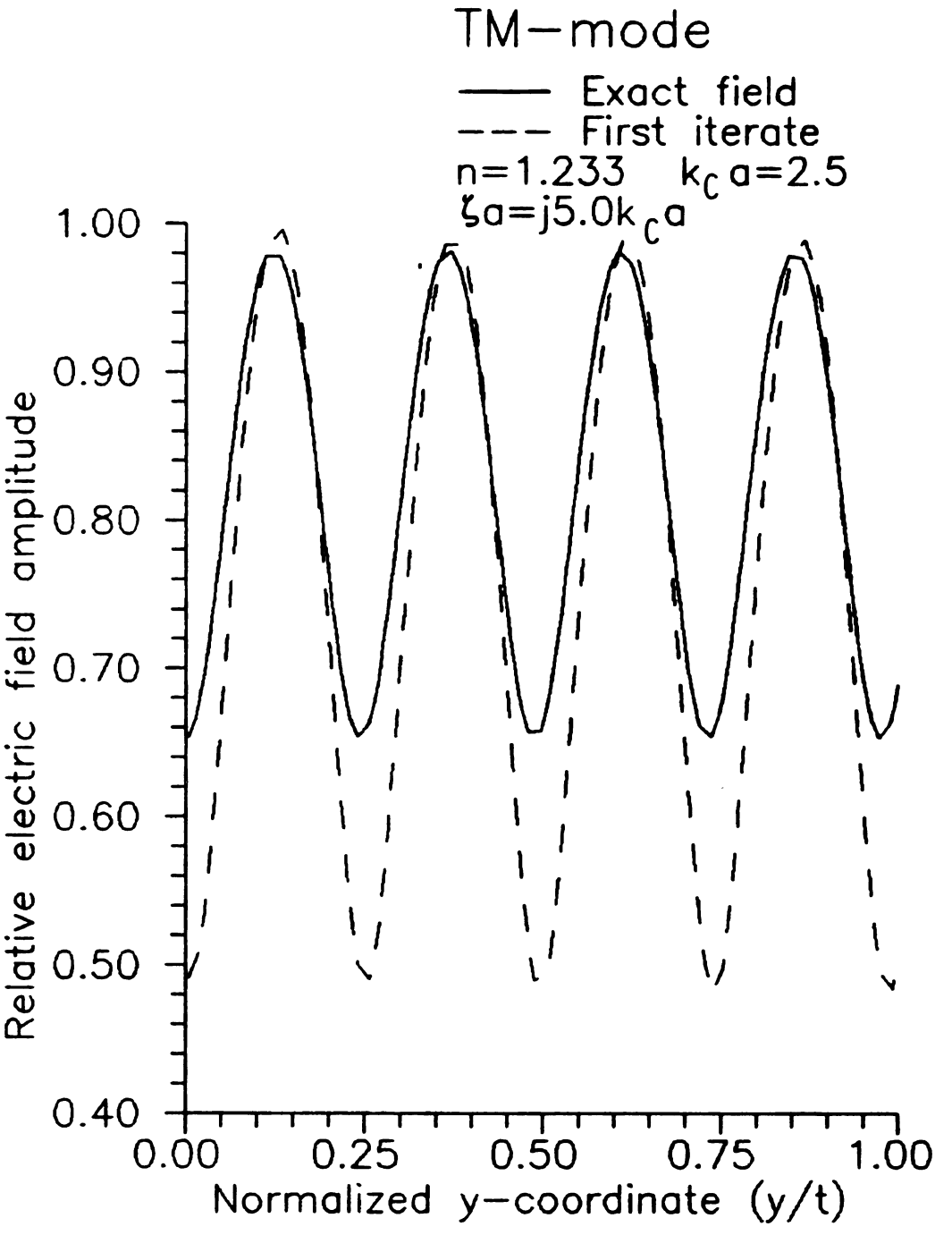

Figure 35. Relative field amplitudes for TM mode (Δn^2 = .520).

relative simplicity of the operators allowed some rather crude estimates of operator norms to lead to useful results. Attempts to estimate operator norms of more complicated operators by similar methods often fail. An examination of the operator for the radiation modes of the circular fiber exposes this difficulty.

Consider the circular fiber of Chapter five modified by allowing the refractive index to have radial grading with $\delta n^2(\rho) = \delta n^2(\rho)$. Then, specialization of (5.35) leads to the coupled pair of integral equations

$$e_\rho(\rho,\zeta) = e^i_\rho(\rho,\zeta) - \frac{\partial}{\partial\rho}\left\{\frac{a\delta n^2(a)}{n_c^2}\int_{-\pi}^{\pi}\left[e_\rho(\rho',\zeta)\, g^p_\zeta(\rho|\rho')\right]\Big|_{\rho'=a} d\varphi'\right\} \quad (17a)$$

$$+ \frac{\partial}{\partial\rho}\int_0^a \frac{2n'(\rho')}{n(\rho')}\left[\int_{-\pi}^{\pi} e_\rho(\rho',\zeta)\, g^p_\zeta(\rho|\rho')\, d\varphi'\right]\rho'd\rho'$$

$$+ k_0^2\int_0^a \delta n^2(\rho')\left[\int_{-\pi}^{\pi}\cos(\varphi-\varphi')\, e_\rho(\rho',\zeta)\, g^p_\zeta(\rho|\rho')\, d\varphi'\right]\rho'd\rho'$$

$$+ k_0^2\int_0^a \delta n^2(\rho')\left[\int_{-\pi}^{\pi}\sin(\varphi-\varphi')\, e_\varphi(\rho',\zeta)\, g^p_\zeta(\rho|\rho')\, d\varphi'\right]\rho'd\rho'$$

$$e_\varphi(\rho,\zeta) = e^i_\varphi(\rho,\zeta) - \frac{1}{\rho}\frac{\partial}{\partial\varphi}\left\{\frac{a\delta n^2(a)}{n_c^2}\int_{-\pi}^{\pi} e_\rho(\rho',\zeta)\, g^p_\zeta(\rho|\rho')\Big|_{\rho'=a} d\varphi'\right\} \quad (17b)$$

$$+ \frac{1}{\rho}\frac{\partial}{\partial\varphi}\int_0^a \frac{2n'(\rho')}{n(\rho')}\left[\int_{-\pi}^{\pi} e_\rho(\rho',\zeta)\, g^p_\zeta(\rho|\rho')\, d\varphi'\right]\rho'd\rho'$$

$$+ k_0^2\int_0^a \delta n^2(\rho')\left[\int_{-\pi}^{\pi}\cos(\varphi-\varphi')\, e_\varphi(\rho',\zeta)\, g^p_\zeta(\rho|\rho')\, d\varphi'\right]\rho'd\rho'$$

$$- k_0^2\int_0^a \delta n^2(\rho')\left[\int_{-\pi}^{\pi}\sin(\varphi-\varphi')\, e_\rho(\rho',\zeta)\, g^p_\zeta(\rho|\rho')\, d\varphi'\right]\rho'd\rho'.$$

Along the relevant branch cut, the principal Green's function assumes the form given by (3.16b)

$$g_\zeta^p(\rho|\rho') = -\frac{i}{4} H_0^{(2)}(\Omega_c|\rho-\rho'|).$$

Exploiting the circular symmetry greatly reduces the complexity of the problem.

6.4.1 FOURIER SERIES EXPANSION

Assume that for each $\rho \in [0,a]$, e (e^i) is a continuous function of φ and that $\partial e/\partial\varphi$ ($\partial e^i/\partial\varphi$) is a square integrable function of φ on the interval $-\pi \le \varphi \le \pi$. Then, the Fourier series for the transverse components of e (e^i) converge uniformly [17, p.84] and are written

$$e_\rho(\rho) = \Sigma\, e_{\rho n}(\rho)\, e^{jn\varphi}$$

$$e_\varphi(\rho) = \Sigma\, e_{\varphi n}(\rho)\, e^{jn\varphi}$$

$$e^i_\rho(\rho) = \Sigma\, e^i_{\rho n}(\rho)\, e^{jn\varphi}$$

$$e^i_\varphi(\rho) = \Sigma\, e^i_{\varphi n}(\rho)\, e^{jn\varphi}$$

where the summation extends over all integer valued n. Note that the ζ-dependence of e and e^i has been suppressed. Substitution of these series into (17a) and (17b), with the summing notation implied, yields

$$e_{\rho n}(\rho)\, e^{jn\varphi} = e^i_{\rho n}(\rho)\, e^{jn\varphi} - \frac{\partial}{\partial\rho}\left\{\frac{a\delta n^2(a)}{n_c^2} e_{\rho n}(a)\, M_n(\rho,a;\varphi)\right\} \qquad (18a)$$

$$+ \frac{\partial}{\partial\rho}\int_0^a \frac{2n'(\rho')}{n(\rho')} e_{\rho n}(\rho')\, M_n(\rho,\rho';\varphi)\, \rho' d\rho'$$

$$+ k_0^2 \int_0^a \delta n^2(\rho')\, e_{\rho n}(\rho')\, M_n^c(\rho,\rho';\varphi)\, \rho' d\rho'$$

$$+ k_0^2 \int_0^a \delta n^2(\rho')\, e_{\varphi n}(\rho')\, M_n^s(\rho,\rho';\varphi)\, \rho' d\rho'$$

$$e_{\varphi n}(\rho)\, e^{jn\varphi} = e^{i}_{\varphi n}(\rho)\, e^{jn\varphi} - \frac{1}{\rho}\frac{\partial}{\partial\varphi}\left\{ \frac{a\delta n^2(a)}{n_c^2}\, e_{\rho n}(a)\, M_n(\rho, a;\varphi)\right\} \quad (18b)$$

$$+ \frac{1}{\rho}\frac{\partial}{\partial\varphi}\int_0^a \frac{2n'(\rho')}{n(\rho')}\, e_{\rho n}(\rho')\, M_n(\rho,\rho';\varphi)\, \rho' d\rho'$$

$$+ k_0^2 \int_0^a \delta n^2(\rho')\, e_{\varphi n}(\rho')\, M_n^c(\rho,\rho';\varphi)\, \rho' d\rho'$$

$$- k_0^2 \int_0^a \delta n^2(\rho')\, e_{\rho n}(\rho')\, M_n^s(\rho,\rho';\varphi)\, \rho' d\rho'$$

where the quantities M_n^c, M_n^s, and M_n abbreviate the integrals

$$\begin{Bmatrix} M_n^c(\rho,\rho';\varphi) \\ M_n^s(\rho,\rho';\varphi) \\ M_n(\rho,\rho';\varphi) \end{Bmatrix} = \int_{-\pi}^{\pi} \begin{Bmatrix} \cos(\varphi-\varphi') \\ \sin(\varphi-\varphi') \\ 1 \end{Bmatrix} e^{jn\varphi'}\, g_z^p(\rho|\rho')\, d\varphi'.$$

Making the change of variable $\theta = \varphi - \varphi'$ gives

$$\begin{Bmatrix} M_n^c(\rho,\rho';\varphi) \\ M_n^s(\rho,\rho';\varphi) \\ M_n(\rho,\rho';\varphi) \end{Bmatrix} = -\frac{1}{4} e^{jn\varphi} \int_{-\pi}^{\pi} \begin{Bmatrix} \cos\theta \\ \sin\theta \\ 1 \end{Bmatrix} e^{-jn\theta}\, H_0^{(2)}(Q_c R_0)\, d\theta \quad (19)$$

where $R_0 = (\rho^2 + \rho'^2 - 2\rho\rho'\cos\theta)^{1/2}$.

Closed form expressions for the integrals in (19) can be obtained by using the following expansion found in Gradshteyn [25, p.979].

$$H_0^{(2)}(Q_c R_0) = \sum_m J_m(Q_c\rho_<)\, H_m^{(2)}(Q_c\rho_>)\, e^{jm\theta} \quad (20)$$

where $\rho_<$ ($\rho_>$) is the smaller (larger) of ρ and ρ'. Now, substitute the series (20) into (19) and formally interchange the summation with the integral (this is justifiable by uniform convergence of (20)). The remaining integrations are trivial and are evaluated by exploiting the

orthogonality of the complex exponentials. This reduces (19) to the closed form expressions

$$M_n^c(\rho,\rho';\varphi) = -\frac{j\pi}{4} e^{jn\varphi} \left(J_{n-1}(Q_c\rho_<) H_{n-1}^{(2)}(Q_c\rho_>) + J_{n+1}(Q_c\rho_<) H_{n+1}^{(2)}(Q_c\rho_>)\right)$$

$$M_n^s(\rho,\rho';\varphi) = -\frac{\pi}{4} e^{jn\varphi} \left(J_{n-1}(Q_c\rho_<) H_{n-1}^{(2)}(Q_c\rho_>) - J_{n+1}(Q_c\rho_<) H_{n+1}^{(2)}(Q_c\rho_>)\right)$$

$$M_n(\rho,\rho';\varphi) = -\frac{j\pi}{2} e^{jn\varphi} J_n(Q_c\rho_<) H_n^{(2)}(Q_c\rho_>)$$

After substituting the expressions above into equations (18a) and (18b), the orthogonality of the complex exponentials are used again allowing Fourier coefficients to be equated term by term. This results in the following pair of coupled integral equations.

$$e_{\rho n}(\rho) = e_{\rho n}^i(\rho) + \frac{j\pi}{2}\frac{\delta n^2(a)}{n_c^2}\left[e_{\rho n}(a)\,(Q_c a)\,H_n^{(2)}(Q_c a)\right] J_n'(Q_c\rho) \qquad (21a)$$

$$-\frac{j\pi}{2}\frac{\partial}{\partial\rho}\int_0^a \frac{2n'(\rho')}{n(\rho')} e_{\rho n}(\rho')\, J_n(Q_c\rho_<) H_n^{(2)}(Q_c\rho_>)\,\rho'd\rho'$$

$$-\frac{j\pi}{4}k_o^2\int_0^a \delta n^2(\rho')\, e_{\rho n}(\rho')\, J_{n-1}(Q_c\rho_<) H_{n-1}^{(2)}(Q_c\rho_>)\,\rho'd\rho'$$

$$-\frac{j\pi}{4}k_o^2\int_0^a \delta n^2(\rho')\, e_{\rho n}(\rho')\, J_{n+1}(Q_c\rho_<) H_{n+1}^{(2)}(Q_c\rho_>)\,\rho'd\rho'$$

$$-\frac{\pi}{4}k_o^2\int_0^a \delta n^2(\rho')\, e_{\varphi n}(\rho')\, J_{n-1}(Q_c\rho_<) H_{n-1}^{(2)}(Q_c\rho_>)\,\rho'd\rho'$$

$$+\frac{\pi}{4}k_o^2\int_0^a \delta n^2(\rho')\, e_{\varphi n}(\rho')\, J_{n+1}(Q_c\rho_<) H_{n+1}^{(2)}(Q_c\rho_>)\,\rho'd\rho'$$

$$e_{\varphi n}(\rho) = e^{i}_{\varphi n}(\rho) - \frac{\pi}{2}\frac{na}{\rho}\frac{\delta n^2(a)}{n_c^2}\left[e_{\rho n}(a)\, H_n^{(2)}(Q_c a)\right] J_n(Q_c\rho) \qquad (21b)$$

$$+ \frac{\pi}{2}\frac{n}{\rho}\int_0^a \frac{2n'(\rho')}{n(\rho')}\, e_{\rho n}(\rho')\, J_n(Q_c\rho_<)\, H_n^{(2)}(Q_c\rho_>)\, \rho' d\rho'$$

$$+ \frac{\pi}{4} k_o^2 \int_0^a \delta n^2(\rho')\, e_{\rho n}(\rho')\, J_{n-1}(Q_c\rho_<)\, H_{n-1}^{(2)}(Q_c\rho_>)\, \rho' d\rho'$$

$$- \frac{\pi}{4} k_o^2 \int_0^a \delta n^2(\rho')\, e_{\rho n}(\rho')\, J_{n+1}(Q_c\rho_<)\, H_{n+1}^{(2)}(Q_c\rho_>)\, \rho' d\rho'$$

$$- \frac{j\pi}{4} k_o^2 \int_0^a \delta n^2(\rho')\, e_{\varphi n}(\rho')\, J_{n-1}(Q_c\rho_<)\, H_{n-1}^{(2)}(Q_c\rho_>)\, \rho' d\rho'$$

$$- \frac{j\pi}{4} k_o^2 \int_0^a \delta n^2(\rho')\, e_{\varphi n}(\rho')\, J_{n+1}(Q_c\rho_<)\, H_{n+1}^{(2)}(Q_c\rho_>)\, \rho' d\rho'$$

It can be seen that the estimates used in the previous section are not adequate to obtain analytic bounds for the operator norm. Nevertheless, a single iteration might still provide a "good" approximation for waveguides with sufficiently small contrast of refractive indices for those spectral components of sufficiently high spatial frequency. As a simple example, the n = 0 mode of a step-index fiber is investigated. Excitation is provided by an axially-polarized point source and a comparison of one iteration with the exact solution is made.

6.4.2 IMPRESSED FIELD

Consider an axially-polarized point source of current located at (ρ^s, z^s) where $\rho^s > a$. Then, $J = \hat{z}\, J\, \delta(\rho-\rho^s)\, \delta(z-z^s)$. As usual the impressed field is given by

$$e^i(\rho) = (k_c^2 + \tilde{\tilde{\nabla}}\tilde{\tilde{\nabla}}\cdot) \int_{CS_\infty} g_z^p(\rho|\rho')\, \frac{F_z(J)}{j\omega\epsilon_c}\, dS'.$$

The radial component of field can be written

$$e^i_\rho(\rho) = j\zeta \frac{\partial}{\partial\rho} \int_{CS_\infty} (-\tfrac{j}{4})\, H_0^{(2)}(Q_c|\rho-\rho'|)\, (J/j\omega\epsilon_c)\, e^{-j\zeta z''}\, \delta(\rho'-\rho'')\, dS'$$

from which use of (20) allows the Fourier coefficient $e^i_{\rho n}$ to be extracted. Then,

$$e^i_{\rho n}(\rho) = -\frac{jJ}{4\omega\epsilon_c}\left(\zeta Q_c\right) H_n^{(2)}(Q_c\rho'')\, e^{-j\zeta z''}\, e^{-jn\varphi''}\, J_n'(Q_c\rho)$$

and for n = 0

$$e^i_{\rho 0}(\rho) = \frac{jJ}{4\omega\epsilon_c}\left(\zeta Q_c\right) H_0^{(2)}(Q_c\rho'')\, e^{-j\zeta z''}\, J_1(Q_c\rho)$$

$$= A(\zeta)\, J_1(Q_c\rho) \qquad (22)$$

where $A(\zeta) = (jJ/4\omega\epsilon_c)\left(\zeta Q_c\right) H_0^{(2)}(Q_c\rho'')\, e^{-j\zeta z''}$ is a spatial constant. Similarly, the φ-component of field is expressed as

$$e^i_\varphi(\rho) = j\zeta \frac{1}{\rho}\frac{\partial}{\partial\varphi} \int_{CS_\infty} (-\tfrac{j}{4})\, H_0^{(2)}(Q_c|\rho-\rho'|)\, (J/j\omega\epsilon_c)\, e^{-j\zeta z''}\, \delta(\rho'-\rho'')\, dS'$$

so that $e^i_{\varphi n}$ becomes

$$e^i_{\varphi n}(\rho) = \left(\frac{J}{4\omega\epsilon_c}\,\zeta\right) H_n^{(2)}(Q_c\rho'')\, e^{-j\zeta z''}\, e^{-jn\varphi''}\left(\frac{n}{\rho}\right) J_n(Q_c\rho).$$

Therefore, the φ-component of the n = 0 radiation mode is not excited by a z-directed current source.

6.4.3 SPECIALIZED EFIE

When equations (21a) and (21b) are specialized for the n = 0 mode, an uncoupling of the transverse components results. To see this, invoke the relations $J_{-1} = -J_1$ and $H^{(2)}_{-1} = -H^{(2)}_1$ found in [16, p.360]. Then, (21a) becomes

$$e_{\rho 0}(\rho) = e^{i}_{\rho 0}(\rho) - \frac{j\pi}{2}\frac{\delta n^2(a)}{n_c^2}\left[e_{\rho 0}(a)\,(Q_c a)\,H_0^{(2)}(Q_c a)\right] J_1(Q_c\rho)$$

$$- \frac{j\pi}{2}\frac{\partial}{\partial\rho}\int_0^a \frac{2n'(\rho')}{n(\rho')}\, e_{\rho 0}(\rho')\, J_0(Q_c\rho_<)\, H_0^{(2)}(Q_c\rho_>)\,\rho'd\rho'$$

$$- \frac{j\pi}{2} k_0^2 \int_0^a \delta n^2(\rho')\, e_{\rho 0}(\rho')\, J_1(Q_c\rho_<)\, H_1^{(2)}(Q_c\rho_>)\,\rho'd\rho'$$

which for the step-index guide simplifies to

$$e_{\rho 0}(\rho) = e^{i}_{\rho 0}(\rho) - \frac{j\pi}{2}\frac{\Delta n^2}{n_c^2}\left[e_{\rho 0}(a)\,(Q_c a)\,H_0^{(2)}(Q_c a)\right] J_1(Q_c\rho) \qquad (23)$$

$$- \frac{j\pi}{2} k_0^2 \left\{\int_0^\rho \delta n^2(\rho')\, e_{\rho 0}(\rho')\, J_1(Q_c\rho')\,\rho'd\rho'\right\} H_1^{(2)}(Q_c\rho)$$

$$- \frac{j\pi}{2} k_0^2 \left\{\int_\rho^a \delta n^2(\rho')\, e_{\rho 0}(\rho')\, H_1^{(2)}(Q_c\rho')\,\rho'd\rho'\right\} J_1(Q_c\rho)$$

where the integral has been split into a sum of integrals. Obviously, this mode uncouples the transverse components of field. The φ-component of field for the n = 0 mode is given by

$$e_{\varphi 0}(\rho) = e^{i}_{\varphi 0}(\rho) - \frac{j\pi}{2} k_0^2 \int_0^a \delta n^2(\rho')\, e_{\varphi 0}(\rho')\, J_1(Q_c\rho_<)\, H_1^{(2)}(Q_c\rho_>)\,\rho'd\rho'$$

which is also an uncoupled EFIE.

6.4.4 EXACT FIELD

Exact solution for spectral components for the step-index circular fiber have been discussed by Snyder [28]. Eigenfunction expansions of unknown interior and exterior fields are made and boundary conditions at the dielectric interface are enforced. An alternative and equivalent

approach in which the exterior field is written as the sum of the known impressed field and the unknown scattered field may be also be used. In either case, the closed form solution for the n = 0 mode excited by the axially-polarized point source is

$$e_{\rho 0}(\rho) = A(z)\left(\frac{j2n_c^2}{\pi a}\right) W^{-1} J_1(Q\rho) \tag{24}$$

where $W = n_c^2 Q J_0(Qa) H_1^{(2)}(Q_c a) - n^2 Q J_1(Qa) H_0^{(2)}(Q_c a)$.

6.4.5 FIRST ITERATE

The first iterate is obtained as usual, by substituting (22) in the right side of (23). This yields

$$\begin{aligned} e_{\rho 0}^{(1)}(\rho) = A(z) \Bigg\{ & J_1(Q_c\rho) - \frac{j\pi}{2}\frac{\Delta n^2}{n_c^2}\left[J_1(Q_c a)\,(Q_c a)\,H_0^{(2)}(Q_c a)\right] J_1(Q_c\rho) \\ & - \frac{j\pi}{2}\Delta k^2 \left(\int_0^{\rho} J_1(Q_c\rho')\, J_1(Q_c\rho')\,\rho' d\rho'\right) H_1^{(2)}(Q_c\rho) \\ & - \frac{j\pi}{2}\Delta k^2 \left(\int_{\rho}^{a} J_1(Q_c\rho')\, H_1^{(2)}(Q_c\rho')\,\rho' d\rho'\right) J_1(Q_c\rho) \Bigg\} \end{aligned} \tag{25}$$

where as in Chapter five, $\Delta k^2 = \Delta n^2 k_0^2$.

Each of the integrals in (25) can be evaluated in closed form. The first integral is given in Gradshteyn [25, p.634] as

$$\int [J_1(Q_c\rho)]^2 \rho d\rho = \frac{\rho^2}{2}\left([J_1(Q_c\rho)]^2 - J_0(Q_c\rho)\, J_2(Q_c\rho)\right). \tag{26}$$

Writing J_2 in terms of J_0 and J_1 through use of the recurrence relation [16, p.361]

$$J_2(Q_c\rho) = -J_0(Q_c\rho) + \frac{2}{Q_c\rho} J_1(Q_c\rho)$$

allows (26) to be written

$$\int J_1^2(Q_c\rho)\ \rho d\rho = \frac{\rho^2}{2}\left(J_1^2(Q_c\rho) - J_0^2(Q_c\rho)\right) - \frac{\rho}{Q_c} J_0(Q_c\rho)\ J_1(Q_c\rho). \quad (27)$$

The second integral is evaluated in Appendix E (E.9) and is given by

$$\int J_1(Q_c\rho)\ H_1^{(2)}(Q_c\rho)\ \rho d\rho = \frac{\rho^2}{2}\left[J_1(Q_c\rho)\ H_1^{(2)}(Q_c\rho) + J_0(Q_c\rho)\ H_0^{(2)}(Q_c\rho)\right] - \frac{\rho}{Q_c} J_1(Q_c\rho)\ H_0^{(2)}(Q_c\rho). \quad (28)$$

Substituting (27) and (28) into (25) gives first iterate

$$e_{\rho 0}^{(1)}(\rho) = A(z)\left\{J_1(Q_c\rho) - \frac{j\pi}{2}\frac{\Delta n^2}{n_c^2}\left[(Q_c a)\ J_1H_0\right] J_1(Q_c\rho) - \frac{j\pi}{2}\Delta k^2\left[\frac{\rho^2}{2} J_0^2(Q_c\rho)\ H_1^{(2)}(Q_c\rho) + \frac{\rho^2}{2} J_1^2(Q_c\rho)\ H_1^{(2)}(Q_c\rho) - \frac{\rho}{Q_c} J_0(Q_c\rho)\ J_1(Q_c\rho)\ H_1^{(2)}(Q_c\rho) + \frac{\rho}{Q_c} J_1^2(Q_c\rho)\ H_0^{(2)}(Q_c\rho) - \frac{\rho^2}{2} J_0(Q_c\rho)\ J_1(Q_c\rho)\ H_0^{(2)}(Q_c\rho) - \frac{\rho^2}{2} J_1^2(Q_c\rho)\ H_1^{(2)}(Q_c\rho) + \frac{a^2}{2}\left(J_0H_0 + J_1H_1\right) J_1(Q_c\rho) - \frac{a}{Q_c}\left(J_1H_0\right) J_1(Q_c\rho)\right]\right\}$$

where Bessel functions without specified arguments are assumed to have argument $Q_c a$. Judicious factorizations and use of Wronskian derived in Appendix E (E.8) simplify the first iterate to

$$e_{\rho 0}^{(1)}(\rho) = A(z)\left\{J_1(Q_c\rho) + \frac{j\pi}{2}\frac{\Delta n^2}{n_c^2}\left[(z^2 a/Q_c)J_1H_0\right] J_1(Q_c\rho) + \frac{\Delta k^2}{2Q_c^2}\left[(Q_c\rho)\ J_0(Q_c\rho) - 2J_1(Q_c\rho)\right] - \frac{j\pi}{4}\Delta k^2 a^2\left(J_0H_0 + J_1H_1\right) J_1(Q_c\rho)\right\}. \quad (29)$$

6.4.6 COMPARISON

As with the modes of the slab waveguide, the first iterate (29) is directly shown to be equivalent to a first-order expansion in Δn^2 of the exact solution (24). The following expansions facilitate this development.

$$n^2 = n_c^2 + \Delta n^2 \tag{31a}$$

$$\begin{aligned} J_0(Q\rho) &= J_0(Q_c\rho) + \frac{\Delta k^2}{2Q_c^2}(Q_c\rho)\, J_0'(Q_c\rho) + O[(\Delta n^2)^2] \\ &= J_0(Q_c\rho) - \frac{\Delta k^2}{2Q_c^2}(Q_c\rho)\, J_1(Q_c\rho) + O[(\Delta n^2)^2] \end{aligned} \tag{31b}$$

$$\begin{aligned} J_1(Q\rho) &= J_1(Q_c\rho) + \frac{\Delta k^2}{2Q_c^2}(Q_c\rho)\, J_1'(Q_c\rho) + O[(\Delta n^2)^2] \\ &= J_1(Q_c\rho) + \frac{\Delta k^2}{2Q_c^2}[(Q_c\rho)\, J_0 Q_c\rho) - J_1(Q_c\rho)] \\ &\quad + O[(\Delta n^2)^2] \end{aligned} \tag{31c}$$

Now, the quantity W appearing in (24) can be approximated by using equations (31a) through (31c), retaining terms of order Δn^2 and manipulating the resulting expression. This reveals

$$n_c^2\, Q\, J_0(Qa)\, H_1^{(2)}(Qa) \approx n_c^2\, Q_c H_1 \left\{ J_0 + \frac{\Delta k^2}{2Q_c^2}[J_0 - (Q_c a)J_1] \right\}$$

$$n^2\, Q_c J_1(Qa)\, H_0^{(2)}(Q_c a) \approx n_c^2\, Q_c H_0 \left\{ J_1 + \frac{\Delta k^2}{2Q_c^2}\left(\frac{2Q_c^2}{k_c^2} J_1 + (Q_c a)J_0 - J_1 \right) \right\}.$$

Forming the difference in these expressions yields

$$W = n_c^2\, Q\, J_0(Qa)\, H_1^{(2)}(Q_c a) - n^2\, Q_c J_1(Qa)\, H_0^{(2)}(Q_c a)$$

$$W \approx n_c^2 Q_c(J_0H_1 - J_1H_0) + \frac{\Delta k^2}{2Q_c^2}\left\{n_c^2 Q_c(J_0H_1 + J_1H_0) - n_c^2 Q_c^2 a(J_0H_0 + J_1H_1) - \frac{2Q_c^3}{k_0^2} J_1H_0\right\} \tag{32}$$

Use of Wronskian (E.8) shows that $J_0H_1 - J_1H_0 = 2j/(\pi Q_c a)$, whereby (32) becomes

$$W \approx n_c^2 Q_c(j2/\pi Q_c a) + \frac{\Delta k^2}{2Q_c^2}\left\{n_c^2 Q_c\,(2J_1H_0 + (j2/\pi Q_c a)) - n_c^2 Q_c^2 a(J_0H_0 + J_1H_1) - \frac{2Q_c^3}{k_0^2} J_1H_0\right\}$$

$$\approx (j2n_c^2/\pi a)\left\{1 + \frac{\Delta k^2}{2Q_c^2}\left(1 + \frac{j\pi}{2}(Q_c a)^2(J_0H_0 + J_1H_1) - j\pi\frac{\zeta^2 Q_c a}{k_c^2} J_1H_0\right)\right\}.$$

With $e_{\rho 0} = A(\zeta)\,(j2n_c^2/\pi a)\,W^{-1}\,J_1(Q\rho)$, the first order approximation is given by

$$e_{\rho 0}(\rho) = A(\zeta)\left\{1 - \frac{\Delta k^2}{2Q_c^2}\left(1 + \frac{j\pi}{2}(Q_c a)^2(J_0H_0 + J_1H_1) - j\pi\frac{\zeta^2 Q_c a}{k_c^2} J_1H_0\right)\right.$$
$$\left. \times\left(J_1(Q_c\rho) + \frac{\Delta k^2}{2Q_c^2}\left[Q_c\rho\, J_0Q_c\rho) - J_1(Q_c\rho)\right]\right)\right\}$$
$$= A(\zeta)\left\{J_1(Q_c\rho) + \frac{j\pi}{2}\frac{\Delta n^2}{n_c^2}\,[(\zeta^2 a/Q_c)J_1H_0]\,J_1(Q_c\rho)\right.$$
$$+ \frac{\Delta k^2}{2Q_c^2}\,[Q_c\rho\, J_0(Q_c\rho) - 2J_1(Q_c\rho)]$$
$$\left. - \frac{j\pi}{4}\Delta k^2 a^2\,(J_0H_0 + J_1H_1)\,J_1(Q_c\rho)\right\}$$

which as expected is the first iterate.

6.4.7 RESULTS

A comparison between the first iterate and the exact solution of the n = 0 mode was made. Again, n_c was taken as vacuum index. In order to guarantee mono-mode surface-wave propagation, $\Delta k^2 a^2$ must be less than $(2.405)^2$. If k_0 is chosen such that $k_0 = .75k_{co}$, where k_{co} is the cutoff wavenumber of the first higher order surface-wave mode, then $\Delta k^2 a^2 = 3.25$. Figures 36 through 38 show relative error versus the normalized wavenumber Q_c/k_c. It appears that a reasonably good approximation to the relative error is given by $(\Delta n^2/n_c^2 + \Delta(\bar{k})^2/2\bar{Q}_c)^2$. This correspondence may be explained by examining the large argument approximations of the Bessel functions. With the apriori knowledge of solution, it can be seen that $|e_{\rho 0}(a)| = \|e_{\rho 0}\| \times |J_1(Qa)|/\|J_1\|$. Then for large Q_c, the relative error asymptotically approaches $(\Delta n^2/n_c^2)^2$.

In Figures 39 through 44, relative field amplitude $|e_{\rho 0}/A(\zeta)|$ and $|e_{\rho 0}^{(1)}/A(\zeta)|$ versus normalized radius ρ/a are shown. It is apparent that for small Δn^2, the field amplitudes compare well at relatively low spatial frequencies. In fact, it appears that the difference between the relative field amplitudes is much closer than the absolute error. This suggests that an alternative normed vector space might be more suitable for analysis.

6.5 SUMMARY

Numerical approximation of spectral components of the continuous spectrum is required for all but a few guiding structures. Standard numerical techniques such as the method of moments are ineffective in approximating those spectral components having high spatial frequencies due to limitations on computation. The method of successive

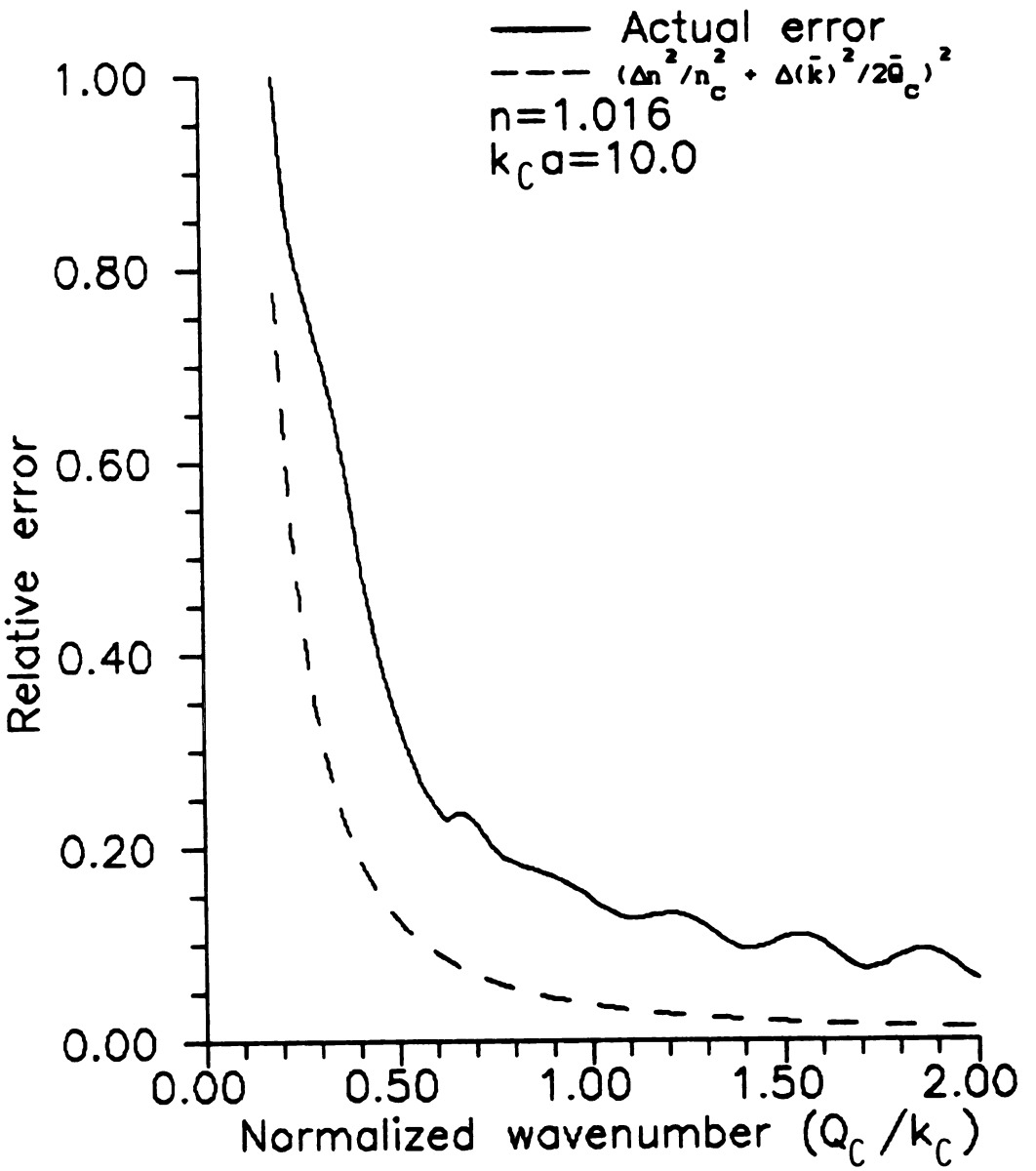

Figure 36. Relative error vs. (Q_c/k_c) for n = 0 mode (Δn^2 = .032).

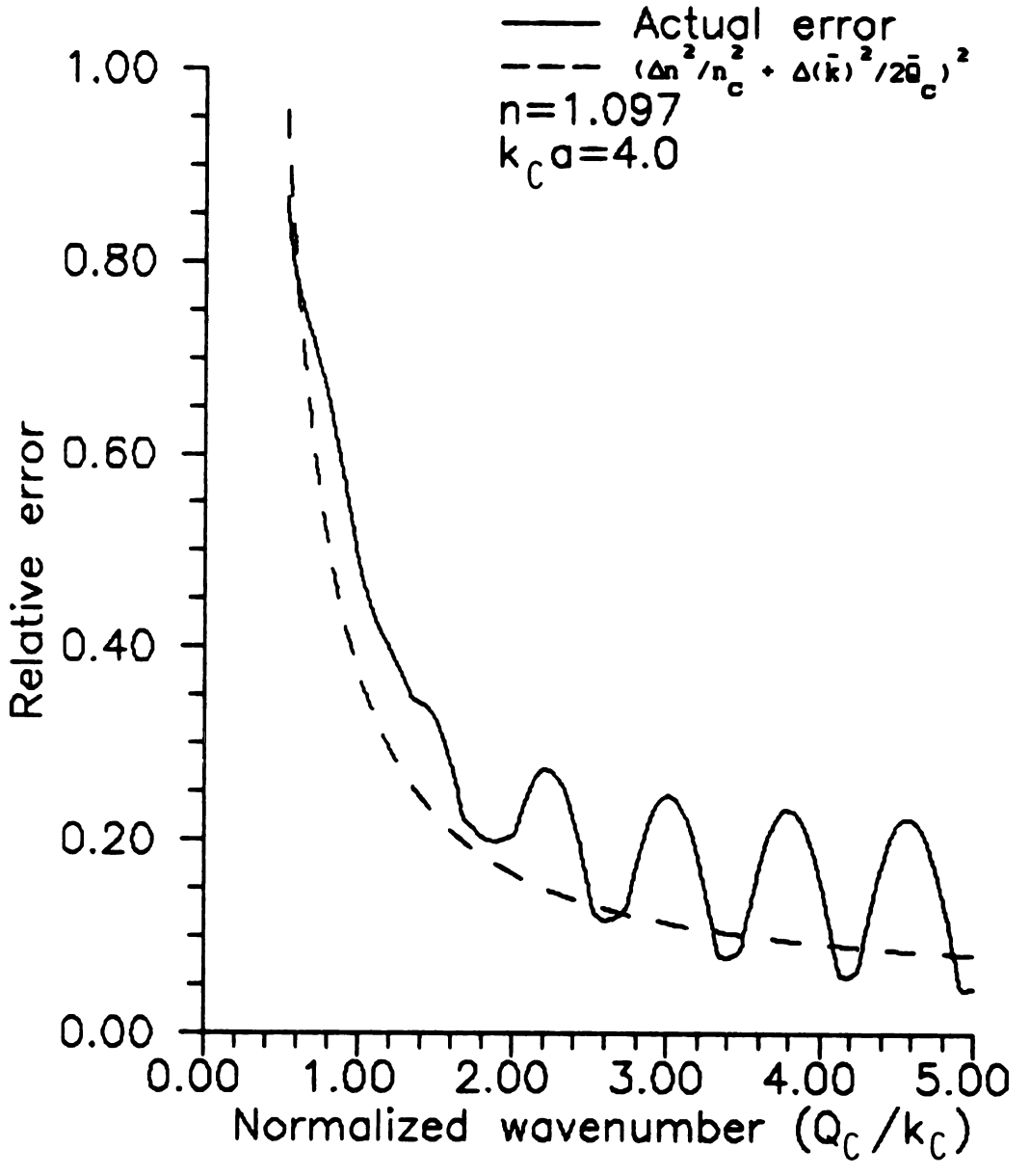

Figure 37. Relative error vs. (Q_c/k_c) for n = 0 mode (Δn^2 = .203).

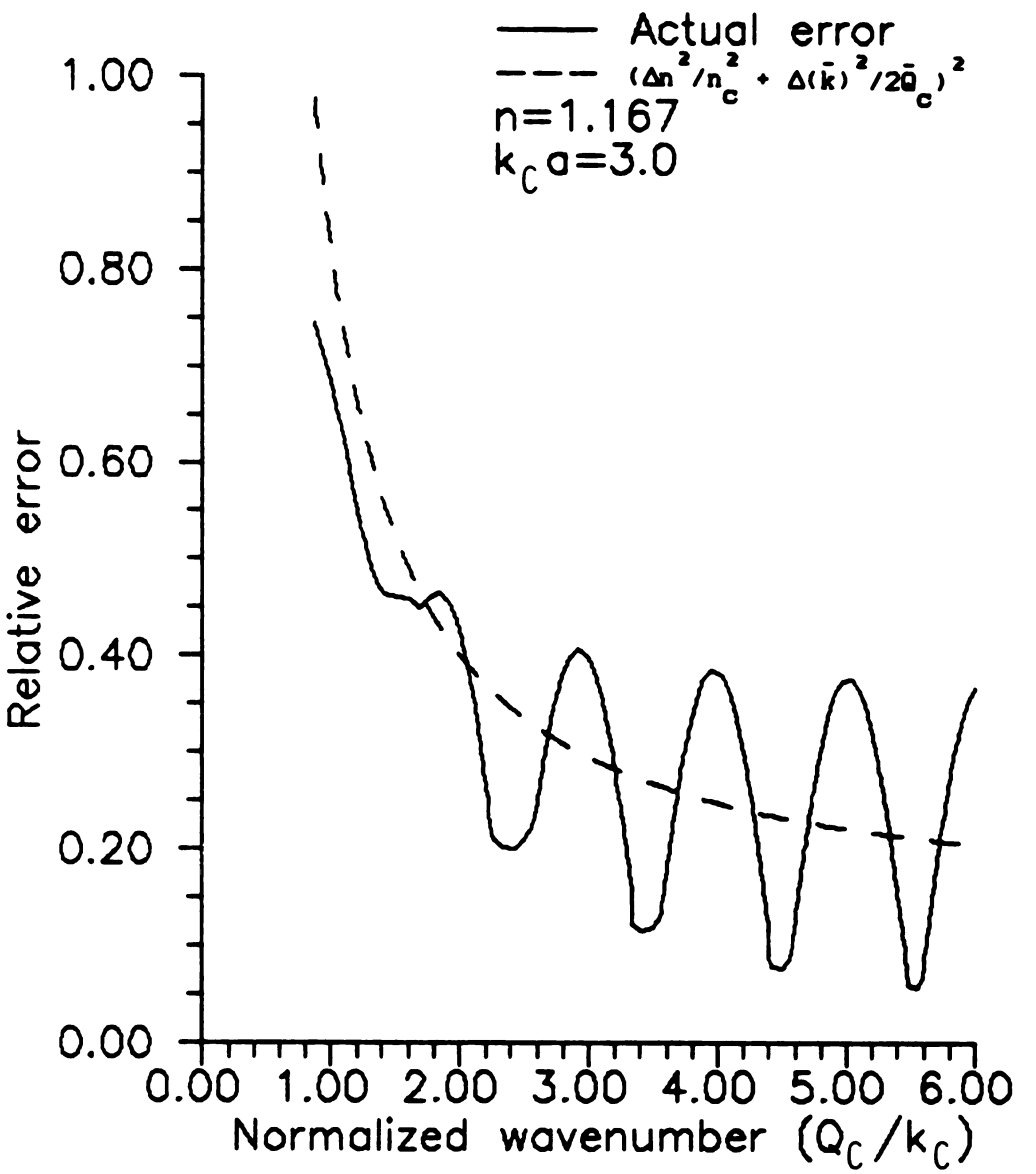

Figure 38. Relative error vs. (Q_c/k_c) for n = 0 mode (Δn^2 = .362).

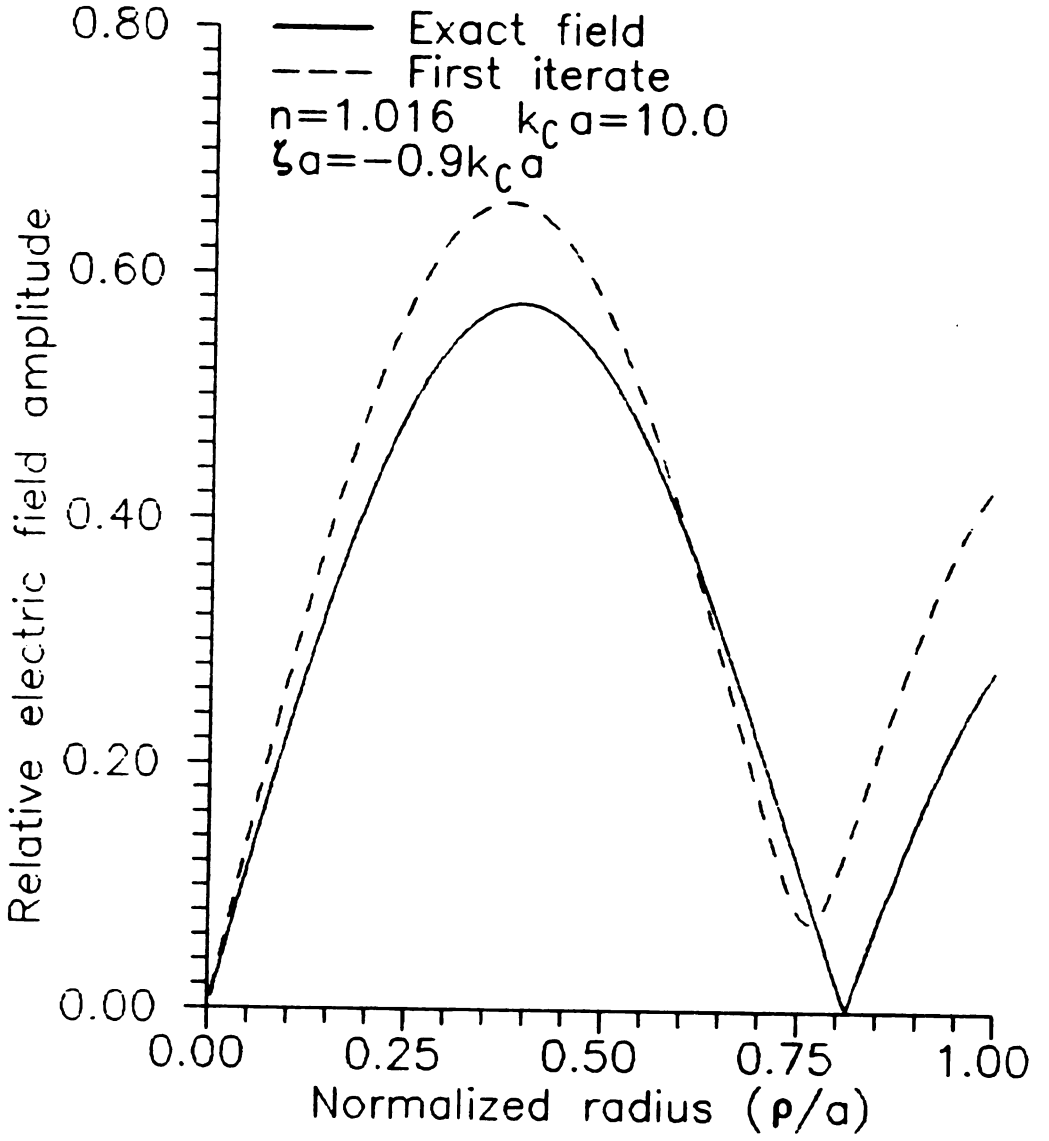

Figure 39. Relative field amplitudes for n = 0 mode (Δn^2 = .032).

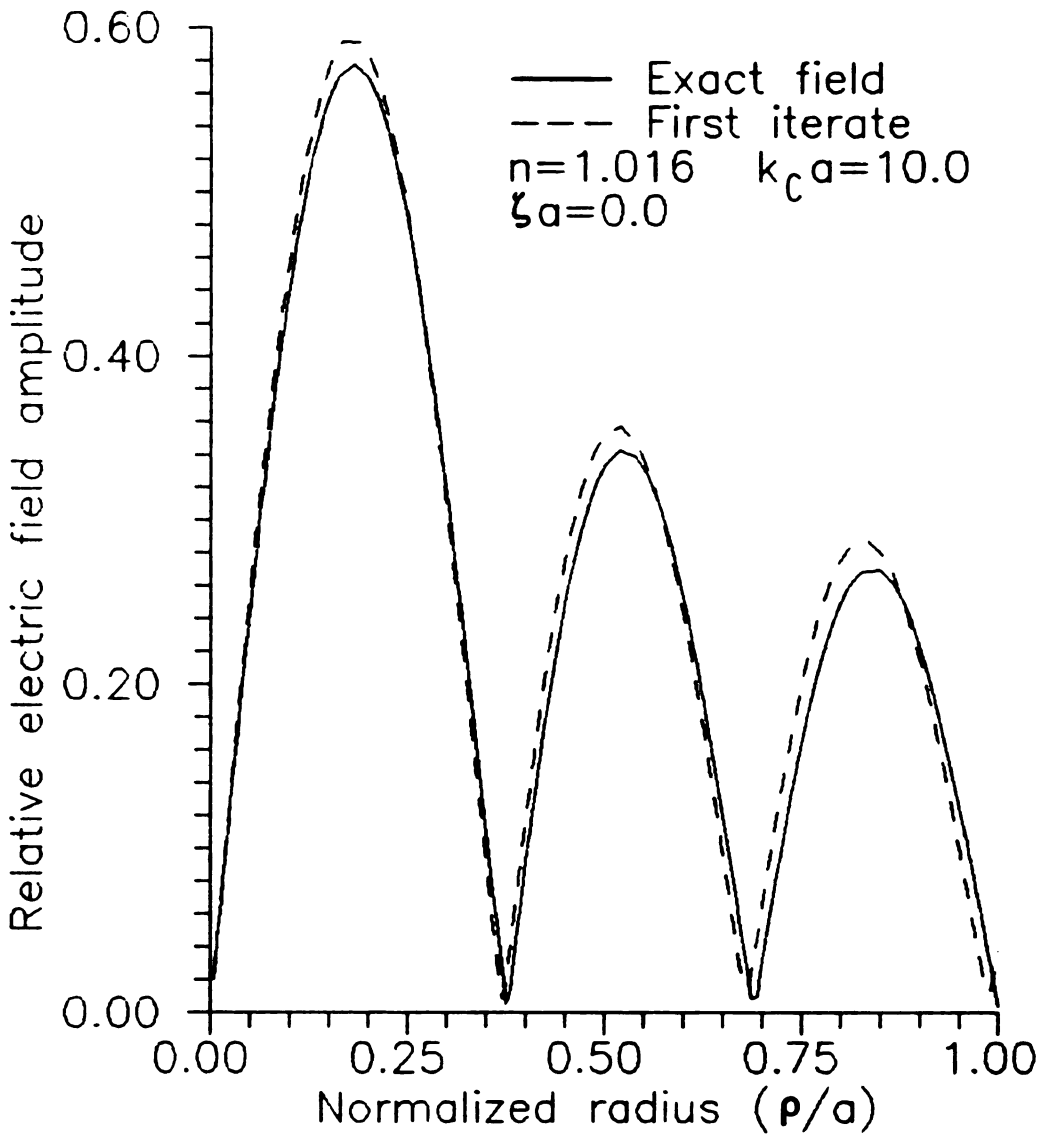

Figure 40. Relative field amplitudes for n = 0 mode (Δn^2 = .032).

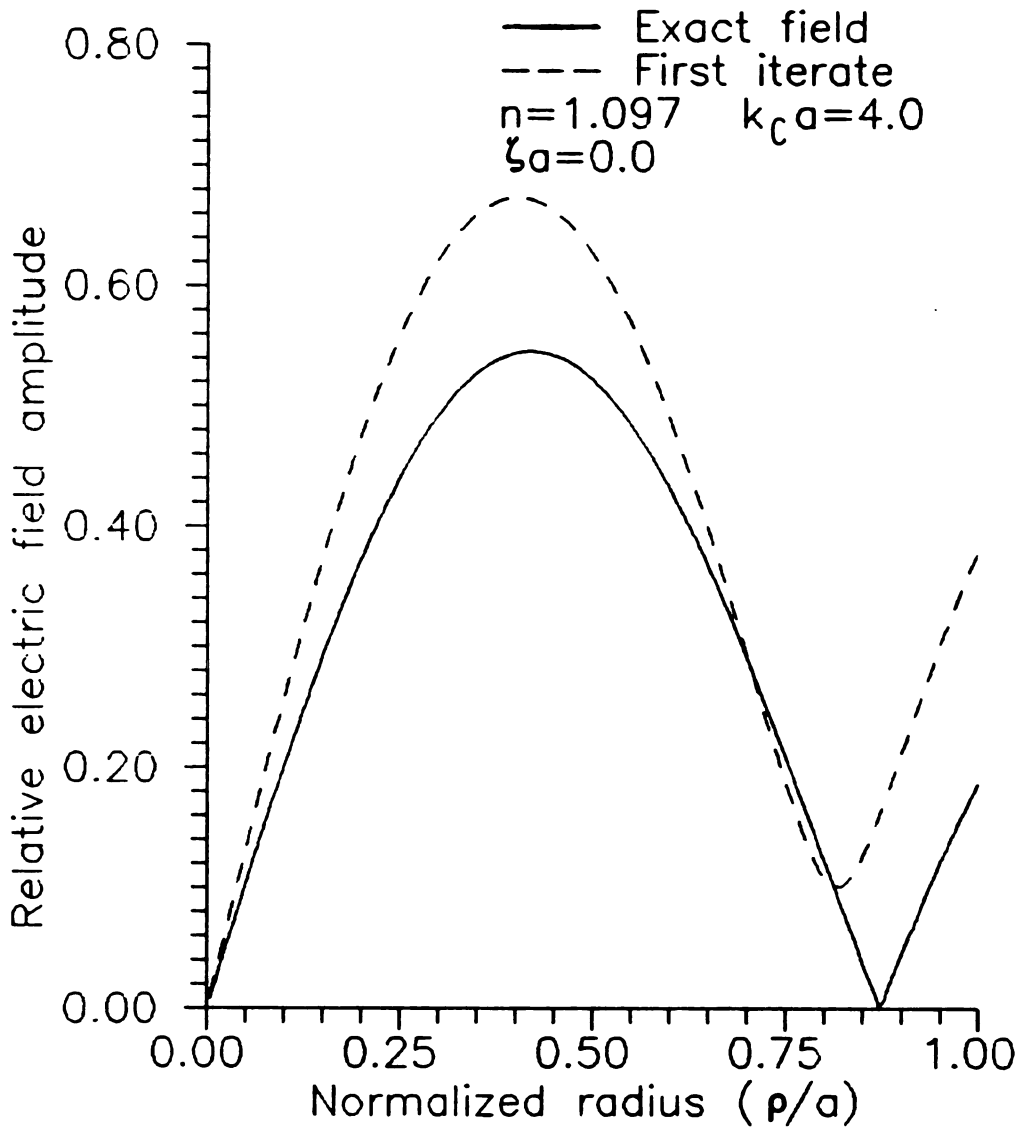

Figure 41. Relative field amplitudes for n = 0 mode (Δn^2 = .203).

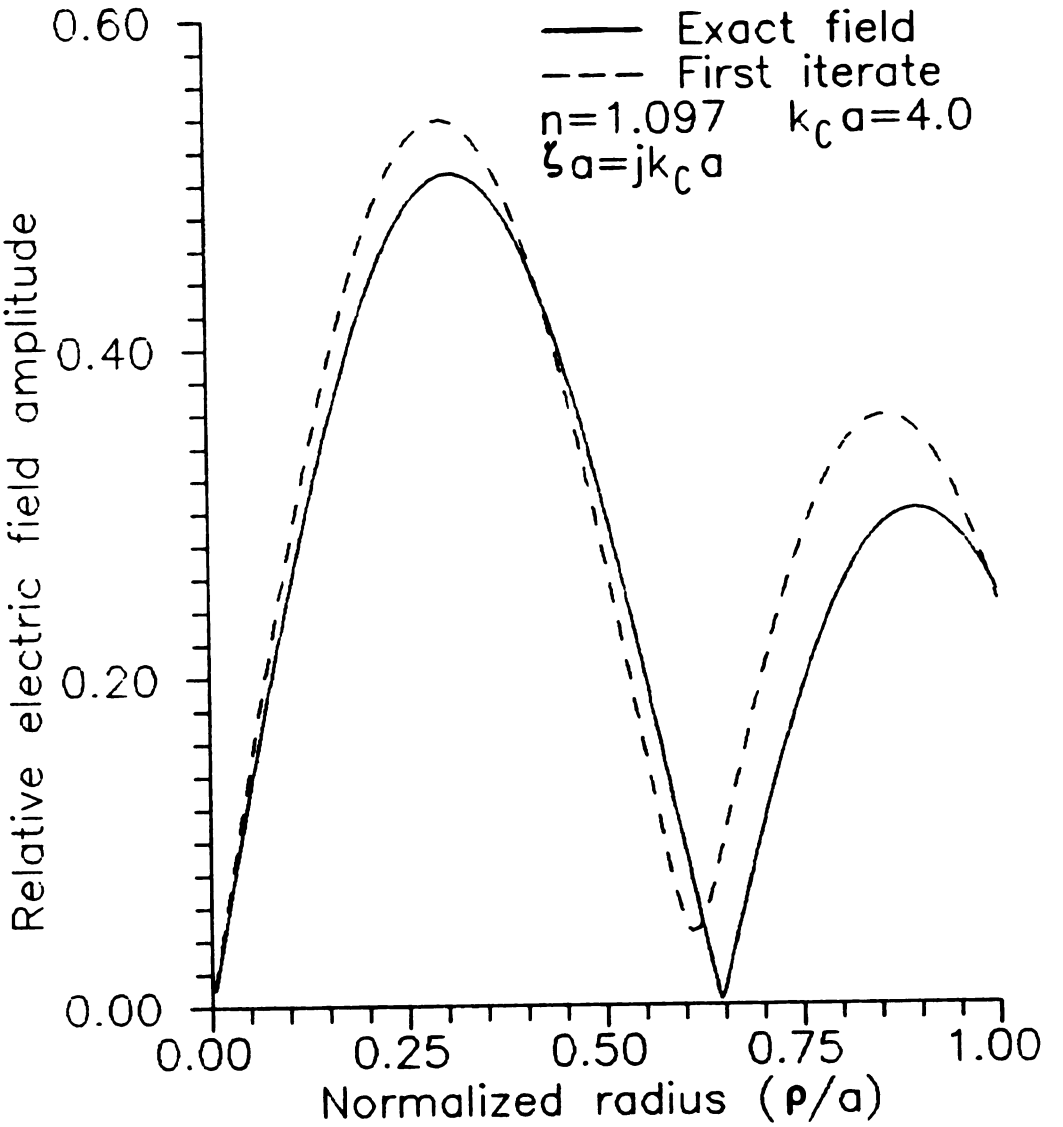

Figure 42. Relative field amplitudes for n = 0 mode (Δn^2 = .203).

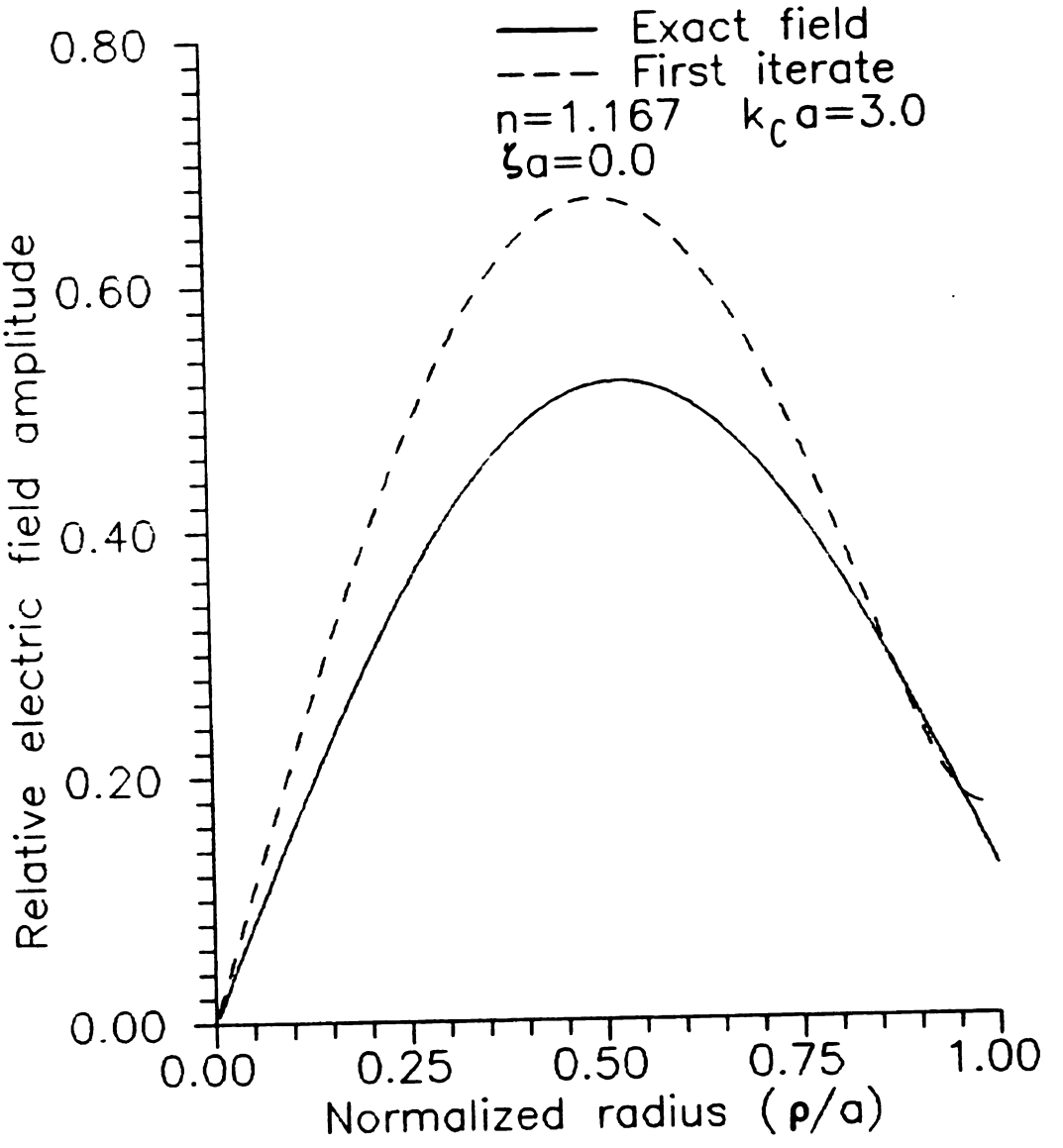

Figure 43. Relative field amplitudes for n = 0 mode (Δn^2 = .362).

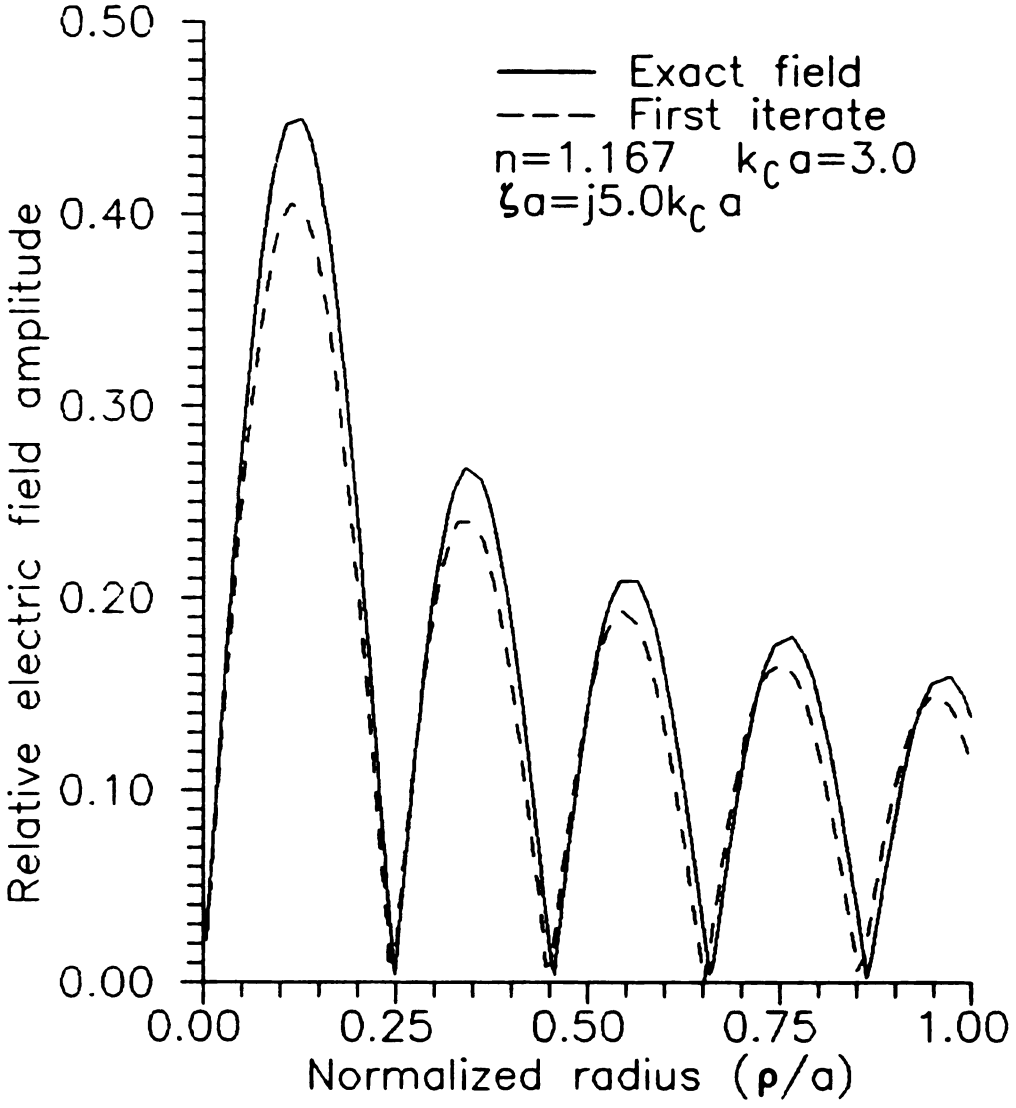

Figure 44. Relative field amplitudes for n = 0 mode (Δn^2 = .362).

approximations avoids these deficiencies.

Transform-domain EFIE (3.29) may be expressed in operator form as

$$e = \mathcal{L}_{op}(e) + e^{i} \tag{33}$$

where the operator $\mathcal{L}_{op}$ is given by

$$\mathcal{L}_{op}(\cdot) = (k_c^2 + \tilde{\tilde{\nabla}}\tilde{\tilde{\nabla}}\cdot) \int_{CS} \frac{\delta n^2(\rho')}{n_c^2} \tilde{\tilde{g}}_z(\rho|\rho') \cdot (\cdot)\, dS'.$$

Heuristic reasoning suggests that the total field should be close to the impressed field provided that δn^2 is adequately small. An iterative sequence is generated by the recursive formula

$$e^{(0)} = e^{i} \qquad e^{(n)} = e^{i} + \mathcal{L}_{op}(e^{(n-1)}), \quad (n \geq 1).$$

A theorem from functional analysis guarantees that this sequence converges to solution of (33) if the operator norm $\|\mathcal{L}_{op}\|$ defined by

$$\|\mathcal{L}_{op}\| = \sup_{f \in B} \frac{\|\mathcal{L}_{op}(f)\|}{\|f\|}, \quad (f \neq 0)$$

is less than one.

Usually in practice, only one iteration is feasible. The relative error of the first iterate is defined by

$$\epsilon_{rel}^{(1)} = \frac{\|e - e^{(1)}\|}{\|e\|}$$

and is bounded above by the square of the operator norm. Therefore, an estimate of the operator norm provides an estimate of the relative error. As a consequence of the definition of the operator norm, any estimate of the form $\|\mathcal{L}_{op}(e)\| \leq \alpha \|e\|$ implies that $\|\mathcal{L}_{op}\| \leq \alpha$.

Analyses of the slab waveguide and the circular fiber indicate that one iteration can provide a "good" approximation to solution of (33) for

sufficiently high spatial frequency provided that $(\delta n^2)^2 << 1$. The results quantify the accuracy of the first iterate.

CHAPTER SEVEN

CONCLUSIONS AND RECOMMENDATIONS

An integral-equation formulation, providing a conceptually exact description of the electromagnetic field within a fairly general class of integrated optical circuits, has been presented. This formulation affords an extremely powerful method of analysis for both theoretical and practical applications. Apparently, the integral-operator approach is particularly useful in the investigation of axially-invariant waveguides.

A detailed discussion of the electric dyadic Green's function for a tri-layered substrate/film/cover dielectric structure was given in Chapter two. Knowledge of this dyad was of utmost importance since it was used throughout this dissertation as the kernel in the EFIE for integrated optics. The development of the electric Green's dyad demanded a mathematically rigorous treatment and revealed a natural depolarizing dyad appropriate for the Sommerfeld-integral representation of dyadic components. Again, rigorous analysis effected the subsequent identification of the corresponding principal volume. This development is believed to be new and is the subject of a paper which is currently in the review cycle [29].

In Chapter three, a transform-domain EFIE was developed to facilitate the study of axially-invariant dielectric waveguides. A straightforward derivation resulted in an EFIE for the transverse field, thereby uncoupling the axial field component. This derivation is presented in a

forthcoming paper [30] as a potentially new contribution.

Complex-plane analysis effected the identification of the propagation-mode spectrum for axially-uniform integrated dielectric waveguides in Chapter four. Pole singularities of the transform-domain field were observed to comprise a discrete spectrum associated with surface waves, while hyperbolic branch cuts corresponded to a continuous spectrum. Regimes of purely-guided and leaky wave poles were also identified.

An asymptotic EFIE, appropriate to the study of dielectric waveguides capable of supporting a surface-wave mode with no low-frequency cutoff, was derived in Chapter five. It was conjectured that such a surface wave can exist on any axially-invariant dielectric waveguide immersed in a uniform surround. Applications of the AEFIE to the graded-index asymmetric slab and the step-index circular fiber provided evidence to support this conjecture. Aside from the academic purpose of proving the aforementioned hypothesis, the AEFIE provides a favorable alternative to numerically implementing the non-asymptotic EFIE in the investigation of surface waves propagating in the regime where the phase constant approaches the wavenumber of the surround.

Finally, standard numerical techniques were observed to be ineffective in approximating spectral components of the continuous spectrum having high spatial frequencies. An iterative scheme was proposed which avoids deficiencies in such methods. Analyses of the slab waveguide and the circular fiber indicated that a single iteration can provide an adequate approximation to high-frequency spectral components when the contrast of refractive indices is sufficiently small. These analyses were performed on the space of continuous functions equipped with sup norm. This space is quite restrictive and future endeavors are encouraged to

investigate other normed vector spaces (e.g. the Hilbert space of square integrable functions). At this time, there seems to be little hope in successfully approximating high spectral components for guides having high refractive-index contrast. Research in this area is also recommended.

APPENDICES

APPENDIX A

APPENDIX A

ELECTRIC HERTZIAN POTENTIAL

The Hertzian potential is developed by observing the nonexistence of magnetic monopoles through (1.1d). Borrowing a theorem from vector calculus [15, pp.640-643], the magnetic field $\mathbf{H}$ may be expressed as the curl of a vector potential. In an electrically homogeneous medium, $\mathbf{H}$ may be expressed in terms of the Hertzian potential $\boldsymbol{\Pi}$ as

$$\mathbf{H} = j\omega\epsilon\, \nabla\times\boldsymbol{\Pi}. \tag{1}$$

Substitution of (1) into Faraday's law (1.1b) yields

$$\nabla\times(\mathbf{E} - k^2\boldsymbol{\Pi}) = 0 \tag{2}$$

where $k^2 = \omega^2\mu\epsilon$ is the wavenumber in the medium. Under suitable conditions (see [15, p.639]), (2) implies

$$\mathbf{E} = k^2\boldsymbol{\Pi} - \nabla\varphi \tag{3}$$

where φ is a suitable scalar field. Use of (1) and (3) into Ampere's law (1.1c) yields

$$(\nabla^2 + k^2)\boldsymbol{\Pi} = -\mathbf{J}/j\omega\epsilon + \nabla(\nabla\cdot\boldsymbol{\Pi} + \varphi) \tag{4}$$

where use of the vector identity $\nabla\times\nabla\times\mathbf{F} = \nabla\nabla\cdot\mathbf{F} - \nabla^2\mathbf{F}$ has been made. According to a well known theorem from potential theory [31, pp.66-67], a vector field is uniquely determined through knowledge of its curl and divergence. Therefore, at this stage, $\boldsymbol{\Pi}$ is arbitrary since its divergence is unspecified. Choosing $\nabla\cdot\boldsymbol{\Pi} = -\varphi$ uniquely determines $\boldsymbol{\Pi}$. Thus (4) simplifies to

$$(\nabla^2 + k^2)\boldsymbol{\Pi} = -\mathbf{J}/j\omega\epsilon$$

which is the Helmholtz equation for the Hertzian potential subject to the Lorentz gauge $\nabla\cdot\Pi = -\varphi$. Use of this gauge in (3) yields

$$\mathbf{E} = (k^2 + \nabla\nabla\cdot)\Pi \tag{5}$$

which relates the electric field to the Hertzian potential.

APPENDIX B

APPENDIX B

HERTZIAN POTENTIAL GREEN'S DYAD

The boundary conditions for the scalar components of the transform-domain Hertzian potential are given in [13] and may be expressed as

$$\pi_{c\alpha} = N_{fc}^2 \, \pi_{f\alpha} \ldots \alpha = x, y, z \tag{1a}$$

$$\frac{\partial \pi_{c\alpha}}{\partial y} = N_{fc}^2 \, \frac{\partial \pi_{f\alpha}}{\partial y} \ldots \alpha = x, z \qquad \text{at } y = 0 \tag{1b}$$

$$\frac{\partial \pi_{cy}}{\partial y} - \frac{\partial \pi_{fy}}{\partial y} = (N_{fc}^{-2} - 1)\,(j\xi\, \pi_{cx} + j\zeta\, \pi_{cz}) \tag{1c}$$

$$\pi_{f\alpha} = N_{sf}^2 \, \pi_{s\alpha} \ldots \alpha = x, y, z \tag{1d}$$

$$\frac{\partial \pi_{f\alpha}}{\partial y} = N_{sf}^2 \, \frac{\partial \pi_{s\alpha}}{\partial y} \ldots \alpha = x, z \qquad \text{at } y = -t \tag{1e}$$

$$\frac{\partial \pi_{fy}}{\partial y} - \frac{\partial \pi_{sy}}{\partial y} = -(N_{sf}^2 - 1)\,(j\xi\, \pi_{sx} + j\zeta\, \pi_{sz}) \tag{1f}$$

where $N_{fc} = (n_f/n_c)$ and $N_{sf} = (n_s/n_f)$. Additionally, the potential must vanish as $|y| \to \infty$. These boundary conditions are implemented below for the situation in which currents are immersed exclusively within the film region of the tri-layered dielectric structure.

As shown in Chapter two, the transform-domain potentials decompose into reflected and principal parts. Enforcing the boundary condition at $y = \pm\infty$, the potentials for sources in the film are given by

$$\pi_{c\alpha}(\lambda, y) = W_{c\alpha}(\lambda)\, e^{-p_c y} \qquad \ldots\ y > 0$$

$$\pi_{f\alpha}(\lambda, y) = W^{+}_{f\alpha}(\lambda)\, e^{p_f y} + W^{-}_{f\alpha}(\lambda)\, e^{-p_f y} + \pi^{p}_{\alpha}(\lambda, y) \qquad \ldots\ 0 > y > -t$$

$$\pi_{s\alpha}(\lambda, y) = W_{s\alpha}(\lambda)\, e^{p_s y} \qquad \ldots\ -t > y$$

where the principal part π^{p}_{α} of the transform-domain potential is

$$\pi^{p}_{\alpha}(\lambda, y) = \int_V \frac{e^{-p_f |y-y'|}}{2p_f}\, e^{-j\lambda\cdot r'}\, \frac{J_\alpha(r')}{j\omega\epsilon_f}\, dV'.$$

It will be useful to abbreviate the following quantities. Let $u_\alpha(\lambda)$ and $v_\alpha(\lambda)$ be defined as

$$u_\alpha(\lambda) \equiv \pi^{p}_{\alpha}(\lambda, 0)$$
$$= \int_V \frac{e^{p_f y'}}{2p_f}\, e^{-j\lambda\cdot r'}\, \frac{J_\alpha(r')}{j\omega\epsilon_f}\, dV'$$

$$v_\alpha(\lambda) \equiv \pi^{p}_{\alpha}(\lambda, -t)$$
$$= \int_V \frac{e^{-p_f (t+y')}}{2p_f}\, e^{-j\lambda\cdot r'}\, \frac{J_\alpha(r')}{j\omega\epsilon_f}\, dV'$$

Then, it is easy to see that

$$\left.\frac{\partial \pi^{p}_{\alpha}(\lambda, y)}{\partial y}\right|_{y=0} = -\, p_f u_\alpha(\lambda)$$

$$\left.\frac{\partial \pi^{p}_{\alpha}(\lambda, y)}{\partial y}\right|_{y=-t} = p_f v_\alpha(\lambda)$$

Now, implementing the boundary conditions (1a)-(1f), the following sys-

tem of equations is generated.

$$W_{c\alpha} = N_{fc}^2 \, (W_{f\alpha}^+ + W_{f\alpha}^- + u_\alpha) \quad \ldots(\alpha = x,y,z) \tag{2a}$$

$$- p_c W_{c\alpha} = N_{fc}^2 (p_f W_{f\alpha}^+ - p_f W_{f\alpha}^- - p_f u_\alpha) \quad \ldots(\alpha = x,z) \tag{2b}$$

$$- p_c W_{cy} - (p_f W_{fy}^+ - p_f W_{fy}^- - p_f u_y) = (N_{fc}^{-2} - 1) \, (j\xi \, W_{cx} + j\zeta \, W_{cz}) \tag{2c}$$

$$W_{f\alpha}^+ \, e^{-p_f t} + W_{f\alpha}^- \, e^{p_f t} + v_\alpha = N_{sf}^2 \, W_{s\alpha} \, e^{-p_s t} \quad \ldots(\alpha = x,y,z) \tag{2d}$$

$$p_f W_{f\alpha}^+ \, e^{-p_f t} - p_f W_{f\alpha}^- \, e^{p_f t} + p_f v_\alpha = N_{sf}^2 \, p_s W_{s\alpha} \, e^{-p_s t} \quad \ldots(\alpha = x,z) \tag{2e}$$

$$p_f (W_{fy}^+ \, e^{-p_f t} - W_{fy}^- \, e^{p_f t} + v_y) - p_s W_{sy} \, e^{-p_s t} = - (N_{sf}^2 - 1)(j\xi \, W_{sx} \, e^{-p_s t} + j\zeta \, W_{sz} \, e^{-p_s t}). \tag{2f}$$

Tangential components of potential ($\alpha = x,z$) satisfy the boundary conditions (2a), (2b), (2d), and (2e). These relations provide a system of eight linear equations in eight unknowns. Solving (2a) and (2b) simultaneously for $W_{c\alpha}$ and $W_{f\alpha}^+$ in terms of $W_{f\alpha}^-$ and u_α yields

$$W_{c\alpha} = T_{fc}^t (W_{f\alpha}^- + u_\alpha) \tag{3a}$$

$$W_{f\alpha}^+ = R_{cf}^t (W_{f\alpha}^- + u_\alpha) \tag{3b}$$

where the tangential reflection and transmission coefficients associated with the cover-film interface are

$$R_{cf}^t = (p_f - p_c)/(p_f + p_c) \qquad T_{fc}^t = 2N_{fc}^2 p_f/(p_f + p_c).$$

Similarly, solving (2d) and (2e) simultaneously for $W_{f\alpha}^-$ and $W_{s\alpha}$ in terms of $W_{f\alpha}^+$ and v_α yields

$$W_{f\alpha}^- = R_{sf}^t (W_{f\alpha}^+ \, e^{-2p_f t} + v_\alpha \, e^{-p_f t}) \tag{4a}$$

$$W_{s\alpha} = T_{fs}^t (W_{f\alpha}^+ \, e^{(p_s - p_f)t} + v_\alpha \, e^{p_s t}) \tag{4b}$$

where the tangential reflection and transmission coefficients associated with the film-substrate interface are given by

$$R^t_{sf} = (p_f - p_s)/(p_f + p_s) \qquad T^t_{fs} = 2N^{-2}_{sf}p_f/(p_f + p_s).$$

Finally, solving the resulting equations (3a), (3b), (4a) and (4b) simultaneously yields

$$W_{c\alpha} = (T^t_{fc}\, u_\alpha + T^t_{fc}R^t_{sf}e^{-p_f t}\, v_\alpha)/D^t \tag{5a}$$

$$W^+_{f\alpha} = (R^t_{cf}\, u_\alpha + R^t_{cf}R^t_{sf}e^{-p_f t}\, v_\alpha)/D^t \tag{5b}$$

$$W^-_{f\alpha} = (R^t_{cf}R^t_{sf}e^{-2p_f t}\, u_\alpha + R^t_{sf}e^{-p_f t}\, v_\alpha)/D^t \tag{5c}$$

$$W_{s\alpha} = (R^t_{cf}T^t_{fs}e^{(p_s - p_f)t}\, u_\alpha + T^t_{fs}e^{p_s t}\, v_\alpha)/D^t \tag{5d}$$

where the quantity D^t is defined as $D^t = 1 - R^t_{cf}R^t_{sf}e^{-2p_s t}$.

Normal components of potential ($\alpha = y$) satisfy the boundary conditions (1a), (1c), (1d), and (1f). These relations provide a system of four linear equations in four unknowns. Solving (2a) and (2c) simultaneously for W^+_{fy} in terms of W^-_{fy}, u_y, W_{cx}, and W_{cz} yields

$$W^+_{fy} = -R^n_{fc}\, W^-_{fy} - R^n_{fc}\, u_y - \frac{N^{-2}_{fc} - 1}{N^2_{fc}p_c + p_f}(j\xi\, W_{cx} + j\xi\, W_{cz}) \tag{6}$$

where the normal reflection and transmission coefficients associated with the cover-film interface are

$$R^n_{fc} = (N^2_{fc}p_c - p_f)/(N^2_{fc}p_c + p_f) \qquad T^n_{fc} = 2N^2_{fc}p_f/(N^2_{fc}p_c + p_f).$$

Similarly, solving (2d) and (2f) simultaneously for W^-_{fy} in terms of W^+_{fy}, v_y, W_{sx}, and W_{sz} yields

$$W_{fy}^{-} = R_{sf}^{n} e^{-2p_f t} W_{fy}^{+} + R_{sf}^{n} e^{-p_f t} v_y + \frac{N_{sf}^2 (N_{sf}^2 - 1)}{N_{sf}^2 p_f + p_s} (j\xi W_{sx} + j\zeta W_{sz}) \times e^{-(p_s + p_f)t} \tag{7}$$

where the reflection and transmission coefficients associated with the film-substrate interface are

$$R_{sf}^{n} = (N_{sf}^2 p_f - p_s)/(N_{sf}^2 p_f + p_s) \qquad T_{fs}^{n} = 2p_f/(N_{sf}^2 p_f + p_s).$$

Now, equations (6) and (7) can be solved simultaneously for W_{fy}^{+} and W_{fy}^{-} revealing

$$W_{fy}^{+} = -\frac{R_{fc}^{n}}{D^n} u_y - \frac{R_{fc}^{n} R_{sf}^{n} e^{-p_f t}}{D^n} v_y - \frac{N_{fc}^{-2} - 1}{(N_{fc}^2 p_c + p_f) D^n} (j\xi W_{cx} + j\zeta W_{cz}) - \frac{N_{sf}^2 (N_{sf}^2 - 1)}{(N_{sf}^2 p_f + p_s) D^n} R_{fc}^{n} e^{-(p_s + p_f)t} (j\xi W_{sx} + j\zeta W_{sz}) \tag{8}$$

$$W_{fy}^{-} = -\frac{R_{fc}^{n} R_{sf}^{n} e^{-2p_f t}}{D^n} u_y + \frac{R_{sf}^{n} e^{-p_f t}}{D^n} v_y - \frac{N_{fc}^{-2} - 1}{(N_{fc}^2 p_c + p_f) D^n} R_{sf}^{n} e^{-2p_f t} \times (j\xi W_{cx} + j\zeta W_{cz}) + \frac{N_{sf}^2 (N_{sf}^2 - 1)}{(N_{sf}^2 p_f + p_s) D^n} e^{-(p_s + p_f)t} (j\xi W_{sx} + j\zeta W_{sz}) \tag{9}$$

where the quantity D^n is defined as $D^n \equiv 1 + R_{fc}^{n} R_{sf}^{n} e^{-2p_f t}$.

Now, the reflected part of the potential in the film can be calculated by inverse Fourier transforming the transform-domain potentials. First, use equations (5a)-(5d), (8) and (9) to express tangential components as

$$\pi_{f\alpha}(\lambda, y) = \pi_{\alpha}^{p}(\lambda, y) + [(R_{cf}^{t} u_\alpha + R_{cf}^{t} R_{sf}^{t} e^{-p_f t} v_\alpha)/D^t] e^{p_f y} + [(R_{cf}^{t} R_{sf}^{t} e^{-2p_f t} u_\alpha + R_{sf}^{t} e^{-p_f t} v_\alpha)/D^t] e^{-p_f y}. \tag{10}$$

Then, application of the inverse Fourier-transform operator

$$F^{-1}\{\cdot\} = \frac{1}{(2\pi)^2}\iint \{\cdot\}\, e^{j\lambda\cdot r}\, d^2\lambda$$

to (10) yields the tangential components ($\alpha = x,z$) of potential

$$\Pi_{f\alpha}(r) = \lim_{v\to 0}\int_{V-v} G^p(r|r')\,\frac{J_\alpha(r')}{j\omega\epsilon_f}\,dV'$$

$$+\int_V G_t^r(r|r')\,\frac{J_\alpha(r')}{j\omega\epsilon_f}\,dV'.$$

Here, G^p is the principal dyad discussed extensively in Chapter two, and the tangential component of the reflected dyad G_t^r is expressed as the spectral integral

$$G_t^r(r|r') = \iint \sum_{i=1}^{4} R_i^t(\lambda)\,\frac{e^{-p_f\varphi_i}}{2(2\pi)^2 p_f}\, e^{j\lambda\cdot(r-r')}\, d^2\lambda. \tag{11}$$

The tangential reflection coefficients R_i^t are given by

$$\begin{aligned} R_1^t &= R_{cf}^t/D^t \\ R_2^t &= R_{sf}^t/D^t \\ R_3^t &= R_{cf}^t R_{sf}^t/D^t \\ R_4^t &= R_3^t \end{aligned} \tag{12}$$

and the phase lengths φ_i are given in Section 2.2.3.

Calculation of the normal component of potential is slightly more elaborate due to their coupling with the tangential components of current. Therefore, define π_{fyy} as that part of π_{fy} produced by J_y. Then, the potential Π_{fyy} becomes

$$\Pi_{fyy}(r) = \lim_{v\to 0}\int_{V-v} G^p(r|r')\,\frac{J_y(r')}{j\omega\epsilon_f}\,dV'$$

$$+\int_V G_n^r(r|r')\,\frac{J_y(r')}{j\omega\epsilon_f}\,dV'.$$

The normal component of the reflected dyad G_n^r is expressed as the spectral integral

$$G_n^r(r|r') = \iint \sum_{i=1}^{4} R_i^n(\lambda) \frac{e^{-p_f \Psi_i}}{2(2\pi)^2 p_f} e^{j\lambda\cdot(r-r')} \, d^2\lambda. \tag{13}$$

where the normal reflection coefficients R_i^n are given by

$$\begin{aligned} R_1^t &= - R_{fc}^n / D^n \\ R_2^n &= R_{sf}^n / D^n \\ R_3^n &= - R_{fc}^n R_{sf}^n / D^n \\ R_4^n &= R_3^n. \end{aligned} \tag{14}$$

Likewise, define $\pi_{fy\alpha}$ as that part of π_{fy} produced by tangential current J_α. Then, the potential $\Pi_{fy\alpha}$ becomes

$$\Pi_{fy\alpha}(r) = \int_V \frac{\partial}{\partial x_\alpha} G_c^r(r|r') \frac{J_\alpha(r')}{j\omega\epsilon_f} \, dV'$$

where the coupling component of the reflected dyad G_c^r is expressed as the spectral integral

$$G_c^r(r|r') = \iint \sum_{i=1}^{4} C_i(\lambda) \frac{e^{-p_f \Psi_i}}{2(2\pi)^2 p_f} e^{j\lambda\cdot(r-r')} \, d^2\lambda. \tag{15}$$

and the coupling coefficients C_i are given by

$$\begin{aligned} C_1 &= - \frac{1}{D^t D^n} \left\{ \frac{N_{fc}^{-2} - 1}{N_{fc}^2 p_c + p_f} T_{fc}^t + \frac{N_{sf}^2 (N_{sf}^2 - 1)}{N_{sf}^2 p_f + p_s} R_{cf}^t R_{fc}^n T_{fs}^t e^{-2p_f t} \right\} \\ C_2 &= - \frac{1}{D^t D^n} \left\{ \frac{N_{fc}^{-2} - 1}{N_{fc}^2 p_c + p_f} R_{sf}^t R_{sf}^n T_{fc}^t e^{-2p_f t} - \frac{N_{sf}^2 (N_{sf}^2 - 1)}{N_{sf}^2 p_f + p_s} T_{fs}^t \right\} \\ C_3 &= - \frac{1}{D^t D^n} \left\{ \frac{N_{fc}^{-2} - 1}{N_{fc}^2 p_c + p_f} R_{sf}^n T_{fc}^t - \frac{N_{sf}^2 (N_{sf}^2 - 1)}{N_{sf}^2 p_f + p_s} R_{cf}^t T_{fs}^t \right\} \\ C_4 &= - \frac{1}{D^t D^n} \left\{ \frac{N_{fc}^{-2} - 1}{N_{fc}^2 p_c + p_f} R_{sf}^t T_{fc}^t + \frac{N_{sf}^2 (N_{sf}^2 - 1)}{N_{sf}^2 p_f + p_s} R_{fc}^n T_{fs}^t \right\}. \end{aligned} \tag{16}$$

Finally, the potential in the film can be expressed as

$$\Pi_f(r) = \lim_{v \to 0} \int_{V-v} \bar{\bar{G}}^p(r|r') \cdot \frac{J(r')}{j\omega\epsilon_f} dV' + \int_V \bar{\bar{G}}^r(r|r') \cdot \frac{J(r')}{j\omega\epsilon_f} dV'$$

where the principal dyad is $\bar{\bar{I}}G^p$ and the reflected dyad is written in terms of scalar components as

$$\bar{\bar{G}}^r(r|r') = \hat{x}G_t^r\hat{x} + \hat{y}\left(\frac{\partial G_c^r}{\partial x}\hat{x} + G_n^r\hat{y} + \frac{\partial G_c^r}{\partial z}\hat{z}\right) + \hat{z}G_t^r\hat{z}.$$

The scalar components of the reflected dyad are calculated by using equations (11)-(16).

APPENDIX C

APPENDIX C

DIFFERENTIATION UNDER SPECTRAL INTEGRALS

It is now shown that the differentiation under the spectral integral of (2.3) is a legitimate operation. Without loss of generality, justifying this interchange of operations for the following is sufficient.

$$\iint_{\lambda} \nabla\nabla\cdot\left[e^{j\lambda\cdot r}\int_V g^p(\lambda;y,r')\,J(r')\,dV'\right]d^2\lambda \qquad (1)$$

In (1), k_r is the real part of k_c and evaluation of p_c is made on the Riemann sheet with $Re(p_c) > 0$.

Assuming that J and $\nabla\cdot J$ are continuous and have compact support in V, use of the vector identity $\nabla\cdot(\varphi A) = \varphi\,\nabla\cdot A + \nabla\varphi\cdot A$ along with the divergence theorem on (1) yields

$$\iint_{\lambda} \nabla\nabla\cdot\left[e^{j\lambda\cdot r}\int_V g^p(\lambda;y,r')\,J(r')\,dV'\right]d^2\lambda = \iint_{\lambda} \nabla\left[e^{j\lambda\cdot r}\int_V \nabla'\cdot J(r') \times g^p(\lambda;y,r')\,dV'\right]d^2\lambda$$

$$= \iint_{\lambda} \nabla\left[e^{j\lambda\cdot r}\int F(\nabla'\cdot J(r'))\,\frac{e^{-p_c|y-y'|}}{2p_c}\,dy'\right]d^2\lambda \qquad (2)$$

where $F(\nabla\cdot J)$ is the Fourier transform of $\nabla\cdot J$ as defined in Chapter two. Next, use $p_c = p_r + jp_i$, where p_r and p_i are the real and imaginary parts of p_c respectively. The exponential $e^{-p_r|y-y'|}$ is of constant sign for all y. Using the generalized form of the first mean value theorem for integrals [15, p.117], the right side of (2) may be written

as

$$\iint_{\lambda \leq k_r} \nabla\left[e^{j\lambda\cdot r}\, \mathrm{Re}\left\{F(\nabla'\cdot J(x',\eta,z'))e^{-jp_i|y-\eta|}\right\} \int_{y_{min}}^{y_{max}} \frac{e^{-p_r|y-y'|}}{2p_c}\, dy'\right] d^2\lambda \quad (3)$$

$$+j \iint_{\lambda \leq k_r} \nabla\left[e^{j\lambda\cdot r}\, \mathrm{Im}\left\{F(\nabla'\cdot J(x',\theta,z'))e^{-jp_i|y-\theta|}\right\} \int_{y_{min}}^{y_{max}} \frac{e^{-p_r|y-y'|}}{2p_c}\, dy'\right] d^2\lambda,$$

where $y_{min} < \eta, \theta < y_{max}$ ($J = 0$ for all $y < y_{min}$, $y > y_{max}$). The spatial integral in (3) is trivial and leads to

$$\iint_{\lambda \leq k_r} \nabla\left[e^{j\lambda\cdot r}\, \mathrm{Re}\left\{F(\nabla'\cdot J(x',\eta,z'))e^{-jp_i|y-\eta|}\right\} \frac{\varphi(p_r;y)}{2p_r p_c}\right] d^2\lambda \quad (4)$$

$$+j \iint_{\lambda \leq k_r} \nabla\left[e^{j\lambda\cdot r}\, \mathrm{Im}\left\{F(\nabla'\cdot J(x',\theta,z'))e^{-jp_i|y-\theta|}\right\} \frac{\varphi(p_r;y)}{2p_r p_c}\right] d^2\lambda,$$

where $\varphi(p_r;y) = (2 - e^{-p_r(y-y_{min})} - e^{-p_r(y_{max}-y)})$. Since $\nabla\cdot J$ is continuous and of compact support in V, $\nabla\cdot J \in L^2$ (i.e. the space of square integrable functions). In particular, for each y, $\nabla\cdot J$ is an L^2 function in the x-z plane. Using a standard theorem from Fourier transform theory [17, pp.310-313], the 2-D Fourier transform of $\nabla\cdot J$ is an L^2 function in the ξ-ζ plane. Thus, $F(\nabla\cdot J) = O(\lambda^{-1-\varepsilon})$ as ($\lambda\to\infty$, $\varepsilon>0$). The integrand in (4) is dominated in magnitude by a function which is independent of r and $O(\lambda^{-2-\varepsilon})$. The Weierstrauss M-test [15, p.470] guarantees that the integral in (4) converges uniformly. A standard theorem from advanced calculus [15, p.474] justifies the interchange of differentiation and spectral integration.

APPENDIX D

APPENDIX D

ELECTRIC DYADIC GREEN'S FUNCTION IN THE SOURCE REGION

A classical development of the electric dyadic Green's function for observation points within the source region proceeds as follows. The Hertzian potential maintained by electric current sources J in an unbounded medium is given by

$$\Pi(r) = \lim_{v \to 0} \int_{V-v} \psi(r|r') \frac{J(r')}{j\omega\epsilon} \, dV' \tag{1}$$

where v is any volume containing r'=r, and

$$\psi(r|r') = \frac{e^{-jk|r-r'|}}{4\pi|r-r'|}$$

is the familiar representation for the free-space Green's function. Since (1) is independent of the shape of v, it is often written without the limit.

The electric field E is related to Π by $E = (k^2 + \nabla\nabla\cdot)\Pi$. Evidently, calculation of E requires evaluation of the derivatives of Π. Fikioris [32] has shown that first derivatives of Π may be obtained by formally differentiating under the integral in (1) provided that J is continuous in V. Therefore

$$\nabla\cdot\Pi(r) = \frac{1}{j\omega\epsilon} \int_V \nabla\psi(r|r')\cdot J(r') \, dV' \tag{2a}$$

$$= -\frac{1}{j\omega\epsilon} \int_V J(r')\cdot \nabla'\psi(r|r') \, dV' \tag{2b}$$

where the relation $\nabla\psi = -\nabla'\psi$ has been used in going from (2a) to (2b). Now, under the additional assumption that $\nabla\cdot J$ is continuous throughout V, use of the vector identity $\nabla\cdot(\psi A) = \nabla\psi\cdot A + \psi\nabla\cdot A$ allows (2b) to be written

$$\nabla\cdot\Pi(r) = -\frac{1}{j\omega\epsilon}\int_V \left\{ \nabla'\cdot[J(r')\,\psi(r|r')] - \psi(r|r')\,\nabla'\cdot J(r') \right\} dV'. \quad (3)$$

Application of the divergence theorem to (3) yields

$$\nabla\cdot\Pi(r) = \frac{1}{j\omega\epsilon}\left\{ \int_V \psi(r|r')\,\nabla'\cdot J(r')\,dV' - \int_S \hat{n}\cdot J(r')\,\psi(r|r')\,dS' \right\} \quad (4)$$

where S is the boundary of V and $\hat{n}$ is the outward unit normal to S. Since J is assumed to have compact support in V, $\hat{n}\cdot J = 0$ on S. Thus (4) simplifies to

$$\nabla\cdot\Pi(r) = \frac{1}{j\omega\epsilon}\int_V \psi(r|r')\,\nabla'\cdot J(r')\,dV'. \quad (5)$$

Now second derivatives of Π may be obtained by formally differentiating under the integral in (5). Thus

$$\begin{aligned}\nabla\nabla\cdot\Pi(r) &= \frac{1}{j\omega\epsilon}\int_V \nabla\psi(r|r')\,\nabla'\cdot J(r')\,dV' \\ &= -\frac{1}{j\omega\epsilon}\int_V \nabla'\psi(r|r')\,\nabla'\cdot J(r')\,dV'. \end{aligned} \quad (6)$$

Writing $\nabla'\cdot J(r') = \nabla'\cdot\{J(r') - J(r)\}$ in (6) yields

$$\begin{aligned}\nabla\nabla\cdot\Pi(r) &= -\frac{1}{j\omega\epsilon}\int_V \nabla'[\psi(r|r')]\,\nabla'\cdot\{J(r') - J(r)\}\,dV' \\ &= -\frac{1}{j\omega\epsilon}\lim_{v\to 0}\left\{ \int_{S+s} \{J(r') - J(r)\}\cdot \hat{n}'\nabla'\psi(r|r')\,dS' \right. \\ &\qquad \left. - \int_{V-v} \{J(r') - J(r)\}\cdot \nabla'\nabla'\psi(r|r')\,dV' \right\} \end{aligned} \quad (7)$$

where as before v is any volume which contains r, and s is the boundary of v. By differentiability of J at r, the volume integral in (7) con-

verges as $v \to 0$. However, it may be illegitimate to separate this integral into the sum

$$\lim_{v\to 0}\left\{\int_{V-v} J(r')\cdot\nabla'\nabla'\psi(r|r')\,dV' - \int_{V-v} J(r)\cdot\nabla'\nabla'\psi(r|r')\,dV'\right\} \qquad (8)$$

since each integral in (8) may not converge. However, evaluation of the second integral in (8) reveals

$$\lim_{v\to 0}\int_{V-v} J(r)\cdot\nabla'\nabla'\psi(r|r')\,dV' = -\,J(r)\cdot\left\{\lim_{v\to 0}\int_{V-v}\nabla'\nabla'\psi(r|r')\,dV'\right\}$$

which upon application of the divergence theorem becomes

$$\begin{aligned}\lim_{v\to 0}\int_{V-v} J(r)\cdot\nabla'\nabla'\psi(r|r')\,dV' &= J(r)\cdot\left\{\lim_{v\to 0}\int_{S+s}\hat{n}'\nabla'\psi(r|r')\,dS'\right\}\\ &= J(r)\cdot\left\{\int_S \hat{n}'\nabla'\psi(r|r')\,dS'\right.\\ &\quad\left.+\lim_{v\to 0}\int_s \hat{n}'\nabla'\psi(r|r')\,dS'\right\}. \qquad (9)\end{aligned}$$

Clearly the limit in (9) is convergent. Consequently, convergence of the first integral in (8) is now established since it is equal to the sum of convergent integrals. Now, substitution of (8) and (9) into (7) reveals

$$\begin{aligned}\nabla\nabla\cdot\Pi &= \frac{1}{j\omega\epsilon}\lim_{v\to 0}\left\{\int_{V-v}\nabla'\nabla'\psi(r|r')\cdot J(r')\,dV' - \int_{S+s}\nabla'\psi(r|r')\hat{n}'\cdot J(r')\,dS'\right.\\ &\quad\left.-\left[\int_{S+s}\nabla'\psi(r|r')\hat{n}'\,dS'\right]\cdot J(r) + \left[\int_{S+s}\nabla'\psi(r|r')\hat{n}'\,dS'\right]\cdot J(r)\right\}\\ &= \frac{1}{j\omega\epsilon}\lim_{v\to 0}\left\{\int_{V-v}\nabla'\nabla'\psi(r|r')\cdot J(r')\,dV' - \int_{S+s}\nabla'\psi(r|r')\hat{n}'\cdot J(r')\,dS'\right\}\\ &= \frac{1}{j\omega\epsilon}\lim_{v\to 0}\left\{\int_{V-v}\nabla'\nabla'\psi(r|r')\cdot J(r')\,dV' - \int_{s}\nabla'\psi(r|r')\hat{n}'\cdot J(r')\,dS'\right\}\end{aligned}$$

where again the vanishing of $\hat{n}\cdot J$ on S has been observed. Finally, the electric field is given by

$$\mathbf{E}(\mathbf{r}) = \frac{1}{j\omega\epsilon} \lim_{v \to 0} \int_{V-v} (\bar{\bar{I}}k^2 + \nabla'\nabla')\psi(\mathbf{r}|\mathbf{r}') \cdot \mathbf{J}(\mathbf{r}')\, dV' + \mathbf{E}^c(\mathbf{r})$$

where the correction term $\mathbf{E}^c$ is given by

$$\mathbf{E}^c(\mathbf{r}) = -\frac{1}{j\omega\epsilon} \lim_{v \to 0} \int_s \nabla'\psi(\mathbf{r}|\mathbf{r}')\hat{n}' \cdot \mathbf{J}(\mathbf{r}')\, dS'.$$

APPENDIX E

APPENDIX E

EVALUATION OF AN INDEFINITE INTEGRAL

Evaluation of the indefinite integral $\int x\, Z_p(\beta x)\, B_p(\beta x)\, dx$ where Z_p and B_p are arbitrary Bessel functions, can be found as the limit of the following integral which appears in Gradshteyn [25, p.634].

$$\int x\, Z_p(\alpha x)\, B_p(\beta x)\, dx = \frac{\beta x Z_p(\alpha x) B_{p-1}(\beta x) - \alpha x Z_{p-1}(\alpha x) B_p(\beta x)}{\alpha^2 - \beta^2} \qquad (1)$$

for $\alpha \neq \beta$. An initial inspection of (1) seems to indicate an inconsistency. The left side of this expression is clearly well-behaved for $\alpha = \beta$. However, the right side is not of indeterminate form as $\alpha \to \beta$. This apparent discrepancy is reconciled by remembering that (1) is an indefinite integral. It is shown below that addition of an appropriately chosen constant to the right side of (1) results in an indeterminate form.

Let V be defined by the limit

$$V \equiv \lim_{\alpha \to \beta} \{\beta x\, Z_p(\alpha x)\, B_{p-1}(\beta x) - \alpha x\, Z_{p-1}(\alpha x)\, B_p(\beta x)\}$$

$$= \beta x \{Z_p(\beta x)\, B_{p-1}(\beta x) - Z_{p-1}(\beta x)\, B_p(\beta x)\}. \qquad (2)$$

Noting that the following Wronskians [16, p.360] hold,

$$J_p(\beta x)\, Y_{p-1}(\beta x) - J_{p-1}(\beta x)\, Y_p(\beta x) = 2/(\pi \beta x) \qquad (3)$$

$$H_p^{(1)}(\beta x)\, H_{p-1}^{(2)}(\beta x) - H_{p-1}^{(1)}(\beta x)\, H_p^{(2)}(\beta x) = -4j/(\pi \beta x)$$

it can be seen from (2) that V is independent of x for integer valued p. Subtracting V from the numerator of the right side of (1) yields

$$\int x\, Z_p(\alpha x)\, B_p(\beta x)\, dx = \frac{\beta x Z_p(\alpha x) B_{p-1}(\beta x) - \alpha x Z_{p-1}(\alpha x) B_p(\beta x) - V}{\alpha^2 - \beta^2} \qquad (4)$$

which is clearly of indeterminate form.

Now, application of L'hopitals rule [15, pp.95-102] to the right side of (4) allows evaluation of the following integral.

$$\begin{aligned}\int x\, Z_p(\beta x)\, B_p(\beta x)\, dx &= \lim_{\alpha\to\beta} \int x\, Z_p(\alpha x)\, B_p(\beta x)\, dx \\ &= \frac{1}{2\beta} \lim_{\alpha\to\beta} \frac{\partial}{\partial\alpha} \left(\beta x Z_p(\alpha x) B_{p-1}(\beta x) - \alpha x Z_{p-1}(\alpha x) B_p(\beta x)\right) \\ &= \frac{1}{2\beta} \left(\beta x^2 Z_p'(\beta x)\, B_{p-1}(\beta x) - x\, Z_{p-1}(\beta x)\, B_p(\beta x)\right. \\ &\qquad \left. - \beta x^2 Z_{p-1}'(\beta x)\, B_p(\beta x)\right). \end{aligned} \qquad (5)$$

The derivatives Z_p' and Z_{p-1}' are related to Z_p and Z_{p-1} through the recurrence relations [16, p.361]

$$Z_p'(\beta x) = Z_{p-1}(\beta x) - \frac{p}{\beta x} Z_p(\beta x) \qquad (6a)$$

$$Z_{p-1}'(\beta x) = - Z_p(\beta x) + \frac{p-1}{\beta x} Z_{p-1}(\beta x). \qquad (6b)$$

Substitution of (6a) and (6b) into (5) shows

$$\begin{aligned}\int x\, Z_p(\beta x)\, B_p(\beta x)\, dx = \frac{1}{2\beta} &\left(\beta x^2 B_{p-1}(\beta x) \left[Z_{p-1}(\beta x) - \frac{p}{\beta x} Z_p(\beta x)\right]\right. \\ &- \beta x^2 B_p(\beta x) \left[-Z_p(\beta x) + \frac{p-1}{\beta x} Z_{p-1}(\beta x)\right] \\ &\left. - x\, B_p(\beta x)\, Z_{p-1}(\beta x)\right)\end{aligned}$$

$$= \frac{x^2}{2}\left[Z_p(\beta x)\, B_p(\beta x) + Z_{p-1}(\beta x)\, B_{p-1}(\beta x)\right] - \frac{px}{2\beta}\left[Z_p(\beta x)\, B_{p-1}(\beta x) + Z_{p-1}(\beta x)\, B_p(\beta x)\right]. \tag{7}$$

This expression is used below to evaluate a specific indefinite integral.

Let $p = 1$, $Z_p = J_1$, $B_p = H_1^{(2)}$ and $\beta x = Q_c\rho$ in (7). Then,

$$\int J_1(Q_c\rho)\, H_1^{(2)}(Q_c\rho)\, \rho d\rho = \frac{\rho^2}{2}\left[J_1(Q_c\rho)\, H_1^{(2)}(Q_c\rho) + J_0(Q_c\rho)\, H_0^{(2)}(Q_c\rho)\right] - \frac{\rho}{2Q_c}\left[J_1(Q_c\rho)\, H_0^{(2)}(Q_c\rho) + J_0(Q_c\rho)\, H_1^{(2)}(Q_c\rho)\right].$$

An alternative form of this integral is obtained by application of the Wronskian (3) and the relation $H_p^{(2)}(\beta x) = J_p(\beta x) - jY_p(\beta x)$ [16, p.358]. It is easy to show from these relations that

$$J_p(\beta x)\, H_{p-1}^{(2)}(\beta x) - J_{p-1}(\beta x)\, H_p^{(2)}(\beta x) = -j2/(\pi\beta x)$$

which for $p = 1$, $\beta = Q_c$, and $x = \rho$ can be written

$$J_0(Q_c\rho)\, H_1^{(2)}(Q_c\rho) = J_1(Q_c\rho)\, H_0^{(2)}(Q_c\rho) + j2/(\pi Q_c\rho). \tag{8}$$

Substituting (8) into (7) yields

$$\int J_1(Q_c\rho)\, H_1^{(2)}(Q_c\rho)\, \rho d\rho = \frac{\rho^2}{2}\left[J_1(Q_c\rho)\, H_1^{(2)}(Q_c\rho) + J_0(Q_c\rho)\, H_0^{(2)}(Q_c\rho)\right] - \frac{\rho}{2Q_c}\left[2J_1(Q_c\rho)\, H_0^{(2)}(Q_c\rho) + j2/(\pi Q_c\rho)\right].$$

Stressing that this is an indefinite integral, the last term may be omitted since it is constant. Therefore,

$$\int J_1(Q_c\rho)\, H_1^{(2)}(Q_c\rho)\, \rho d\rho = \frac{\rho^2}{2}\left[J_1(Q_c\rho)\, H_1^{(2)}(Q_c\rho) + J_0(Q_c\rho)\, H_0^{(2)}(Q_c\rho)\right] - \frac{\rho}{Q_c} J_1(Q_c\rho)\, H_0^{(2)}(Q_c\rho). \tag{9}$$

LIST OF REFERENCES

LIST OF REFERENCES

[1] E.A.J. Marcatili, "Dielectric waveguide and directional coupler for integrated optics," BSTJ, vol. 48, no. 9, pp. 2071-2102, Sept. 1969.

[2] S-T. Peng, and A.A. Oliner, "Guidance and leakage properties of a class of open dielectric waveguides: part I--mathematical formulation," IEEE MTT-S Trans., vol. MTT-29, no. 9, pp. 843-855, Sept. 1981.

[3] A.A. Oliner, S-T. Peng, T-I. Hsu and A. Sanchez, "Guidance and leakage properties of a class of open dielectric waveguides: part II--new physical effects," IEEE MTT-S Trans., vol. MTT-29, no.9, pp. 855-869, Sept. 1981.

[4] V. Daniele, I. Montrosset, and R. Zich, "Boundary formulation of propagation problems in guiding structures for integrated optics," Radio Science, vol. 16, no. 4, pp. 461-465, July-August 1981.

[5] C-C, Su, "A combined method for dielectric waveguides using the finite-element technique and the surface integral equations method," IEEE MTT-S Trans., vol. 34, pp. 1140-1146, 1986.

[6] R.E. Collin and D.A. Kajenski, "Boundary element method for dielectric resonators and waveguides," Radio Science, vol. 22, no. 7, pp. 1155-1167, Dec. 1987.

[7] Y. Chang and R.F. Harrington, "A surface formulation for characteristic modes of material bodies, Rep. TR-74-7 p. 124, Syracuse, New York, 1974.

[8] D.R. Johnson and D.P. Nyquist, "Integral-operator analysis for dielectric waveguides--theory and application," National Radio Science (USNC/URSI) Meeting, University of Colorado, Boulder, Co. digest p. 104, Nov. 1978.

[9] J.S. Bagby, "Integral equation analysis of integrated dielectric waveguides," Ph.D. dissertation, Michigan State University, 1984.

[10] D. Marcuse, Theory of Dielectric Optical Waveguides, New York: Academic Press, 1974.

[11] A.W. Snyder, Optical Waveguide Theory, New York: Chapman and Hall, 1983.

[12] A. Sommerfeld, "Ueber die Ausbreitung der Wellen in der drahtlosen Telegraphie," Ann. Physik, vol. 28, p. 665, 1909.

[13] J.S. Bagby and D.P. Nyquist. "Dyadic Green's functions for integrated electronic and optical circuits," IEEE MTT-S Trans., vol. MTT-35, pp. 206-210, Feb. 1987.

[14] A. Sommerfeld, Partial Differential Equations in Physics, New York: Academic Press, 1964, pp.236-265.

[15] M.N. Olmsted, Advanced Calculus, Englewood Cliffs: Prentice-Hall, Inc., 1961.

[16] M. Abramovitz and I.A. Stegun. Handbook of Mathematical Functions, New York: Dover Publications, Inc., 1972.

[17] H,F. Weinberger, A First Course in Partial Differential Equations, New York: John Wiley & Sons, Inc., 1965.

[18] A.D. Yaghjian, "Electric dyadic Green's function in the source region," Proc. IEEE, vol. 68, pp. 248-263, Feb. 1980.

[19] O.D. Kellog, Foundations of Potential Theory, New York: Dover, 1953.

[20] R.E. Collin, Field Theory of Guided Waves, New York: McGraw Hill, 1960.

[21] J.S. Bagby, D.P. Nyquist and B.C. Drachman, "Integral formulation for analysis of integrated dielectric waveguides," IEEE MTT-S Trans., vol. MTT-33, pp.906-915, Oct. 1985.

[22] Private conversation with D.P. Nyquist.

[23] D.P. Nyquist, D.R. Johnson, and S.V. Hsu, "Ortogonality and amplitude spectrum of radiation modes along open-boundary waveguides," JOSA, vol. 71, no. 1, pp. 49-54, Jan. 1981.

[24] C.C. Johnson, Field and Wave Electro-Dynamics, New York: McGraw Hill, 1965, p. 175.

[25] I.S. Gradshteyn and I.M. Ryzhik, Table of Integrals, Series, and Products, Orlando: Academic Press, 1980.

[26] R.F. Harrington, Field Computation by Moment Methods, New York: The MacMillan Co., 1968.

[27] V. Hutson and J.S. Pym, Applications of Functional Analysis and Operator Theory, London: Academic Press, 1980.

[28] A.W. Snyder, "Continuous mode spectrum of a circular dielectric rod," IEEE MTT-S Trans., vol. 19, no. 8, pp. 720-727, August, 1971.

[29] M.S. Viola and D.P. Nyquist, "An observation on the Sommerfeld-integral representation of the electric dyadic Green's function for layered media," submitted to MTT-S Trans., August 1987.

[30] M.S. Viola and D.P. Nyquist, "An electric field integral-equation for the transverse field components of integrated optical waveguides," forthcoming.

[31] G. Arfken, Mathematical Methods for Physicists, New York: Academic Press, Inc., 1970, pp. 66-67.

[32] J.G. Fikioris, "Electromagnetic field inside a current carrying region," Journal of Mathematical Physics, vol. 6, no. 11, pp. 1617-1620, Nov. 1965.